1989

Development and Field Applications of Shaly Sand Petrophysical Models.

Milton Noel Lau
Louisiana State University and Agricultural & Mechanical College

Order Number 9025317

Development and field applications of shaly sand petrophysical models

Lau, Milton Noel, Ph.D.

The Louisiana State University and Agricultural and Mechanical Col., 1989

U·M·I
300 N. Zeeb Rd.
Ann Arbor, MI 48106

DEVELOPMENT AND FIELD APPLICATIONS OF SHALY SAND PETROPHYSICAL MODELS

A Dissertation

Submitted to the Graduate Faculty of the
Louisiana State University and
Agricultural and Mechanical College
in partial fulfillment of the
requirements for the degree of
Doctor of Philosophy

in

The Department of Petroleum Engineering

by

Milton N. Lau
B.S., Louisiana State University, 1985.
M.S., Louisiana State University, 1987.
December,1989.

ACKNOWLEDGEMENT

At this time the author would like to express his most sincere gratitude to Dr. Zaki Bassiouni, Chairman of the Petroleum Engineering Department, for his insightful guidance, and genuine interest in this project. The author also wishes to thank Dr. Robert Desbrandes, Dr. Adam T. Bourgoyne, Dr. William Bernard, and Dr. William Moore for their suggestions and assistance.

In addition, appreciation is extended to Mobil Exploration and Producing U.S. Inc., ARCO Oil and Gas Co. and Freeport Mc Moran for providing the data necessary to complete this study.

Finally, the author recognizes the financial support of the LSU-Mineral Research Institute and the Petroleum Engineering Department, which made this study possible.

TABLE OF CONTENTS

	Page
ACKNOWLEDGEMENT	ii
TABLE OF CONTENTS	iii
LIST OF TABLES	viii
LIST OF FIGURES	ix
ABSTRACT	xii
1.- INTRODUCTION	1
1.1- SHALY SAND MODELS	3
1.1.1- V_{sh} MODELS	3
1.1.2- CATION EXCHANGE CAPACITY MODELS	6
1.2.- PROPOSED NEW MODEL	8
2.- THE SILVA-BASSIOUNI MODELS	10
2.1- THE CONDUCTIVITY MODEL	10
2.1.1- DETERMINATION OF THE FRACTIONAL VOLUME OF THE DOUBLE LAYER, v_{fdl}	11
2.1.2- DETERMINATION OF EQUIVALENT COUNTERION CONDUCTIVITY, C_{eq}:	13
2.2- MEMBRANE POTENTIAL IN SHALY SANDS	15
2.2.1- TRANSPORT NUMBERS IN SHALY SANDS	16
2.2.2- CALCULATION OF THE MEAN ACTIVITY COEFFICIENT	17
2.2.3- CALCULATION OF THE HITTORF TRANSPORT NUMBER, tna^h	17
2.2.4- CALCULATION OF THE MEMBRANE POTENTIAL	17

2.3- CRITIQUE OF THE S-B MODELS..... 18
3- THE LSU SHALY-SANDS MODELS 19
3.1- THE LSU CONDUCTIVITY MODEL..... 19
3.1.1- DETERMINATION OF THE EQUIVALENT COUNTERION CONDUCTIVITY, C_{eq}..... 20
3.1.2- DETERMINATION OF COUNTERION CONCENTRATION, n_{eq}..... 24
3.1.3- DETERMINATION OF THE FRACTIONAL VOLUME OCCUPIED BY THE DOUBLE LAYER, v_{fdl}... 26
3.1.4- PREDICTION OF CORE CONDUCTIVITIES.. 27
3.1.5- CONDUCTIVITIES OF CORES WITH Qv<.1 meq/cc..... 27
3.2- MEMBRANE POTENTIAL MODEL..... 31
3.2.1- CALCULATION OF THE NaCl TRANSPORT NUMBER, tna^+..... 31
3.2.1.1- THE WATER TRANSPORT NUMBER, tw 35
3.2.2- SOLUTION OF THE MEMBRANE POTENTIAL EQUATION..... 37
4- THE LSU MODEL IN HYDROCARBON BEARING FORMATIONS..... 40
5- MODEL EXTENSION TO FIELD CONDITIONS..... 45
5.1- DESCRIPTION OF EXPERIMENTAL DATA..... 45
5.2- EFFECT OF TEMPERATURE ON THE PARAMETERS APPEARING IN THE LSU MODEL..... 46
5.2.1- TEMPERATURE EFFECT ON WATER CONDUCTIVITY, C_w..... 46

5.2.2- EFFECT OF TEMPERATURE ON THE FRACTIONAL VOLUME OF THE DOUBLE LAYER, v_{fdl}.... 47
5.2.3- EFFECT OF TEMPERATURE ON THE COUNTERION CONDUCTIVITY..... 48
5.2.4- DETERMINATION OF THE FRACTIONAL VOLUME OF THE DOUBLE LAYER, n_{eq}, AT HIGH TEMPERATURES..... 49
5.3- TEST OF THE MODEL..... 49
5.3.1- CALCULATION OF CORE CONDUCTIVITIES AT MOLAL CONCENTRATIONS OF m<.26..... 49
5.3.2- CALCULATION OF CORE CONDUCTIVITIES AT MOLAL CONCENTRATIONS OF m>.26..... 50
6.- SP LOG INTERPRETATION IN SHALY SANDS USING THE LSU MODEL..... 53
6.1- THE SP MODEL..... 55
6.2- DETERMINATION OF Tna^{ss} AT FORMATION TEMPERATURE..... 56
6.2.1- VARIATIONS OF THE SODIUM TRANSPORT NUMBER, tna^{*}, WITH TEMPERATURE..... 56
6.2.2- VARIATIONS OF THE ACTIVITY COEFFICIENT WITH TEMPERATURE:..... 57
6.3- DEFINITION AND DETERMINATION OF MEMBRANE EFFICIENCY, m_{eff}..... 59
6.4- DETERMINATION OF R_w IN SHALY SANDS WHEN Qv IS KNOWN..... 61
6.5- DETERMINATION OF Qv WHEN R_w IS KNOWN.... 62

7.- EVALUATION OF SHALY SAND FORMATIONS USING THE LSU MODEL..... 66
7.1- CURRENT METHODS TO DETERMINE Qv AND C_w.. 66
7.1.1- DETERMINATION OF Qv..... 66
7.1.2- DETERMINATION OF C_w..... 67
7.2- DETERMINATION OF Qv AND C_w IN WATER BEARING ZONES USING THE LSU MODEL..... 68
7.3- EVALUATION OF HYDROCARBON BEARING FORMATIONS 78
8- FIELD APPLICATION OF LSU MODELS..... 79
8.1- DETERMINATION OF S_w USING ARCHIE'S EQUATION 80
8.2- THE CYBERLOOK WATER SATURATION MODEL.... 81
8.2.1- DETERMINATION OF S_{wb}..... 82
8.3- THE LSU MODEL..... 84
8.3.1- INPUT DATA NEEDED IN THE LSU MODEL. 86
8.4- FIELD TEST OF LSU MODEL..... 88
8.5- DISCUSSION OF RESULTS..... 114
CONCLUSIONS..... 115
RECOMMENDATIONS..... 117
NOMENCLATURE..... 118
BIBLIOGRAPHY..... 122
APPENDIX A: DETERMINATION OF COUNTERION CONCENTRATION..... 125
APPENDIX B: COMPARISON OF EXPERIMENTAL AND CALCULATED CORE CONDUCTIVITIES..... 132
APPENDIX C: MEMBRANE POTENTIALS..... 160

APPENDIX D: EXPERIMENTAL DATA OF SHALY SAND CORES WITH DIFFERENT WATER SATURATIONS..... 170

APPENDIX E: COMPARISON OF EXPERIMENTAL AND CALCULATED CORE CONDUCTIVITIES AT DIFFERENT TEMPERATURES..... 177

APPENDIX F: CORE CONDUCTIVITIES AT DIFFERENT TEMPERATURES..... 188

VITA..... 198

LIST OF TABLES

	Page
3.1- IONIC MOBILITY COEFFICIENTS.....	22
3.2- SATURATED COUNTERION CONCENTRATIONS.....	26
3.3- HITTORF TRANSPORT NUMBER IN AQUEOUS SOLUTIONS AT 25 C.....	33
5.1- PETROPHYSICAL PARAMETERS.....	46
5.2- EQUIVALENT CONDUCTIVITY OF NaCl SOLUTIONS	46
6.1- TRANSPORT NUMBER OF THE CATION IN NaCl SOLUTIONS.....	58
8.1- EVALUATION OF WELL A	99
8.2- EVALUATION OF WELL B	100
8.3- EVALUATION OF WELL C	108
8.4- EVALUATION OF WELL D	108
8.5- EVALUATION OF WELL E	114

LIST OF FIGURES

Figure		Page
2.1-	TYPICAL C_o-C_w PLOT.....	12
2.2-	DISTRIBUTION OF CHARGES IN PORE SPACE....	14
3.1-	TRANSPORT COEFFICIENTS vs. FREE ELECTROLYTE CONCENTRATION.....	23
3.2-	DETERMINATION OF n_{eq}.....	25
3.3-	DETERMINATION OF FREE ELECTROLYTE CONCENTRATION.....	28
3.4-	COMPARISON OF CALCULATED vs. EXPERIMENTAL CORE CONDUCTIVITIES.....	29
3.5-	COMPARISON OF CALCULATED vs. EXPERIMENTAL CONDUCTIVITIES FOR CORES WITH Qv<.1.....	30
3.6-	DATA PUBLISHED ON THE HITTORF TRANSPORT NUMBER OF NaCl SOLUTIONS.....	34
3.7-	DETERMINATION OF twf.....	38
3.8-	COMPARISON OF CALCULATED vs. EXPERIMENTAL MEMBRANE POTENTIALS.....	39
4.1-	COMPARISON OF CALCULATED vs. EXPERIMENTAL Ct's.....	42
4.2-	COMPARISON OF CALCULATED vs. EXPERIMENTAL S_w's.....	44
5.1-	COMPARISON OF EXPERIMENTAL vs. CALCULATED CONDUCTIVITIES FOR CORES WITH Qv<.1.....	51
5.2-	COMPARISON OF EXPERIMENTAL vs. CALCULATED CONDUCTIVITIES FOR CORES WITH Qv>.1.....	52

6.1- COMPONENTS OF SP DEFLECTION..... 54

6.2- NEW SP MODEL..... 63

6.3- DETERMINATION OF R_w FROM SP MODEL..... 64

6.4- DETERMINATION OF Qv USING NEW SP MODEL... 65

7.1- COMPARISON OF CALCULATED Qv's vs. Qv's FROM SIMULTANEOUS SOLUTION..... 72

7.2- COMPARISON OF CALCULATED Qv's vs. Qv's FROM SIMULTANEOUS SOLUTION..... 73

7.3- COMPARISON OF CALCULATED Qv's vs. Qv's FROM SIMULTANEOUS SOLUTION..... 74

7.4- COMPARISON OF EXPERIMENTAL C_w's vs. C_w's FROM SIMULTANEOUS SOLUTION..... 75

7.5- COMPARISON OF MEASURED vs. CALCULATED C_w's

7.6- COMPARISON OF CALCULATED (LSU) vs. CHEMICALLY DETERMINED Qv's..... 76

8.1- CYBERLOOK FDC-CNL CROSSPLOT..... 81

8.2- FDC-CNL CROSSPLOT..... 87

8.3- RESISTIVITY LOGS - WELL A..... 90

8.4- POROSITY LOGS - WELL A..... 91

8.5- COMPARISON OF V_{sh} INDICATORS..... 92

8.6- S_w vs. DEPTH - WELL A..... 95

8.7- COMPARISON OF CYBERLOOK, ARCHIE AND LSU MODELS WELL - A..... 96

8.8- RESISTIVITY LOGS - WELL B..... 97

8.9- POROSITY LOGS - WELL B..... 98

8.10- COMPARISON OF CYBERLOOK, ARCHIE AND LSU MODELS
WELL - B..... 101
8.11- RESISTIVITY LOGS - WELL C..... 103
8.12- POROSITY LOGS - WELL C..... 104
8.13- RESISTIVITY LOGS - WELL D..... 105
8.14- POROSITY LOGS - WELL D..... 106
8.15- RESISTIVITY LOGS - WELL E..... 109
8.16- RESISTIVITY LOGS - WELL E..... 110
8.17- POROSITY LOGS - WELL E..... 111
8.18- POROSITY LOGS - WELL F..... 112

ABSTRACT

A new, theoretically derived model expressing shaly sand conductivity is presented. The proposed model is based on dual water and cation exchange capacity concepts.

The new model is based on the Waxman and Smits concept of supplementing the water conductivity with a clay counterions conductivity. The model also utilizes the dual water theory, which relates each conductivity term to a particular type of water, each occupying a specific volume of the total pore space.

The proposed model, however, assumes that the counterion conductivity can be represented by a hypothetical electrolyte. The properties of this electrolyte were derived from electrochemical and irreversible thermodynamics theory.

From the conductivity model a spontaneous potential model was also developed. Both models have been tested using accurate core data published by Waxman and Smits. The conductivity and spontaneous potential models were also validated by log data. They have been successfully applied to the interpretation of multiple intervals of 15 wells.

The use of these newly developed models is the first shaly sand interpretation technique based on sound scientific principles, which determines hydrocarbon potential as well as shale and formation water electrical properties directly from well logs readings obtained within the formation analyzed.

CHAPTER # 1

INTRODUCTION

In 1953 H. G. Doll[1] wrote, "the most important problem that has received thus far no satisfactory solution is that of shaly sands". Recently, in a comprehensive study on shaly-sand interpretation models published by Worthington[1], he stated, "Doll's comment is equally applicable today. The shaly sand problem as we know it will not be solved until electrical shale parameters, determined directly from downhole measurements can be input to a reliable and generally applicable predictive algorithm for S_w, that is based on a sound scientific shaly-sand model." A model comprising all these requirements has now been developed, and it is presented in this dissertation.

The main purpose of open hole well log interpretation is the identification of potential hydrocarbon bearing formations. The potential of a zone is measured by estimating its water saturation, S_w.

In shale-free formations, water saturation can be calculated using the well known Archie's formula:

$$S_w^n = \frac{C_t}{\phi^m C_w} = \frac{R_w}{\phi^m R_t} \qquad [1.1]$$

where:

C_t = conductivity of the reservoir rock

R_t = resistivity of the reservoir rock

C_w = formation water conductivity

R_w = formation water resistivity

ϕ = porosity

m = cementation exponent

n = saturation exponent.

Customarily, the water conductivity, R_w, is determined from the spontaneous potential (SP) log deflection, which in clean sandstones can be represented by[2]:

$$SP=-K\cdot\log(R_{mfe}/R_{we}) \qquad [1.2]$$

where K is a temperature dependent parameter. R_{mfe} and R_{we} are the equivalent mud filtrate and formation water resistivity, respectively. R_{mfe} and R_{we} are related empirically to the mud filtrate, R_{mf}, and formation water resistivity, R_w.
The conductivity and porosity of the rock are obtained from log measurements. The exponents m and n are usually determined from core analysis or approximated by generalized values.

Equations 1.1 and 1.2 are based on the assumption that brine is the only electric conductor in the formation. However, this is not the case in shaly formations, where counterions associated with clay minerals also transport electricity. This results in a reduction of the SP deflection, and an increase of the rock conductivity, C_t. Consequently, the use of clean sand models to estimate water saturation suppresses the potential of hydrocarbon zones. In some cases, hydrocarbon zones may even appear water bearing and can be

completely overlooked.

1.1 SHALY SAND MODELS:

Available shaly-sand models can be divided in two groups:

i) V_{sh} models: These models have the disadvantage of being inexact. They are open to misunderstanding and misuse.

ii) Models based on the cation excange and the ionic double-layer concepts. These models are based on sound principles. However, current models require laboratory determined core data which in the most part are determined at 25°C.

1.1.1. V_{sh} Models:

The quantity V_{sh} is defined as the volume of wetted shale per unit volume of reservoir rock. There are over 30 V_{sh} models[1], only the better known models will be presented hereafter:

Simandoux[1] reported experiments on homogeneous mixtures of sand and montmorillonite. Based on his experimental data he proposed the following expression:

$$C_t=(C_w \cdot S_w^n)/F + V_{sh} \cdot C_{sh} \qquad [1.3]$$

where:

F=formation factor

V_{sh}=fractional volume of shale

C_{sh}=conductivity of pure shale

Poupon and Leveaux[1] proposed the so called "Indonesia Formula":

$$C_t^{1/2}=(C_w \cdot S_w^n/F)^{1/2}+V_{sh}^{1-Vsh/2}(C_{sh} \cdot S_w^n)^{1/2} \qquad [1.4]$$

This formula was developed for use in Indonesia were fresh formation waters and high degrees of shaliness are common.

Fertl and Hammack presented a modified version of Simandoux equation. Their model can be written in the form[3]:

$$S_w=(F\cdot R_w/R_t)^{1/2}-(V_{sh}\cdot R_w)/(0.4\cdot\phi\cdot R_{sh}) \qquad [1.5]$$

where:

R_w=formation water resistivity, ohm/m

R_t=formation resistivity, ohm/m

R_{sh}=shale resistivity, ohm/m

The Cyberlook model[2] is a computer assisted wellsite interpretation model developed by Schlumberger. It uses pseudo-dual-water concepts to account for the effects of the shale fraction.

In the Cyberlook model, the resistivity of a water bearing shaly sand is given by[2]:

$$R_o=\frac{R_w\cdot R_{wb}}{\phi_t^2 S_{wb}\cdot R_w+(1-S_{wb})R_{wb}} \qquad [1.6]$$

where:

R_{wb}=bound water resistivity

S_{wb}=bound water saturation

The Cyberlook water saturation is given by:

$$S_w^n=R_o/R_t \qquad [1.7]$$

where:

R_o=resistivity of the shaly formation fully saturated with water.

In this model, ϕ_t, is derived from porosity crossplots, S_{wb} is obtained from traditional shale indicators. R_{wb} and R_w

must be determined by the field engineers and entered as input parameters. A more detailed presentation of the Cyberlook model is given in sec. 8.2.

V_{sh} models present serious interpretation problems. First, there is no universally accepted V_{sh} indicator. Furthermore, the V_{sh} parameter does not take account the mode of distribution or the composition of the different clay-types. Various clay types can give rise to markedly different shale effects for the same numerical shale fraction, V_{sh}.

The principal clay types are: kaolinite, montmorillonite/smectite, illite and chlorites. These clay minerals, because of their composition and structure, have an excess of negative charges. In the presence of an electrolyte, this excess of negative charge is compensated by the adsorption of cations on the clay surface. These cations are called counterions, and the clay property of exchanging cations is called cation exchange capacity (CEC).

Smectite and illite have high cation exchange capacities, while kaolinite and chlorite show small to zero CEC values. Table 1.1 lists the average CEC's of the different clay types

TABLE 1.1

PROPERTIES OF CLAY TYPES

Clay	Density (g/cc)	Hydrogen (%)	CEC (meq/cc)
Kaolinite	2.69	1.5	0.03
Illite	2.76	0.5	0.20
Smectite	2.33	0.5	1.00
Chlorite	2.77	1.2	0.00

One of the problems associated with V_{sh} models is their assumption that there is a correlation between the non-conductive (i.e. density, hydrogen content, and radioactivity) and the conductive (i.e. CEC) shale properties.

In addition, the V_{sh} models do not present a method for determining C_w from downhole measurements. For these reasons, improved models were sought which did take account of the geometry and electrochemistry of mineral-electrolyte interfaces, i.e., double layer models.

1.1.2 Cation Exchange Capacity Models:

Waxman and Smits[4] proposed a simple model, consisting of two conductance elements in parallel. One element represents the clay counterion contribution to the total conductance. The other element is the contribution of the free electrolyte. The Waxman-Smits model is given by the equation:

$$C_t = S_w^{n_e}[B \cdot Qv' + C_w]/F^* \qquad [1.8]$$

where:

C_t= rock conductivity

n_e= saturation exponent for shaly formations

B= empirically determined equivalent counterion conductivity

C_w= water conductivity

F^*= formation factor

and

S_w= water saturation

Qv' is defined as:

$$Qv'=Qv/S_w \qquad [1.9]$$

where:

Qv=cation exchange capacity.

Clavier, Coates and Dumanoir[5] proposed the Dual Water Model, which considers the presence of a double layer. This double layer is formed by: i) the water associated with the clay which is salt free, but contains all the necessary counterions, and ii) the electrolyte solution which is found at a distance away from the clay surface, and serves as the equilibrating media. The Dual Water Model is given by:

$$C_t=S_w^{ne}[\beta \cdot Qv'+(1-.28 \cdot \alpha \cdot Qv')C_w]/F_o \qquad [1.10]$$

where:

β= 2.05 (constant)

α= double layer's expansion factor

F_o= formation factor.

In 1985, Silva and Bassiouni[6] presented the S-B conductivity model. This model is based on dual water concepts. However, it considers that the counterion conductivity can be represented by that of an equivalent

sodium chloride solution. The general expression of this model is as follows:

$$C_t=S_w^{ne}[C_{eq}'\cdot Qv'+(1-v'_{fdl})C_w]/F_e \qquad [1.11]$$

where:

C_{eq}'= counterion conductivity

v'_{fdl}= fractional volume of the double layer

F_e= equivalent formation factor

The most severe restriction of the three forementioned models is that none of them can be applied at field conditions. All three, in their present form, represent the conductivity behavior of a shaly sand at 25°C. In fact, the Dual Water and Waxman and Smits models use empirically determined factors, namely, β and B respectively, to represent the clay conductivity, which cannot be used at higher temperatures. Moreover, they also require laboratory determination of Qv. This fact makes the use of these models impractical.

The S-B model is the more accurate of the models[6]. Furthermore, it uses a sodium chloride solution to represent the clay counterions. Since conductivity data for sodium chloride solutions are available at high temperatures, this model can be adapted to field conditions.

1.2 PROPOSED NEW MODEL:

The purpose of this study is to develop a sound method to evaluate shaly sand formations at field conditions. To pursue this objective, the basic idea of the S-B model, i.e.

counterions can be represented by a sodium chloride solution, is retained to model the conductivity behavior of shaly sands.

Silva and Bassiouni[7] have also presented a model predicting the membrane potential of shaly sands. In a water bearing zone, both models, i.e. the conductivity and membrane potential models, are expressed in terms of the cation exchange capacity of clays, Qv, and the free electrolyte conductivity, C_w. Hence, it is possible to solve simultaneously for these two parameters in a water zone. F_e can be calculated from porosity logs. This data can then be used to estimate the water saturation of an adjacent hydrocarbon bearing zone. If a representative adjacent water bearing zone is absent, an iterative process can be used to obtain S_w, C_w and Qv using data pertaining to the hydrocarbon zone only.

CHAPTER # 2

THE SILVA-BASSIOUNI MODELS

2.6 THE CONDUCTIVITY MODEL:

The presence of clay minerals in the formation increases its conductivity beyond that of an otherwise clean rock of the same porosity saturated with the same electrolyte. The excess conductivity is due to the transport of electric current by the counterions associated with clay minerals forming what is termed the double layer. The double layer contains the positive ions necessary to balance the internal negative charge of the clay particles. The determination of hydrocarbon saturation in shaly sands requires petrophysical models that account for the presence of the double layer.

Silva and Bassiouni[6] presented a theoretical model, which treats the "excess conductivity" generated by the counterions as that of an equivalent sodium chloride solution. The Silva-Bassiouni (S-B) model is based on the premise that the conductivity behavior of a shaly sand can be defined using an expression similar to that of a clean sand. According to this model the total conductivity of a core fully saturated with water is defined by[6]:

$$C_o = C_{we}/F_e \qquad [2.1]$$

where:

$$C_{we} = v_{fdl} \cdot C_{cl} + (1 - v_{fdl}) \cdot C_w \qquad [2.2]$$

C_{cl} and C_w are the conductivity contributions of the exchange cations associated with the clay, and the free electrolyte, respectively. V_{fdl} is the fractional volume occupied by the

double layer, expressed in terms of total porosity.

In electrochemical terms, the conductance contribution of the clay counterions can be defined by

$$C_{cl}=C_{eq}\cdot n_{eq} \qquad [2.3]$$

where C_{eq} and n_{eq} represent the equivalent conductivity and concentration of the clay counterions, respectively. By substituting equations 2.2 and 2.3 into equation 2.1 the conductivity of a core fully saturated with water is:

$$C_o=[C_{eq}\cdot n_{eq}\cdot v_{fdl}+(1-v_{fdl})C_w]/F_e \qquad [2.4]$$

where F_e is the formation factor of an equivalent clean formation of the same total porosity. F_e can be expressed as:

$$F_e=\phi^{-me} \qquad [2.5]$$

where m_e is the cementation exponent. Also n_{eq} can be expressed in terms of the counterion concentration per total pore volume, Qv, as

$$n_{eq}=Qv/v_{fdl} \qquad [2.6]$$

The S-B model given by equation 2.4 describes the typical C_o-C_w curve representative of shaly formations, illustrated in Fig. 2.1.

2.1.1 Determination of the fractional volume of the double layer, v_{fdl}:

The proposed use of the S-B model presented above requires the estimation of the fractional volume of the double layer, v_{fdl}, in terms of the unkowns C_w and Qv. This fractional volume is related to the distance from the clay surface up to

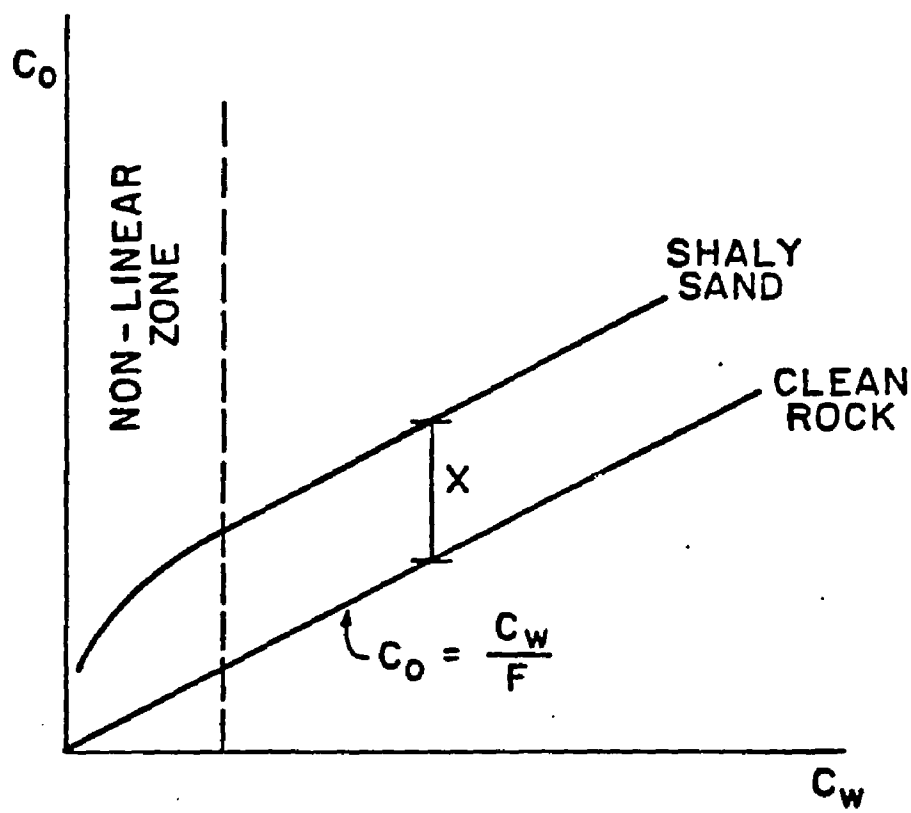

Fig. 2.1 Typical C_o-C_w Plot

the point where the number of positive ions are equal to the number of negative ions (Fig. 2.2). The volume of the double layer can be expressed by[8]:

$$v_{fdl}=0.084 \cdot Qv/C_w+0.22 \qquad [2.7]$$

2.1.2 Calculation of Equivalent Counterion Conductivity, C_{eq}:

The use of the S-B model requires also the estimation of the equivalent counterion conductivity. The model defines the concentrations and conductivity of the equivalent sodium chloride solution n_{eq} and C_{eq} as[3]:

$$n_{eq}=\frac{3.571}{(f_{dl}^{1/2}-.188)^2} \qquad [2.8]$$

$$C_{eq}=C_{eq}'/(fg \cdot F(ne)) \qquad [2.9]$$

where, C_{eq}' is the equivalent conductivity of the equivalent NaCl solution, representing the double layer. At a temperature of 25 degrees centigrade, C_{eq}', is expressed as:

$$C_{eq}'=\frac{12.645+7.6725(n_{eq})^{1/2}}{1+1.3164 \cdot n_{eq}} \qquad [2.10]$$

F(ne) and fg are empirically determined correction factors. At 25°C they are given by[3]:

$F(ne)=1+3.83\times10^{-2}(n_{eq}-.5)+1.761\times10^{-2}(n_{eq}-.5)^2$ for $n_{eq}>.5$ mol/l

$F(ne)=1.0$ for $n_{eq}\leq.5$ mol/l [2.11]

$$fg=f_{dl}^{1/nc} \qquad [2.12]$$

$$n_c=.6696+1.1796f_{dl}-0.14426f_{dl}^2 \qquad [2.13]$$

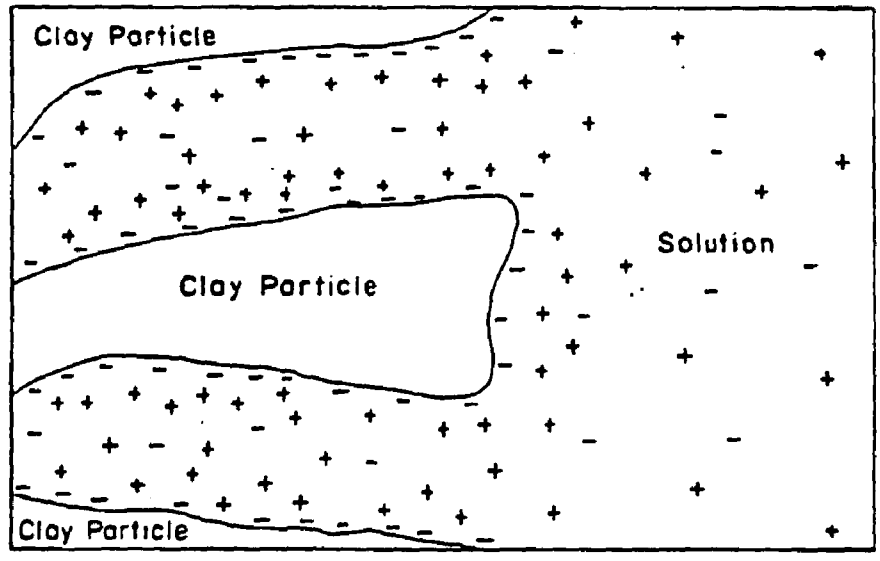

Fig. 2.2 Distribution of charges in the pore space

2.2 MEMBRANE POTENTIALS IN SHALY SANDS:

The general expression for the membrane potential, Em, reported by Thomas[9] is in the form:

$$Em=-\frac{2RT}{F}\int_{m2}^{m1} Tna^{+}d\ln(m\gamma\pm) \qquad [2.14]$$

where:

R=universal gas constant

F=Faraday constant

T=absolute temperature (°K)

Tna^{+}=sodium transport number

m=molal concentration (mol/kg H_2O)

$\gamma\pm$=mean activity coefficient

In the case of saturated salt solutions this form was found to give membrane potentials that deviate from experimental values. To account for this effect Silva and Bassiouni modified equation 2.14, by introducing a correction factor, τ.

Consequently, the model for membrane potentials is given by:

$$Em=-\frac{2RT}{F}\int_{m2}^{m1}\tau Tna^{+}d\ln(m\gamma\pm) \qquad [2.15]$$

where

$$\tau=1-.28Qv(C_w-C_{wn})/C_w \qquad \text{for } C_w>C_{wn} \qquad [2.16]$$

$$\tau=1 \qquad \text{for } C_w\leq C_{wn} \qquad [2.17]$$

and

C_{wn}=16.61 mho/m at 25°C

2.2.1 Transport Numbers in Shaly Sands:

Transport numbers are defined as the ratio of the electrical current carried by an ion to the total electrical current, when an electrical potential difference is applied under conditions where pressure and concentration gradients are both zero[14].

In the case of shaly sands the S-B model[7] assumes that the current carried by the clay counterions is parallel to the current carried by the far water, and that both currents are related to the same potential gradient by the same cell constant. It is assumed that both electrolytes can be treated as NaCl solutions. Hence, the transport number is defined as follows,

$$Tna^{+}=(J_{Na}{}^{c}+J_{Na}{}^{b})/J \qquad [2.18]$$

where:

$J_{Na}{}^{c}$ is the current carried by the clay counterions

$J_{Na}{}^{b}$ is the current carried by the far water

J is the total current of the system.

According to the S-B model:

$$Tna^{+}=\frac{C_{eq}\cdot Qv+tna^{h}\cdot(1-v_{fdl})\cdot C_{w}}{C_{eq}\cdot Qv+(1-v_{fdl})\cdot C_{w}} \qquad [2.19]$$

tna^{h} is the sodium's Hittorf transport number. Hittorf defines, for convenience, the motion of ions relative to that of water.

2.2.2 Calculation of the Mean Activity Coefficient:

For sodium chloride solutions at 25°C the mean activity coefficient can be defined by:

$$\log(\gamma\pm)=\frac{-.05115\cdot n^{1/2}}{1+1.3065\cdot n^{1/2}}-1.75\log(a_A)-\log(1-.027m) \qquad [2.20]$$

where:

n=molar concentration (mol/l)

$$a_A=.99948-.03959m-.0015075m^2 \qquad [2.21]$$

2.2.3 Calculation of the Hittorf Transport Number, tna^h:

Based on the Fouss-Onsager theory of conductance, Stokes derived a theoretical expression to approximate the Hittorf transport number. For NaCl solutions at 25°C tna^h expression is expressed as[11]:

$$tna^h=\frac{50.1+55.402\cdot n^{1/2}}{126.45+155.726\cdot n^{1/2}} \qquad [2.22]$$

where n is the molar concentration of the far water.

2.2.4 Calculation of the Membrane Potential:

The equation of membrane potentials can be solved as Thomas[9] suggested. First, the concentration interval between the electrolytes is divided into 100 subintervals. The magnitudes of C_{eq}, v_{fdl}, tna^h, $\pm$, and C_w are evaluated for each molal concentration subinterval, and each Tna^+ is computed. The 100 subintervals are evaluated and summed. The result is then multiplied by -51.38, which is the value of -2RT/F at 25°C. The final result is then taken as the magnitude of the membrane potential.

2.3 CRITIQUE OF THE S-B MODELS:

The S-B models accurately describe the resistivity behavior and membrane potential of a shaly sand. However, the application of the models require the use of empirically determined parameters, namely, fg, F(ne) and τ, which in their present form can not be practically adapted to high temperature applications. This fact complicates the use of the models at field conditions.

CHAPTER # 3

THE LSU SHALY-SAND MODELS

The S-B model is modified to eliminate the use of empirically derived correction factors. This elimination permits the extension of the model to temperatures other than 25°C. Every modification was based on electrochemical properties of NaCl solutions, or experimental observations. The modified model is referred to as the LSU model. The accuracy of the S-B model was maintained or improved.

3.1 THE LSU CONDUCTIVITY MODEL:

The conductivity of a shaly formation fully saturated with water is defined according the S-B model as:

$$C_o=[v_{fdl}C_{cl}+(1-v_{fdl})\cdot C_w]/F_e \qquad [3.1]$$

where F_e is the shaly sand formation resistivity factor, and v_{fdl} is the fractional volume of the double layer. Eq. 3.1 can be rewritten in terms of molar conductivities as:

$$C_o=[C_{eq}\cdot n_{eq}\cdot v_{fdl}+(1-v_{fdl})\cdot C_w]/F_e \qquad [3.2]$$

where C_{eq} and n_{eq} are the molar counterion conductivity and concentration, respectively. From equation 3.2, it can be observed that the LSU model uses a very basic formulation, and unlike the S-B model it does not assume that:

$$n_{eq}=Qv/v_{fdl} \qquad [2.6]$$

The counterion concentration, instead, is directly determined from published experimental data.

3.1.1 Determination of the Equivalent Counterion Conductivity, C_{eq}:

The S-B model assumes that the clay counterions mimic the conductive properties of a sodium chloride solution. Hence, well known electrochemical relationships can be used to define C_{eq}.

According to electrochemistry theory of 1-1 electrolytes the equivalent conductivity, C_{eq}, is proportional to the total current in the system. For molar concentrations of less than .5 mol/l, C_{eq} can be defined by[3]:

$$C_{eq} = C_{eq}^{\circ} - \frac{B_2 n^{1/2}}{1+Bo \cdot a \cdot n^{1/2}} \qquad [3.3]$$

where:

C_{eq}°= equivalent conductivity at infinite dilution (mho/mol)

B_2= electrophoretic term

n= molar concentration (mol/l)

a= equivalent ion size (Å)

For sodium chloride solutions at 25°C equation 3.3 can be rewritten as[6]:

$$C_{eq} = \frac{12.645+7.6725 n_{eq}^{1/2}}{1+1.3164 n_{eq}^{1/2}} \qquad [3.4]$$

This relationship is valid in dilute aqueous electrolyte solutions, where the ions are so far apart that ionic interactions and specific ion effects are negligible. In concentrated solutions, however, specific ion effects become

important. Hence, the flow of ions is influenced by the presence of other ions and the rate of change of their properties as well[12]. The original S-B model utilizes the empirically determined factor, F(ne), to correct equation 3.4 for the ionic interactions occurring at moderate and high concentrations.

The LSU model uses the theory of irreversible thermodynamics to define the equivalent conductance of an 1-1 electrolyte at moderate and high concentrations. By assuming that the clay counterions behave as a sodium chloride solution C_{eq} can be defined by[12]:

$$C_{eq}=F^2(l_{33}+l_{44}-2l_{34})/n_{eq} \qquad [3.5]$$

where F is the Faraday constant and l_{ij} are the ionic transport coefficients. These ionic transport coefficients represent relatively complex functions of mobilities of ions and of water. The transport coefficients, l_{33} and l_{44} represent the ionic mobilities and the gradient of properties of the Na^+ and Cl^-, respectively. The l_{34} coefficients represent the ionic interactions that occur at moderate and high concentrations. To obtain quantitative expressions for the transport coefficients four properties of the electrolyte under investigation are needed, namely, conductance, diffusion coefficient, Hittorf transport number, and emf transference number. Carman[13] defined the transport coefficients as:

$$l_{33}=(q_3)\cdot n_{eq} \qquad [3.6]$$

$$l_{44}=(q_4)\cdot n_{eq} \qquad [3.7]$$

and

$$l_{34}=n_{eq}\cdot\beta/2 \qquad [3.8]$$

Substituting equations 3.6, 3.7 and 3.8 in 3.5 yields:

$$C_{eq}=F^2(q_3+q_4-2\cdot\beta) \qquad [3.9]$$

Data on conductance, diffusion coefficients, Hittorf transport numbers and emf transference numbers for sodium chloride solutions compiled by Miller[12] was used to determined the values of the ionic transport coefficients, which in turn was used to obtain q_3, q_4 and β, listed in table 3.1

Table 3.1

n_{eq}	$q_3 x10^9$	$q_4 x10^9$	$\beta x10^9$
0.5	5.16	7.46	1.28
1.0	4.96	7.15	1.46
1.5	4.75	6.75	1.50
2.0	4.55	6.50	1.52
2.5	4.35	6.15	1.50
3.0	4.15	5.80	1.46
4.0	3.75	5.04	1.32
5.0	3.37	4.31	1.18

These values were curve fitted using regression analysis. As seen from Fig 3.1, q_3, q_4, β and can be represented by the following equations:

$$q_3 x10^9=-.3989n_{eq}+5.35 \qquad [3.10]$$

$$q_4 x10^9=-.699n_{eq}+7.849 \qquad [3.11]$$

$$\beta x10^9=-.00326n_{eq}^4+.05n_{eq}^3-.3n_{eq}^2+.68n_{eq}+1.014 \qquad [3.12]$$

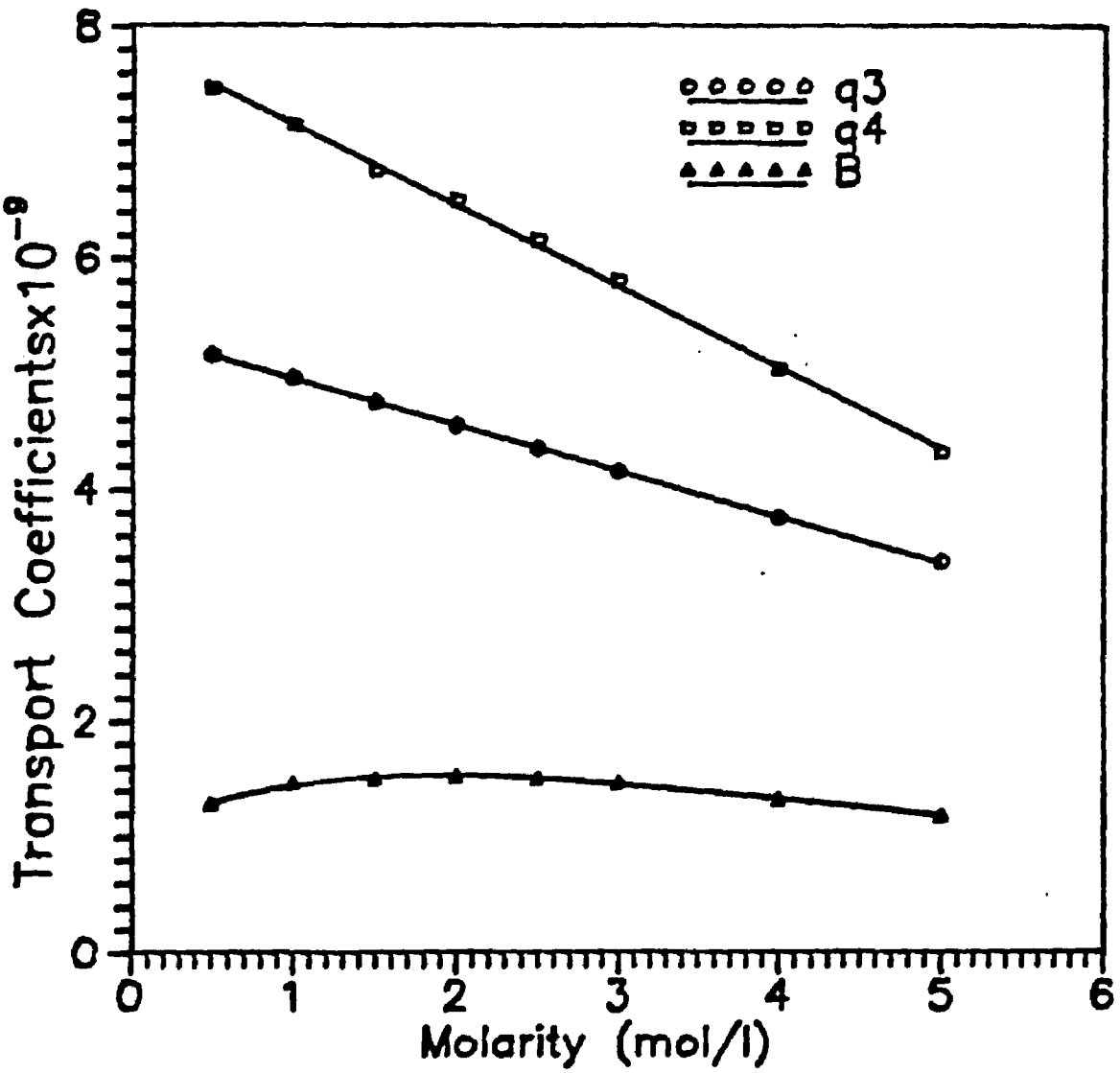

Fig. 3.1 Transport coefficients vs. free electrolyte concentrations

3.1.2 Determination of Counterion Concentration, n_{eq}:

Another main modification to the original S-B model is the calculation of n_{eq}. The S-B model assumes that the counterion concentration can be represented by:

$$n_{eq}=3.5714/(f_{dl}^{1/2}-.188)^2 \qquad [2.8]$$

which implies that n_{eq} is independent of Qv, and only a function of the free electrolyte concentration. This assumption necessitated the introduction of the empirically determined factor 'fg' to improve the quality of curve fitting. The LSU model assumes instead, that the counterion concentration is a function of both Qv and the free electrolyte concentration. This assumption eliminated the need for correction factors. This fact is supported by the experimental data published by Waxman and Smits[4].

If the core conductivity, C_o, is known the magnitude of the equivalent counterion conductivity can be calculated from equation 3.2. The data published by Waxman and Smits[12] was used to determine $n_{eq,}$ and the results are presented in Fig. 3.2, and appendix A. From figure 3.2 it can be observed that n_{eq} is a function of Qv and far water concentration, n. N_{eq} increases with Qv and n but as any other solution the bound water reaches a saturation point. Saturation is reached at a value n_{eq} dependent on n as shown by the following Table 3.2:

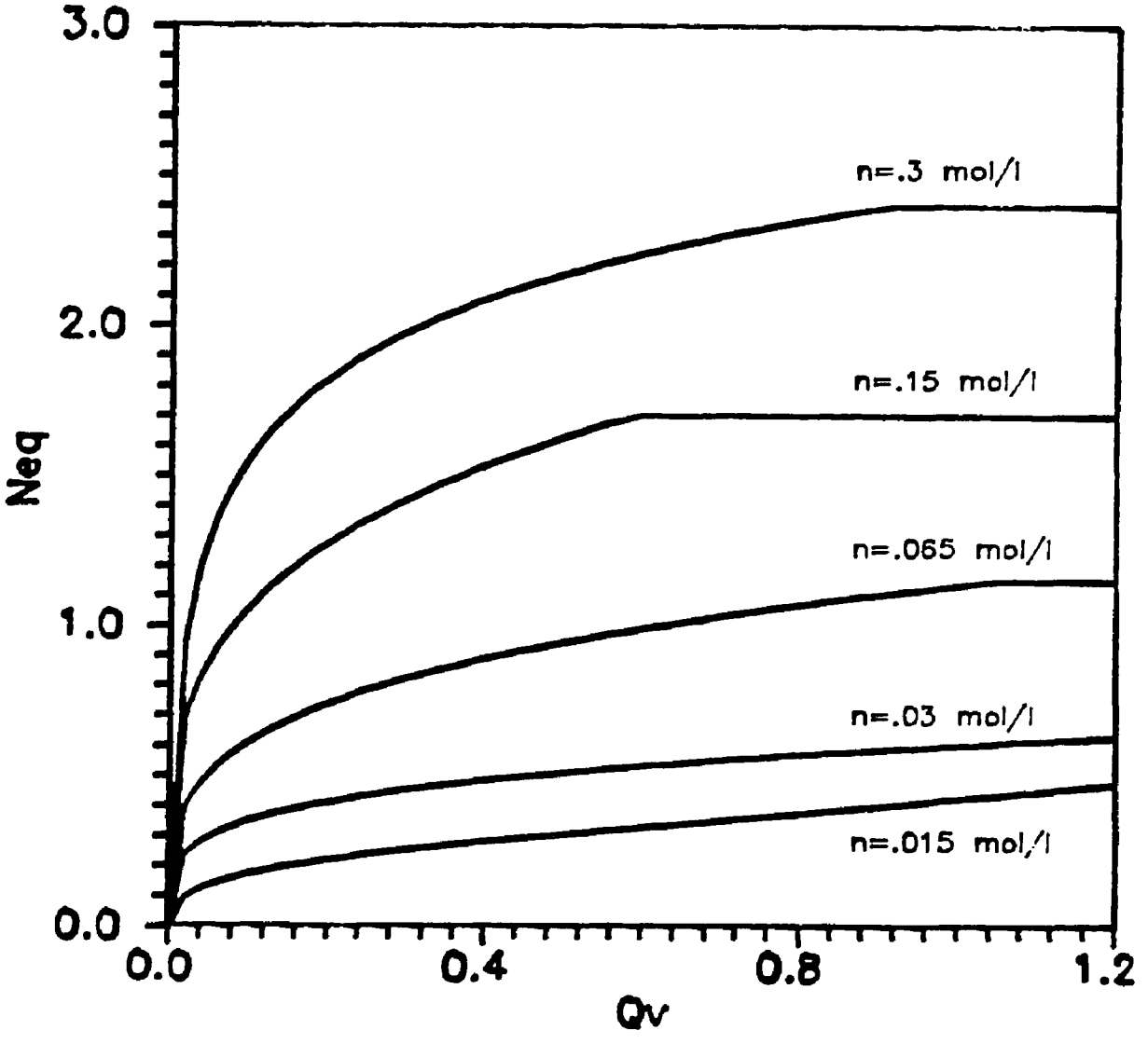

Fig. 3.2 Determination of Neq

Table 3.2

n mol/l	n_{eq} @ sat. mol/l	Qv @ sat. meq/l
.015	0.50	1.20
.030	0.60	1.20
.065	1.20	1.04
.150	1.70	0.60
.300	2.40	0.76

At concencentrations higher than .3 mol/lt the straight line portion of the C_o-C_w plot is reached, at this molarity and at a Qv=.76 meq/l, the highest possible counterion concentration, n_{eq}= 2.40 mol/l, is attained.

3.1.3 Estimation of the Fractional Volume Occupied by the Double Layer, v_{fdl}:

The fractional volume of the double layer , v_{fdl}, can be expressed by the following relationship derived by Clavier et al.[5]

$$v_{fdl}=.28\cdot f_{dl}\cdot Qv \qquad [3.13]$$

The parameter f_{dl} is known as the double layer expansion factor and is given by[6]:

$$f_{dl}=(X_h^2\cdot Bo^2\cdot n)^{-1/2} \qquad [3.14]$$

X_h was determined by Clavier et al.[5] to be 6.18Å, and Bo can be calculated using the following polynomial[3]:

$$Bo=.3248+1.5108x10^{-4}T+8.935x10^{-7}T^2 \qquad [3.15]$$

The far water concentration, n, can be calculated from the conductivity data published by Miller[12], see Fig.3.3:

for C_w<10 mho/m

$$n=-2.81x10^{-5}C_w^3+.003C_w^2+.0931C_w \qquad [3.16a]$$

for $C_w \geq 10$ mho/m

$$n=8.63x10^{-5}C_w^4-.0046C_w^3+.0915C_w^2-.63C_w+2.052 \qquad [3.16b]$$

The use of two equations to determine 'n' as a function of C_w improves the accuracy of the results at low electrolyte concentrations.

3.1.4 Prediction of Core Conductivities:

In order to evaluate the validity of the modified model, the Waxman and Smits[4] (group 2) data was used as reference for this study. The petrophysical parameters Qv and F_e were obtained from Silva[3]. The C_o-C_w plots for the 27 cores are presented in Appendix B. A good agreement between the calculated and experimental values can be observed, see Fig. 3.4.

3.1.5 Conductivities of cores with Qv≤.1 meq/cc:

It was observed from the experimental data gathered by Waxman and Smits[4], that cores with Qv≤0.1 did not display the curved portion of the C_o-C_w plot, see Appendix B. Hence, for practical purposes, it is possible to use the clean sand model in such cases.

The validity of this assumption can be verified by applying the clean sand model to cores 1 and 2. Fig 3.5 shows

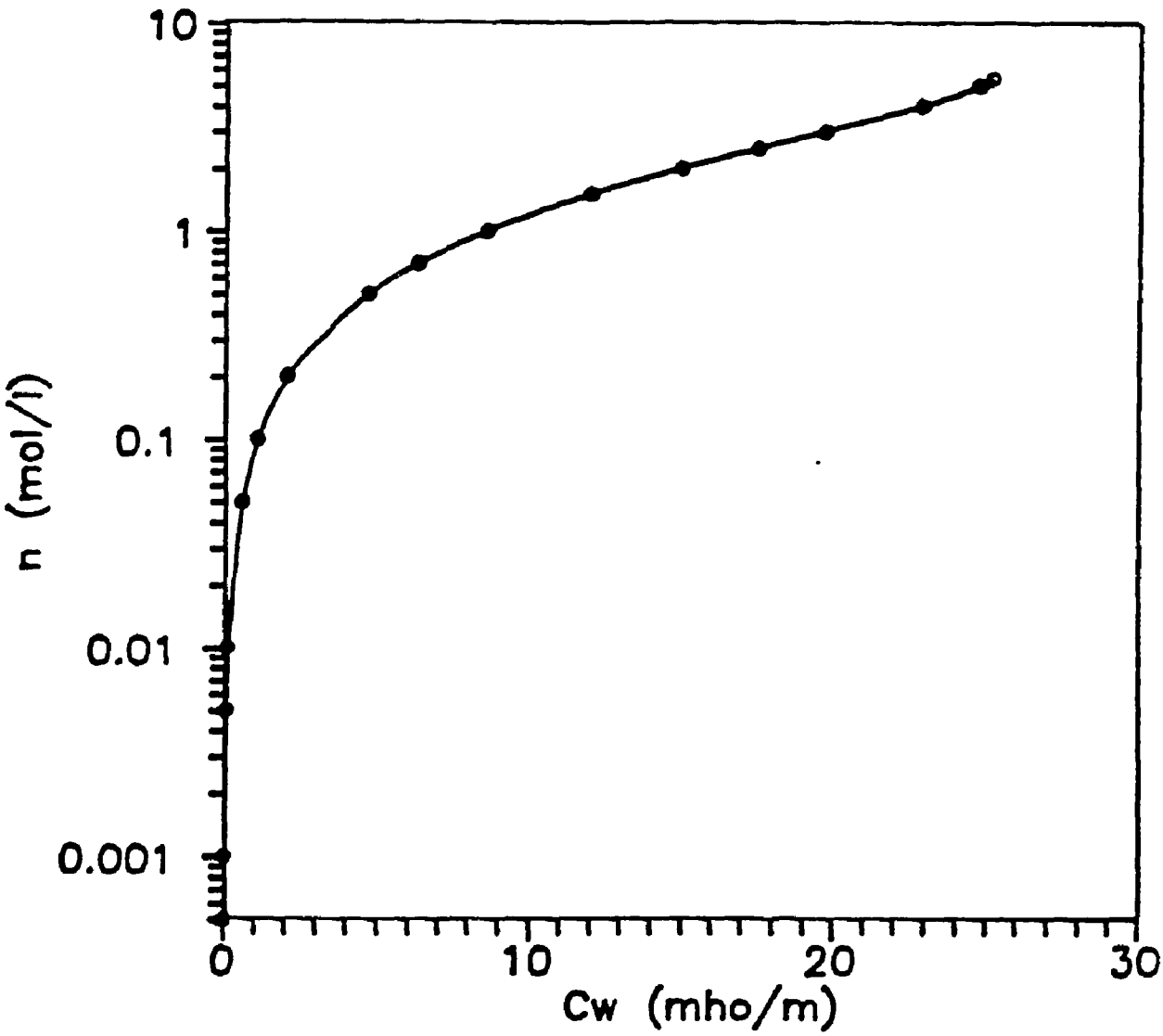

Fig. 3.3 Determination of free electrolyte concentration

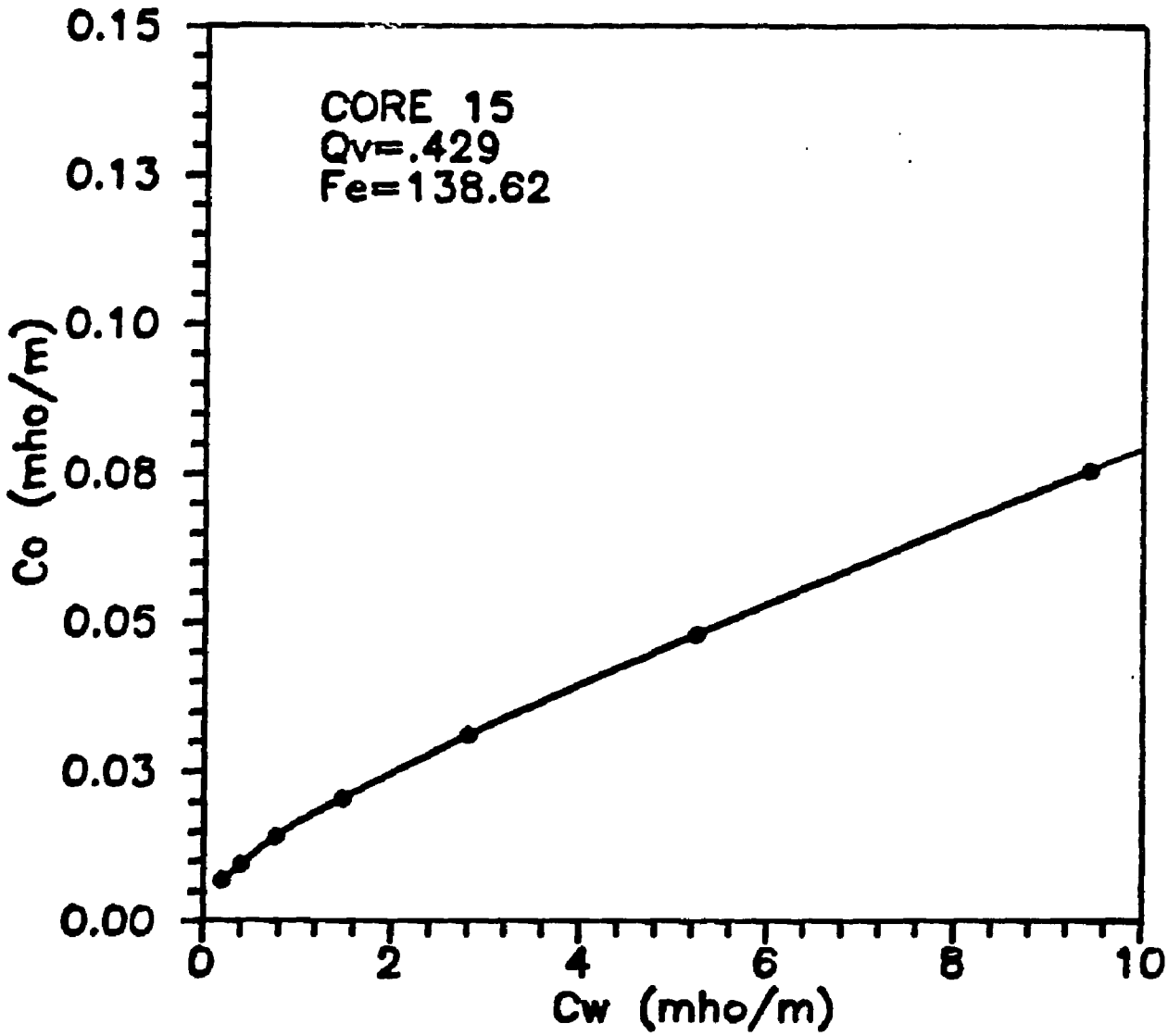

Fig. 3.4 Comparison of calculated vs. experimental core conductivities

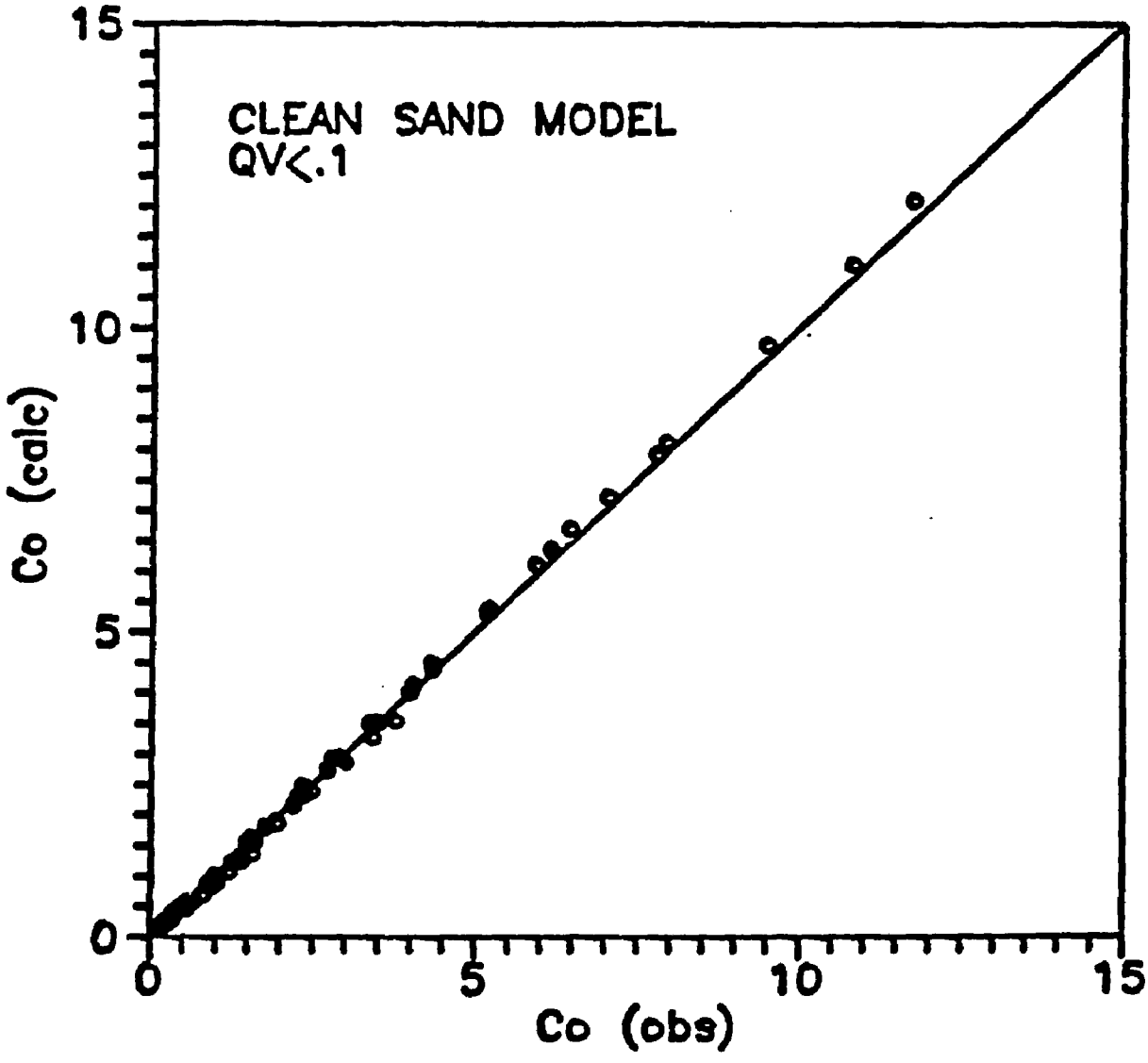

Fig. 3.5 Comparison of calculated vs. experimental conductivities for cores with Qv<.1

the good agreement between the calculated and experimental conductivity data.

3.2 MEMBRANE POTENTIAL MODEL:

The basic expression for the membrane potential, Em, in shaly sands was obtained by Smits[14], and reported by Thomas[9] in the form:

$$Em=\frac{-2RT}{F}\int_{m2}^{m1} Tna^{+}\,d\ln(m\gamma\pm) \qquad [2.14]$$

where, m1 and m2 are the molal concentration of the solution separated by the membrane.

Tna^{+} = the cation transport number of the membrane

R = gas constant

T = Absolute temperature (°K)

F = Faraday Constant

$\gamma\pm$ = mean activity coefficient of the electrolyte.

Using the LSU model Eq. 2.14 becomes:

$$Em=\frac{-2RT}{F}\int_{m2}^{m1}\frac{C_{eq}\cdot n_{eq}\cdot v_{fdl}+tna^{+}(1-v_{fdl})\cdot C_{w}}{C_{eq}\cdot n_{eq}\cdot v_{fdl}+(1-v_{fdl})C_{w}}\,d\ln(m\gamma\pm) \qquad [3.17]$$

where tna^{+} is the transport number of the electrolyte corrected for the transport of water.

The calculation of C_{eq}, n_{eq}, and v_{fdl} have been presented in the previous sections of this chapter. The mean activity coefficient can be calculated using Eq. 2.20. The calculation of tna^{+} is detailed hereafter.

3.2.1 Calculation of the NaCl Transport Number, tna^{+}:

Transport numbers are a function of the mobilities of the

ions of an electrolyte[15]. This quantity is therefore not a characteristic of an isolated ion, but of an ion in a given electrolyte.

Stokes derived a relationship for the Hittorf transport number of NaCl solutions at 25°C[7]

$$tna^h = \frac{50.1+55.402n^{1/2}}{126.45+155726n^{1/2}} \qquad [2.22]$$

which is based on the Fouss-Onsager theory of conductance, and the Debye-Hückel theory. Nevertheless, it is now common knowledge that above 0.3 mol/l the Debye-Hückel model is inadequate to correctly describe the nature and behavior of the ionic transport process[16]. This fact was neglected by the original S-B model.

In this study, to obtain the Hittorf transport number at concentrations greater than 0.3 mol/l, experimental data from several sources were gathered and analyzed. Currie and Gordon[17] have used an "adjusted indicator technique" to measure tna^h up to 2.5 mol/kg. However, in the evaluation of the data no volume correction was applied. The data were later re-evaluated by Miller[12] and Smits and Durvis[18]. Della Monica et al.[16] have measured tna^h up to 5.6 mol/kg, whereas Urban[19] reported values at .5 mol/kg and.75 mol/kg. The data of Caramazza[20] extended to 5 mol/kg, while the data of Smits and Durvis include a value near saturation, i.e. 6.144 mol/kg.

The data reported by Caramazza[20], Currie and Gordon[17], Miller[12], and Della Monica et al.[16] are in excellent agreement, and will be used in this study to obtain tna^+. This data are

reported in Table 3.2. The data by Smits and Durvis diverge from that of previous authors at concentrations higher than 1 mol/kg, as seen in Fig. 3.6. Consequently, it is concluded that the data by Smits and Durvis is in error and was discarded.

The values of Table 3.2 were curve fitted for concentrations between 0.25 and 4. mol/kg, and the following expression was obtained:

$$tna^h = -.009 \ln(n) + .366 \qquad [3.18]$$

In this expression n represents the molar concentration of the electrolyte solution.

Table 3.2

Hittorf Transport Numbers in Aqueous NaCl Solutions at 25°C

m	tna^h	m	tna^h
.25	.379	2.50	.358
.50	.372	2.75	.357
.75	.369	3.00	.356
1.00	.366	3.50	.354
1.25	.364	4.00	.353
1.50	.363	4.50	.353
1.75	.362	5.00	.353
2.00	.360	5.50	.352
2.25	.359	6.00	.352

Notice that tna^h remains unchanged for molalities greater than 4 mol/kg, which implies that the transport of current cannot be improved by adding more salt at concentrations greater than

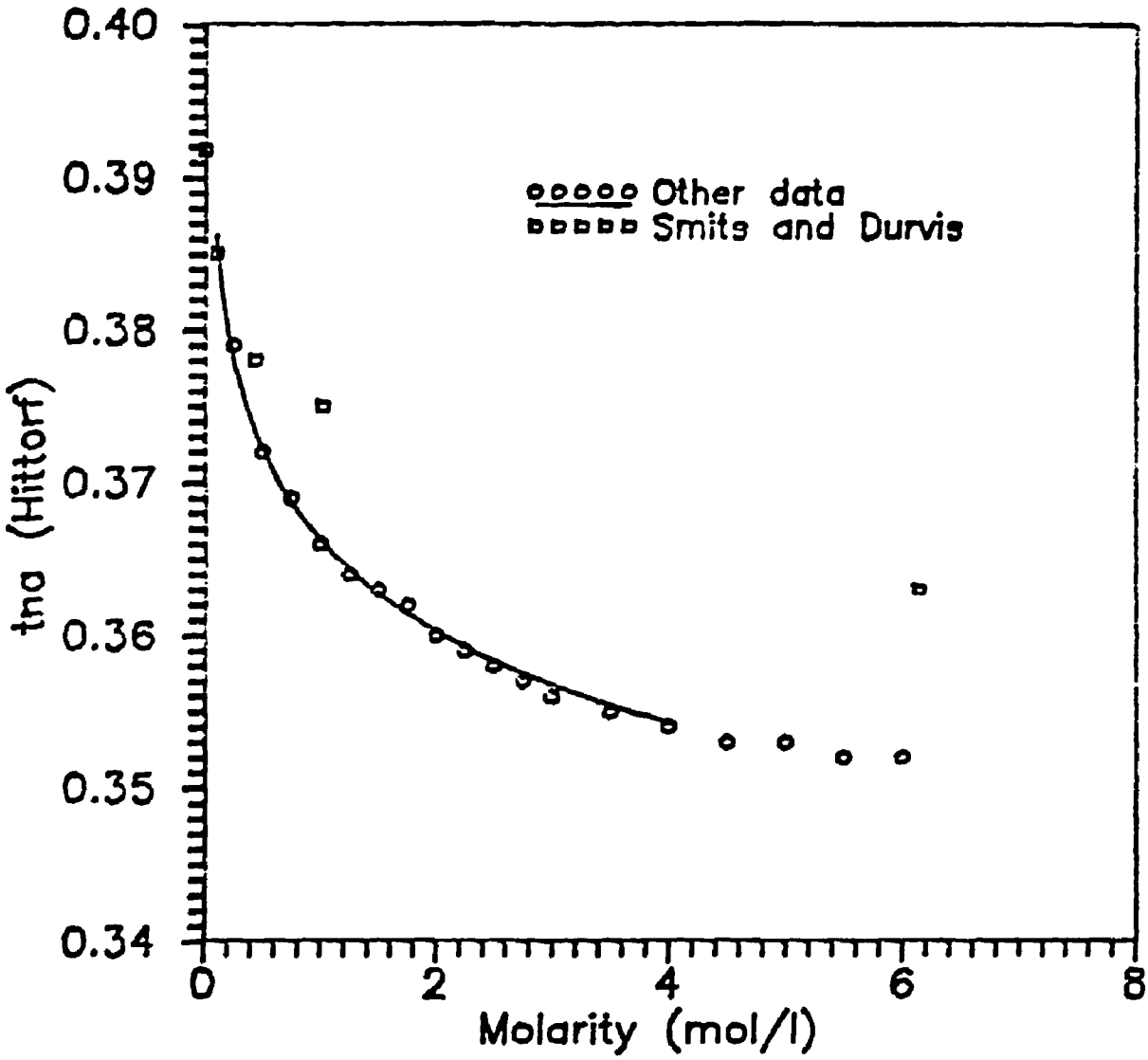

Fig. 3.6 Data Published on the Hittorf Transport number of NaCl solutions

4 mol/kg.

3.2.1.1 The Water Transport Number, tw:

Smits[14] and Silva[7] acknowledged that the introduction of the water transport number in the membrane potential calculations would improve the accuracy of their models. However, it is yet to be formally introduced by any author. The LSU model introduces, hereafter, the water transport number, tw, for shaly sand formations.

It is well known that the Hittorf transport number represents the correct transport number only when the ions are not hydrated in the aqueous solution, which occurs at moderate and high concentrations[7,14]. From the experimental membrane potential data presented by Smits[14], it was determined that the sodium ions become hydrated at concentrations higher than 0.1 mol/l. At this concentration the LSU model defines the sodium transport number, tna^+ by:

$$tna^+=tna^h+tw \qquad [3.19]$$

The water transport number, tw, for shaly sands was derived using published membrane potential values[14]. The sodium transport number, tna^+, can be determined by trial and error using Eq. 3.17, and if the Hittorf transport number is calculated, it is possible to obtain the water transport number by rearranging Eq. 3.19:

$$tw=tna^+-tna^h \qquad [3.20]$$

The water transport number could be positive or negative[21]. If water is transported to the cathode tw>0, while

if water is transported to the anode tw<0. This implies that at dilute and moderate concentrations only the Na^+ ions travel across the membrane. At higher concentrations, however, the membrane is no longer permselective and some Cl^- ions can also travel through it. Hence, depending on the electrolyte concentration both Na^+ and Cl^- ions can transport water molecules. At dilute concentrations most water molecules are transported to the cathode attached to the sodium ions, while at higher concentrations the water molecules can also be transported to the anode by the Cl^- ions, hence, at higher concentrations the water transport number becomes negative because anions and cations carry water in opposite directions. Some preliminary measurements by Trivijitkasem[21] show that the concentration of anions in some cation exchange membranes increases from 1% of the total ion exchange capacity at a normality of 0.01 eq/l to 5% at a normality of 0.1 eq/l. This is in agreement with the observations made by Wills and Lightfoot and the theoretical considerations of Glueckauf[21].

The LSU model presents tw as a function of the bound and far water concentrations, which implies a diffusion of counterions from the double layer to the pore space occupied by the free electrolyte. Consequently, the water transport number, tw, can be written as a function of Qv and free water molar concentration ,n:

$$tw=t_{fw}\cdot Qv \qquad [3.21]$$

where

$$t_{fw}=-.07\ln(n)+.98 \qquad \text{for } n<.7 \qquad [3.22a]$$

$$t_{fw}=-.006n^3-.052n^2-.1626n+.2051 \quad \text{for } n\geq .7 \qquad [3.22b]$$

or as in terms of molality:

For $m\leq 1.0$

$$tw=0.053m-0.43+(0.196\ln(m)+.1244)\cdot Qv \qquad [3.23]$$

For $m>1.0$

$$tw=0.036m^{1.1}-0.04377+.04Qv \qquad [3.24]$$

Figure 3.7 shows the values for t_{fw}. Only two data points were used to determine t_{fw} at higher concentrations. More experimental measurements in this range might improve the accuracy of Eq. 3.18b. Fig. 3.7 also shows that for shaly sands tw decreases with increasing salt concentrations, which is in agreement with the results reported by Trivijitkasem[21]. At high concentrations, $n>4.6$, it is apparent that the hydrated anions reverse directions, traveling from the anode to the cathode. Hence, the water transport number becomes negative.

3.2.2 Solution of the Membrane Potential Equation:

Equation 3.15 can be solved using the same procedure presented in Section 2.1.8. The final results are presented in Appendix C. A good agreement was observed between the calculated and experimental data (Fig. 3.8).

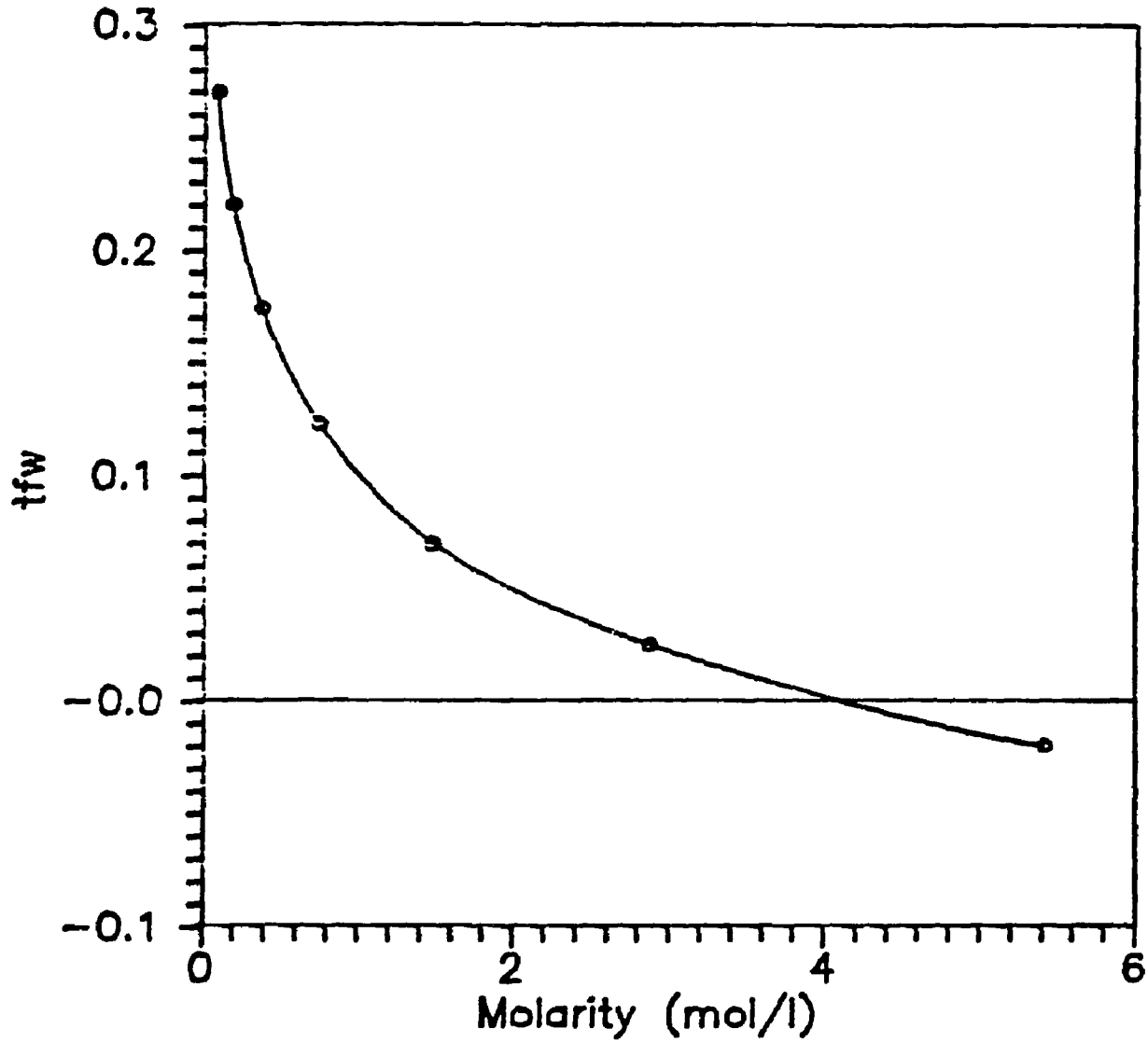

Fig. 3.7 Determination of t_{fw}

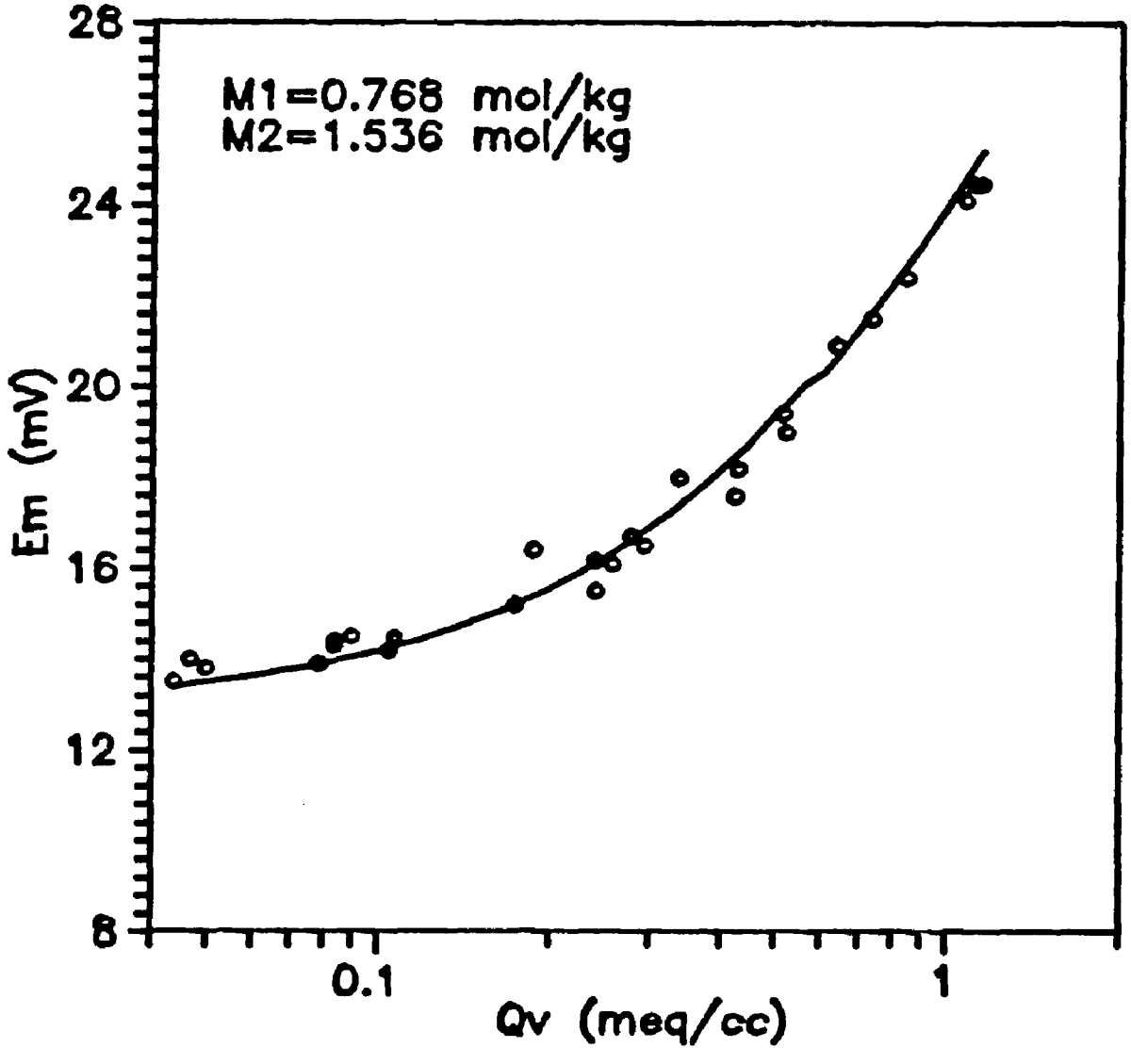

Fig. 3.8 Comparison of experimental and calculated core membrane potentials

CHAPTER # 4

THE LSU MODEL IN HYDROCARBON-BEARING SHALY SANDS

The next step in the development of the LSU model is to test its applicability to hydrocarbon-bearing formations. The model assumes: i) a parallel conductance for the free electrolyte and the bound water, ii) the bound water can be represented by an equivalent sodium chloride solution, iii) the same formation factor affects the conductivity contributions of the free electrolyte and bound water, iv) if hydrocarbons are present, they will preferentially displace the free electrolyte, and v) it is also assumed that when the water saturation, S_w, is less than unity, the exchange cations associated with the clay, Qv, become more concentrated in the pore space[23]. This concentration Qv' is related to Qv and S_w by:

$$Qv'=Qv/S_w \qquad [4.1]$$

In accordance with Archie's model, the conductivity of a hydrocarbon-bearing shaly sand, C_{hsd}, can be expressed as:

$$C_{hsd}=S_w^{ne}\cdot C_{we}'/F_e \qquad [4.2]$$

where:

S_w = total water saturation

n_e = saturation exponent

C_{we}' = equivalent water conductivity

According to the LSU model C_{we}' is defined by:

$$C_{we}' = C_{eq}' \cdot n_{eq}' \cdot v_{fdl}' + (1 - v_{fdl}') \cdot C_w \qquad [4.3]$$

where:

$$v_{fdl}' = .28 \cdot f_{dl} \cdot Qv / S_w \qquad [4.4]$$

The equivalent counterion concentration, n_{eq}', can be obtained from Fig. 3.2 by entering the corresponding Qv' and free electrolyte concentration. Lastly, the equivalent counterion conductance, C_{eq}', can be computed using:

for $n<0.5$

$$C_{eq}' = \frac{12.645 + 7.6725 \cdot n_{eq}'^{1/2}}{1 + 1.3164 \cdot n_{eq}'^{1/2}} \qquad [3.4]$$

for $n \geq 0.5$

$$C_{eq}' = F^2 (q_3 + q_4 - 2\beta) \qquad [3.9]$$

A detailed discussion of Eqs. 3.4 and 3.9 was presented in Section 3.1.1.

To test the reliability of Eq. 4.2, the data obtained by Waxman and Thomas[23], at room temperature was used as reference. This data is presented in Appendix D. The data cover a wide range of water salinities, hence, the validity of the saturation equation can be evaluated with confidence. By assuming that n=m Eq. 4.2 was applied to all the data gathered, the results are reported in Appendix E. The good agreement between experimental and calculated values attest for the reliability of the model, see Fig. 4.1.

One of the purposes of well log evaluation is the determination of water saturation for a given formation. Using the LSU model this can be done by rearranging Eq. 4.2:

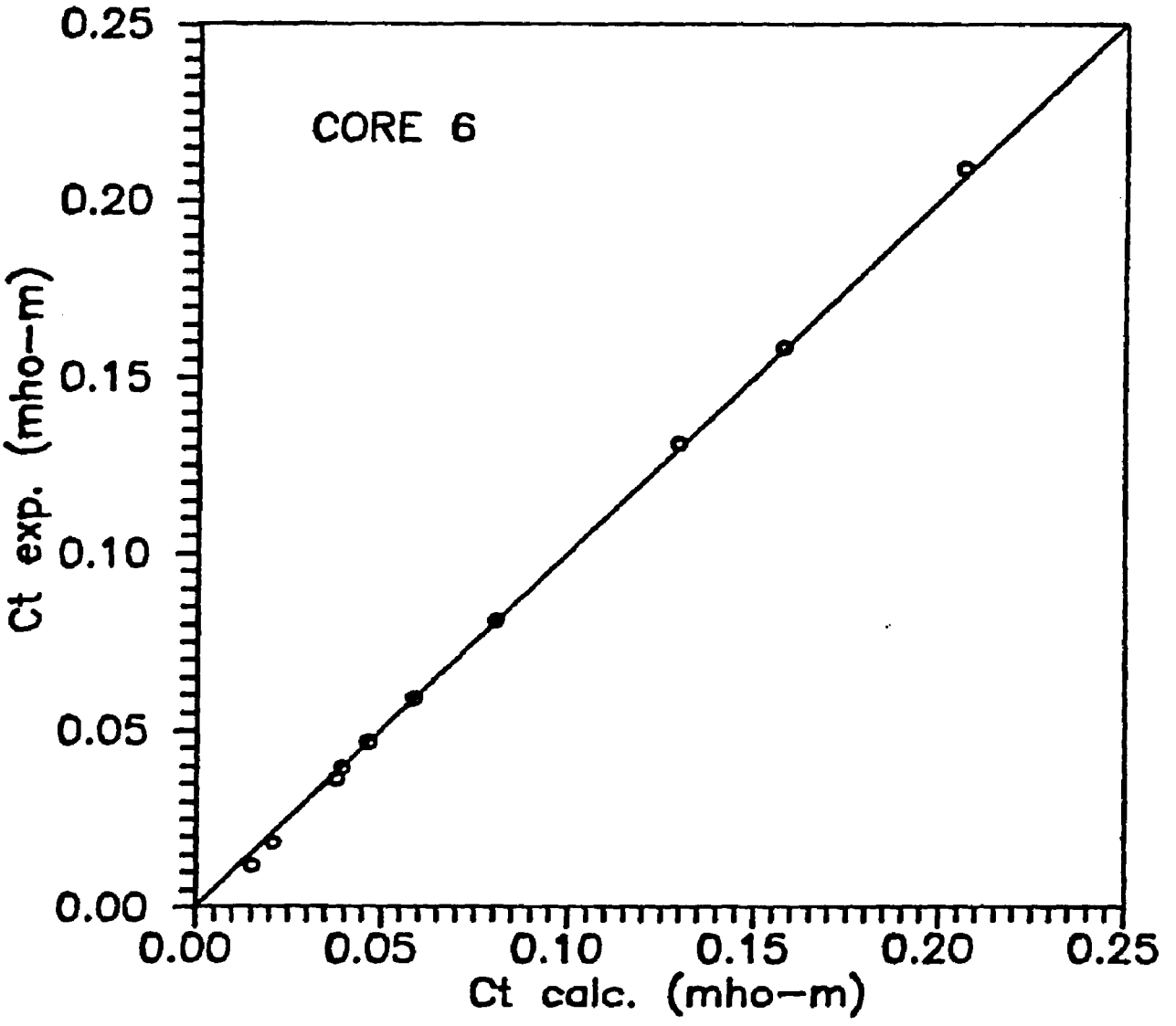

Fig. 4.1 Comparison of experimental Ct versus calculated Ct

$$S_w^{ne} = C_{hsd} \cdot F_e / C_{we}' \qquad [4.5]$$

Unfortunately, C_{we}' is also a function of S_w, and since neq cannot be represented by a unique formulation, a trial and error procedure is required to solve for S_w. However, the use of personal computers makes this calculation an easy task.

The use of Eq. 4.5 to calculate S_w requires the knowledge of C_{hsd}, C_w, F_e, Qv, C_{eq}', v_{fdl}', and n_{eq}'. The parameters C_{hsd} and C_w can be derived from well logs. Currently, the values for Qv and F_e must be determined from special core analysis. The calculation of C_{eq}', v_{fdl}', and n_{eq}' was discussed previously in this chapter. In the case of the saturation exponent, n_e, Silva[3] determined that for practical purposes n=m. Using this assumption S_w values were calculated from the Waxman and Thomas data set, Fig. 4.2. The good agreement between the observed and calculated values shows that the LSU model can be used to interpret resistivity measurements in hydrocarbon bearing formations.

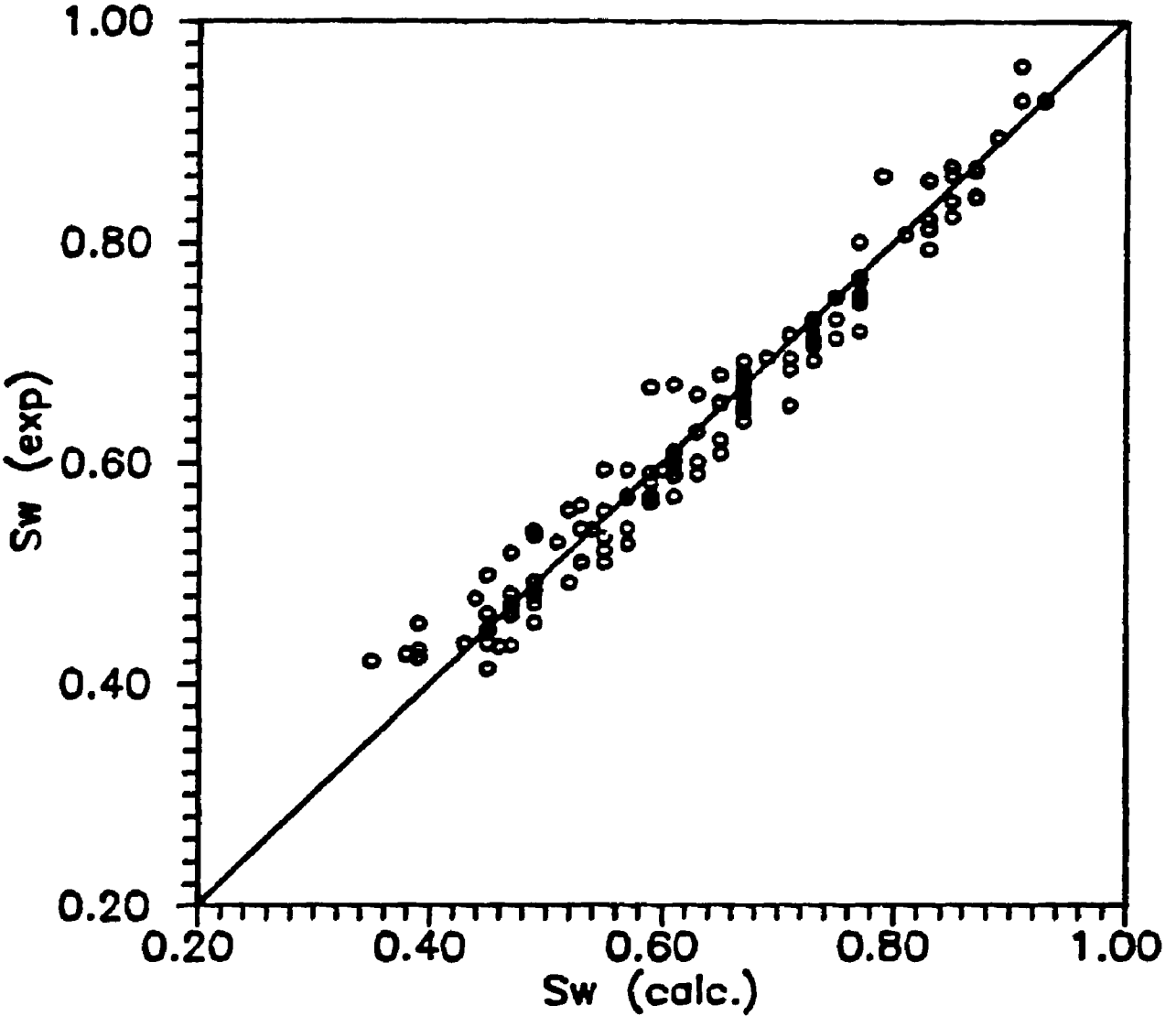

Fig. 4.2 Comparison of calculated vs. experimental Sw values

CHAPTER # 5

MODEL EXTENSION TO FIELD CONDITIONS

The effect of temperature on the conductivity of shaly sands has been experimentally studied by Waxman and Thomas[23]. Their experimental data was used in this study to analyze the effect of temperature on the parameters appearing in the LSU model.

5.1 DESCRIPTION OF EXPERIMENTAL DATA:

The data available consists of the conductance of nine shaly sand cores obtained at seven temperatures (Appendix F) and saturated with water of five different salinities. The seven temperatures used in the experiments were 22, 50, 80, 110, 140, 170 and 200°C. Conductance measurements performed at each temperature were obtained at electrolyte concentrations of 0.09, 0.26, 0.858, 1.76 and 4.74 mol/kg. The data obtained at a temperature of 22°C and electrolyte concentration of 0.09 mol/kg falls in the curved portion of the C_o-C_w plot, while the other conductivity values provide good definition of the linear portion of the C_o-C_w plot.

From the data at 22°C Silva[3] estimated the values of Qv and F_e for each sample. These values are presented in Table 5.1[13].

Table 5.1

Petrophysical Parameters

Core #	Porosity %	F_ϕ	Qv meq/cc
1	29.3	8.12	.098
2	25.6	12.43	.101
3	17.7	23.20	.145
4	15.4	33.86	.256
5	23.5	22.36	.358
6	17.9	49.66	.508
7	19.5	29.31	.739
8	25.6	18.64	.690
9	17.9	54.98	.718

5.2 EFFECT OF TEMPERATURE ON THE PARAMETERS APPEARING IN THE LSU MODEL:

The practical use of the LSU model can be extended to temperatures higher than 25°C, if the effect of temperature on the different parameters can be predicted.

5.2.1 Temperature Effect on Water Conductivity, C_w:

C_w is expected to vary considerably with temperature. The effect of temperature on C_w was empirically determined from the experimental data presented by Lyle and Hosking[24] (Table 5.2). This data covers the range of concentrations and temperatures usually encountered at field conditions.

A multivariable regression analysis was performed on the data. An analytical expression relation C_w to molarity and temperature was obtained:

$$\ln(C_w) = -41.53 + 7.91\ln(Ta) - 1.459\times10^{-5}Ta^2 + .9112\ln(n) - .1026n \qquad [5.1]$$

where:

Ta= absolute temperature, °K.

n = molarity, mol/lt.

The regression coefficient equals 0.9989.

5.2.2 Effect of Temperature on the Fractional Volume of the Double Layer, v_{fl}:

Clavier et al.[15] observed variations in the slope of the C_o-C_w plot for temperatures higher than 25°C. Since F_e and Qv are assumed independent of temperature in the D-W model, Clavier concluded that the unit volume v_Q^H assigned to the bound water decreases as temperature increases. This behavior is attributed to a reduction of the thickness of the double layer.

For the LSU model, the fractional volume occupied by the double layer is expressesed as:

$$v_{fdl}=v_Q^H f_{dl} Qv \qquad [5.2]$$

Silva[3] derived a practical relationship for v_Q^H, which is given by

$$v_Q^H=.28-.0344\ln(T/25) \qquad [5.3]$$

This expression will yield the value assumed correct at 25°C.

Equation 5.3 indicates that the thickness of the double layer is compressed as temperature increases, for f_{dl}=1.0. However, in the curved portion of the C_o-C_w plot f_{dl} increases with temperature. Using the data provided by Waxman for m≤0.26 it was observed that f_{dl} increases proportionally with

temperature following the relationship:

$$f_{dl}^{T}=f_{dl}^{25}(Ta/298)^{1/2} \qquad [5.4]$$

Substituting Eq 3.14 into 5.4 yields:

$$f_{dl}=[Ta/(X_H^2Bo^2n\cdot 298]^{1/2} \qquad [5.5]$$

where:

Ta=absolute temperature, °K.

X_H=6.18 Å

n =molarity mol/lt

and Bo is represented by Eq. 3.15. It is evident that Eq. 5.5 will yield Eq. 3.14 at 25°C.

The free electrolyte concentration, n, can be calculated from the conductivity data published by Lyle and Hosking[24] using the following expression obtained using multivariable regression analysis:

$$\ln(n)=68.1-13.58\ln(Ta)+.0229Ta+1.185\ln(C_w)+.00467C_w \qquad [5.6]$$

A regression coefficient of 0.9952 supports the validity of this expression.

5.2.3 The Effect of Temperature on the Counterion Conductivity, C_{eq}:

The variation of C_{eq} with temperature is identical to that of C_w. This is a result of equating the properties of the double layer solution to those of a sodium chloride solution.

An analytical expression for C_{eq}, can be obtained using published experimental data[24]:

$$\ln(C_{eq}) = -58.84 - .1026 n_{eq} - .0787 \ln(n_{eq}) - 0.0216 Ta + 11.85 \ln(Ta) \qquad [5.7]$$

An adjusted regression coefficient of 0.9971 was obtained for this expression.

5.2.4 Determination of the Fractional Volume of the Double Layer, n_{eq}, at High Temperatures:

The counterion concentration, n_{eq}, at 25°C can be determined using Fig. 3.2. At higher temperatures it was determined from experimental data published by Waxman and Thomas[23] that n_{eq} increases linearly with temperature:

$$n_{eq}^{T} = n_{eq}^{25}(Ta/298) \qquad [5.8]$$

5.3 TEST OF THE MODEL:

As in the case of room temperature conditions, the proposed model can be tested by calculating core conductivities at different temperatures, and comparing them to those obtained experimentaly by Waxman and Thomas[23].

5.3.1 Calculation of Core Conductivities at Molal Concentrations, m≤.26:

The theory predicts that conductivities at m≤0.2 fall in the curved portion of the C_o-C_w plot for temperatures higher than 35°C. Conductivities were calculated for cores with Qv>.1 for temperatures between 50 and 200°C. The overall results of the calculations for the seven cores at m=.09

mol/kg are shown in figure 5.1. It is evident from this figure that the proposed theory allows the calculation of accurate core conductivities at low NaCl concentrations.

5.3.2 Calculation of Core Conductivities at Molal Concentrations, m>0.26 mol/kg:

Conductivities at concentrations higher than 0.26 mol/kg fall on the straight line portion of the C_o-C_w plot. Conductivities for the seven cores with Qv>0.1 are presented in Fig. 5.2. From this figure it can be observed that the proposed theory can accurately predict the conductivity behavior of shaly sands at high salinities and temperatures.

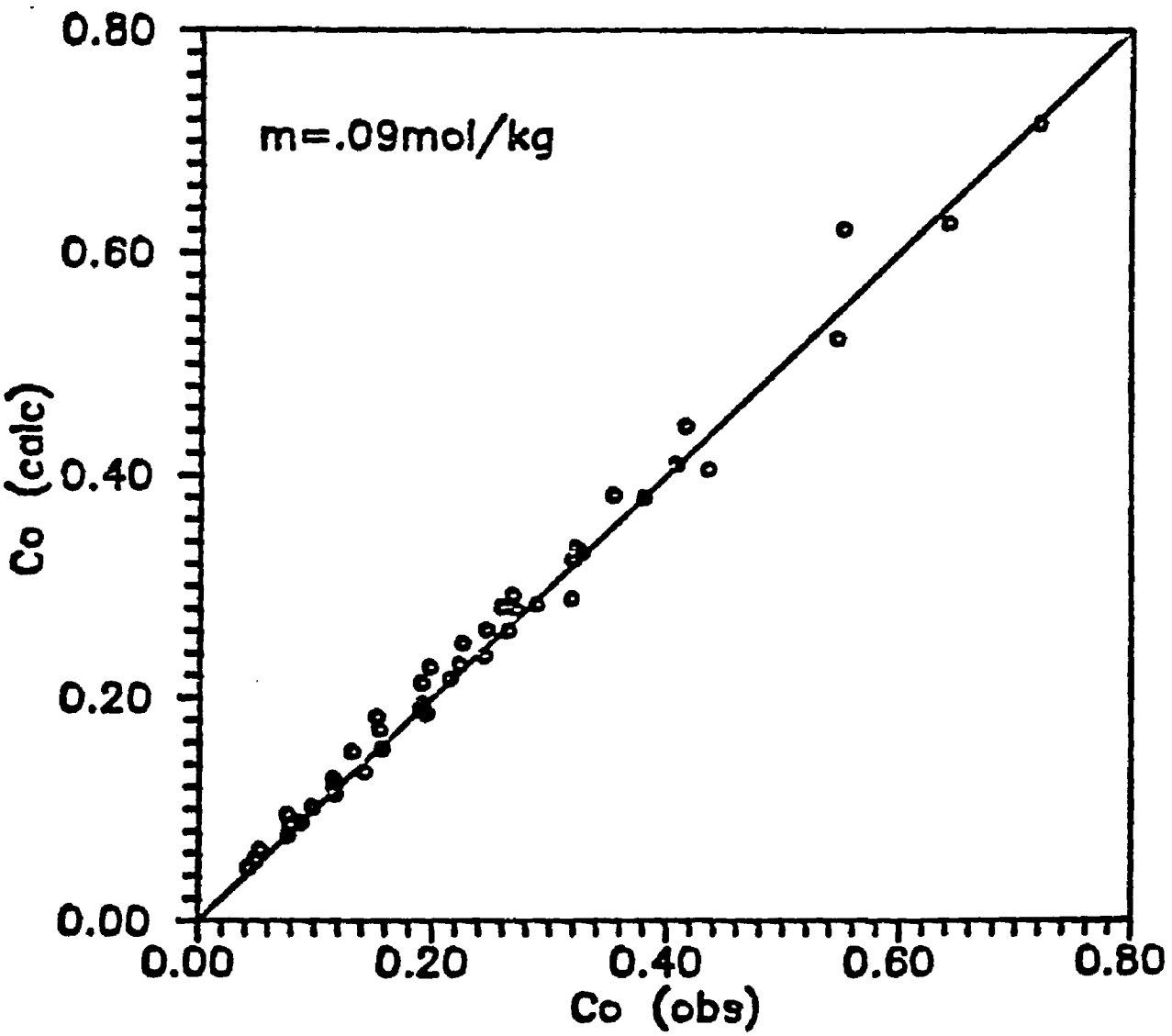

Fig. 5.1 Comparison of experimental to calculated conductivities for cores with Qv>.1

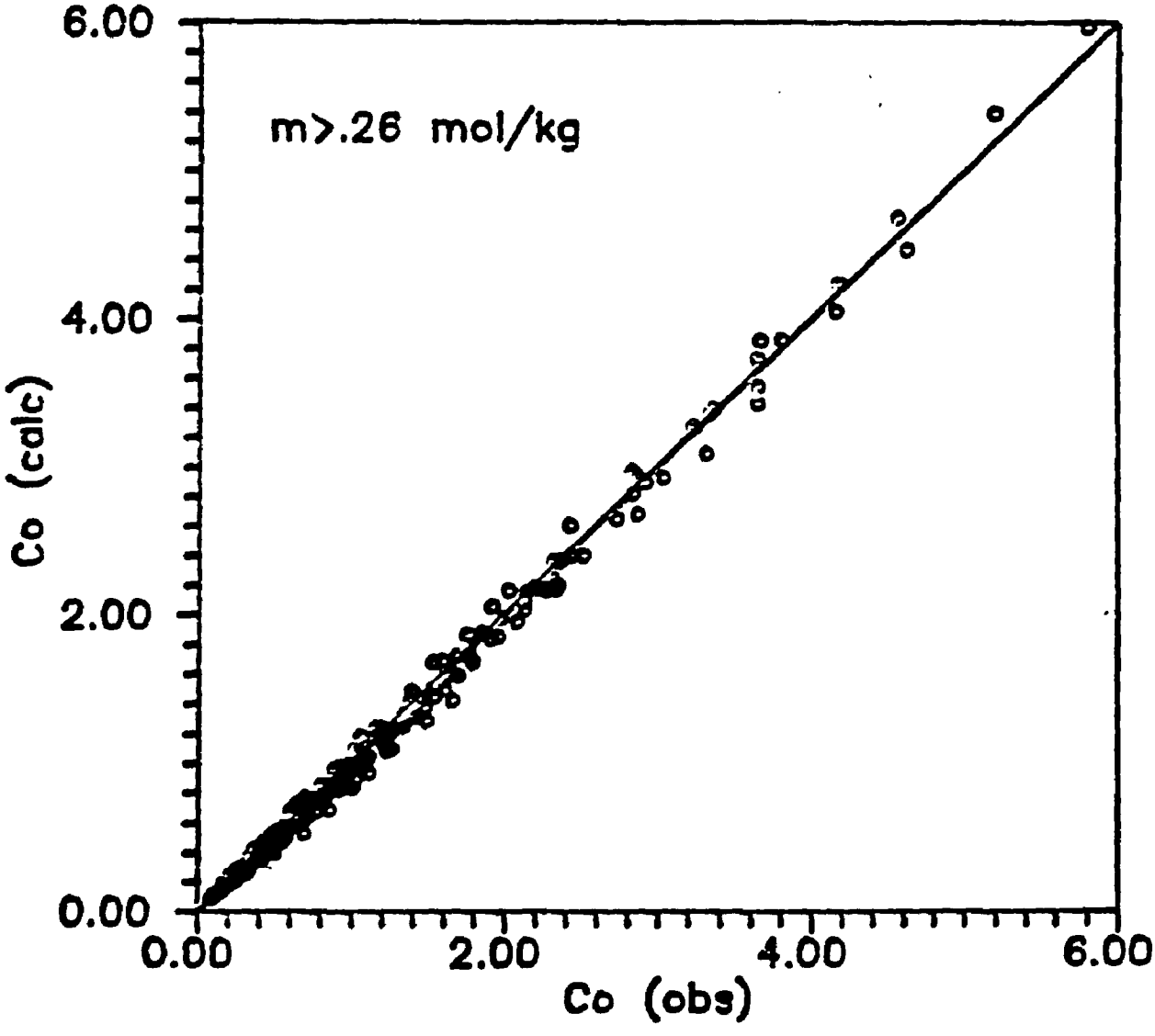

Fig. 5.2 Comparison of calculated vs experimental conductivities for cores with Qv>.1

CHAPTER # 6

SP LOG INTERPRETATION IN SHALY SANDS USING THE LSU MODEL

The LSU conductivity model can be extended to theoretically formulate a model that represents the response of the spontaneous potential (SP) log. Knowing Qv, it is possible to use the model to obtain formation water conductivity, C_w, from the SP log in shaly sand formations. Also a value of Qv can be estimated from the SP response when R_w is known.

An SP log is a record of the way in which the electrical potential of a sonde varies as it passes down a borehole. This electrical potential is a function of formation water salinity and formation shaliness.

The four sources of the SP are illustrated in Fig 6.1. E_1 and E_4 represent streaming potentials generated by the flow of mud filtrate through mud cake opposite permeable formations and through shale respectively.

The remaining part of the SP is called the electrochemical potential, which is divided into two parts: a membrane potential across the shale, E_3, and a junction potential in the permeable sand, E_2.

In clean sands the diffusion potential, i.e. E_2, is small compared to E_3. When the sand is shaly, however, the diffusion potential is helped by the presence of the double layer,

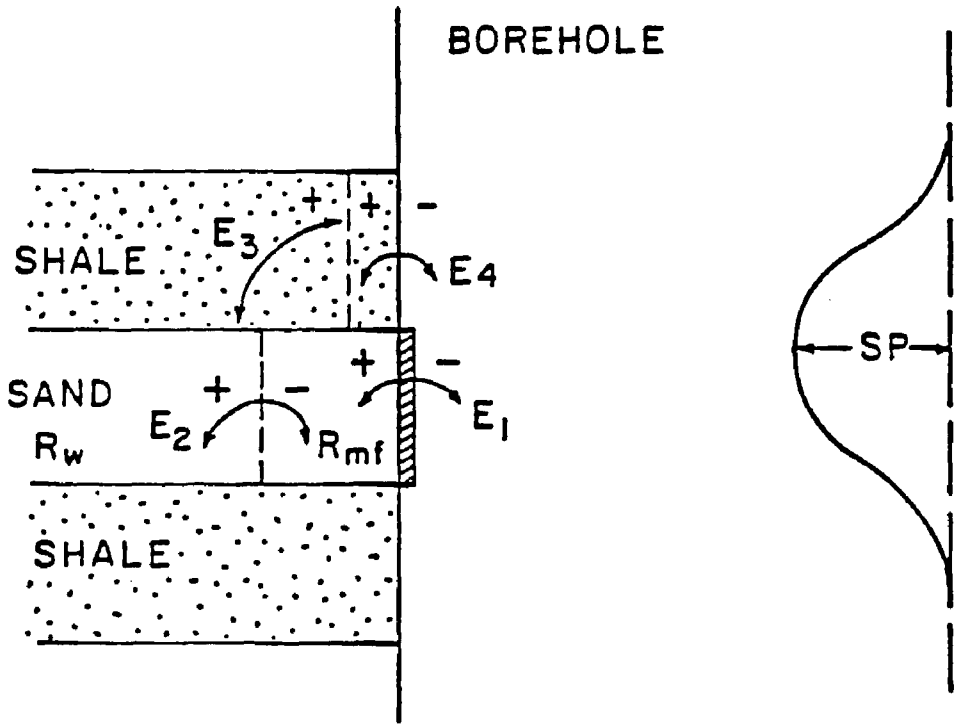

$$SP \approx E_3 - E_2$$

6.1 Components of SP deflection

resulting in a greater potential, E_2. The greater the amount of clay, the stronger this effect will be.

6.1 THE SP MODEL:

The LSU conductivity model can be used to establish a theoretical model for the SP log response. In this model the electrokinetic effects are considered small and are neglected. Hence, the deflection recorded in front of permeable formations, with respect to the shale base line, is given by the difference of the electrochemical potentials of shales, Em_{sh} and adjacent sands[14], Em_{ss}.

$$SP=Em_{sh}-Em_{ss} \qquad [6.1]$$

or in terms of transport numbers:

$$SP=-\frac{2RT}{F}\int_{m2}^{m1}(Tna^{sh}-Tna^{ss})\,d\ln(m_{\pm}) \qquad [6.2]$$

where:

Tna^{sh}=sodium transport number in shales

Tna^{ss}=sodium transport number in sandstones

Both Tna^{ss} and Tna^{sh} can be expressed using the general expression of the sodium transport number, Tna:

$$Tna=\frac{C_{eq}\cdot n_{eq}\cdot v_{fdl}+tna^{+}(1-v_{fdl})C_w}{C_{eq}\cdot n_{eq}\cdot v_{fdl}+(1-v_{fdl})C_w} \qquad [6.3]$$

The parameters C_w and Qv, however, differ for shales and sandstones. In fact, in the case of shales, it is not possible to compute C_w from wireline data. Hence, Tna^{sh} cannot be computed theoretically, and an empirical approach was sought. This approach replaces Tna^{sh} by a term named membrane

efficiency, m_{eff}.

Using this new term and combining Eqs. 6.3 and 6.2, the SP model can be expressed by:

$$SP=\frac{-2RT}{F}\int_{m2}^{m1} m_{eff}\, d\ln(m\gamma_{\pm}) \qquad [6.4]$$

$$+\frac{2RT}{F}\int_{m2}^{m1} \frac{C_{eq}n_{eq}v_{fdl}+tna^{+}(1-v_{fdl})C_{w}}{C_{eq}n_{eq}v_{fdl}+(1-v_{fdl})C_{w}}\, d\ln(m\gamma_{\pm})$$

A discussion of the terms appearing in Eq. 6.4 is presented in Sections 6.2 and 6.3.

6.2 DETERMINATION OF Tna^{ss} AT FORMATION TEMPERATURE:

The determination of Tna^{ss} at elevated temperatures requires special attention, since temperature affects all the parameters present in Eq. 6.3. The effect of temperature on C_{eq}, n_{eq}, and v_{fdl} have been discussed in Chapter 5. Hence, only the effect of temperature on $\gamma_{\pm}$ and tna^{+} have not been considered. The effect of temperature on these parameters is presented hereafter.

6.2.1 Variation of the Sodium Transport Number, tna^{+}, with Temperature:

Transport numbers are a function of the mobilities of the ions of both electrolytes, which in turn are a function of temperature. As discussed in Section 3.2.1 the NaCl transport number can be represented by:

$$tna^{+}=tna^{h}+tw \qquad [3.19]$$

where tna^{h} is the Hittorf transport number and tw is the water transport number. The Hittorf Transport number can be derived

from the experimental data published by Caramazza[20], and presented in Table 6.1.

The values from Table 6.1 were curve fitted and the following expression was developed:

$$\ln(tna^h) = -2.50893 - 1.803769\times10^{-2}\ln(m) + .264709\ln(Ta) - 1.41764\times10^{-5} Ta\ m \qquad [6.5]$$

where:

Ta=absolute temperature, °K.

m=molality, mol/kg.

A regression coefficient of 0.981 was obtained for this expression.

The water transport number, tw, was derived from experimental data in Section 3.2.1.1, and is expressed as a function of molality using Eqs. 3.23 and 3.24

for $m \leq 1.$:

$$tw = .053m - .043 + (.196 \cdot \ln(m) + .1244) \cdot Qv \qquad [3.23]$$

for $m > 1$:

$$tw = .036m^{1.1} - .04377 + .04 \cdot Qv \qquad [3.24]$$

6.2.2 Variations of the Activity Coefficient with Temperature:

As reported by Silva[3] the activity coefficient $\gamma\pm$ is affected by temperature and pressure. However, the effect of pressure is negligible.

The effect of temperature on $\gamma\pm$ has been studied by Millero[25] who developed the expression:

$$\log(\gamma\pm)^t = \log(\gamma\pm)^{298} + .5Y\ L_{298} - .5Z\ J_{298} \qquad [6.6]$$

Table 6.1

Transport Numbers of the Cation in NaCl Solutions

m	0°C	18°	25°	35°	50°
0.05	0.373	0.385	0.389	0.394	0.401
0.10	0.369	0.380	0.384	0.388	0.395
0.20	0.366	0.375	0.378	0.383	0.389
0.50	0.361	0.368	0.371	0.375	0.380
1.00	0.357	0.363	0.366	0.369	0.374
1.50	0.355	0.360	0.362	0.366	0.370
2.00	0.353	0.357	0.360	0.362	0.367
2.50	0.352	0.355	0.357	0.360	0.364
3.00	0.351	0.354	0.356	0.358	0.362
3.50	0.349	0.352	0.354	0.356	0.360
4.00	0.348	0.350	0.352	0.354	0.358
4.50	0.347	0.349	0.351	0.353	0.357
5.00	0.346	0.348	0.349	0.351	0.355

where:

$$Y=\frac{298.15-Ta}{8.3147(298.15)2.3026(Ta)} \qquad [6.7]$$

$$Z=298.15\ Y+\frac{1}{8.3147}\log(Ta/298.15) \qquad [6.8]$$

$$L_{298}=\frac{2878.6m^{1/2}}{1+m^{1/2}}-3182.8m+986.5m^{3/2} \qquad [6.9]$$

$$J_{298}=\frac{43.5\ m^{1/2}}{1+m^{1/2}}+72.m-20.36m^{3/2} \qquad [6.10]$$

where:

Ta=absolute temperature, °K

m =molality, mol/kg

$\gamma_{\pm}^{298}$=activity coefficient at 25°C

6.3 DEFINITION AND DETERMINATION OF MEMBRANE EFFICIENCY, m_{eff}:

Theoretically, the sodium transport number in shales, Tna^{sh}, contains two electric contributions: i) the clay contribution and ii) the free electrolyte contribution. The clay contribution, C_{cl}, can be expressed using:

$$C_{cl}= C_{eq}\cdot n_{eq}\cdot v_{fdl} \qquad [6.11]$$

The free electrolyte contribution to Tna^{sh}, C_{fe}, can be written as:

$$C_{fe}= (1-v_{fdl})C_w \qquad [6.12]$$

Knowing that tna^{+} is less than 0.5, it is apparent from Eqs. 6.3, 6.11 and 6.12 that an increased value of C_w would decrease the magnitude of Tna^{sh}.

The calculation of Tna^{sh} cannot be treated like Tna^{ss} because formation water conductivity, C_w, cannot be obtained directly from wireline data. Hence, it is commonly assumed that shale behaves as a perfect membrane, which implies that the double layer occupies the entire pore volume, i.e. $v_{fdl}=1$; hence, $Tna^{sh}=1.0$. In reality, v_{fdl} is not equal to zero; therefore, free electrolyte exists in the pore space and contributes to Tna^{sh}. This contribution is small, however, not negligible, making $Tna^{sh}<1.0$.

Since a strict theoretical approach cannot be used in the determination of Tna^{sh}, an empirical approach is sought.

In order to account for C_w, a term defined as membrane efficiency, m_{eff}, is introduced. This term replaces Tna^{sh} in Eq. 6.2. Hence, Em_{sh} can be written as:

$$Em_{sh}=\frac{-2RT}{F}\int_{m2}^{m1} m_{eff}\, d\ln(m_{\gamma\pm}) \qquad [6.13]$$

The introduction of m_{eff} can be supported from log data. In cases where water resistivity is high, i.e. shallow wells, m_{eff} values approach one, while in more saline environments, m_{eff} values approximate 0.8. This implies that in high resistivity environments the contribution of the free electrolyte is minimal, and the shale contribution accounts for nearly 100% of Tna^{sh}. On the other hand, in more saline environments, formation water plays a more important role, hence decreasing the value of Tna^{sh}. This explains the fact that in the Gulf Coast Region where R_w's$\leq$.05 are common, m_{eff}=.8. While, in the shallow reservoirs of California where

more resistive formation water are predominant, m_{eff}=1.0.

The determination of m_{eff} is detailed hereafter.

Shale resistivity, R_{sh}, is a function of Qv_{sh} and C_w; hence, constant shale resistivities are usually associated with constant values of Qv_{sh} and C_w. Therefore, if a water bearing sand which exhibits the same R_{sh} as the zone of interest is present, m_{eff} can be calculated by rearranging Eqs. 6.1 and 3.1 as:

$$m_{eff}=\frac{-F\ (SP+Em_{ss})}{2RT\int_{m2}^{m1} d\ln(m_{\pm})} \qquad [6.14]$$

and

$$C_o \cdot F_e=\frac{C_{eq}\cdot n_{eq}\cdot v_{fdl}+(1-v_{fdl})C_w}{Tna^{ss}} \qquad [6.15]$$

The three unknowns in Eqs. 6.14 and 6.15 are: Qv, C_w, and m_{eff}. If a clean sand is present, i.e. Qv=0.0, m_{eff} can be calculated from the simultaneous solution of Eqs. 6.14 and 6.15. If this is not the case, and only shaly sands are present, m_{eff} can be calculated by trial and error using the same set of equations.

6.4 DETERMINATION OF R_w IN SHALY SANDS WHEN Qv IS KNOWN:

The new LSU-SP model is a function of R_w, Qv, and S_w. Hence, it can be used to compute R_w, if Qv is known.

In the case, of hydrocarbon bearing zones, the "hydrocarbon effect" must be considered. This effect can be incorporated in the model by substituting Qv by Qv', where $Qv'=Qv/S_w$.

To facilitate the use of the proposed SP model in the calculation of R_w, charts can be prepared for any temperature, saturation and shale efficiency, an example of such chart for m_{eff}=0.8 and 225°C is illustrated in Fig. 6.2.

The estimation of R_w from these charts is as follows (Fig. 6.3):

1. Draw a vertical line at the appropriate value of R_{mf} up to the known Qv'.
2. From the Qv' line draw a horizontal line to the y-axis, A .
3. Subtract the magnitude of the SP deflection from A. From this point, proceed horizontally to the appropriate Qv line, point B.
4. Determine the value R_w by following a vertical line from B down to the resistivity axis.

6.5 DETERMINATION OF Qv WHEN R_w IS KNOWN:

In some instances, water samples are recovered from the interval of interest; in these cases, Qv can be determined directly from the SP log response. To facilitate this task charts can be prepared for different R_w's and temperatures. An example of such chart is presented in Fig. 6.4.

In conclusion, the LSU-SP model offers several important advantages over previous work. First, it provides means of determining R_w from shaly-sand formations, and second, it is based on solid theoretical principles, which can improve SP log interpretation in shaly or clean formations.

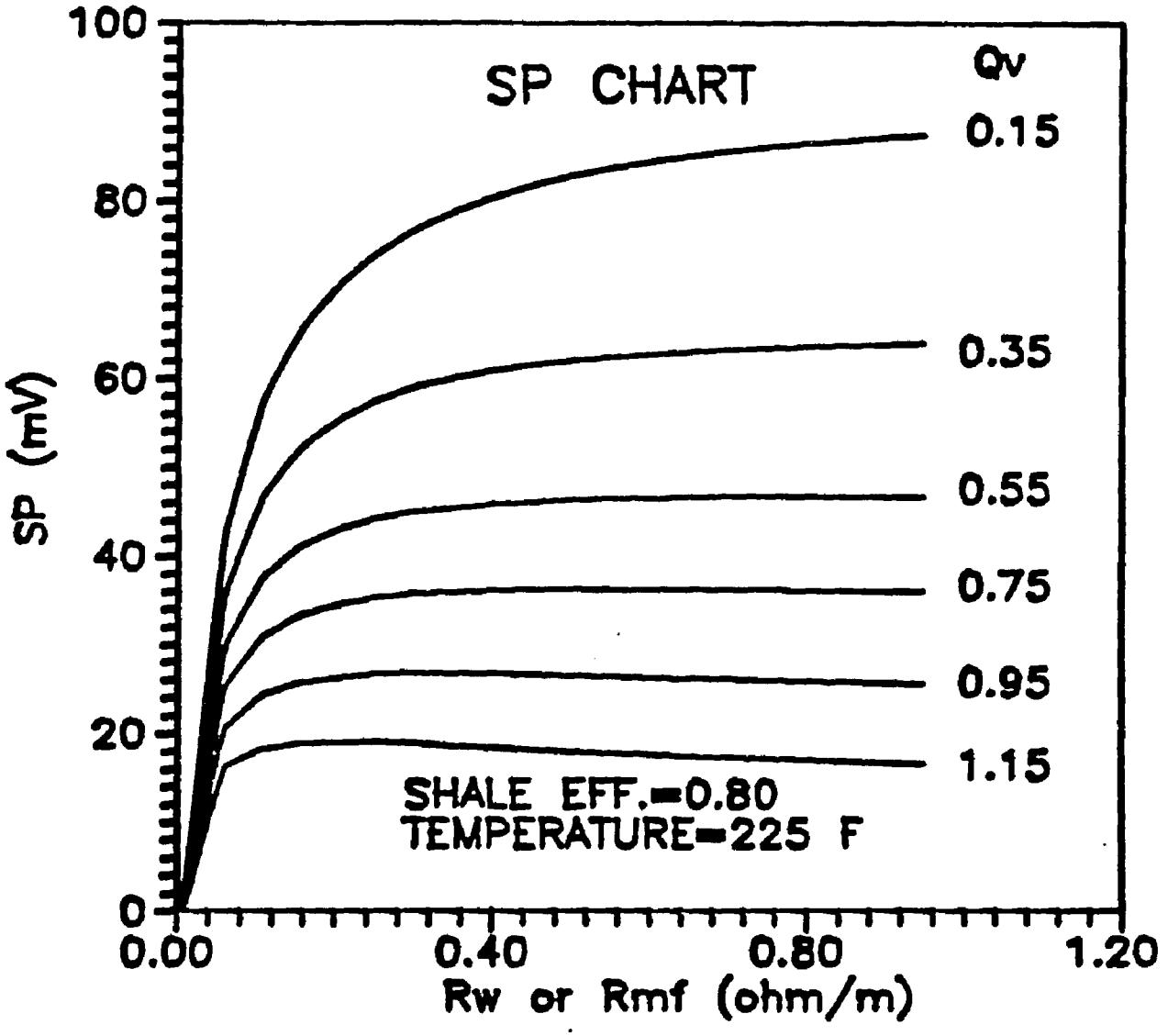

Fig. 6.2 New SP Chart

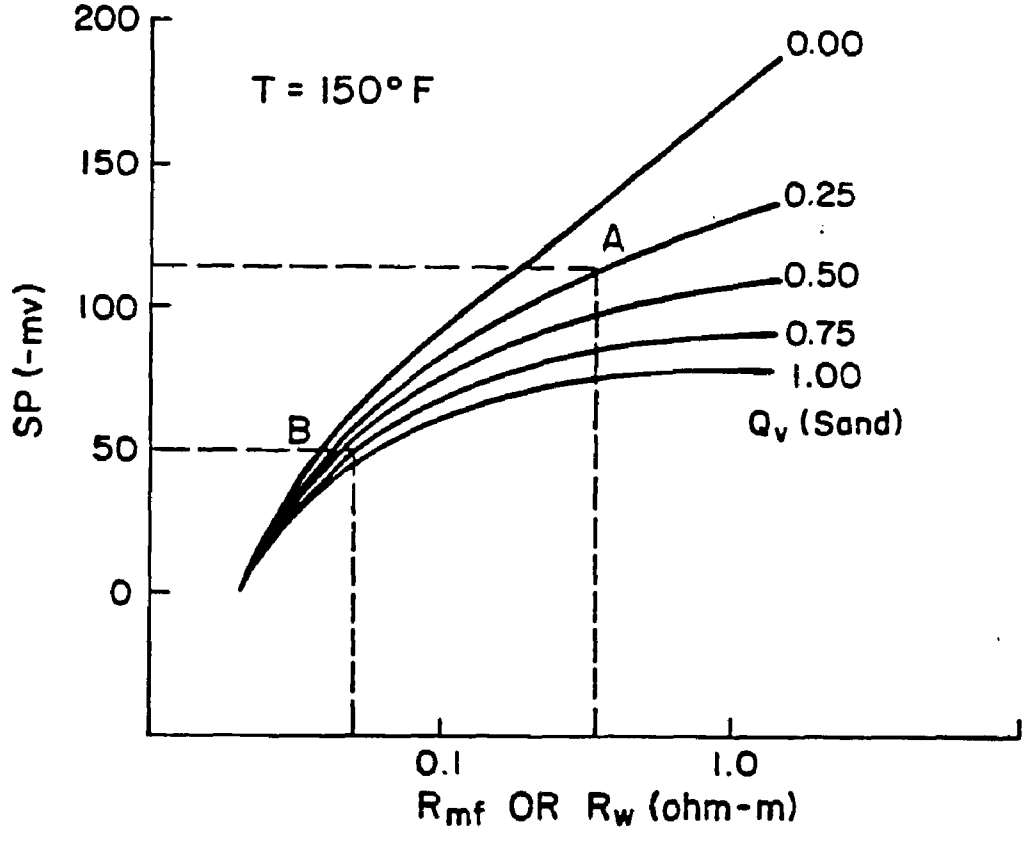

Fig. 6.3 Determination of Rw from LSU model

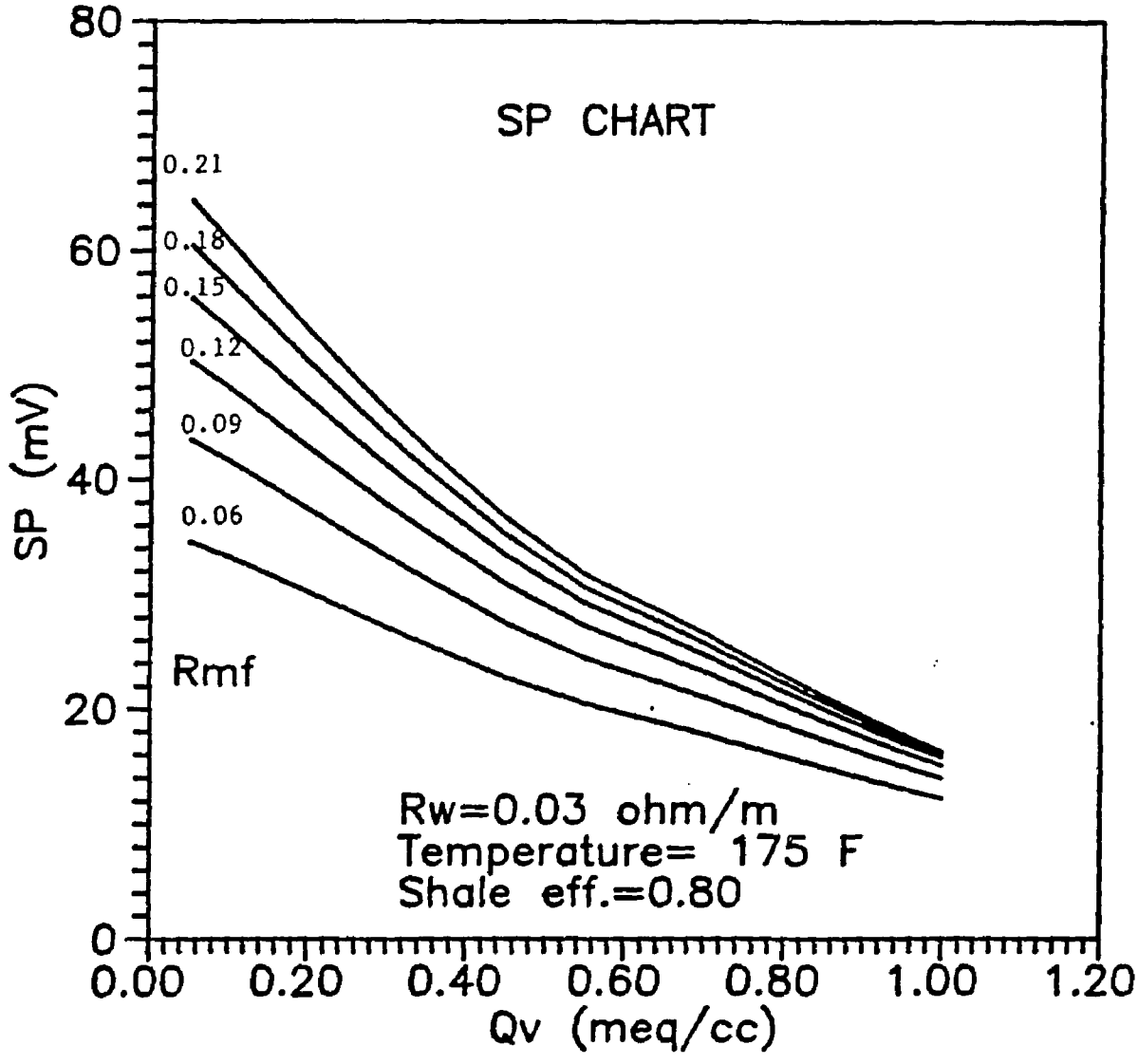

Fig. 6.4 Determination of Qv using new SP Model

CHAPTER # 7

EVALUATION OF SHALY SAND FORMATIONS USING THE LSU MODEL

One of the major shortcoming of current V_{sh} shaly sand models is their inability to predict accurate values of hydrocarbon saturation from wireline data. On the other hand, the use of double layer models require laboratory determined cation exchange capacity, Qv, values. The LSU conductivity and SP models provide, for the first time, means to determine C_w and Qv from conventional well log data. This also leads to a more representative hydrocarbon saturation values.

7.1 METHODS CURRENTLY USED TO DETERMINE Qv AND C_w:

7.1.1 Determination of Qv:

Wet chemistry methods were extensively used in the estimation of Qv. These methods require the physical destruction of the core sample, and the results not only depend on the petrophysical properties of the rock, but also on the method used in the preparation of the sample.

The wet chemistry techniques have been replaced by the multiple salinity and the membrane potential methods[1]. The multiple salinity method appears to be preferable, since information about F_e and Qv can be obtained simultaneously. The method consists in i) measuring core conductivities, C_o, at two or more salinities of the free electrolyte, the salinities must correspond to the straight line portion of

the C_o-C_w plot, and ii) solving simultaneously for F_e and Qv. The results of this procedure depend on the conductivity model used to express C_o.

Even though the multiple salinity technique is accurate, it is not always practical since representative core samples are not available in all cases.

7.1.2 Determination of C_w:

C_w can be estimated from resistivity logs, from the SP log, or from chemical analysis.

Chemical analysis is the most desirable technique, however, its practical application is limited to the cases where non-contaminated water samples can be recovered.

C_w can be obtained from a clean water bearing zone using the equation:

$$C_o=C_w/F \qquad [7.1]$$

where C_o is the conductivity of the rock 100% saturated with water measured by the log and F is the formation factor.

This method requires the knowledge of porosity and the cementation exponent, which are not usually available with the desired accuracy. Eq. 7.1 is not, however, applicable in shaly sand interpretation.

The SP log can be used to calculate C_w from the following expression:

$$SP=-K\cdot\log(R_{mfe}/R_{we}) \qquad [1.2]$$

where:

SP = log reading

R_{mfe}= equivalent mud filtrate resistivity

R_{we}= equivalent formation water resistivity

As discussed in chapter 1, the use of Eq. 1.2 in shaly sands usually underestimates the formation hydrocarbon potential.

7.2 DETERMINATION OF Qv AND C_w IN WATER BEARING ZONES USING THE LSU MODELS:

From the previous section, it is obvious that presently there is no valid and practical technique to obtain reliable values of Qv and C_w. This study presents the first practical method to derive these parameters from the resistivity and SP logs. The behavior of these logs can be described theoretically by the LSU conductivity and membrane potential models, respectively. In water bearing zones, the two log responses are a sole function of Qv and C_w; hence, it is possible to solve for these two variables simultaneously.

The conductivity model is defined by:

$$C_{we}=C_o \cdot F_e=[C_{eq} \cdot n_{eq} \cdot v_{fdl}+(1-v_{fdl}) \cdot C_w] \qquad [3.2]$$

In this equation C_{eq}, n_{eq} and v_{fdl} are a function of Qv and C_w. N_{eq}, as can be observed from Fig. 3.2 is a function Qv and the free electrolyte concentration, n. C_{eq} in turn can be obtained from Qv and C_w from:

$$C_{eq}=\exp(-58.84-.1026n_{eq}-.0787\ln(n_{eq}) -.0216Ta+11.85\ln(Ta)) \qquad [5.8]$$

where:

Ta=absolute temperature, °K

n=molarity,mol/lt

Moreover, by combining Eqs. 3.14, 5.2 and 5.3, the fractional volume of the double layer, v_{fdl}, can be expressed as:

$$v_{fdl}=(.28-.0344\ln(T/25)\cdot(6.18^2\cdot Bo^2\cdot n)^{-1/2}\cdot Qv \qquad [7.2]$$

where:

$$Bo=.3248+1.5108X10^{-4}T+8.935x10^{-7}T^2 \qquad [3.15]$$

and

T=temperature, °F.

Molarity, n, can be related to C_w by:

$$\ln(n)=68.1-13.5791\ln(Ta)+2.289x10^{-2}Ta+1.1854\ln(C_w)$$
$$+4.6761x10^{-3}C_w \qquad [7.3]$$

It is clear from the above stated functions that the conductivity of a water bearing shaly sand is solely a function of Qv and C_w.

On the other hand, the SP model can be expressed by:

$$SP=Em_{sh}-Em_{ss} \qquad [6.1]$$

or

$$SP=\frac{-2RT}{F}\int_{m2}^{m1} m_{eff}\, d\ln(m\gamma_{\pm}) \qquad [6.4]$$

$$+\frac{2RT}{F}\int_{m2}^{m1}\frac{C_{eq}\cdot n_{eq}\cdot v_{fdl}+tna^{+}(1-v_{fdl})\cdot C_w}{C_{we}/F_e}\, d\ln(m\gamma_{\pm})$$

Eq. 6.1 can also be expressed as a function of Qv and C_w, since m_{eff}, $\gamma_{\pm}$ and tna^{+} are also functions of these two variables.

The mean activity coefficient, $\gamma_{\pm}$, can be related to C_w using:

$$\log(\gamma_{\pm}) = \log(\gamma_{\pm}^{298}) + .5Y \cdot L_{298} - .5Z \cdot J_{298} \quad [6.6]$$

where:

$$\log(\gamma_{\pm}^{298}) = \frac{-.05115 \cdot n^{1/2}}{1+1.3065 \cdot n^{1/2}} - 1.75 \cdot \log(a_A) - \log(1-.027m) \quad [2.26]$$

$$a_A = .99948 - 3.0959 \times 10^{-2} m - .00150 m^2 \quad [2.27]$$

$$Y = \frac{298.15 - Ta}{8.3147(298.15)2.3026(Ta)} \quad [6.7]$$

$$Z = 298.15\ Y + \frac{1}{8.3147}\log(Ta/298.15) \quad [6.8]$$

$$L_{298} = \frac{2878.6 m^{1/2}}{1+m^{1/2}} - 3182.8m + 986.5 m^{3/2} \quad [6.9]$$

$$J_{298} = \frac{43.5\ m^{1/2}}{1+m^{1/2}} + 72.m - 20.36 m^{3/2} \quad [6.10]$$

and,

m =molality, mol/kg

$\gamma_{\pm}^{298}$=activity coefficient at 25°C

For sodium chloride solutions molarity, n, and molality, m, can be related using:

$$\ln(m) = -1.5054 + 1.0142 \ln(n) + .2721 \ln(Ta) \quad [7.5]$$

and molarity, n, can be expressed as a function of formation water conductivity, C_w, using Eq. 7.3.

Finally, tna^+ can also be related to Qv and C_w, using the following relationships:

$$tna^h = \exp(-2.5089 - 1.8038 \times 10^{-2} \ln(m) + .2647 \ln(Ta) - 1.4176 \times 10^{-5} Ta \cdot m) \quad [6.5]$$

and

for $m \leq 1.0$

$$tw = 0.053m - 0.43 + (.196\ln(m) + .1244) \cdot Qv \qquad [3.23]$$

for $m > 1.0$

$$tw = 0.036m^{1.1}0.04377 + 0.04Qv \qquad [3.24]$$

Hence, both the conductivity and spontaneous potential models can be formulated as a sole function of Qv and C_w. Furthermore, C_o and SP can be obtained directly from wireline logs, it is possible to solve simultaneously for Qv and C_w using Eqs. 3.2 and 7.4.

This technique was first tested using the data published by Waxman and Smits[4,14]. Results comparing Qv's and C_w's determined from the multiple salinity technique[3], and laboratory samples, respectively, against Qv's and C_w's derived from the simultaneous solution of Eqs. 3.2 and 7.4 are presented in Fig. 7.1, 7.2, 7.3, and 7.4. The good agreement of the calculated and experimental data supports the applicability of the proposed method.

The LSU model was also tested with field data, a comparison of calculated vs. measured water resistivies, from water samples, is illustrated in Fig. 7.5. Fig. 7.6 presents a comparison of calculated (LSU model) vs. chemically determined Qv's. As expected, there is no fair agreement between the results of the two methods; however, a trend between calculated and laboratory determined Qv's is still present.

Field examples using the proposed technique are presented in chapter 8.

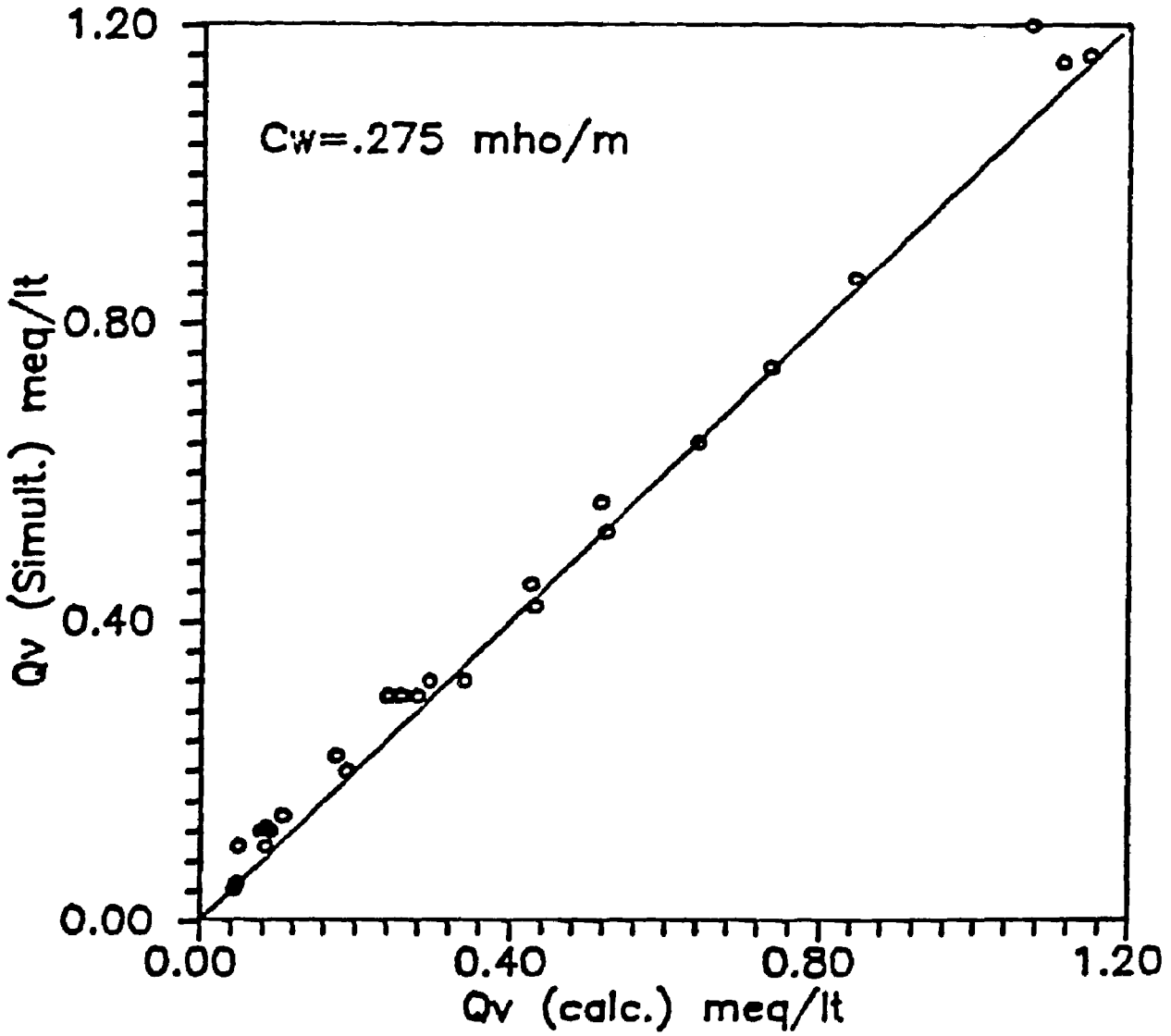

Fig. 7.1 Comparison of calculated Qv's[13] vs Qv's from simultaneous solution

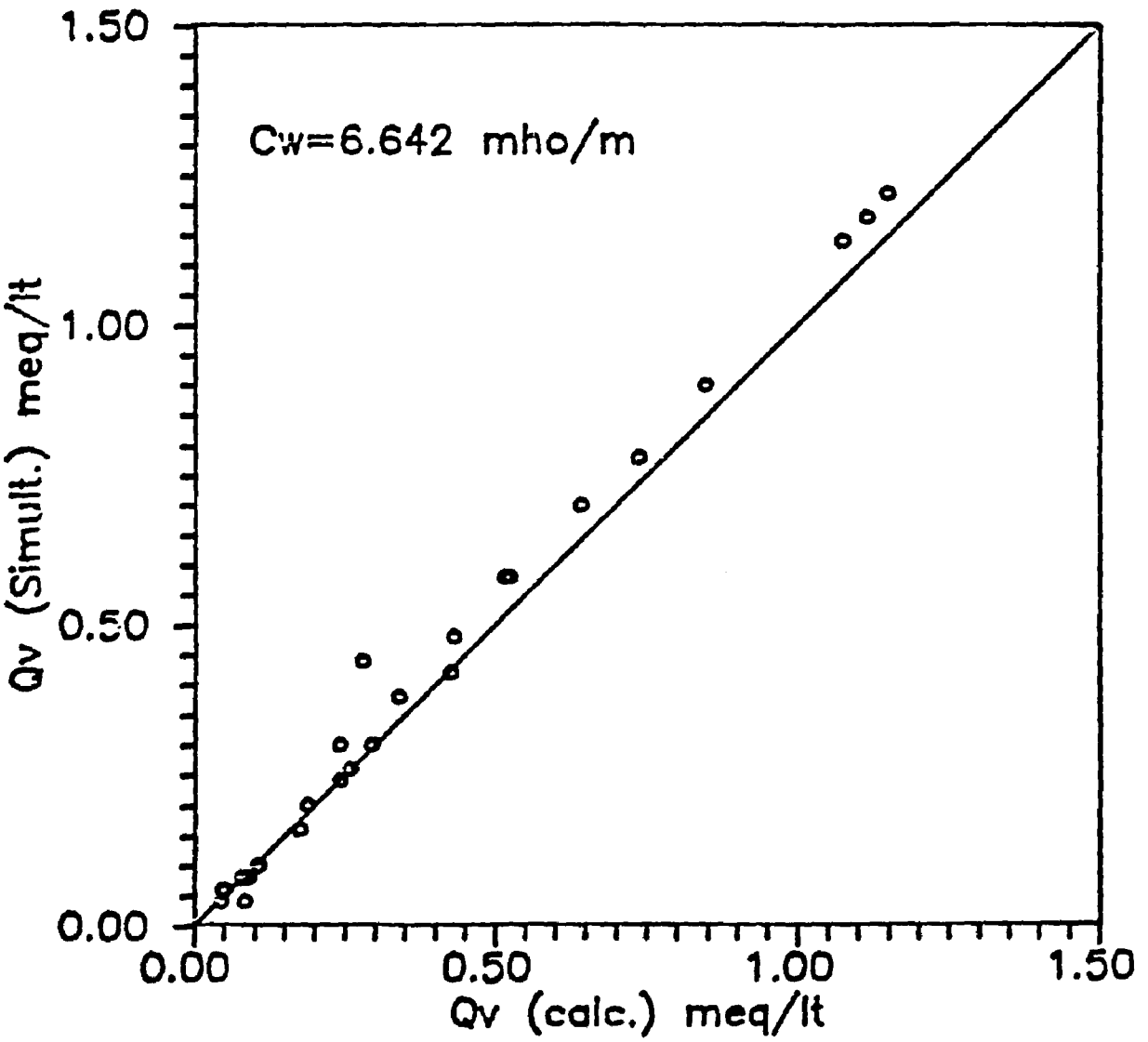

Fig. 7.2 Comparison of calculated Qv's[13] vs. Qv's from simultaneous solution

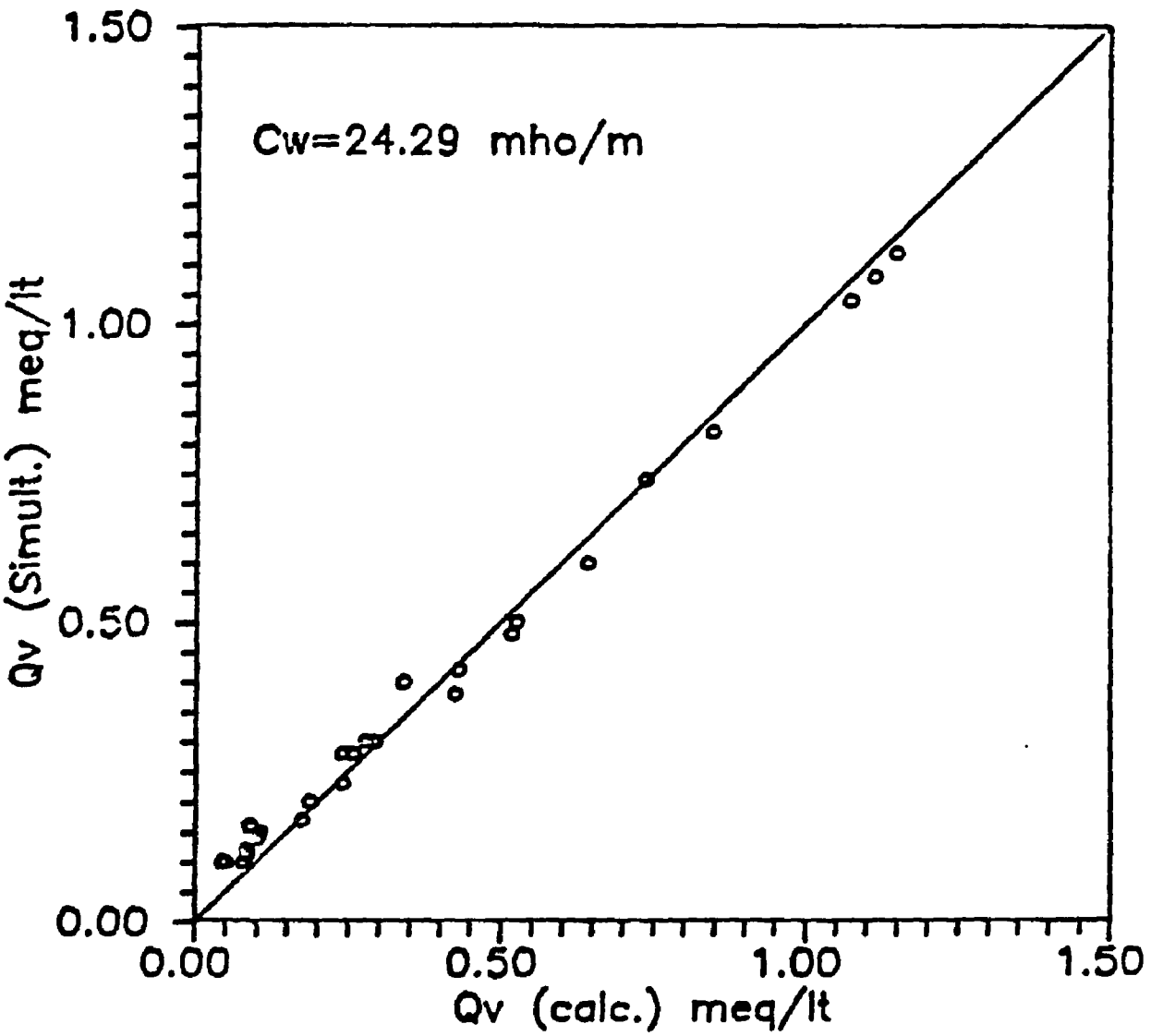

Fig. 7.3 Comparison of calculated Qv's[13] vs Qv's from simultaneous solution

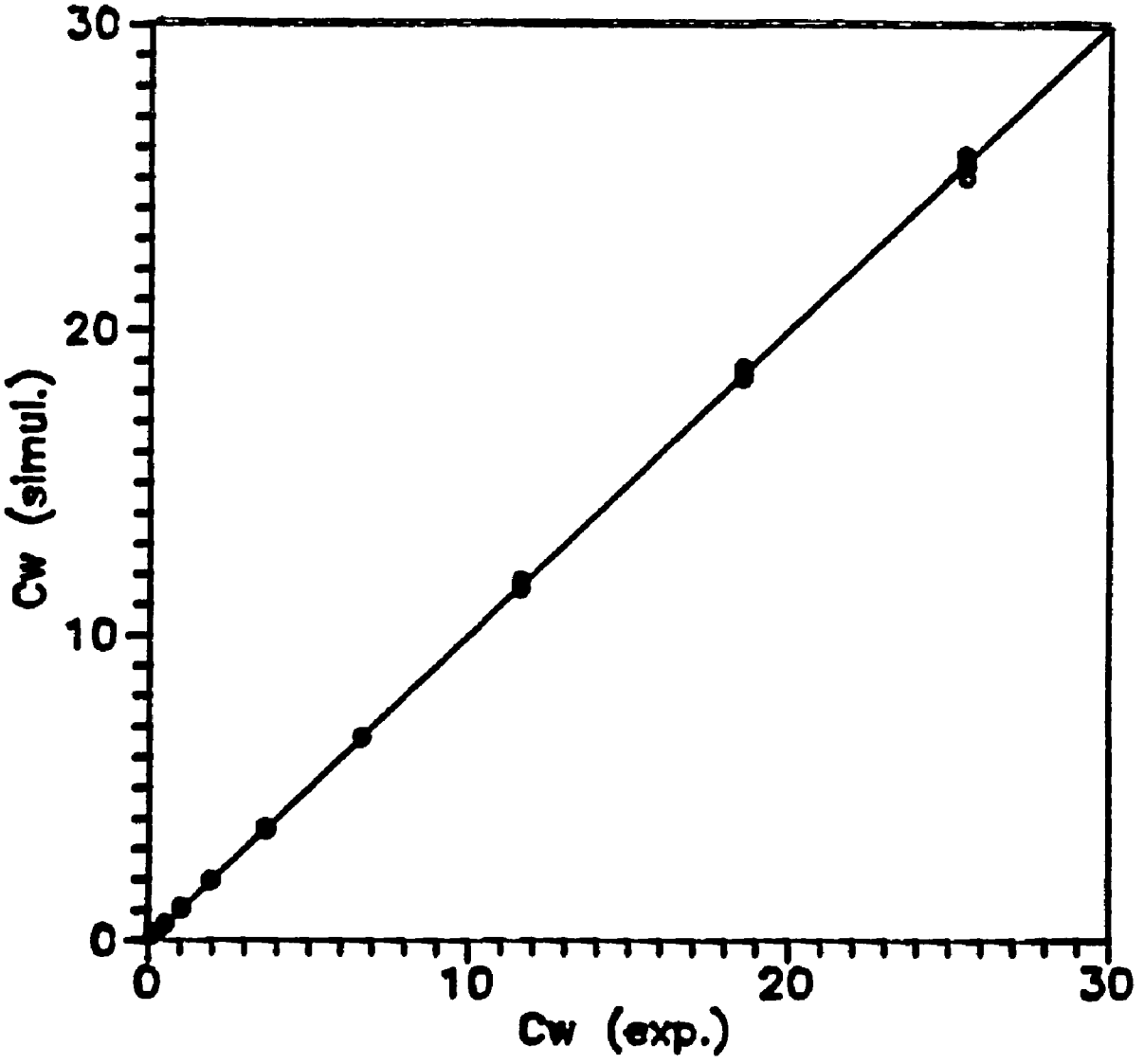

Fig. 7.4 Comparison of experimental Cw's vs. Cw's from simultaneous solution

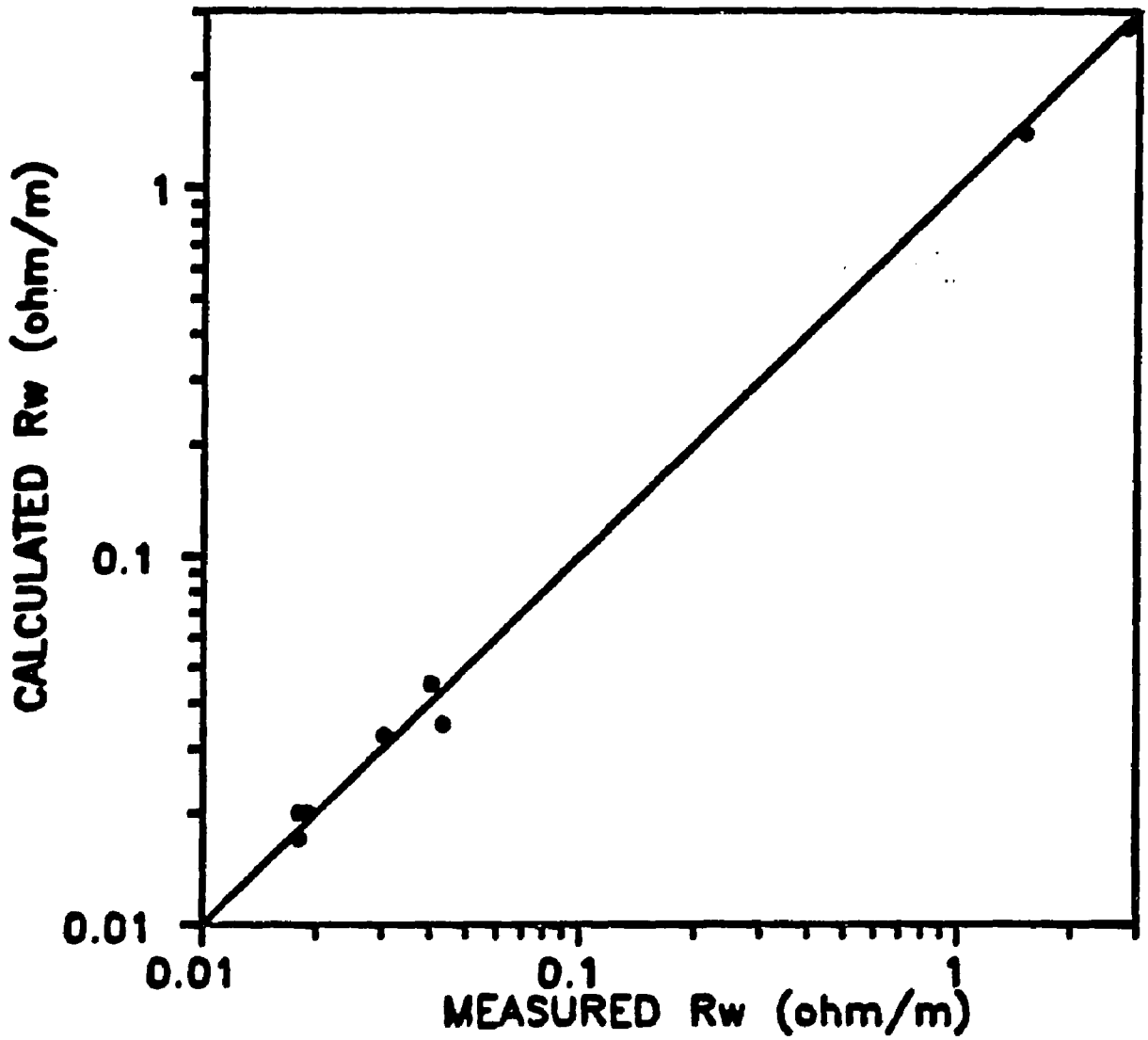

Fig. 7.5 Comparison of measured vs. calculated Rw's

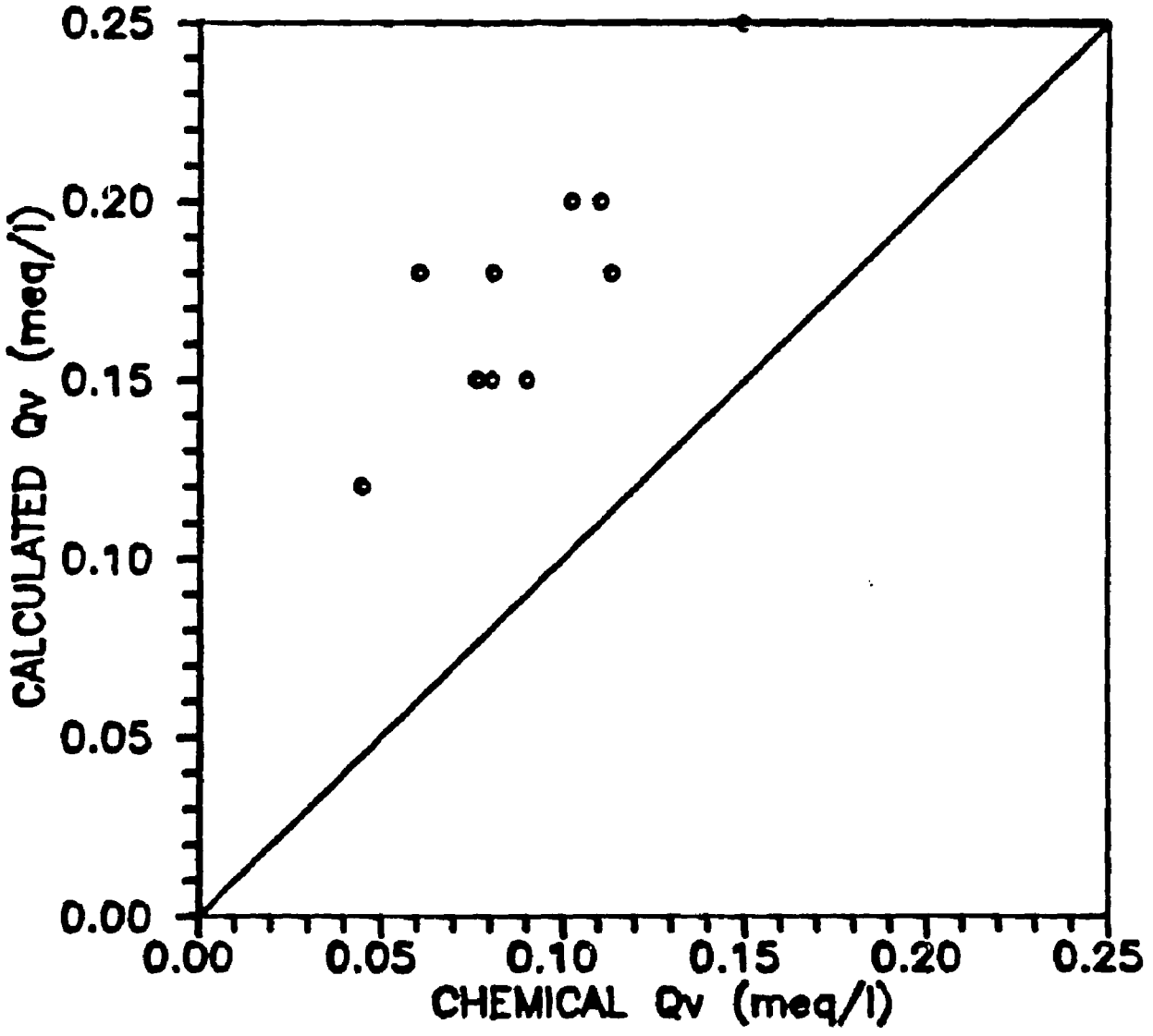

Fig. 7.6 Comparison of calculated (LSU) vs. chemically determined Qv's

7.3 EVALUATION OF HYDROCARBON BEARING FORMATIONS:

As stated previously, the purpose of well log interpretation is the evaluation and detection of potential hydrocarbon bearing zones. This is done by calculating water saturation, S_w, for the intervals of interest. The LSU model expresses S_w as follows:

$$S_w^{ne}=\frac{C_t \cdot F_e}{C_{eq}' \cdot n_{eq}' \cdot v'_{fdi}+(1-v_{fdi}) \cdot C_w} \qquad [7.6]$$

where:

C_t=formation resistivity, ohm/m.

In hydrocarbon bearing formations the SP response can be represented using Eq. 6.1 after substituting Qv by Qv':

$$Qv'=Qv/S_w \qquad [4.1]$$

If a water zone is underlaying a hydrocarbon bearing interval, C_w can be calculated using the procedure outlined in Section 7.2. S_w and Qv can then be obtained from the simultaneous solution of the SP and C_t equations. If a water zone is not present, an iterative procedure can be used to obtain C_w, Qv and S_w. Field examples covering all possible cases are presented in Chapter 8.

In conclusion, the LSU model makes it possible to determine Qv and C_w from simultaneous solution. This is the key that allows the evaluation of the hydrocarbon potential of a shaly formation.

CHAPTER # 8

FIELD APPLICATIONS OF THE LSU MODEL

One of the most important aspects of petroleum exploration is the detection and evaluation of hydrocarbon bearing formations. This task is usually accomplished by calculating water saturation, S_w, from well log readings. When formations are shale-free this task is relatively simple. However, the determination of S_w in shaly sands is usually a complex problem.

The first step towards the understanding of the electrical behavior of shaly sands was the work published in 1968 by Waxman and Smits[4] resulting in their model, which is based on the measurement of Qv from core data. This was followed in 1972 by a paper by Waxman and Thomas[23] incorporating the "hydrocarbon effect" into their model and investigating the effect of temperature on clay conductivity. Since then several authors including Clavier et al.[5] and Juhasz[8] have produced shaly sand saturation models based on Waxman and Smits experimental data, however, none of these have become accepted as a complete solution to the shaly sand problem, mainly because of the core data required for their application.

This study presents the first method based on sound principles that does not require core calibrations. Instead,

the LSU model only requires conventional log data as input parameters.

Several wells were analyzed using the newly developed technique. Examples representing different depositional environments, with formations exhibiting different degrees of shaliness and containing water with different salinities, are presented in this chapter. To show the reliability and uniqueness of the LSU model its results will be compared to those obtained from models currently in use. These models are briefly reviewed hereafter.

8.1 DETERMINATION OF S_w USING ARCHIE'S EQUATION:

In 1942, Archie published his famous saturation model, which can be used to estimate fluid saturation in shale-free formations.

The electrical properties of clean formations are solely related to the fluids saturating the pore space. In these formations the resistivity contrast between the formation resistivity, R_t, and the resistivity of the same formation if 100% saturated with water, R_o, provides a good estimate of S_w:

$$S_w^n = R_o/R_t \qquad [1.7]$$

The magnitude of R_t in Archie's model can be determined directly from resistivity logs. R_o can be equated to the resistivity of an adjacent water bearing formation provided that both strata contain the same formation water and exhibit the same porosity. However, in many cases an adjacent water zone is not available or the constant porosity and/or the

salinity condition is not met. In this situation R_o can be obtained from:

$$R_o=F\cdot R_w \qquad [8.1]$$

where the formation factor, F, can be calculated from porosity logs and R_w can be determined from the SP log using Eqs. 2.5 and 1.2, respectively.

The evaluation of clean formations is therefore straight forward. Unfortunately, this method yields erroneous estimations of S_w in shaly formations. The use of Archie's model in shaly sands results in the underestimation of hydrocarbon potential, which in some cases can result in overlooking a hydrocarbon producing formation.

8.2 THE CYBERLOOK WATER SATURATION MODEL:

The Cyberlook model[2] is a computer-assisted interpretation model. It uses dual water concepts in the derivation of water saturation.

In the Cyberlook model, the resistivity of a water-bearing shaly formation is given by:

$$R_o=\frac{R_w\cdot R_{wb}}{\phi^2[S_{wb}\cdot R_w+(1-S_{wb})\cdot R_{wb}} \qquad [1.6]$$

where:

R_{wb}= bound water resistivity, ohm/m

S_{wb}= bound water saturation, fraction

R_o can then be compared to the measured deep resistivity to determine fluid saturation. The Cyberlook water saturation is given by:

$$S_w^n = R_o/R_t \qquad [1.7]$$

Porosity, ϕ, is derived from special porosity crossplots, S_{wb} is obtained from traditional shale indicators (Sec. 8.2.1). R_{wb} and R_w are determined from a shale section and a clean-water bearing sand, respectively, using the following relationship:

$$R_{wf} = R_o/F \qquad [8.2]$$

where R_{wf} can be substituted by R_w or R_{wb}.

If there are no clean water-bearing zones, R_w has to be estimated by other means, or taken from local experience.

8.2.1 Determination of S_{wb}:

There are several sources for S_{wb}. These include the density-neutron crossplot, SP, Gamma Ray and resistivity logs.

For the density-neutron crossplot, S_{wb} is given by[2]:

$$S_{wb} = \frac{\phi_{tcl} V_{dc}}{\phi_t V_{dccl}} \qquad [8.3]$$

where:

ϕ_{tcl}=wet shale porosity

V_{dc}=volume of dry clay

V_{dccl}=volume of wet clay

These terms can be determined from Fig. 8.1.

For the Gamma Ray Log (GR)[2]:

$$S_{wb} = M(GR/\phi) + B \qquad [8.4]$$

where M and B are the slope and y-intercept of the regression analysis of and I_{gr} vs GR/ϕ crossplot, respectively, and:

$$I_{gr} = \frac{GR - GRmin}{GRmax - GRmin} \qquad [8.5]$$

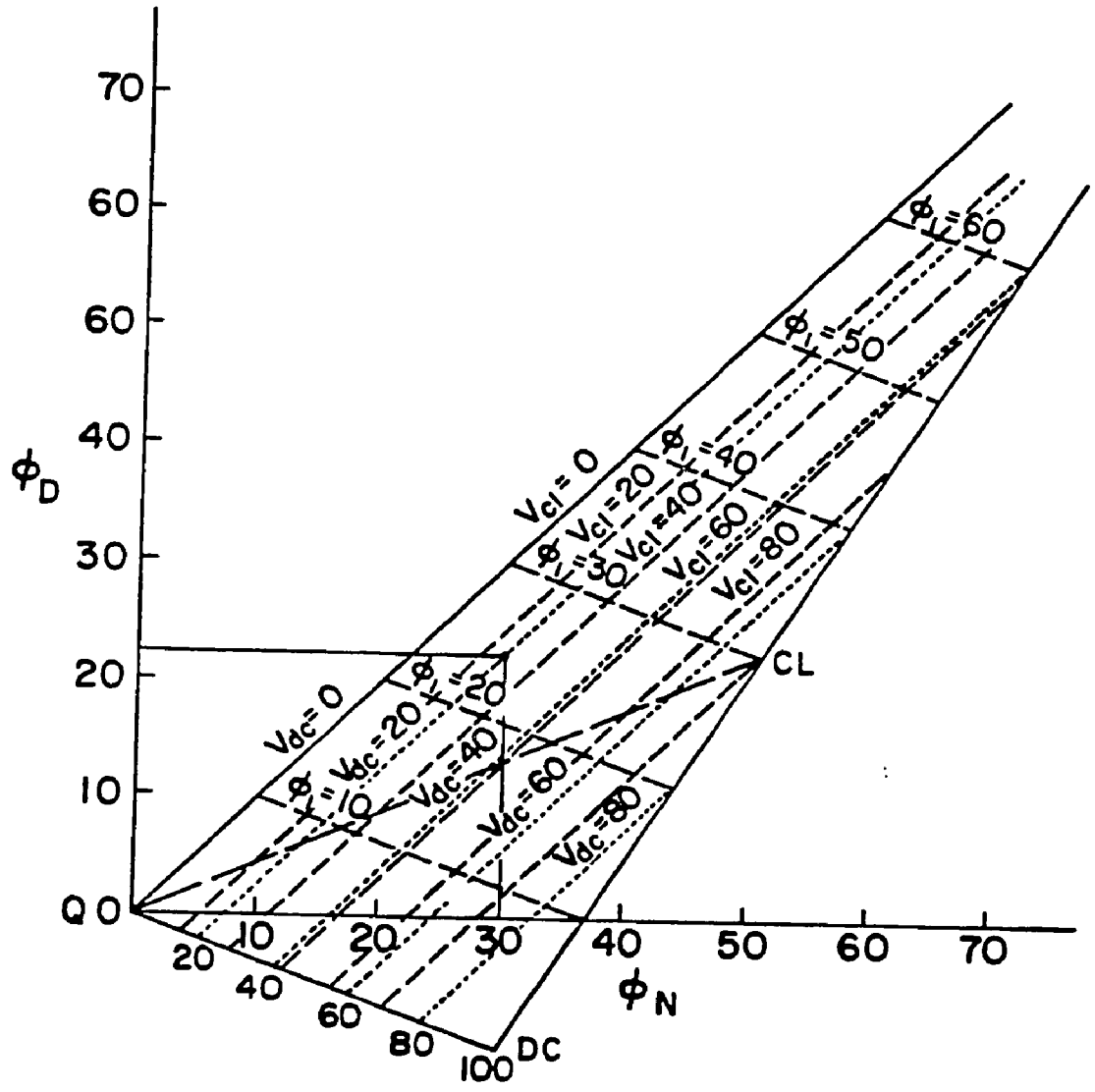

Fig. 8.1 Cyberlook-FDC/CNL Crossplot

where:

GR=gamma ray log reading

GRmin=minimum gamma ray reading

GRmax=maximum gamma ray reading

For the SP log[2]:

$$10^{SP/K}=\frac{[S_w \cdot C_w+S_{wb}(C_{wb}-C_w)]S_{xo}}{[S_{xo} \cdot C_{mf}+S_{wb}(C_{wb}-C_{mf})]S_w} \qquad [8.6]$$

where:

S_{wb}=bound water saturation

S_{xo}=mud filtrate saturation in the invaded zone

C_{mf}=mud filtrate conductivity

C_{wb}=bound water conductivity

Good values of S_w, S_{xo} and C_{wb} are necessary; and iterative process is also required to obtain S_{wb}.

For the resistivity logs:

$$S_{wb}=S_w\frac{(C_{we}-C_w)}{(C_{wb}-C_w)} \qquad [8.7]$$

where $Cwe=F \cdot Ct/S_w^n$ and S_w is initially assumed to be 100%. An iteration process is necessary to obtain S_{wb}. Also, there must be a sufficient difference between C_{wb} and C_w to prevent S_{wb} from being overly sensitive to small anomalies in the data.

8.3 THE LSU MODEL:

The LSU model is based on dual water and cation exchange capacity concepts. This model is built on the premise that clay counterions behave as an equivalent sodium chloride electrolyte. The theoretical principles behind the model have been detailed in Chapters 3 to 6.

The LSU shaly sand interpretation technique consists of two parts:

a.- conductivity model

b.- spontaneous potential model

The conductivity and SP models can be written in resistivity terms as:

$$R_t = \frac{Fe \cdot R'_{eq} \cdot R_w}{S_w^n [R_w \cdot n'_{eq} \cdot v'_{fdl} + (1-v'_{fdl}) R'_{eq}]} \qquad [8.8]$$

and

$$SP = \frac{-2RT}{F} \int_{m2}^{m1} m_{eff} \, d\ln(m'_{\pm}) \qquad [8.9]$$

$$+\frac{2RT}{F} \int_{m2}^{m1} \frac{R_w \cdot n'_{eq} \cdot v'_{fdl} + tna^+ (1-v'_{fdl}) R'_{eq}}{R_w \cdot n'_{eq} \cdot v'_{fdl} + (1-v'_{fdl}) R'_{eq}} \, d\ln(m'_{\pm})$$

Chapter 7 showed that the conductivity and SP models are a function of fluid saturation, Qv and R_w only. Hence, in shaly formations containing a hydrocarbon/water contact, Qv and R_w can be determined from the simultaneous solution of Eqs. 8.7 and 8.8, using log readings from the water bearing zone. Once R_w is calculated the hydrocarbon potential of the interval can be determined by solving simultaneously for Qv and S_w for each depth under analysis.

If a water contact is missing S_w, Qv, and R_w can be determined using an iterative process. This technique can be tedious, however, in exploration situations, this is the only method available to estimate the hydrocarbon potential of a shaly formation.

8.3.1 Input Data Needed in the LSU Model:

Three input data are needed in the LSU model, namely, formation factor, formation resistivity, and spontaneous potential. All three variables can be determined from well logs. Formation Resistivity, R_t, and spontaneous potential, SP, can be read directly from the deep resistivity and the SP logs, respectively. The formation factor in clean sands can be calculated using:

$$F=\frac{a}{\phi^m} \qquad [8.10]$$

In shaly sands the parameters 'a' and 'm' can change from those used in the clean sand model. For an accurate determination of F, these two parameters must be determined from special core analysis. In this study, when core data was not available, 'm' and 'a' were assumed to be equal to 2 and 0.81, respectively.

Porosity in shaly sands can be best determined from neutron-density crossplots (Fig. 8.2). This ternary diagram is defined by the "sand point", "shale point", and "water point" at its vertices. The sand point corresponds to a sandstone neutron porosity of zero, and a bulk density of 2.65 g/cc. The shale point must be determined from the neutron and density readings of an adjacent shale interval. Finally, the water point corresponds to a neutron porosity of 100% and a bulk density of 1.

Porosity crossplots were constructed for all the intervals analyzed. Porosity values derived from the crossplot

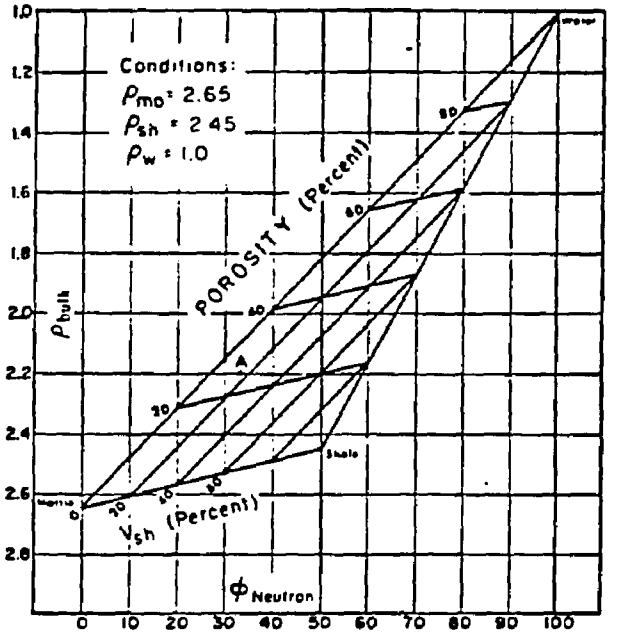

Fig. 8.2 FDC-CNL Crossplot

were compared to porosities obtained from stressed core measurements. Good agreement was observed in liquid filled formations. In gas bearing formations, the "gas effect" must be considered in porosity determination. Hence, an algorithm which accounts for the different clay types and gas densities must be prepared. The development of such algorithm is beyond the scope of this study. In gas bearing formations porosity values were determined from conventional core data when available, or using:

$$\phi=(\phi_n+\phi_d)/2 \qquad [8.11]$$

where:

ϕ_n=sandstone neutron porosity

ϕ_d=sandstone density porosity

Eq. 8.10 is only a porosity estimate, however, it does not differ enough from true porosity to significantly affect fluid saturation calculations.

8.4 FIELD TEST OF THE LSU MODEL:

Multiple intervals from 15 wells were analyzed. These wells were drilled in different geographic locations, and contain different clay types and formation water resistivities. In all cases the newly developed model produced better results than other available techniques.

Examples representing typical situations encountered in shaly sand interpretation are presented hereafter.

EXAMPLE #1: LOW R_w, OIL/WATER CONTACT PRESENT

Well A was drilled in the Gulf Coast Area. The interval of interest is from X298 to X670. From the resistivity curve it is possible to observe that the zone contains an oil/water contact at a depth of X506 (Fig. 8.3). Porosity, Gamma Ray and SP logs (Fig. 8.4) show that shale is present throughout the interval. However, they indicate different proportions of sand and shale. The separation of the neutron-density logs shows that shale content increases with depth, while the gamma ray log shows a constant V_{sh} in the interval of interest. The SP log, on the other hand, illustrates decreasing shale content with depth, see Fig. 8.5. This example shows how V_{sh} models can yield different S_w values depending on the shale indicator used to calculate V_{sh} or S_{wb}.

Core samples from an offset well showed that the reservoir rock contains illite-smectite clays. Formation water resistivity was determined from water samples to be 0.018 ohm/m at formation temperature. This R_w indicates that this example falls on the straight line portion of the C_o-C_w plot.

The LSU model was used to analyze the interval of interest. Shale efficiency was determined to be 0.80 from an adjacent water sand, see Sec. 6.3. Qv and R_w were computed from the water bearing zone, at X680 ft. An R_w=0.02 ohm/m and a Qv=0.25 were determined. The computed and measured R_w's show remarkable agreement attesting to the reliability of the proposed technique. The hydrocarbon bearing interval was evaluated using the technique presented in Sec. 7.3, the

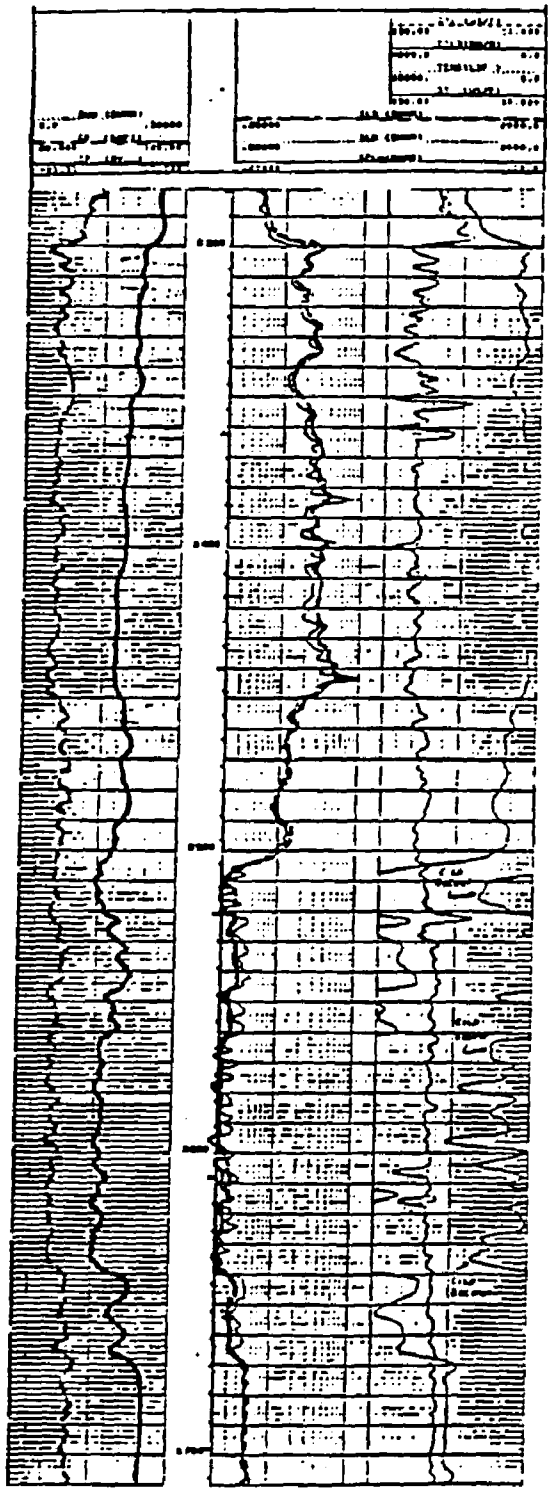

Fig. 8.3 Resistivity Logs-Well A

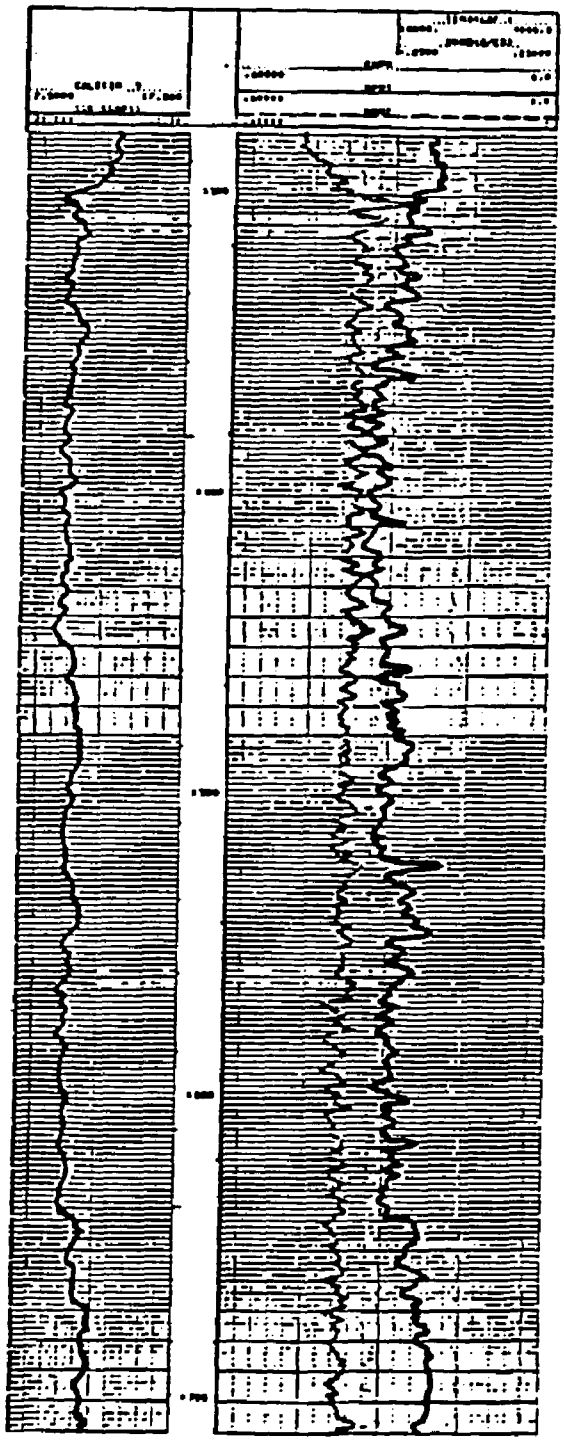

Fig. 8.4 Porosity Logs-Well A

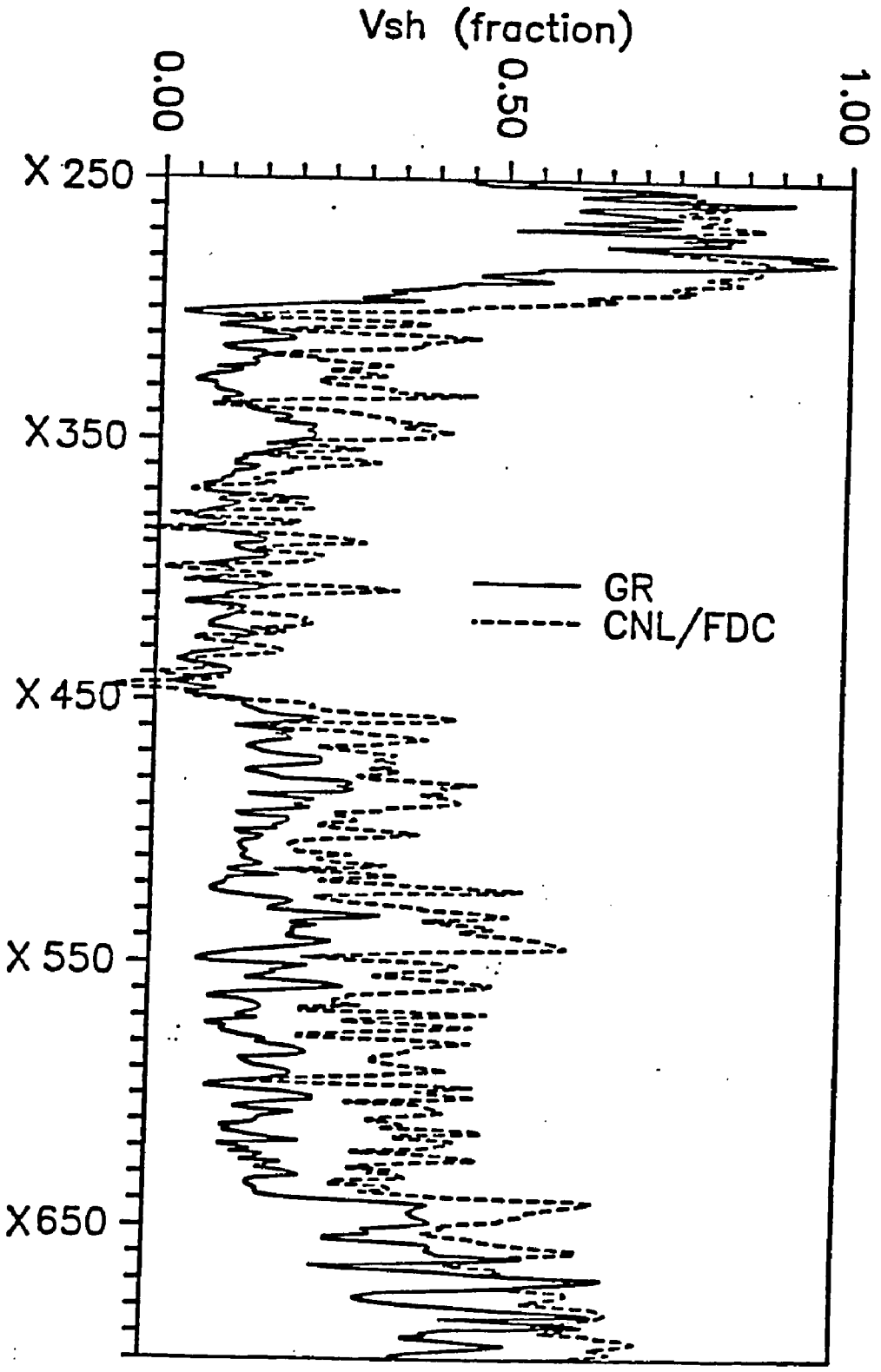

Fig. 8.5 Comparison of different V_{sh} indicators

results are presented in Table 8.1 and Fig. 8.6.

Fig. 8.7 shows a comparison of the Cyberlook, Archie, and the LSU models. From this figure it is apparent that the Cyberlook predicts unlikely low S_w values, i.e. S_w=0.05. Since the formation is not very shaly, saturation values derived from Archie's equation appear reasonable. However, the R_w used in the model was not obtained from clean sand models, instead, it was determined from water samples. A reasonable R_w cannot be obtained from clean sand models.

The LSU model, on the other hand, provided reasonable R_w and S_w values.

EXAMPLE #2: HIGH R_w, OIL/WATER CONTACT PRESENT

Well B was drilled onshore California. The interval studied is between X040 and X462. Resistivity and porosity logs are presented in Figs. 8.8 and 8.9 respectively.

In this example, as in well A, inspection of porosity, gamma ray and SP logs show different V_{sh} trends. Core samples and cuttings from this well show that smectite is the predominant shale type. An R_w=2.57 ohm-m, at formation temperature, was determined from water samples. At this salinity, the free electrolyte conductivity falls on the curved portion of the C_o-C_w plot. This fact, makes this case one of the most complex problems encountered in well log interpretation. Since V_{sh} models cannot be properly calibrated in the curved protion of the C_o-C_w plot.

In this well, the deep induction log shows an increase

Table 8.1

Evaluation of Well A

Depth	Porosity	S_w	Qv
X275	0.39	0.28	0.40
X304	0.30	0.27	0.40
X328	0.31	0.22	0.25
X416	0.36	0.19	0.16
X460	0.35	0.26	0.30
X470	0.34	0.28	0.30
X500	0.35	0.37	0.30
X510	0.35	0.81	0.30

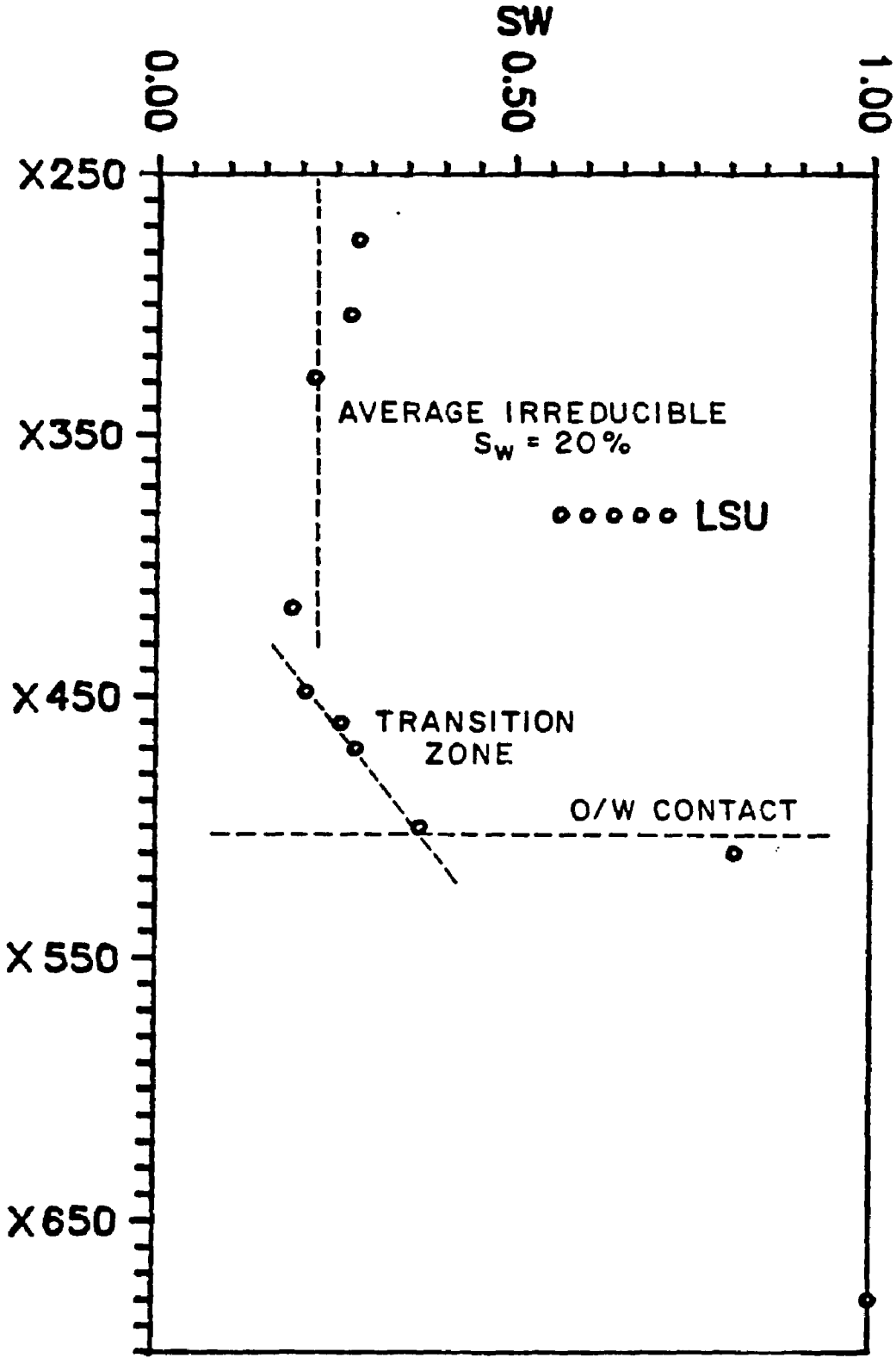

Fig. 8.6 Evaluation of Well A using LSU model

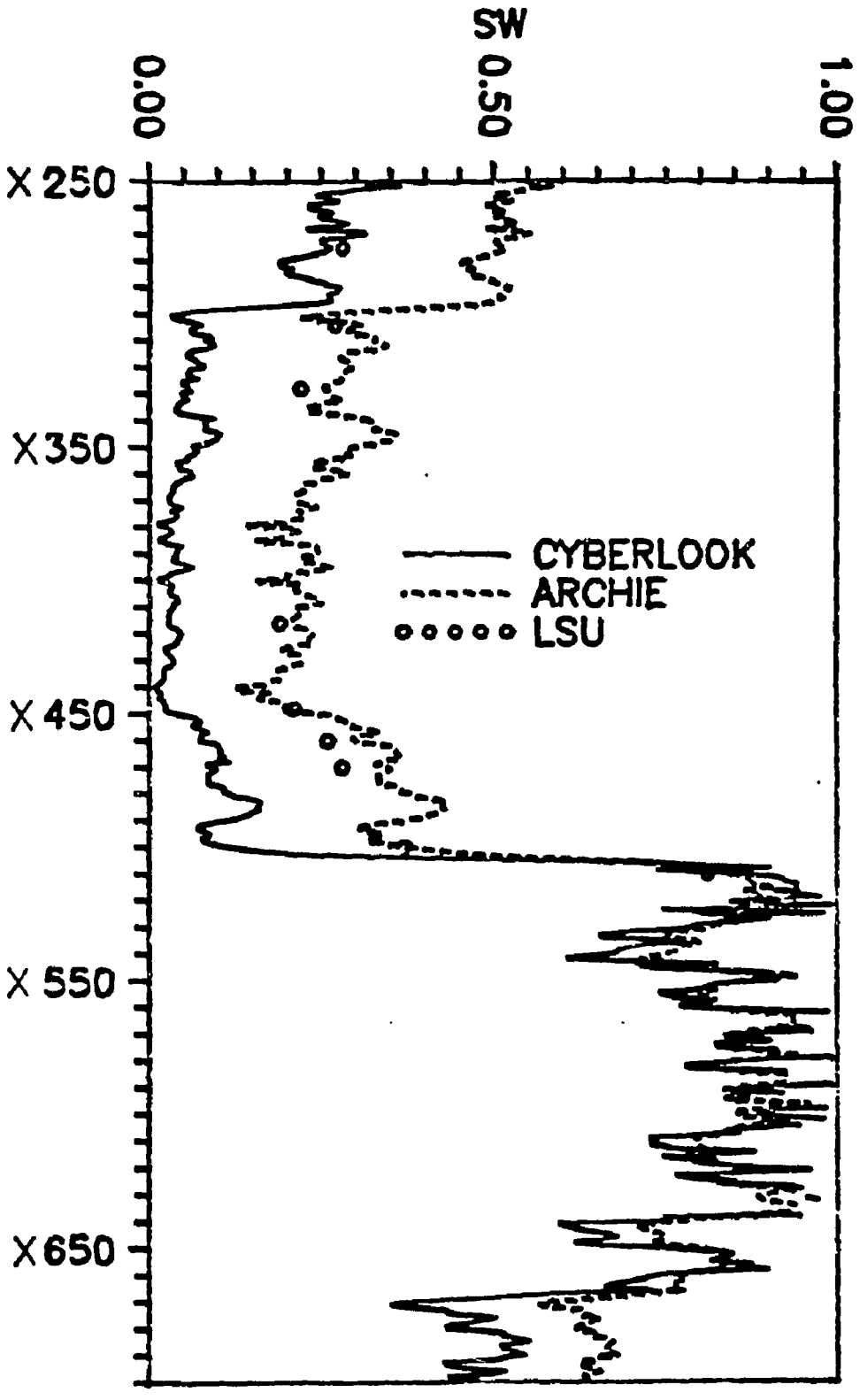

Fig. 8.7 Comparison of Cyberlook, Archie and LSU methods

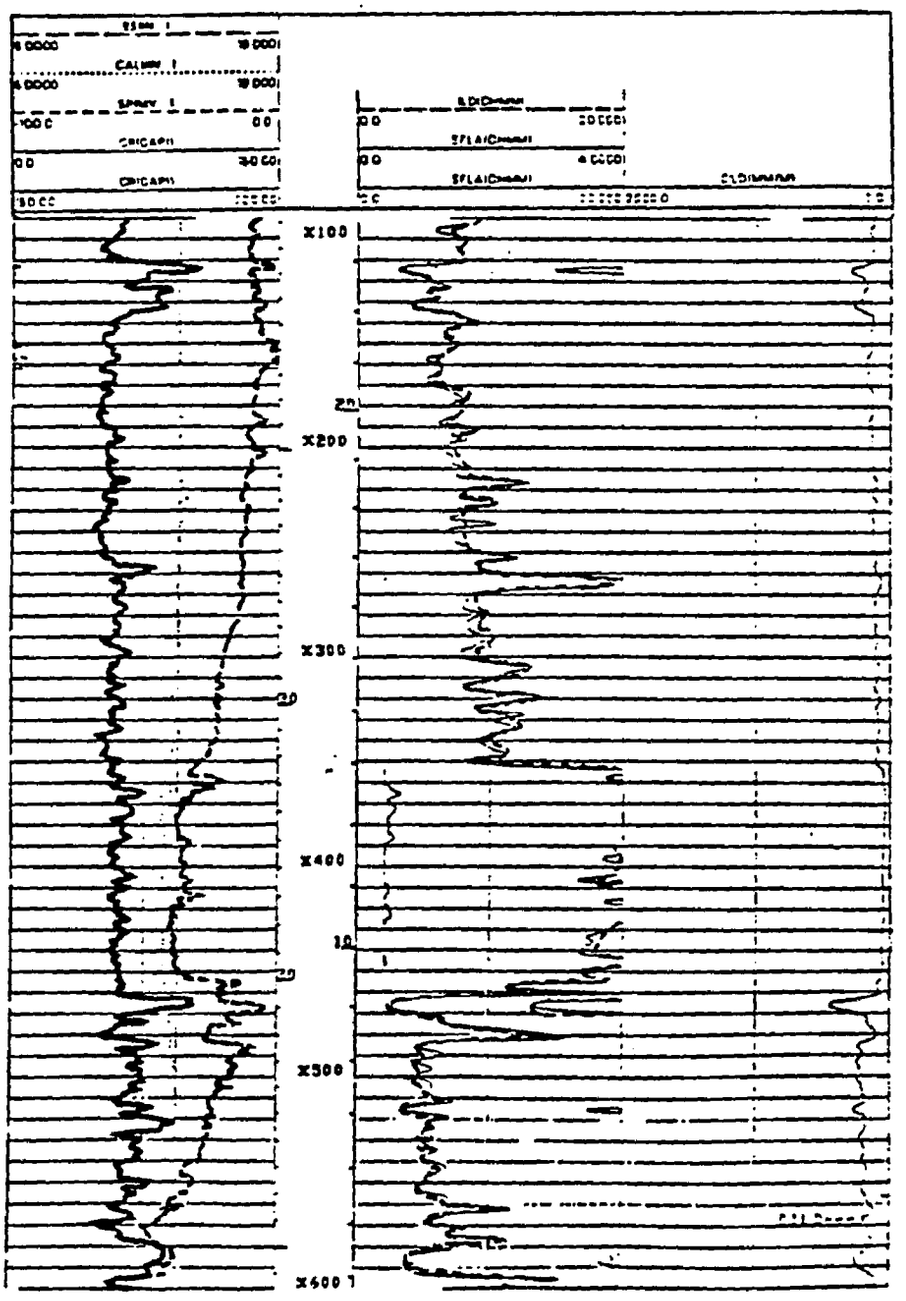

Fig. 8.8 Resistivity Logs-Well B

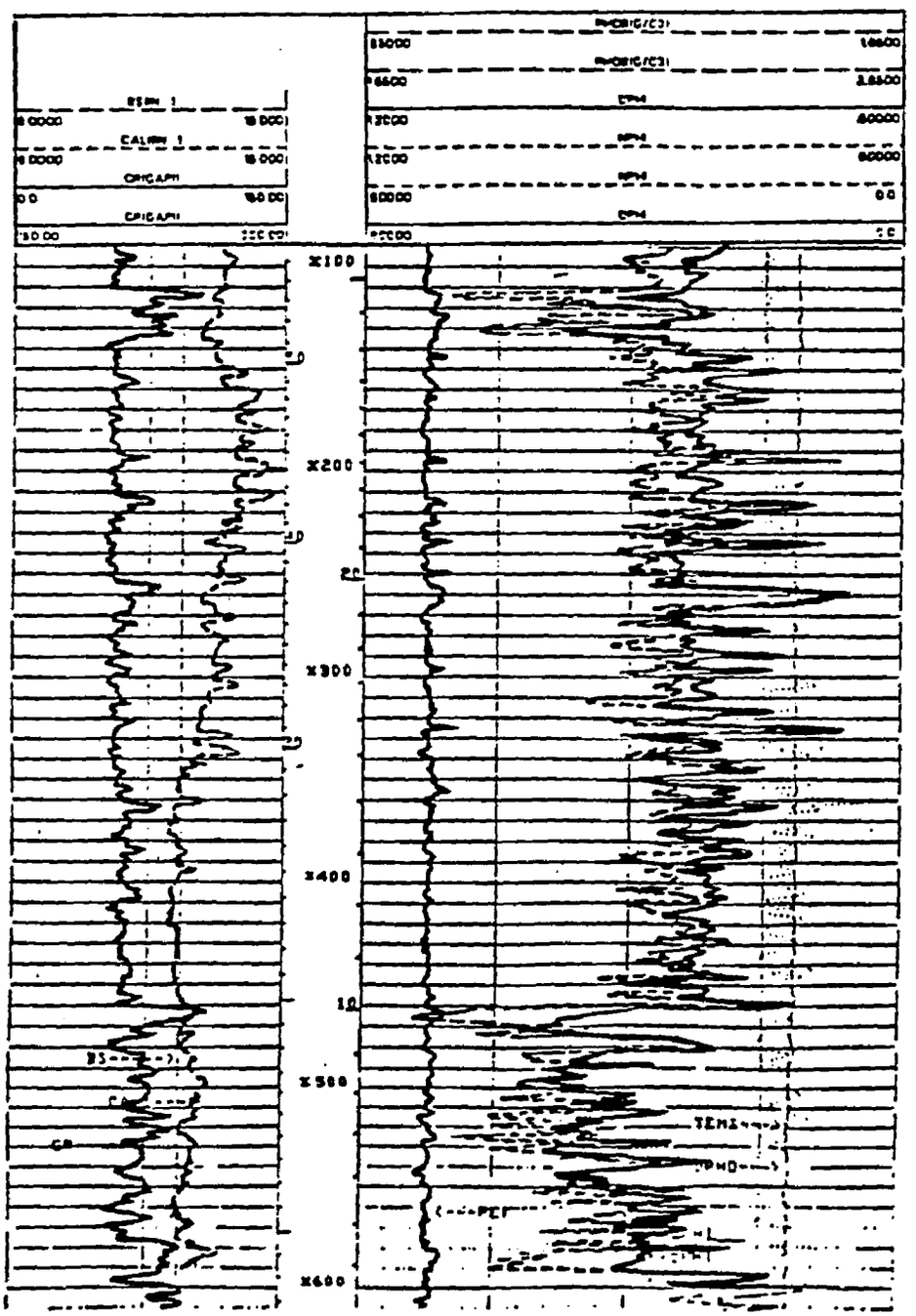

Fig. 8.9 Porosity Logs-Well B

in formation resistivity in the interval between X350 to X462. The high resistivity readings were associated with low water saturations. This interval was tested and produced 100% water. The LSU model was used to estimate fluid saturations in this interval. The proposed model predicted an R_w=2.5 ohm/m and an S_w=100% in this zone. Both values show excellent agreement with water samples and production tests, respectively. A shale efficiency of 1.0 was determined from an adjacent water bearing shaly sand.

The LSU model also predicted that the interval between X040 and X350 ft would be hydrocarbon bearing. This interval was also tested, and produced 90% oil and 10% water. This production test also reflects the calculated S_w values (Table 8.2).

Figure 8.10 compares the Cyberlook, Archie and LSU methods. This figure shows that indeed V_{sh} and clean sand models are inappropriate for formations that fall on the curved portion of the C_o-C_w plot. This example illustrates the absolute need for the LSU interpretation model which does not rely on V_{sh} concepts, but is based on principles that reflect the conductive behavior of the formation water and clay counterions.

EXAMPLE #3: VERY SHALY SANDS, NO OIL/WATER CONTACT

This example presents two wells, Well C and D, from the Gulf Coast Area. Both wells penetrated the same formation, in Well C the formation is present from X480 to X672, while in

Table 8.2

Evaluation of Well B

Depth	Porosity	S_w	Qv
X050	0.23	0.25	1.00
X105	0.27	0.25	1.00
X157	0.23	0.30	0.98
X200	0.25	0.30	0.97
X300	0.24	0.35	0.25
X340	0.23	0.38	0.15
X349	0.28	0.60	0.10
X400	0.22	0.92	0.05
X450	0.22	0.95	0.02

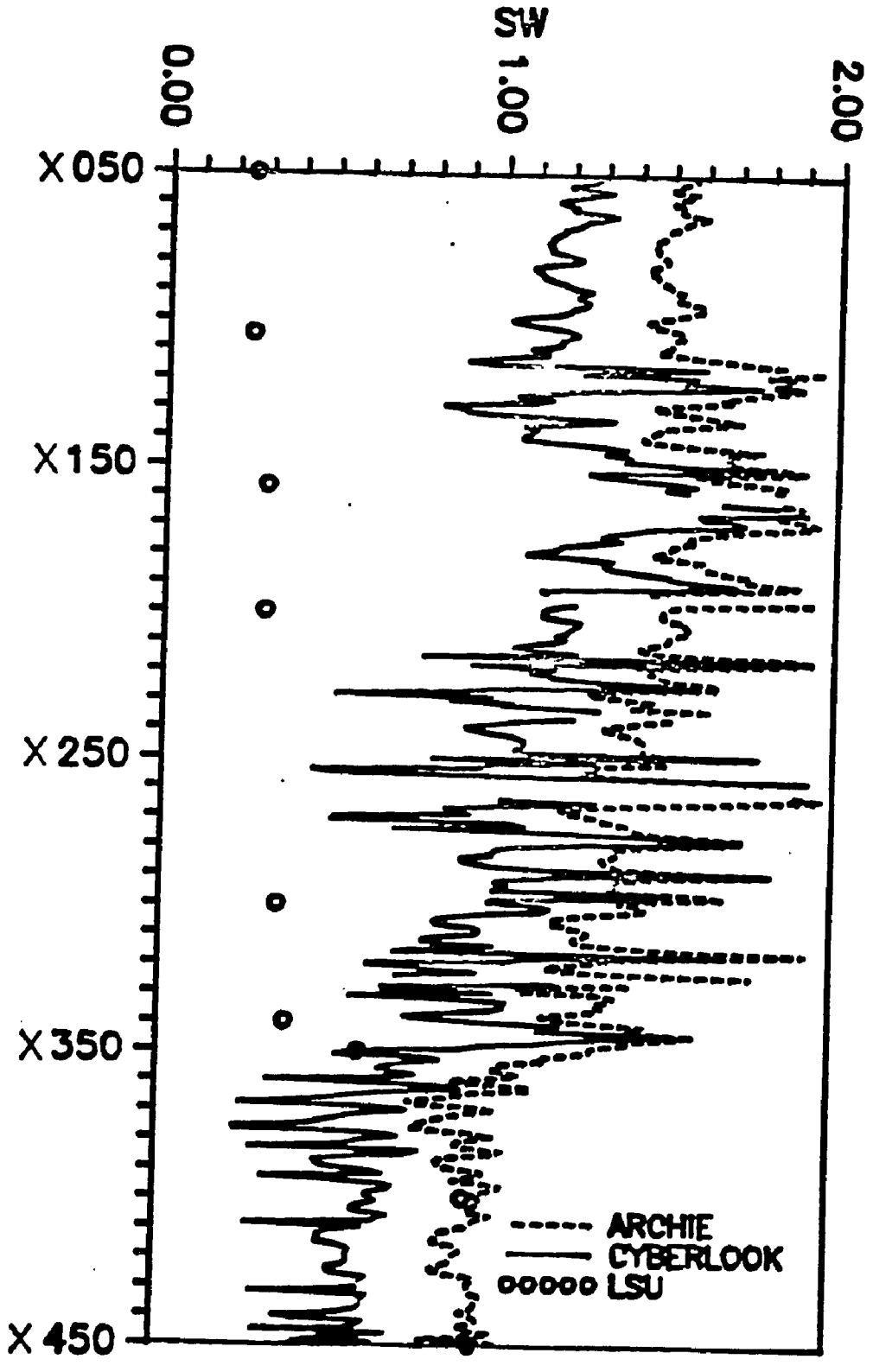

Fig. 8.10 Comparison of Cyberlook, Archie and LSU methods

Well D it is present from X616 to X880. Porosity and resistivity logs are illustrated in Figs. 8.11 and 8.12 for Well C and Figs. 8.13 and 8.14 for well D, respectively.

Porosity logs, Figs. 8.12 and 8.14, show a very shaly interval. Mineralog Analysis performed in core plugs from well D shows that illites-smectites are the predominant clay type, traces of kaolinite also appeared. By mere visual inspection, the resistivity logs, Figs. 8.11 and 8.13, show no apparent hydrocarbon saturation in well C and only few thin zones with high resistivity in well D. Nevertheless, gas shows were clear in mud logs from both wells.

The interval in well C between X606 and X672 was perforated and tested. This test produced 4.6MMCF and no water. Resistivity logs in this lower zone show no deflection from the shale resistivity line.

Since, there are no clean sands in more that 1500 ft above or below the zone of interest V_{sh} models, i.e. Cyberlook, cannot be calibrated, and parameters such as R_w and S_{wb} must be guessed. Archie's equation is completely inappropriate, because the degree of shaliness and the lack of a reliable R_w. For these reasons, neither the Cyberlook or Archie's methods can be used in this case.

The LSU model does not require clean sand calibrations and allows the determination of R_w and S_w from the resistivity data of the interval of interest. Using this model water resistivities of 0.05 and 0.055 ohm/m at 75°C were obtained from wells C and D, respectively. The good agreement between

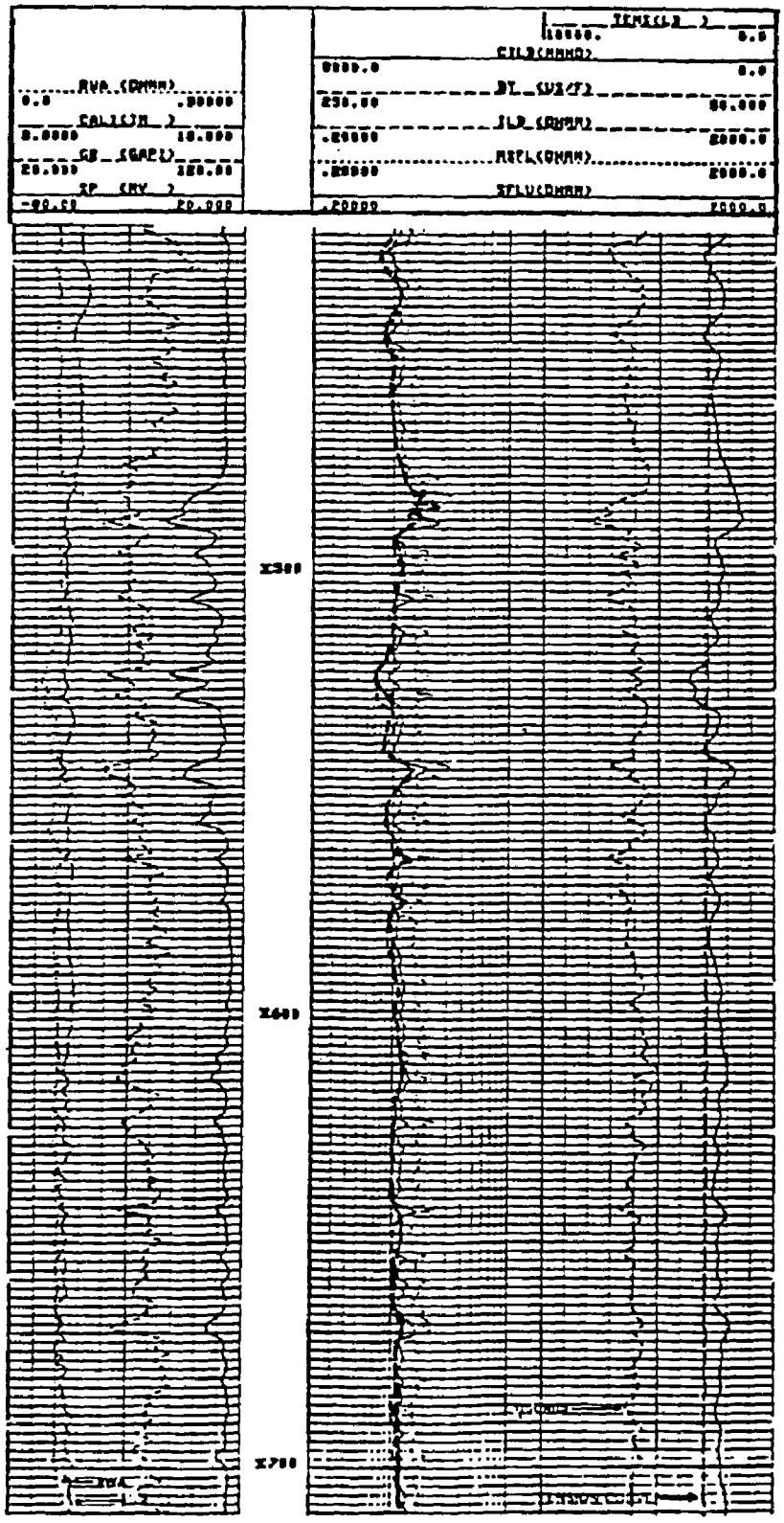

Fig. 8.11 Resistivity Logs-Well C

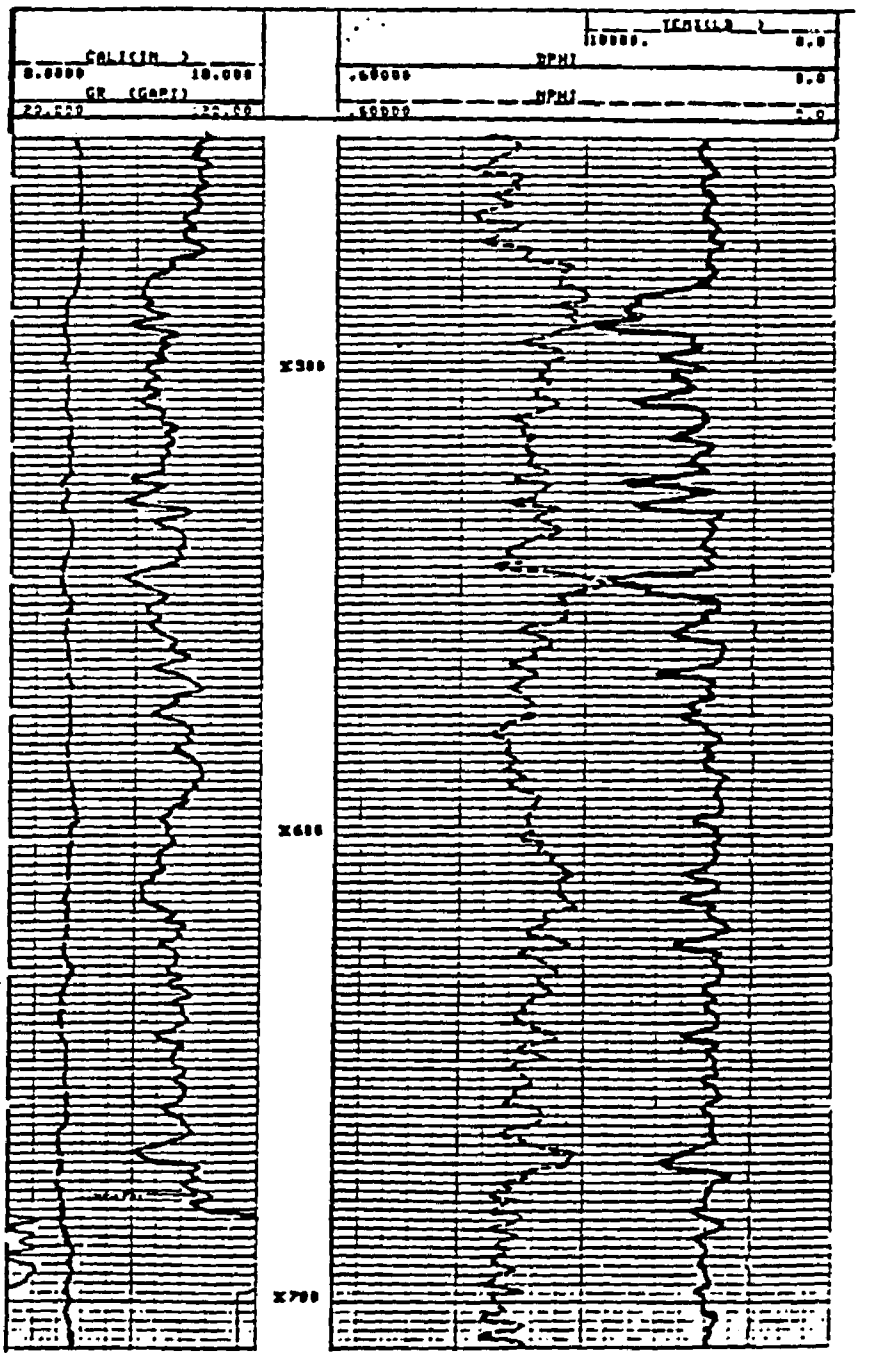

Fig. 8.12 Porosity Logs-Well D

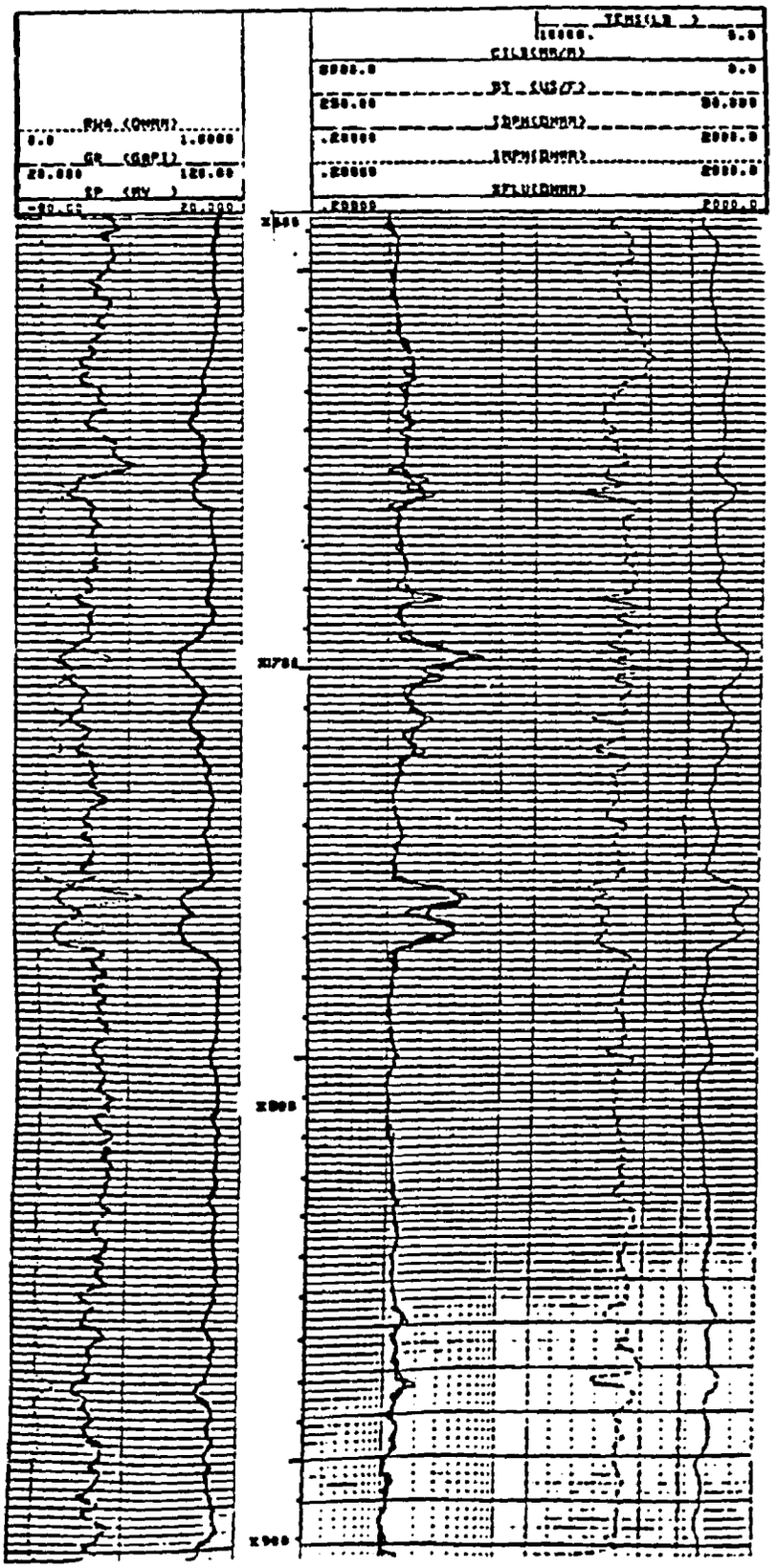

Fig. 8.13 Resistivity Logs-Well D

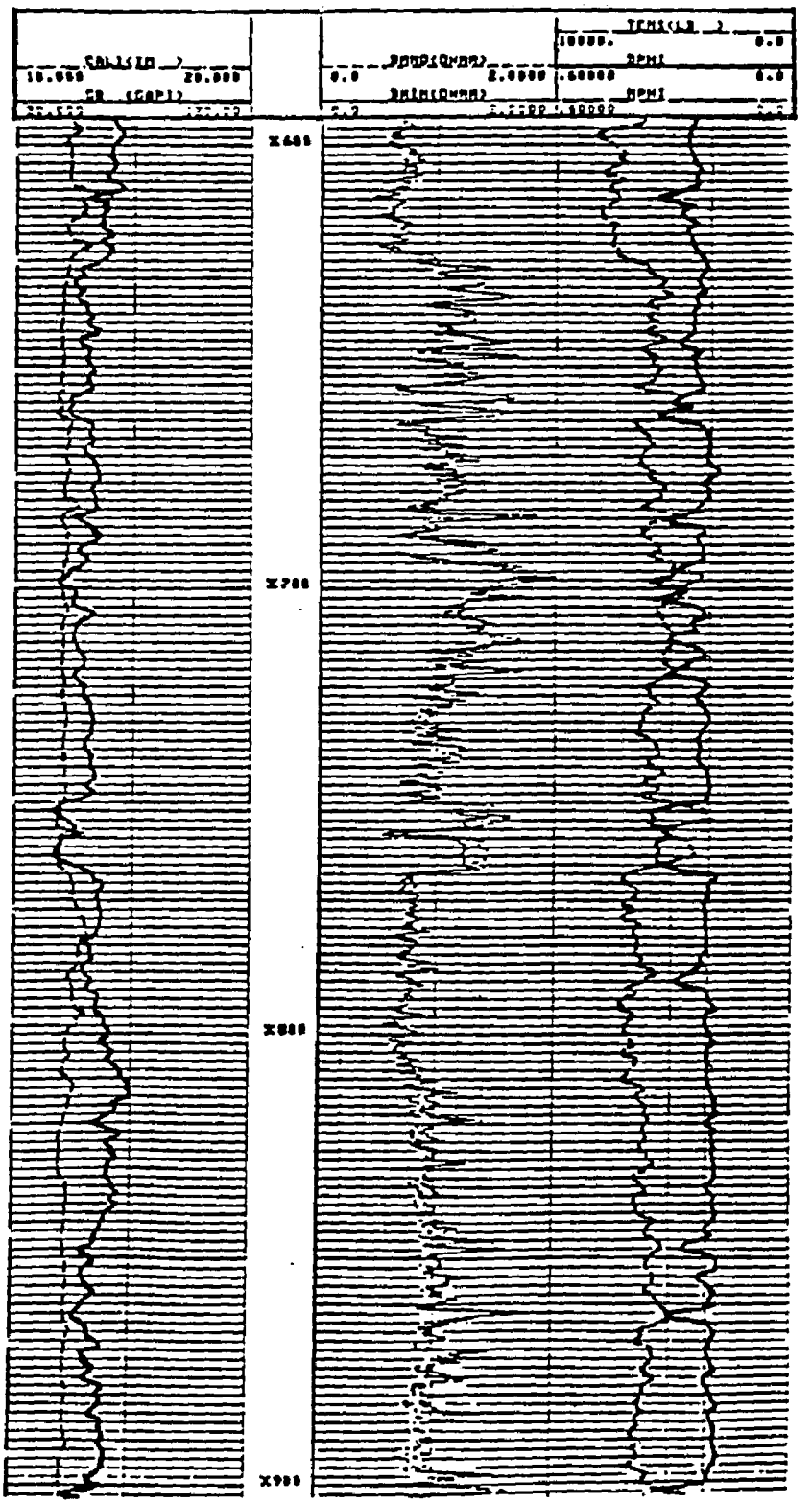

Fig. 8.14 Porosity Logs-Well D

these two values attest for the reliability of the intrepretation. Using log responses from a water bearing shaly sand, a shale efficiency of 0.8 was determined for both wells. S_w values calculated using the iterative process detailed in Sec. 7.3 reflect production test results accurately, see Tables 8.3 and 8.4.

EXAMPLE # 4: TYPICAL GULF COAST SHALY SAND

The section analyzed in well E is between X220 and X580 ft. This interval contains two sands of interest. Porosity and resistivity logs are shown in Figs. 8.15, 8.16, 8.17 and 8.18. This type of sands are commonly found in the Gulf Coast Region. Both sands were cored and showed residual gas saturation in their upper sections.

Porosity logs show that both intervals are shaly. However, gas effect overshadows the shale effect, in fact between X497 and X510 both effects cancel each other. In this case, porosity was determined from conventional core analysis. Formation water resistivity, R_w=0.08 ohm/m at 75°C was calculated from an adjacent clean water bearing sand. From the same clean sand a membrane efficiency, m_{eff}=0.8, was also calculated.

Formation water resistivities were determined using the LSU model. R_w's of 0.084 ohm/m and 0.073 ohm/m at 75°C were obtained from the upper and lower sands, respectively. In both cases, there is good agreement between the R_w's calculated from the shaly interval and the clean sand.

Table 8.3

Evaluation of Well C

Depth	Porosity	S_w	Qv
X488	0.28	0.33	0.15
X506	0.30	0.42	0.75
X522	0.31	0.49	0.50
X528	0.32	0.48	0.50
X546	0.27	0.37	0.60
X556	0.30	0.46	1.10
X614	0.25	0.44	1.10
X643	0.26	0.42	1.10
X649	0.26	0.42	1.0

Table 8.4

Evaluation of Well D

Depth	Porosity	S_w	Qv
X644	0.30	0.30	0.40
X660	0.30	0.26	0.32
X684	0.30	0.29	0.45
X697	0.30	0.20	0.22
X712	0.30	0.28	0.32
X718	0.30	0.30	0.40
X752	0.28	0.20	0.23
X760	0.29	0.22	0.23
X864	0.30	0.32	0.40

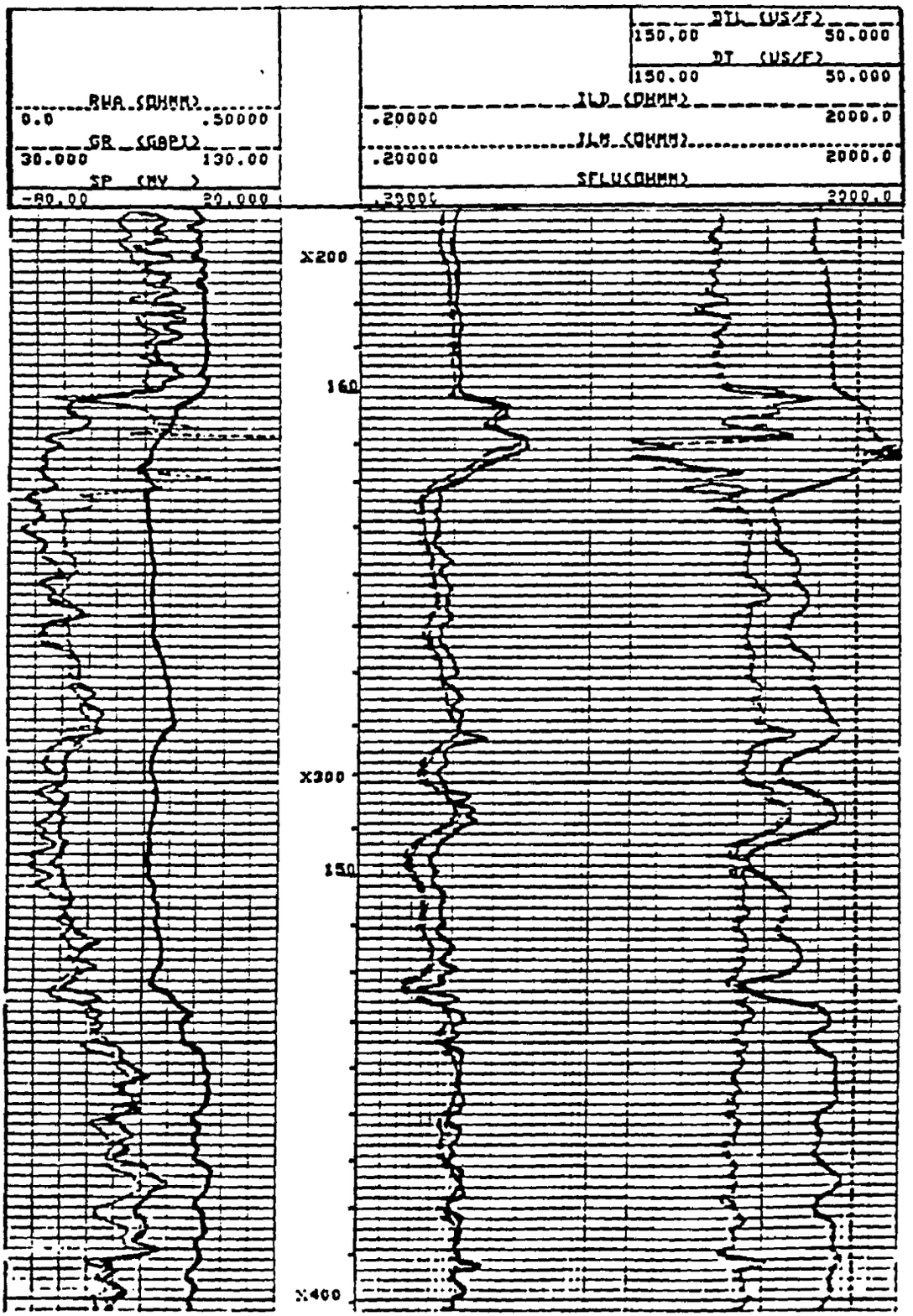

Fig. 8.15 Resistivity Logs-Well E

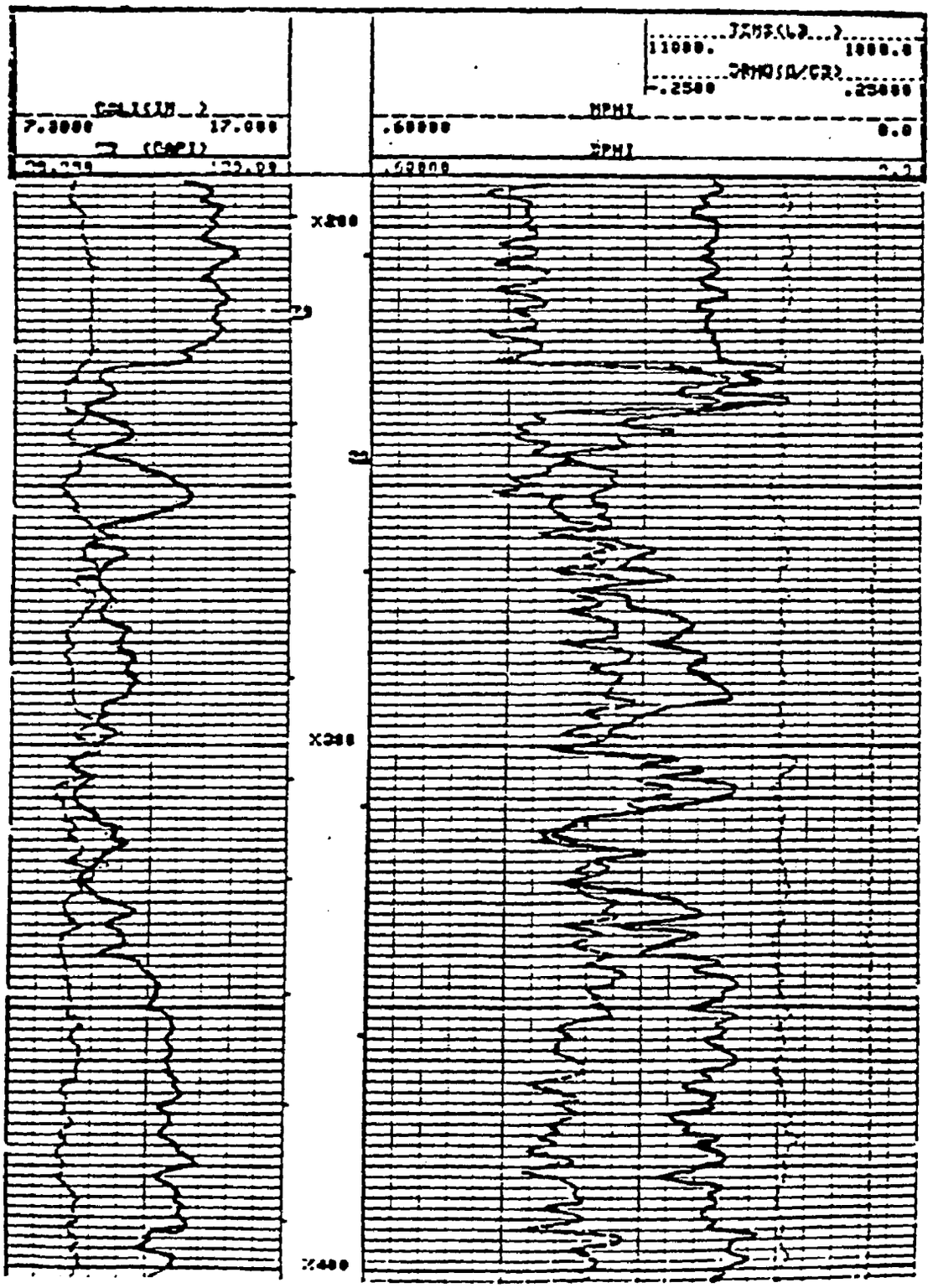

Fig. 8.16 Porosity Logs-Well E

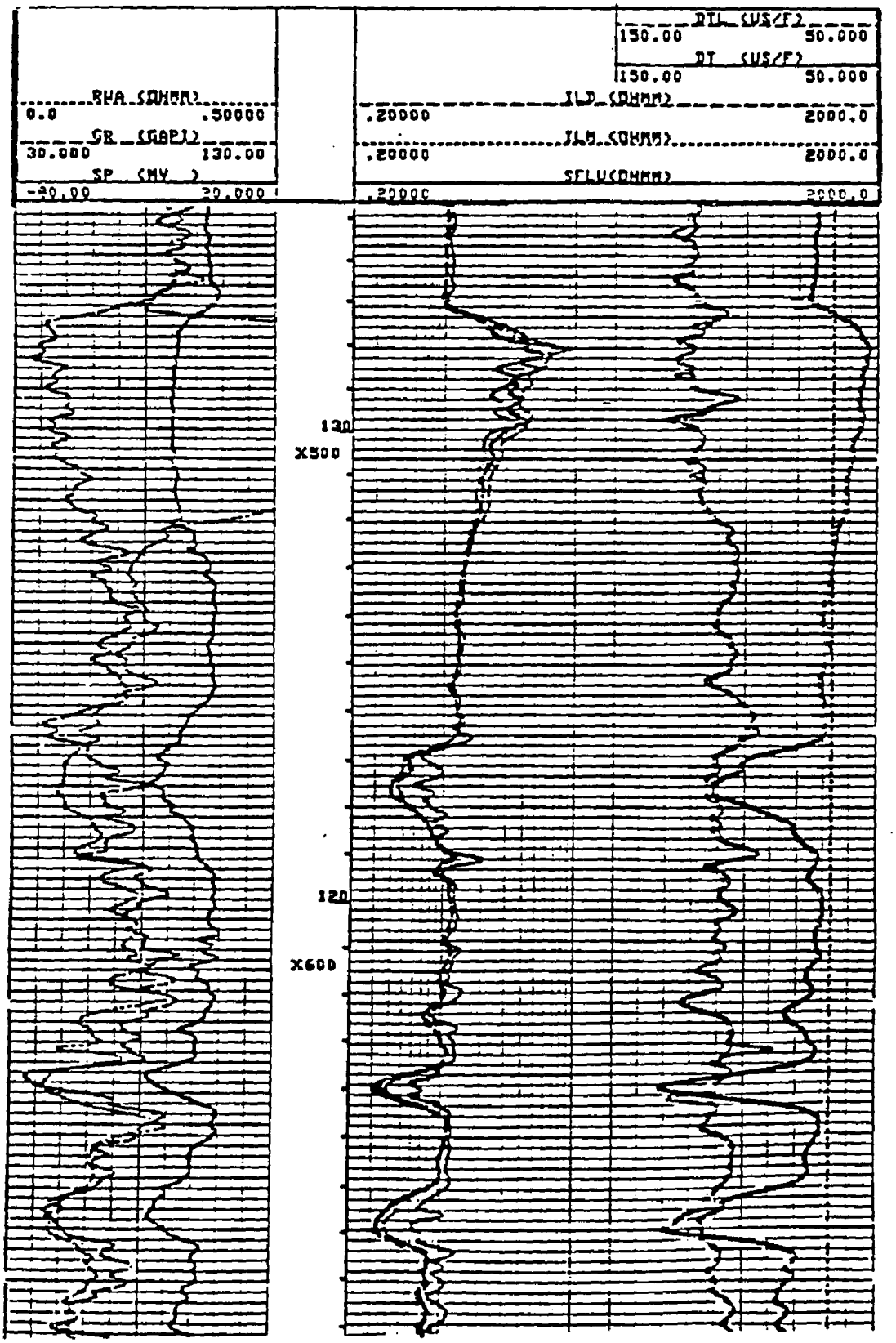

Fig. 8.17 Resistivity Logs-Well E

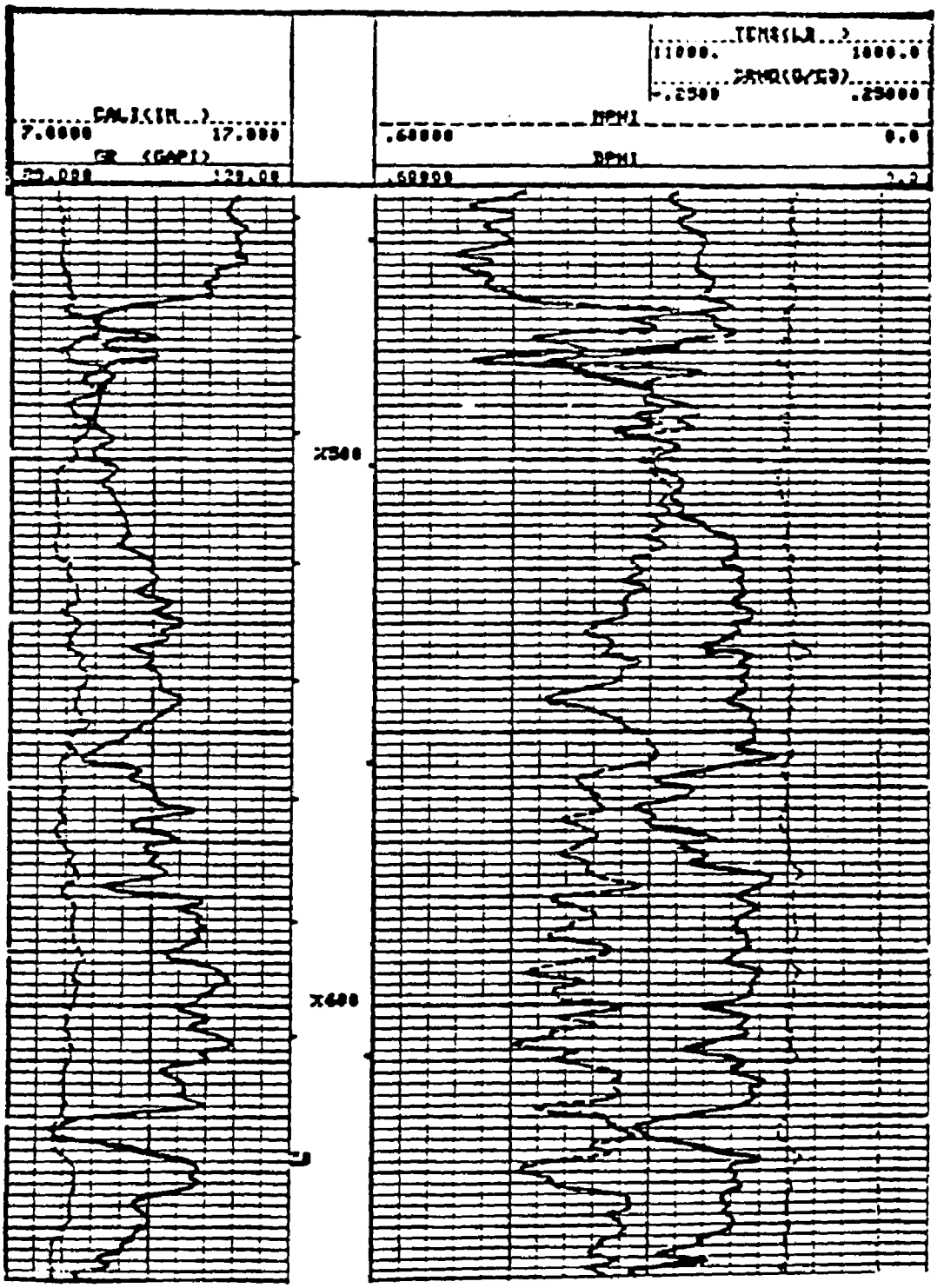

Fig. 8.18 Porosity Logs-Well E

Table 8.5 presents a comparison among the clean sand, Cyberlook and LSU models. S_{wb} for the Cyberlook model was calculated from gamma ray readings. This comparison shows that the 3 methods converge at low Qv values as expected. The difference among the methods increases as Qv increases. However, both Cyberlook and LSU models give similar results.

8.6 DISCUSSION OF RESULTS:

From the examples presented in this chapter, and other wells analysed it is obvious that there is a definite need for a reliable shaly sand interpretation model. It is believed that the LSU model can help to fulfill such a need. In all wells analyzed the LSU model has consistently predicted accurate R_w and S_w values.

The newly developed model is indispensable in two situations: i) when there are no clean water bearing sands near the shaly sand of interest and ii) when the formation water resistivity falls on the curved portion of the C_o-C_w plot. In these two instances, V_{sh} models can not be calibrated to estimate fluid saturations. In cases where R_w falls on the straight line portion of the C_o-C_w plot V_{sh} models can be calibrated by manipulating S_{wb} and R_{wb}, to yield reasonable fluid saturation estimates.

Finally, from all the intervals interpreted, it appears that m_{eff} equals 0.8 for the Gulf Coast Region.

Table 8.5

Evaluation of Well E

Depth	ϕ_{core}	Qv	S_{wLSU}	S_{wcyber}	S_{wclean}
X236	0.29	0.07	0.30	0.35	0.37
X243	0.28	0.16	0.39	0.43	0.56
X249	0.25	0.40	1.00	1.30	1.32
X315	0.27	0.28	1.00	1.30	1.31
X479	0.33	0.13	0.16	0.19	0.23
X485	0.28	0.22	0.25	0.32	0.37
X495	0.28	0.25	0.30	0.37	0.42
X508	0.26	0.38	0.40	0.46	0.61
X561	0.25	0.70	0.90	1.26	1.31
X565	0.25	0.45	0.97	1.34	1.40

CONCLUSIONS

A new shaly sand interpretation technique has been developed. The technique makes use of new conductivity and spontaneous potential models, refered as the LSU models. Both models are based on cation exchange capacity and dual water concepts. The bound water is treated as a hypothetical electrolyte, the properties of which are related to those of an equivalent sodium chloride solution. This approach is the cornerstone of the proposed models, and allows the application of electrochemical and irreversible thermodynamics theory in the determination of the equivalent counterion conductivity. In addition, the proposed spontaneous potential model incorporates the water transport number.

The ability of the new models to accurately predict the electric behavior of shaly sands has been tested at a wide range of temperatures using reliable conductivity and membrane potential data.

Multiple intervals of 15 wells representing different i)geographic locations, ii) degrees of shaliness, iii) clay types and iv) formation water salinities, were used to test the new model at field conditions. In all cases, the LSU model predicted accurate R_w and S_w values, while other methods failed to properly evaluate the potential of the formations analyzed.

In general, the LSU model is a better indicator of the

hydrocarbon potential of shaly sands, because of its solid theoretical foundation. Moreover, the new model acquires all its input parameters from the zone of interest. Consequently, it is the only method capable of determining the hydrocarbon potential when the formation is shaly and contains relatively fresh water and when there are no clean water bearing sands near the shaly sand of interest.

RECOMMENDATIONS

The LSU model is a new approach that better represents the conductivity behavior of shaly sands. However, research work is needed to determine a method to accurately estimate formation factors of shaly sands. The problem is especially complex in gas bearing formations, where a porosity model accounting for the different clay types and gas densities must be developed. Until this problem is resolved, shaly sand interpretation will still present a challenge to log analysts and reservoir engineers.

NOMENCLATURE

a= equivalent ion size (Å)

a= Archie's Constant

B= Waxman's equivalent counterion conductivity (cc-mho-/(meq m)

B_2= electrophoretic constant

C_{cl}= clay conductivity, mho-m

C_{eq}= equivalent counterion conductivity, mho-m

C_{eq}'= equivalent counterion conductivity for $S_w<1$, mho-m

$C_{eq}°$= equivalent conductivity at infinite solution, mho-m

C_{hsh}= conductivity of hydrocarbon bearing shaly sand, mho-m

C_{mf}= mud filtrate conductivity, mho-m

C_{sh}= shale conductivity, mho-m

C_o= conductivity of formation fully saturation with water, mho-m

C_t= formation conductivity, mho-m

C_w= water conductivity, mho-m

C_{wb}= bound water conductivity, mho-m

C_{we}= equivalent water conductivity, mho-m

C_{wn}= water conductivity at the neutral point, mho-m

Em= electrochemical potential, mV

Em_{sh}= electrochemical potential across shales, mV

Em_{ss}= electrochemical potential across shaly sand, mV

F= formation factor

F^*= formation factor in W-S model

F_e= formation factor in LSU model

F_o= formation factor in D-W model

f_{dl}= expansion factor of the double layer

f_{dl}^{25}=expansion factor of the double layer at 25°C

f_{dl}^{t}= expansion factor of the double layer at T>25°C

fg= empirical correction factor

F(ne)=empirical correction factor

GR= gamma ray log readings, API

GRmin= minimum gamma ray log reading, API

GRmax= maximum gamma ray log reading, API

l_{33}= ionic transport coefficient

l_{34}= ionic transport coefficient

l_{44}= ionic interaction coefficient

m= cementation exponent

m= molality, mol/kg H_2O

n= molarity, mol/l

n= saturation exponent

n_e= saturation exponent in W-S model

n_{eq}= equivalent counterion conductivity, mol/l

n_{eq}'= equivalent counterion conductivity for $S_w<1$, mol/l

n_{eq}^{25}=equivalent counterion conductivity at 25°C, mol/l

n_{eq}^{T}= equivalent counterion conductivity at T>25°C, mol/l

q_3= ionic transport coefficient

q_4= ionic transport coefficient

Qv= cation exchange capacity, meq/cc

Qv'= cation exchange capacity for $S_w<1$, meq/cc

R= universal gas constant

R_{eq}= equivalent counterion resistivity, ohm/m

R_{mf}= mud filtrate resistivity, ohm-m

R_{mfe}= equivalent mud filtrate resistivity, ohm-m

R_o= resistivity of formations fully saturated with water, ohm/m

R_t= formation resistivity, ohm/m

R_w= formation water resistivity, ohm/m

R_{wb}= bound water resistivity, ohm/m

R_{we}= equivalent water resistivity, ohm/m

SP= spontaneous potential log reading, mV

S_w= water saturation, fraction

S_{wb}= bound water saturation, fraction

S_{xo}= mud filtrate saturation in the invaded zone, fraction

T= temperature, °C

Ta= absolute temperature, °K

tna^+=sodium transport number

tna^h=Hittorf transport number

Tna^{sh}=shale transport number

Tna^{ss}=shaly sand transport number

tw= water transport number

twf= free water transport number

V_{dc}= volume of dry clay, fraction

V_{dccl}= volume of wet clay, fraction

v_{fdl}= fractional volume of the double layer

v_{fdl}'= fractional volume of the double layer for $S_w<1$

V_{sh}= fractional volume of shale, fraction

X_H= 6.18 Å

α= Clavier's double layer expansion factor

β= 2.05, constant

β= ionic interaction coefficient

$\gamma_{\pm}$= mean activity coefficient

$\gamma_{\pm}^{298}$=mean activity coefficient at 25°C

ϕ= porosity, fraction

ϕ_t= total porosity, fraction

ϕ_{cl}= total clay porosity, fraction

τ= empirical correction factor

BIBLIOGRAPHY

1.- Worthington, P., "The Evolution of Shaly-Sand Concepts in Reservoir Evaluation", The Log Analyst, Jan- Feb. 1985, pp. 23-40.

2.- Log Interpretation Principles/Applications, Schlumberger Document, pp. 111-120, 1987.

3.- Silva P. Development of a New Conductivity Model for Shaly Sand Interpretation, Ph D. Dissertation, LSU, 1986, 117-8.

4.- Waxman M.H. and Smits, L.J.: "Electrical Conductivities in Oil-Bearing Shaly-Sands", J.Pet. Tech., June 1968, 107-122.

5.- Clavier C. Coates G. and Dumanoir J,. "Theoretical and Experimental Bases for the Dual Water Model For Interpretation of Shaly Sands", SPEJ April 1984.

6.- Silva P. and Bassiouni Z., "A Shaly Sand Conductivity Model Based on Variable Equivalent Counter-ion Conductivity and Dual Water Concepts", SPWLA Trans., paper RR, 1985.

7.- Silva P. and Bassiouni Z. "Prediction of Membrane Potentials in Shales and Shaly Sands Using the S-B Conductivity Model", The Log Analyst, March-April 1987, 129-137.

8.- Juhasz I. et al. "The Central Role of Qv and Formation Water Salinity in the Evaluation of Shaly Formations", SPWLA Trans., paper AA, 1979.

9.- Thomas E.C. "The determination of Qv from Membrane Potential Measurements in Shaly Sands", J. Pet. Tech., Sept. 1976.

10.- Staverman A.J.,"Non Equilibrium Thermodynamics of Membrane Processes", Trans. Faraday Soc, v.48, 1952, 176

11.- Stokes R. Electrolyte Solutions, Butterworths Scientific Publications, London, 1955.

12.- Miller D. " Application of Irreversible Thermodynamics to Electrolyte Solutions. I. Determination of Ionic Transport Coefficients l_{ij} for Isothermal Vector Transport Processes in Binary Electrolyte Systems", J. of Phys Chem. v.70, Aug 1966, 2639-59.

13.- Carman P.C. "Transport in Concentrated Solutions of 1-1 electrolytes", J. of Phys. Chem. v.73(4), 1969, 1095-1105.

14.- Smits L.J.M., "SP Log Interpretation in Shaly Sands", J. Pet. Tech., June 1968, 123-136.

15.- Koryta J. and Dvorak J. Principles of Electrochemistry, Jhon Wiley and Sons, 1st ed., 1987, 109.

16.- Della Monica, et al. "Transference Number in Concentrated NaCl Solutions", Electrochim. Acta 24 1013, 1979.

17.- Parropoulus D., Kaneko H. and Spiro M. "Transference Numbers of Sodium Chloride Solutions in Concentrated Aqueos Solutions and Chloride Conductance in Several Concentrated Electrolyte Solutions", J. of Solution Chem., v.15(3), 1986, 243-253.

18.- Smits L, and E.M. Duyvis "Transport Numbers of Concentratede Sodium Chloride Solutions at 25°C", J. of Phys. Chem., 70(9), 1966, 2747-53.

19.- Braun B. and Weingartner H "Transfference Numabers of Aqueous NaCl and $NaSO_4$ at 25°C from EMF measurements with Sodium Selective Glass Electrodes", J. of Solution Chem, v14(9), 1985, 675-686.

20.- Caramazza R. "Transference Numbers of NaCl Solutions", Gazz. Chim Ind., v.90, 1960, 1751.

21.- Trivijitkasem P. and Ostvold T. "Water Transport in Ion Exchange Membranes", Electrochim. Acta, 1987.

22.- Harned, Herbert and Owen, Benton The Physical Chemistry of Electrolyte Solutions, 2nd ed. Reinhold Publishing Co., New York, 1950.

23.- Waxman and Thomas E.C. " Electrical Conductivities in Shaly Sands -I. The Relation of Hydrocarbon Saturation and Resistivity Index; II. The Temperature Coefficient of Electrical Conductivity", J. Pet. Tech., Feb 1974, 213-225.

24.- Lyle T.R. and Hosking R. "The Temperature Variations of the Specific Molecular Conductivity and of the Fluidity of Sodium Chloride Solutions" Phil. Mag. Ser. 6, 3, 487 (1902).

25.- Millero, F.J., "Effects of Pressure and Temperature on Activity Coefficients", Pushished in Activity Coefficients in Electrolyte Solutions, Ricardo M. Pytkowitz, Editor. CRC Press, 1979.

APPENDIX A

Determination of Counterion Concentration

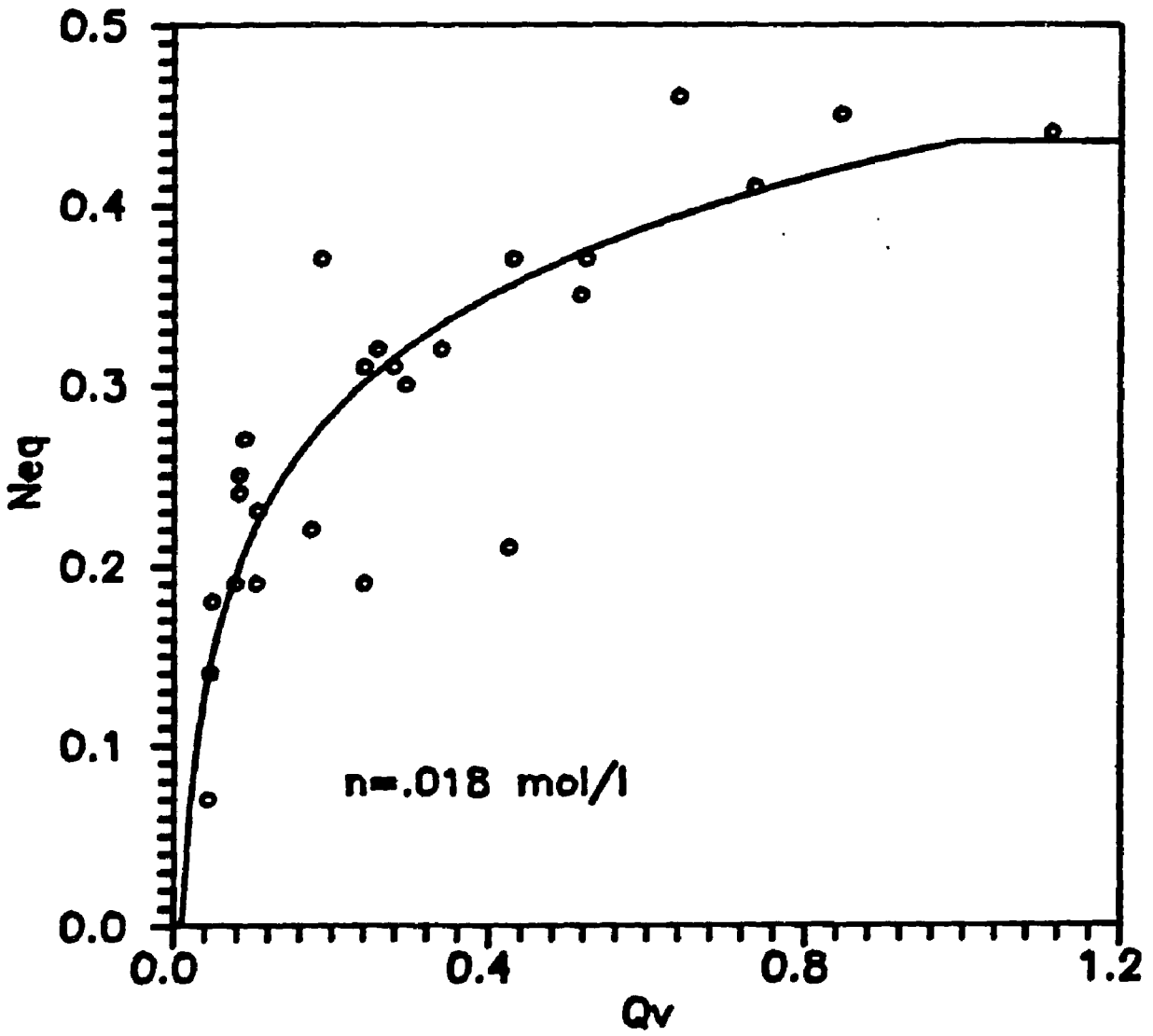
0.5
0.4
0.3
0.2
0.1
0.0
Neq
0.0
0.4
0.8
1.2
Qv
n=.018 mol/l

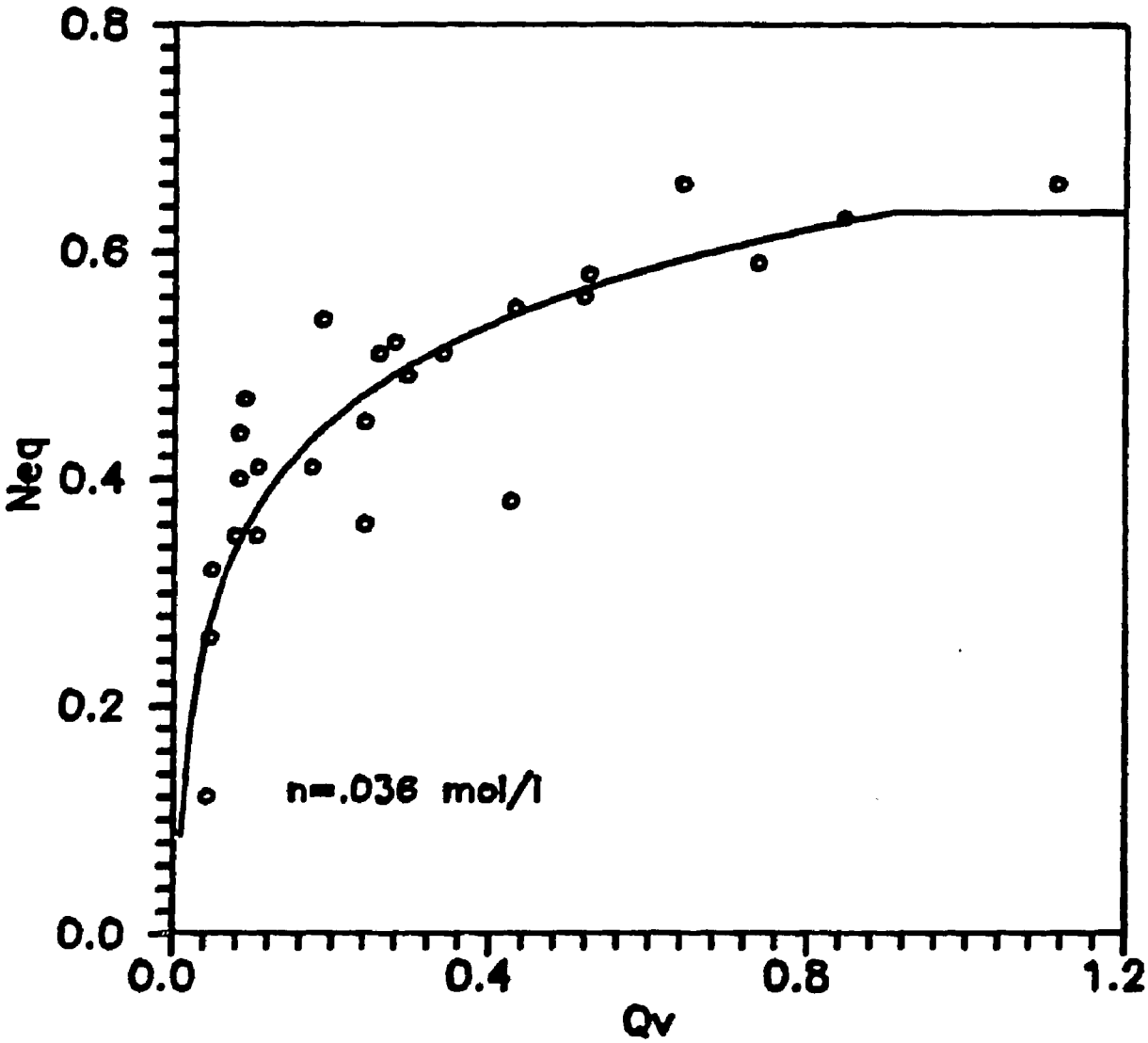
0.8
0.6
0.4
0.2
0.0
Neq
0.0
0.4
0.8
1.2
Qv
n=.036 mol/l

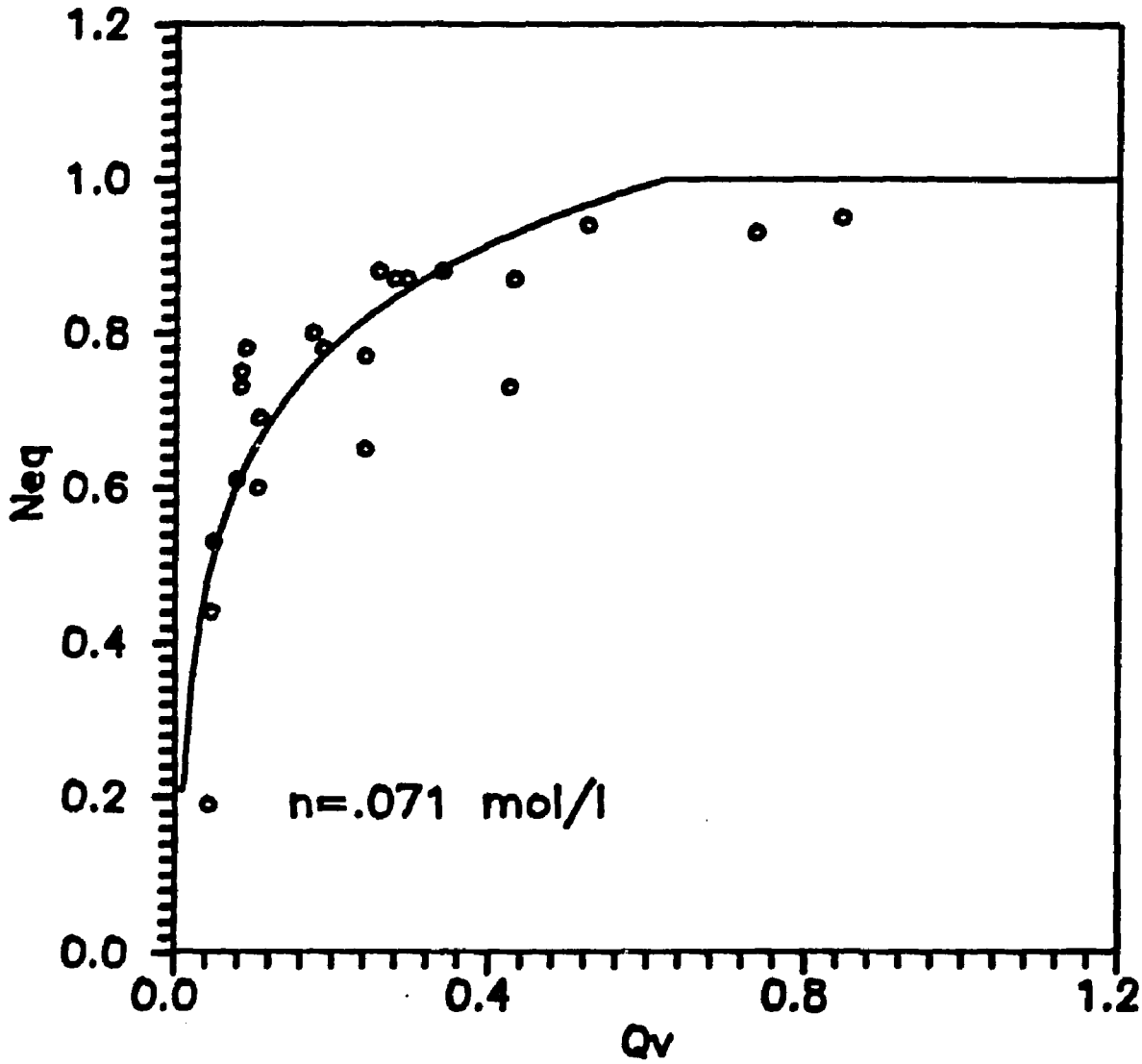
1.2
1.0
0.8
0.6
0.4
0.2
0.0
Neq
0.0
0.4
0.8
1.2
Qv
n=.071 mol/l

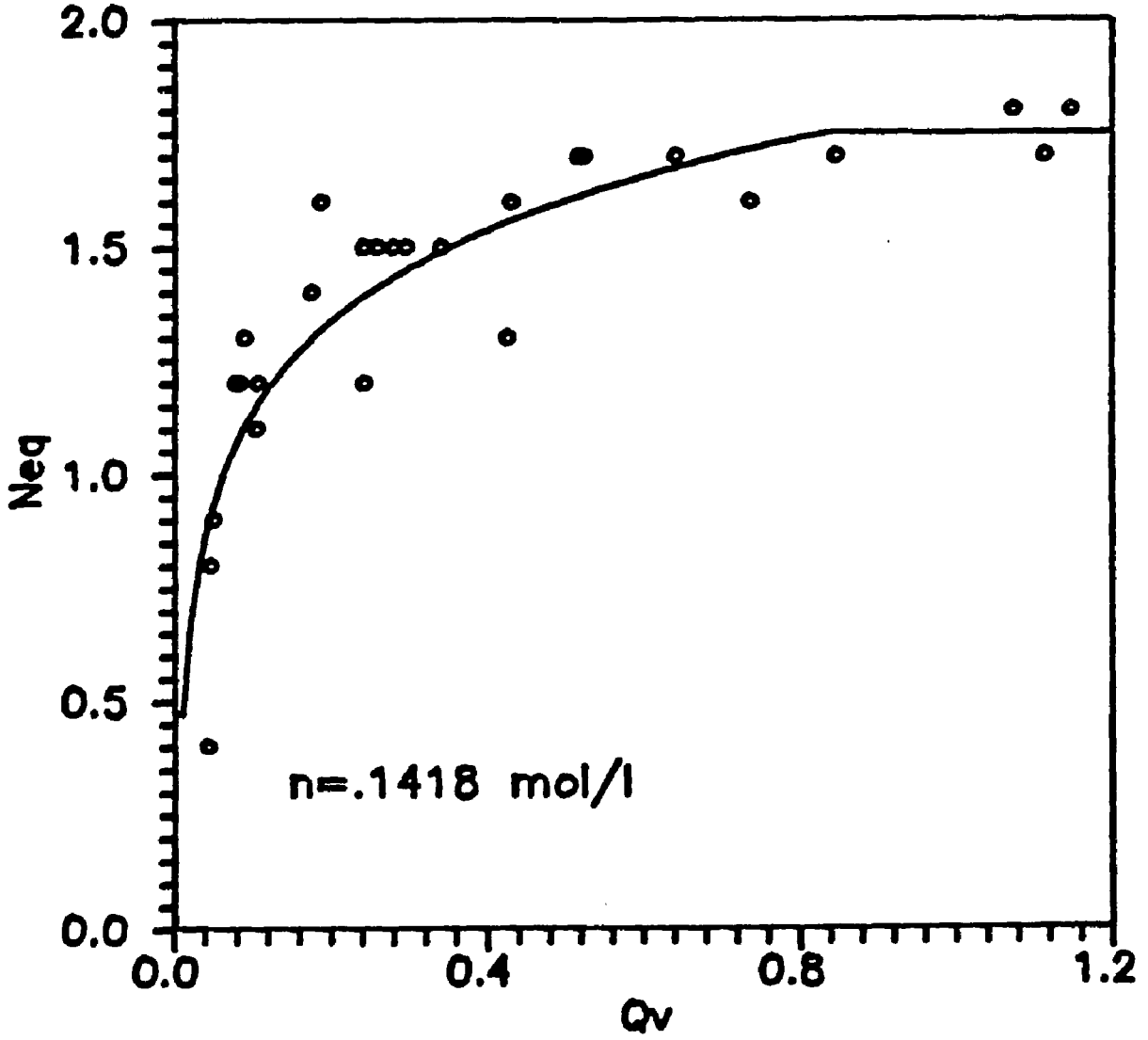
2.0
1.5
1.0
0.5
0.0
Neq
0.0
0.4
0.8
1.2
Qv
n=.1418 mol/l

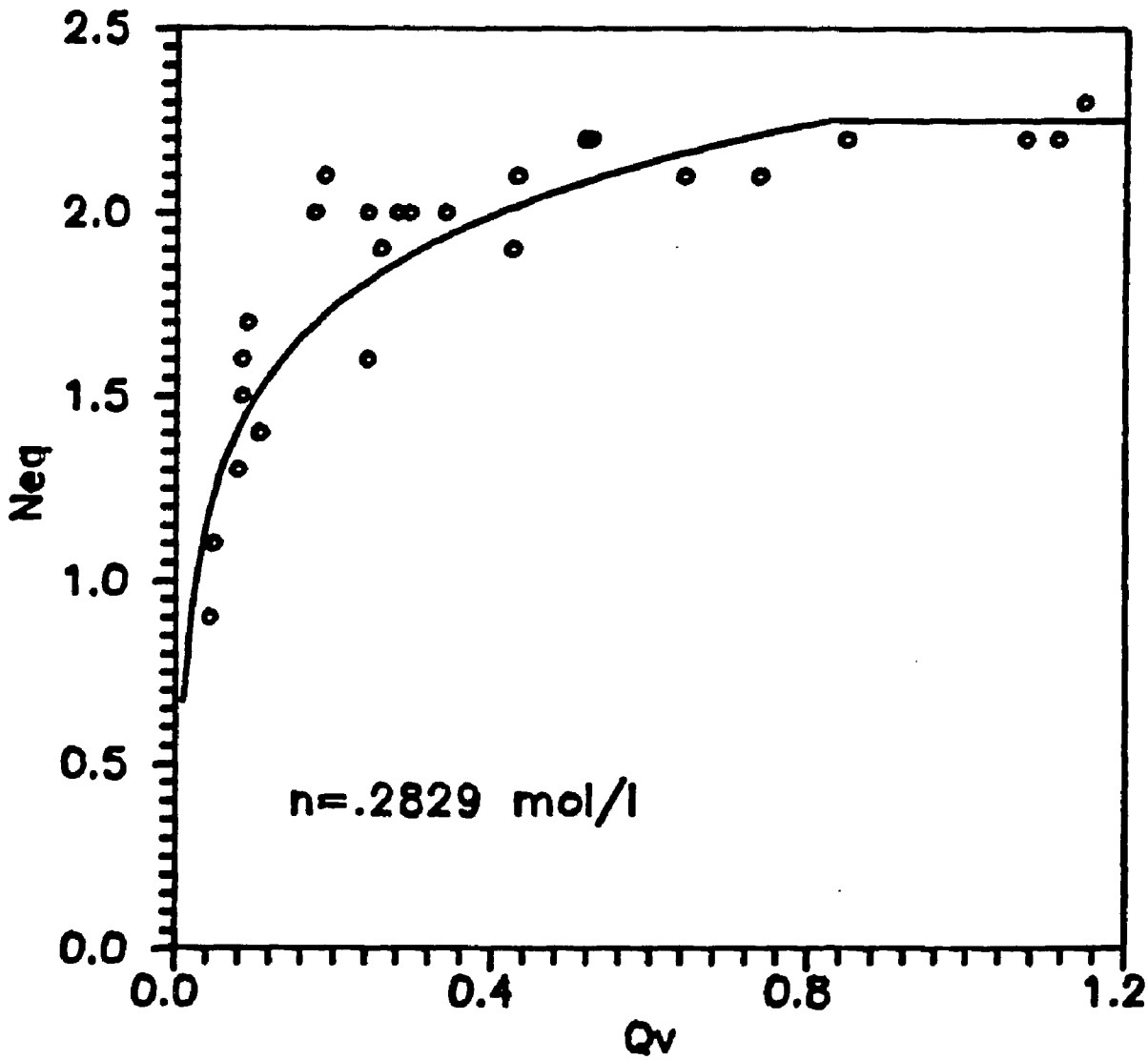
2.5
2.0
1.5
1.0
0.5
0.0
Neq
0.0
0.4
0.8
1.2
Qv
n=.2829 mol/l

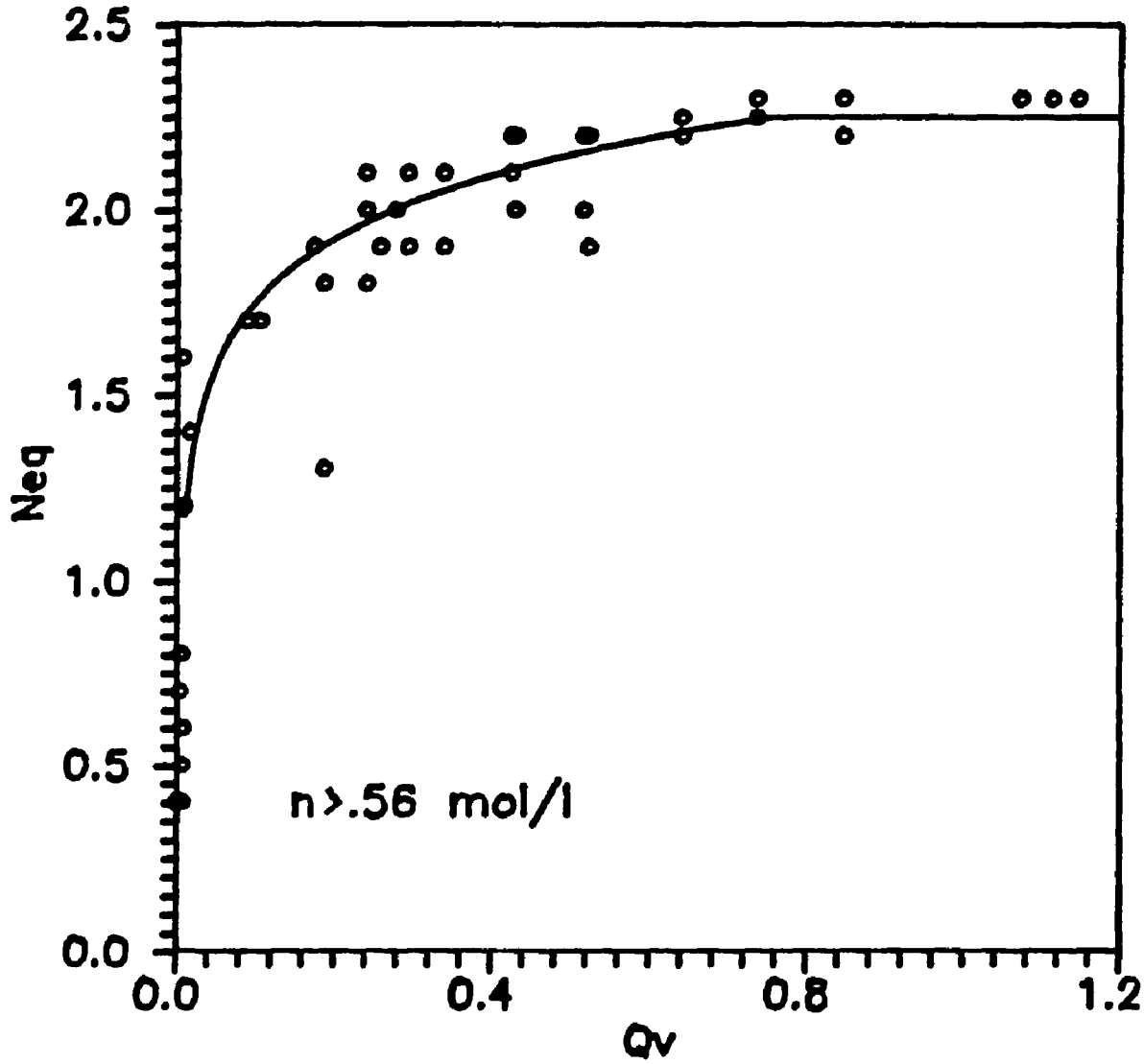
2.5
2.0
1.5
1.0
0.5
0.0
Neq
0.0
0.4
0.8
1.2
Qv
n>.56 mol/l

APPENDIX B

Comparison of Experimental vs. Calculated Core Conductivities

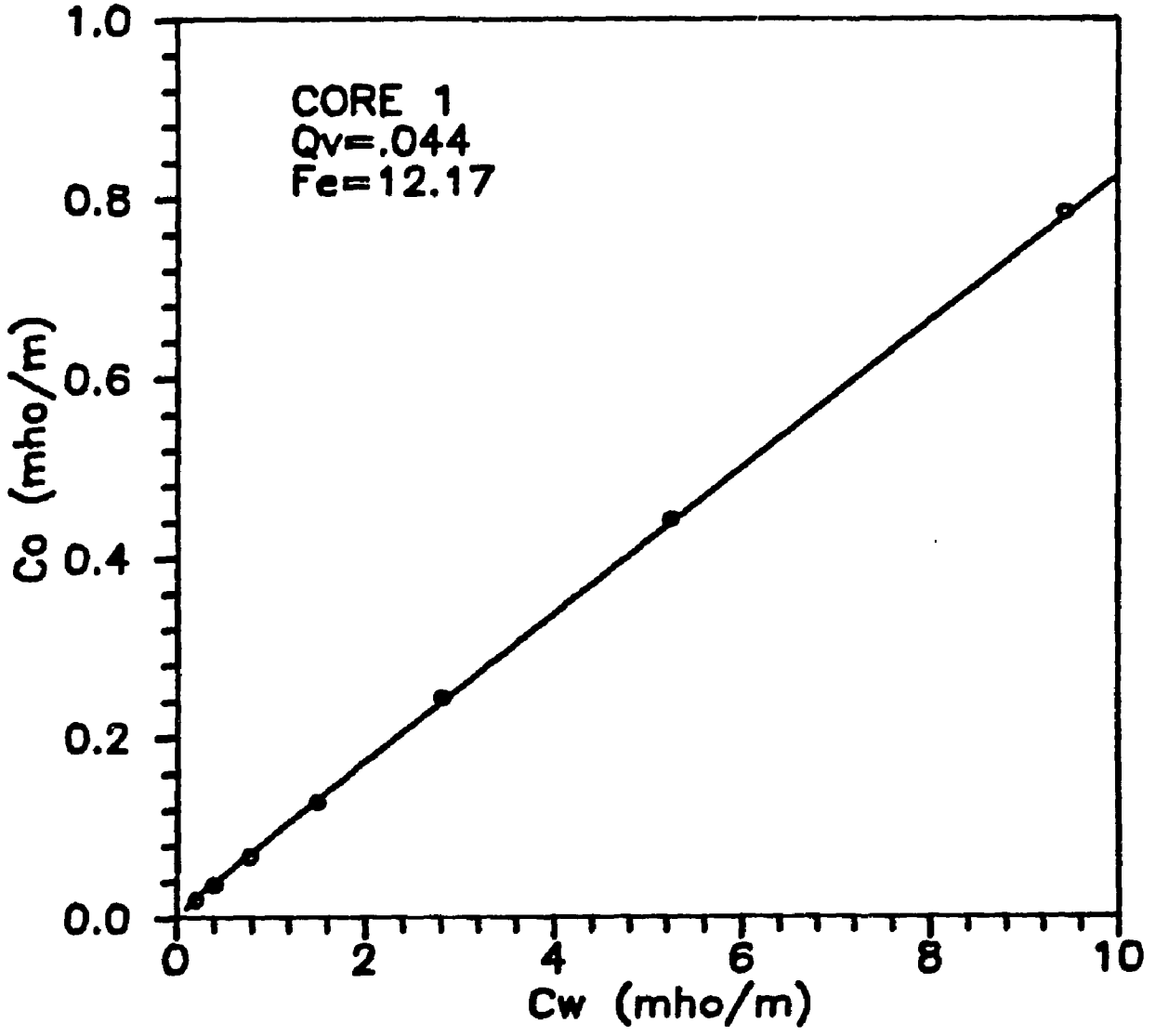
CORE 1
Qv=.044
Fe=12.17
Co (mho/m)
Cw (mho/m)
0.0
0.2
0.4
0.6
0.8
1.0
0
2
4
6
8
10

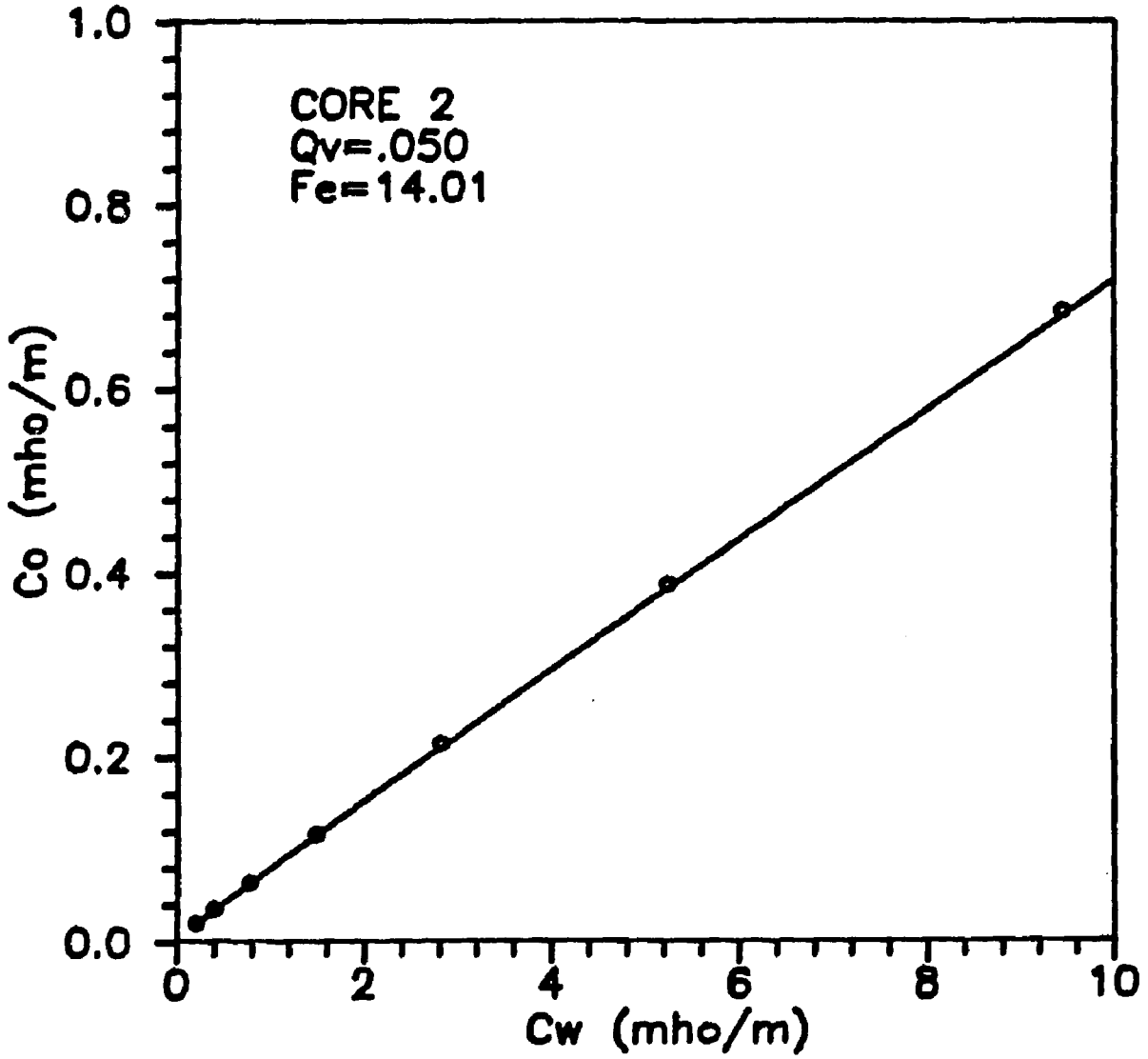
CORE 2
Qv=.050
Fe=14.01
Co (mho/m)
Cw (mho/m)
0.0
0.2
0.4
0.6
0.8
1.0
0
2
4
6
8
10

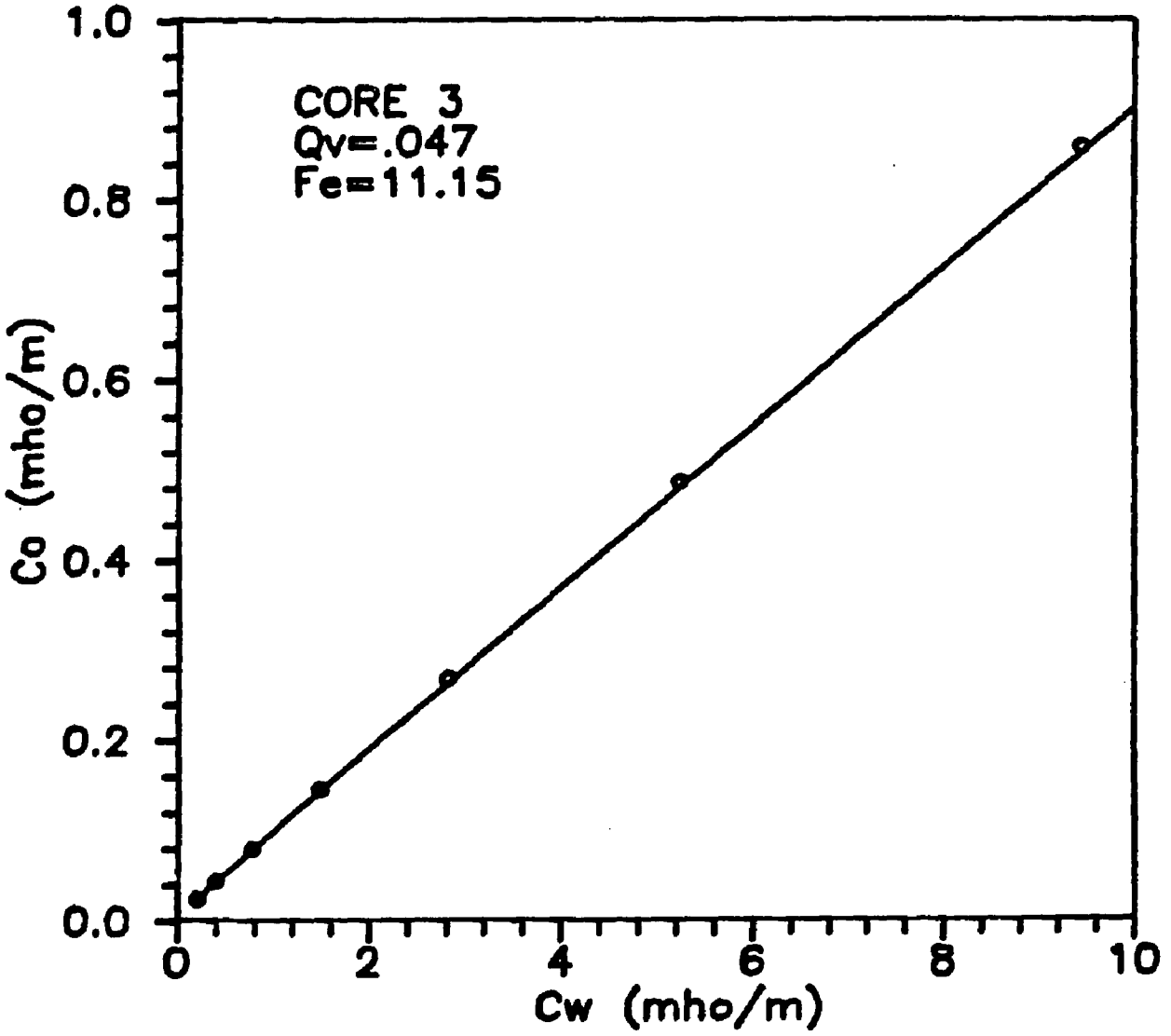
CORE 3
Qv=.047
Fe=11.15
Co (mho/m)
Cw (mho/m)
0.0
0.2
0.4
0.6
0.8
1.0
0
2
4
6
8
10

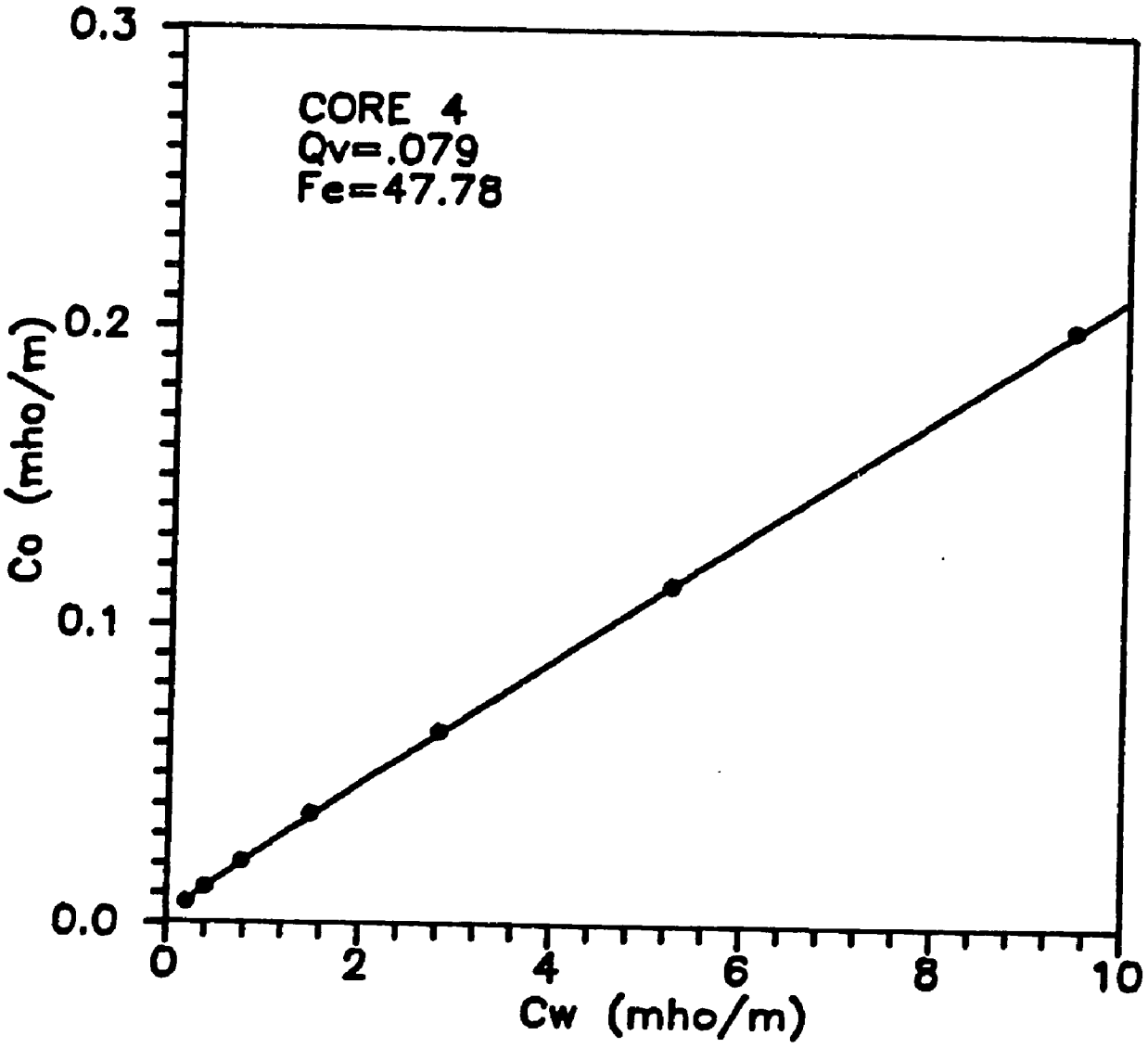
CORE 4
Qv=.079
Fe=47.78
Co (mho/m)
Cw (mho/m)
0.0
0.1
0.2
0.3
0
2
4
6
8
10

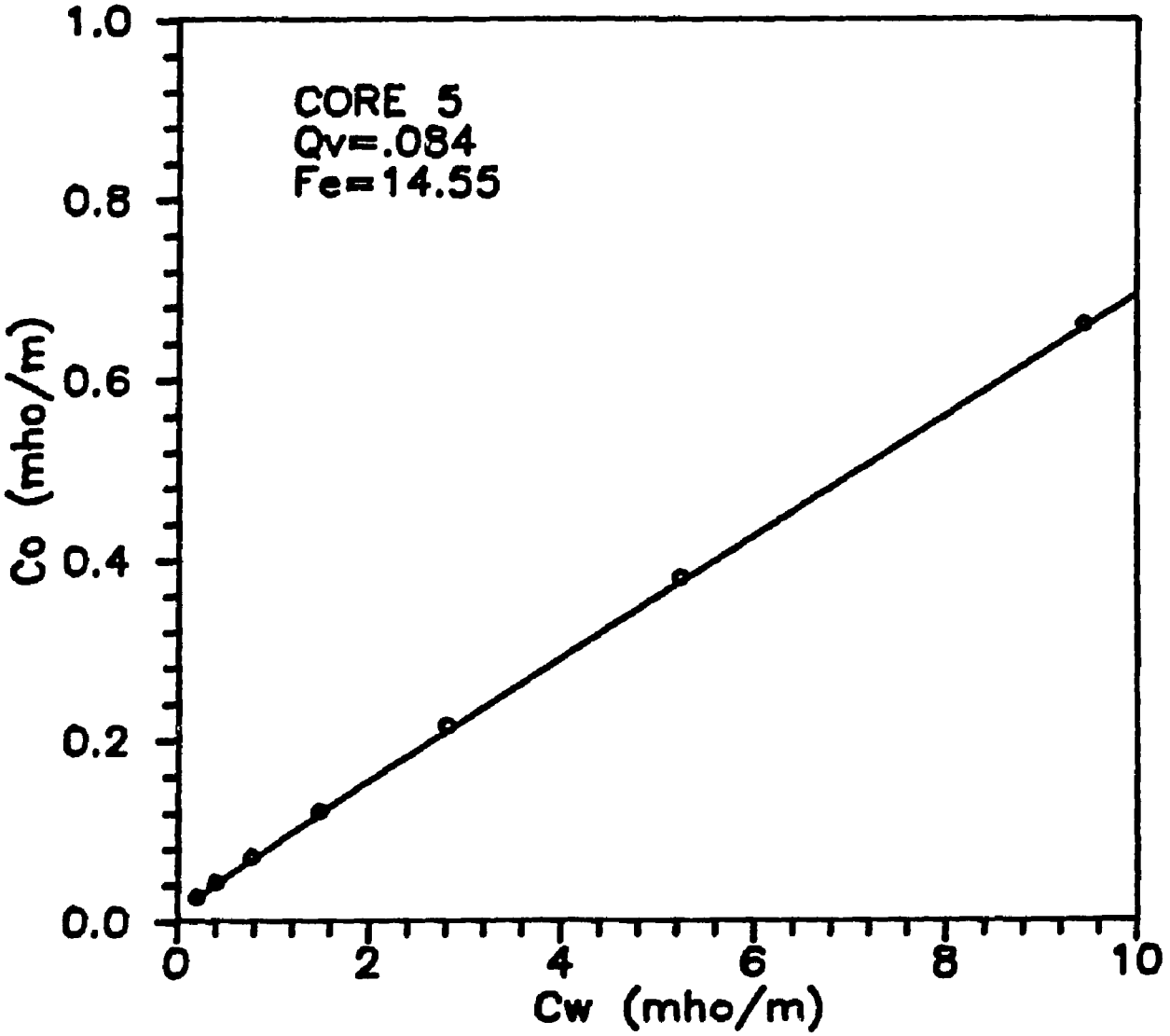
CORE 5
Qv=.084
Fe=14.55
Co (mho/m)
Cw (mho/m)
1.0
0.8
0.6
0.4
0.2
0.0
0
2
4
6
8
10

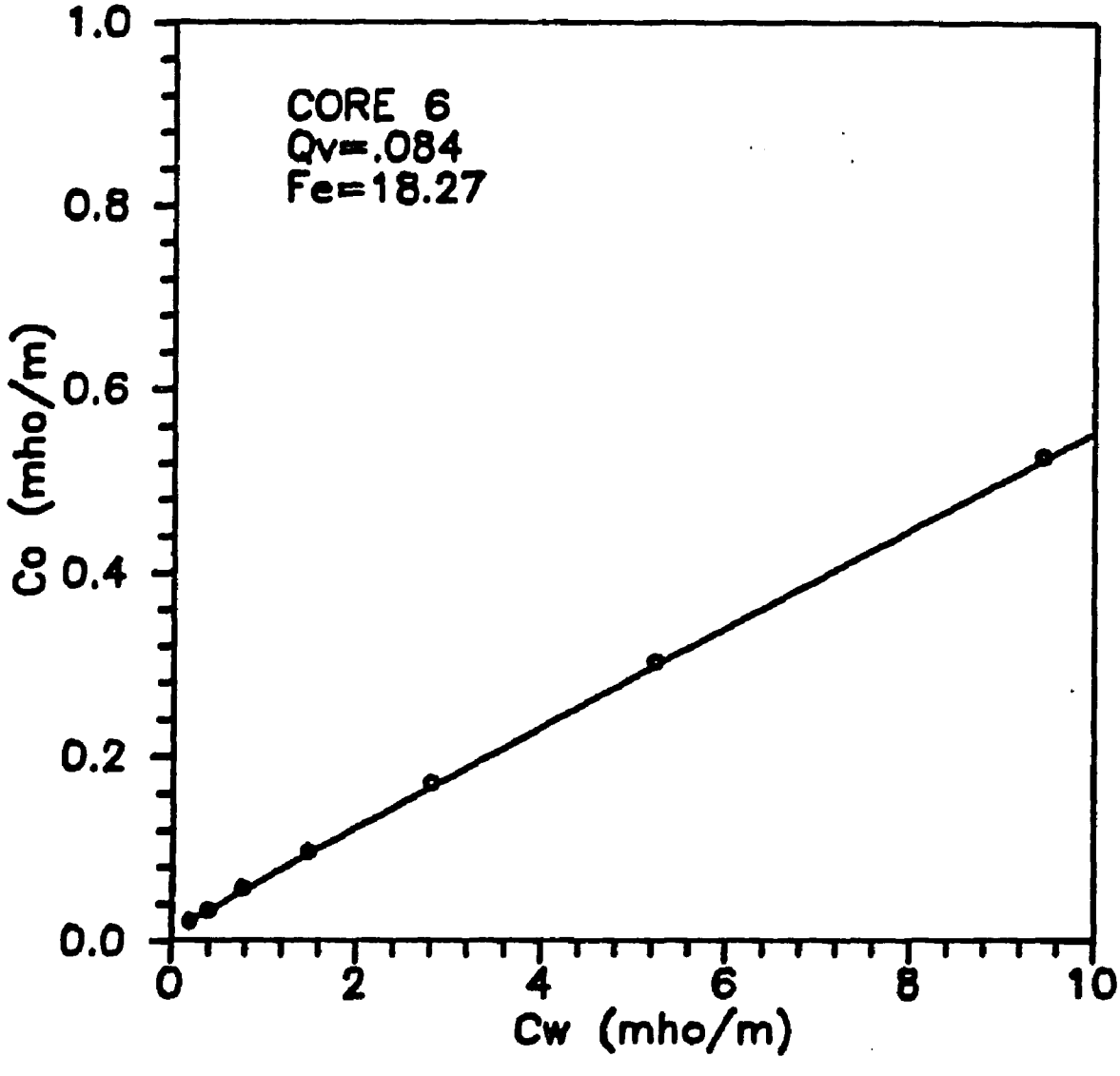
CORE 6
Qv=.084
Fe=18.27
Co (mho/m)
Cw (mho/m)
1.0
0.8
0.6
0.4
0.2
0.0
0
2
4
6
8
10

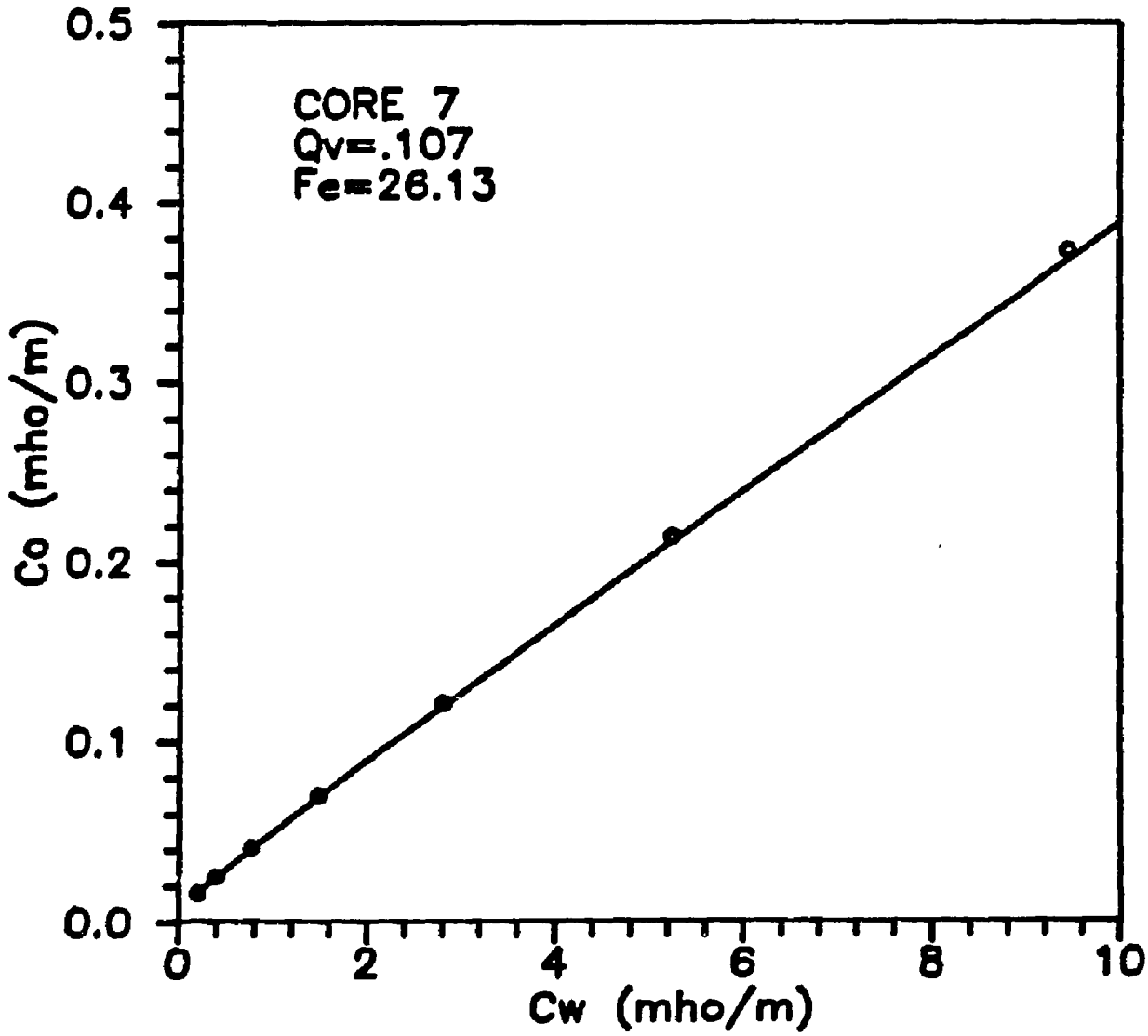
CORE 7
Qv=.107
Fe=26.13
Co (mho/m)
Cw (mho/m)
0.0
0.1
0.2
0.3
0.4
0.5
0
2
4
6
8
10

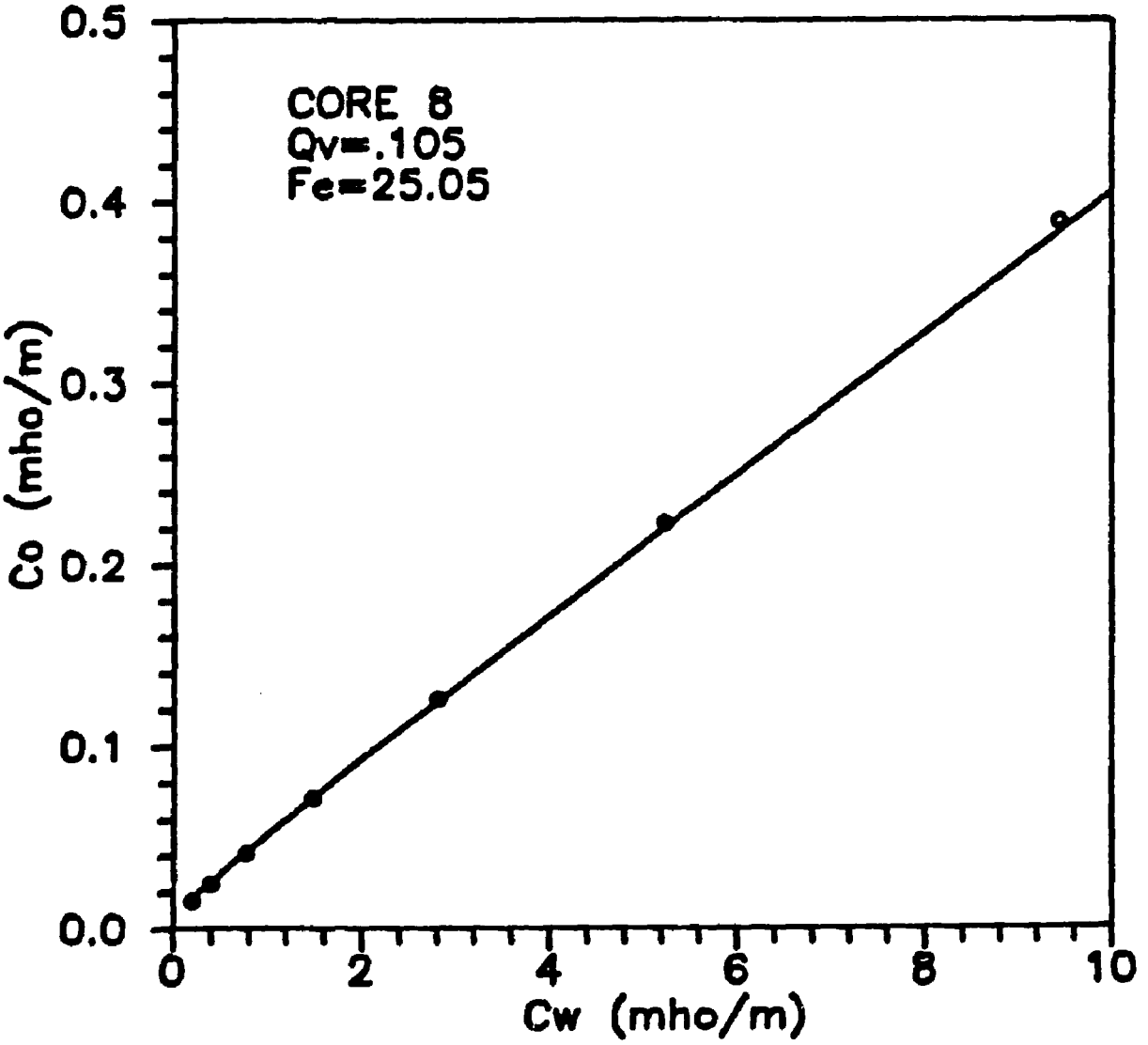
CORE 8
Qv=.105
Fe=25.05
Co (mho/m)
Cw (mho/m)
0.0
0.1
0.2
0.3
0.4
0.5
0
2
4
6
8
10

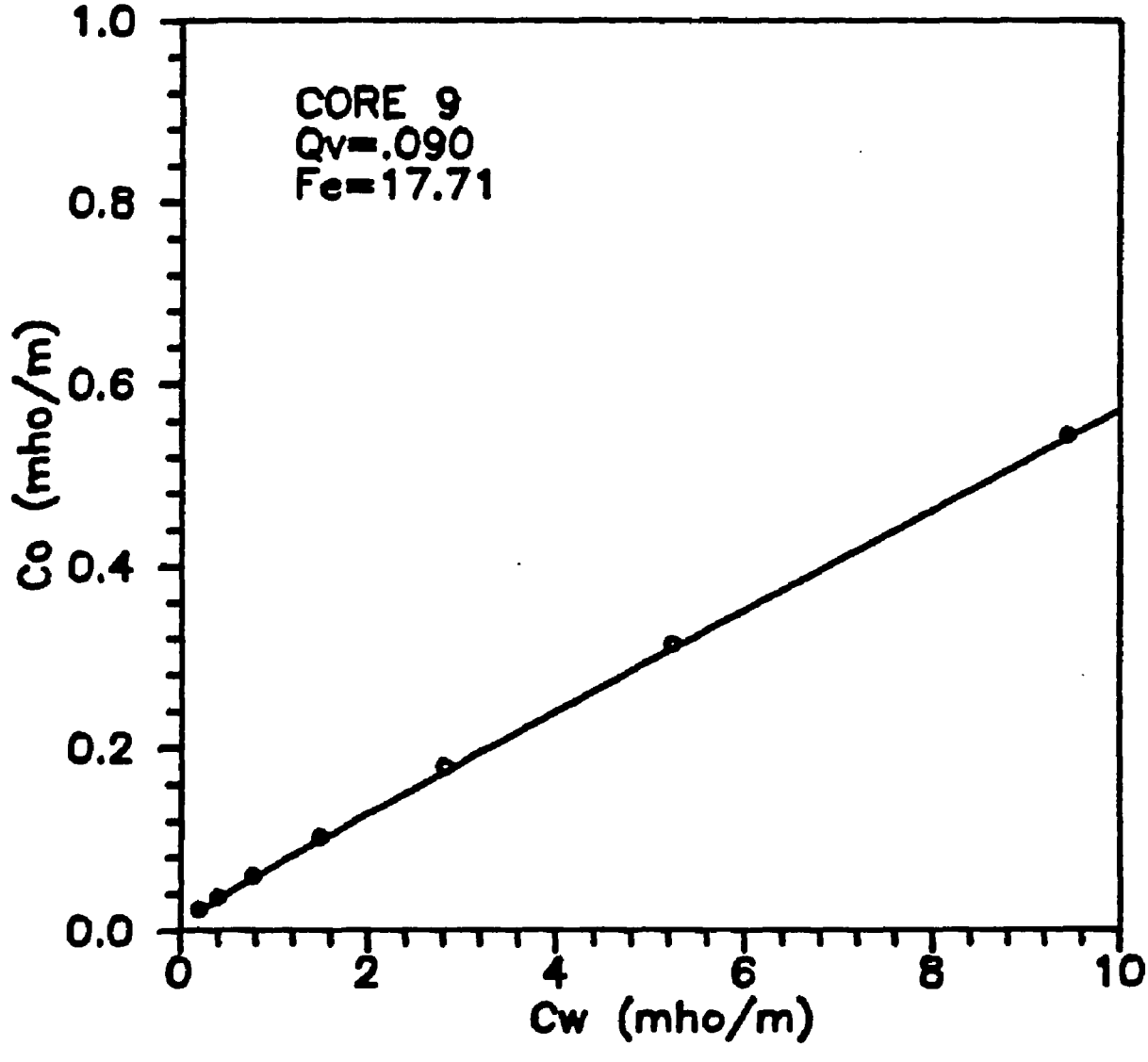
CORE 9
Qv=.090
Fe=17.71
Co (mho/m)
Cw (mho/m)
1.0
0.8
0.6
0.4
0.2
0.0
0
2
4
6
8
10

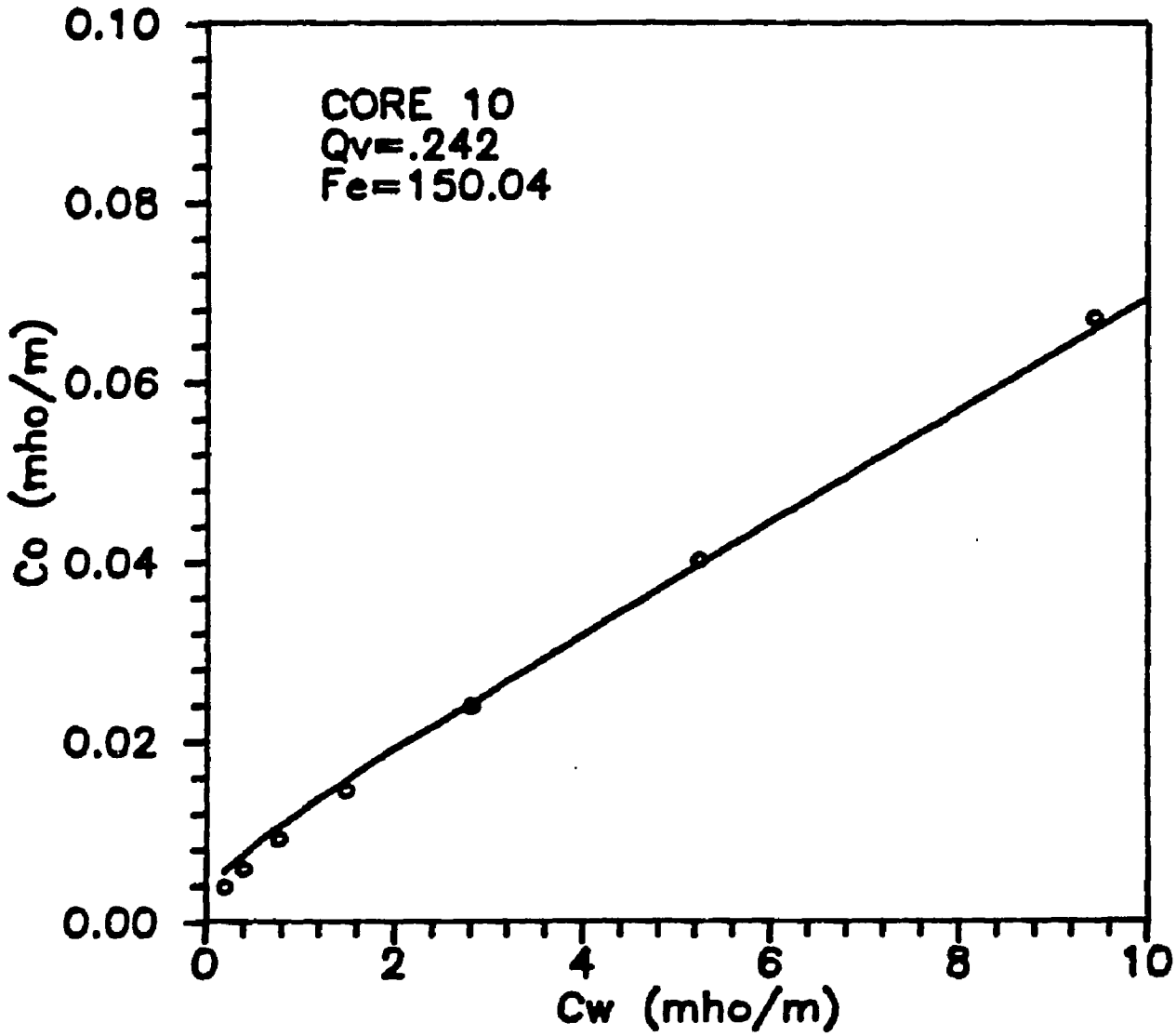
CORE 10
Qv=.242
Fe=150.04
0.10
0.08
0.06
0.04
0.02
0.00
Co (mho/m)
0
2
4
6
8
10
Cw (mho/m)

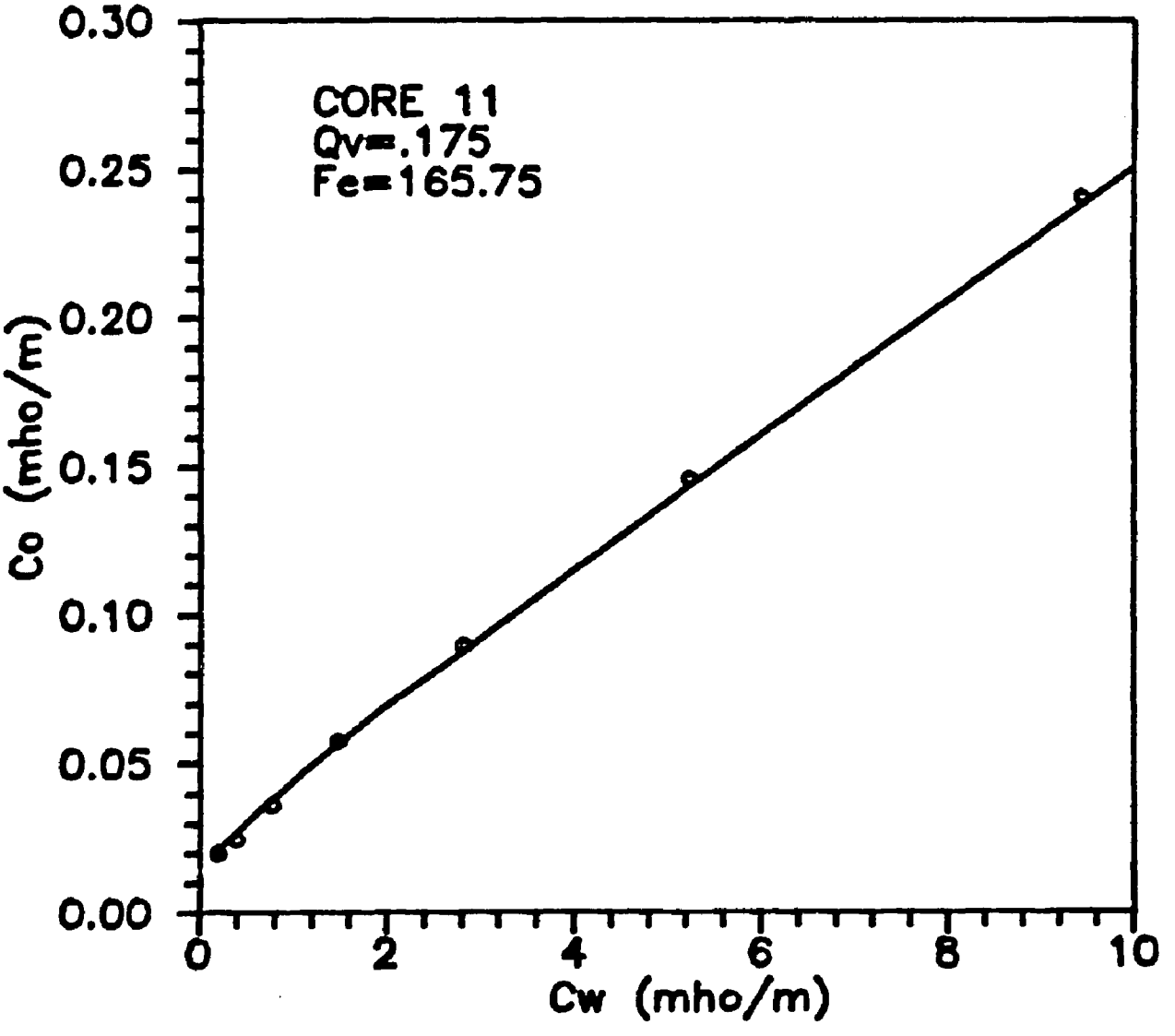
CORE 11
Qv=.175
Fe=165.75
Co (mho/m)
Cw (mho/m)
0.30
0.25
0.20
0.15
0.10
0.05
0.00
0
2
4
6
8
10

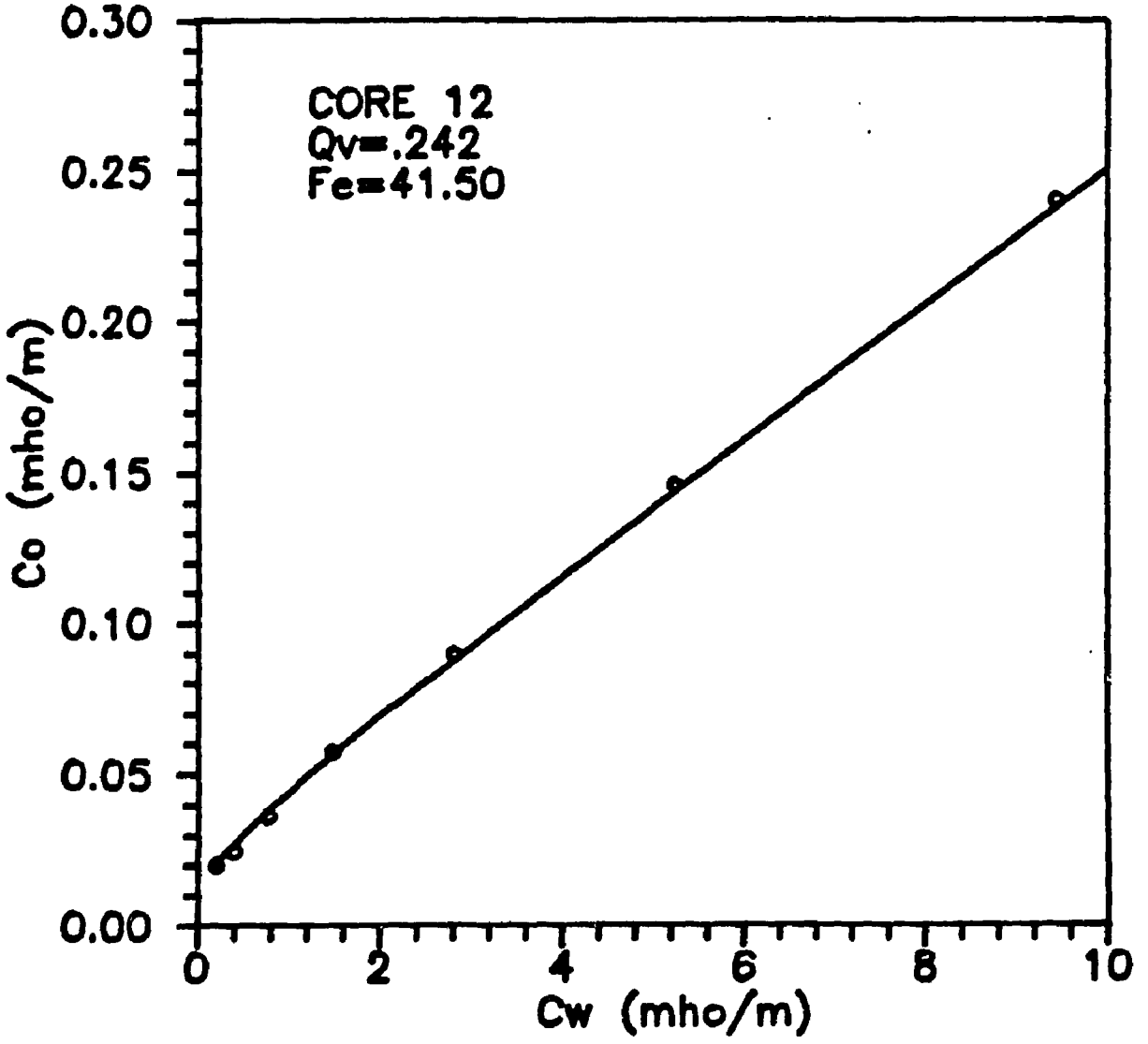
CORE 12
Qv=.242
Fe=41.50
0.30
0.25
0.20
0.15
0.10
0.05
0.00
Co (mho/m)
0
2
4
6
8
10
Cw (mho/m)

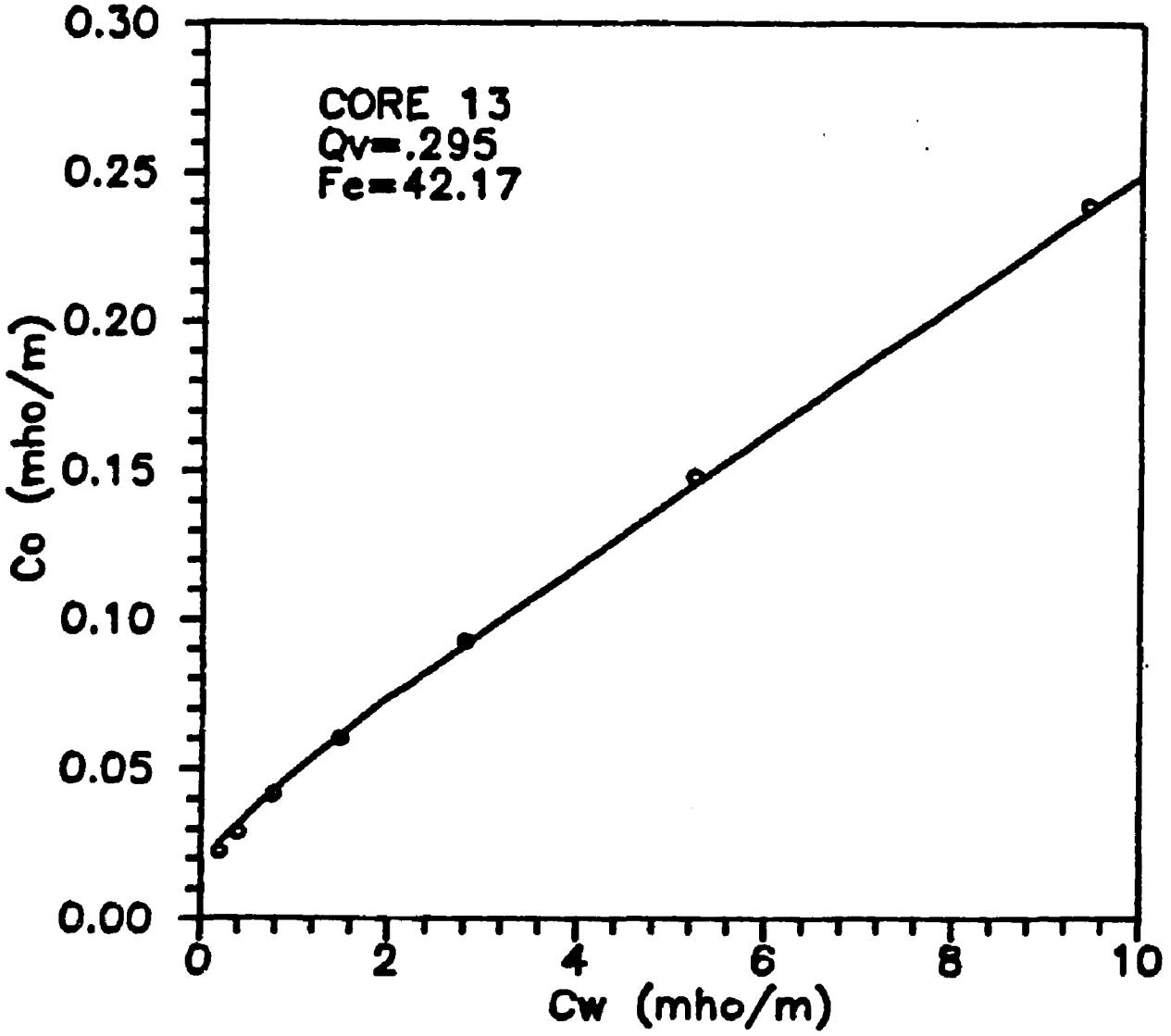
CORE 13
Qv=.295
Fe=42.17
Co (mho/m)
Cw (mho/m)
0.30
0.25
0.20
0.15
0.10
0.05
0.00
0
2
4
6
8
10

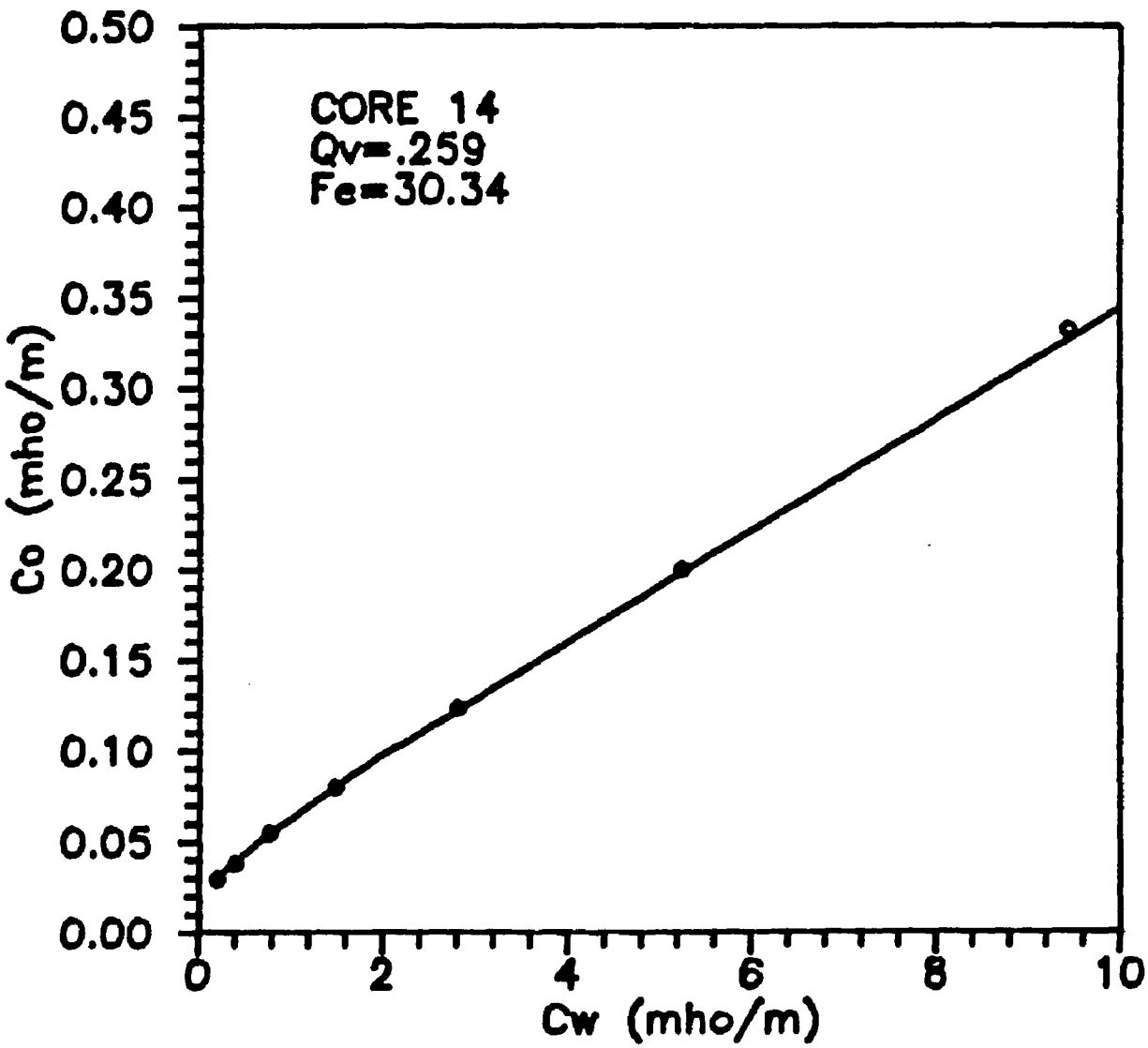
CORE 14
Qv=.259
Fe=30.34
Co (mho/m)
Cw (mho/m)
0.50
0.45
0.40
0.35
0.30
0.25
0.20
0.15
0.10
0.05
0.00
0
2
4
6
8
10

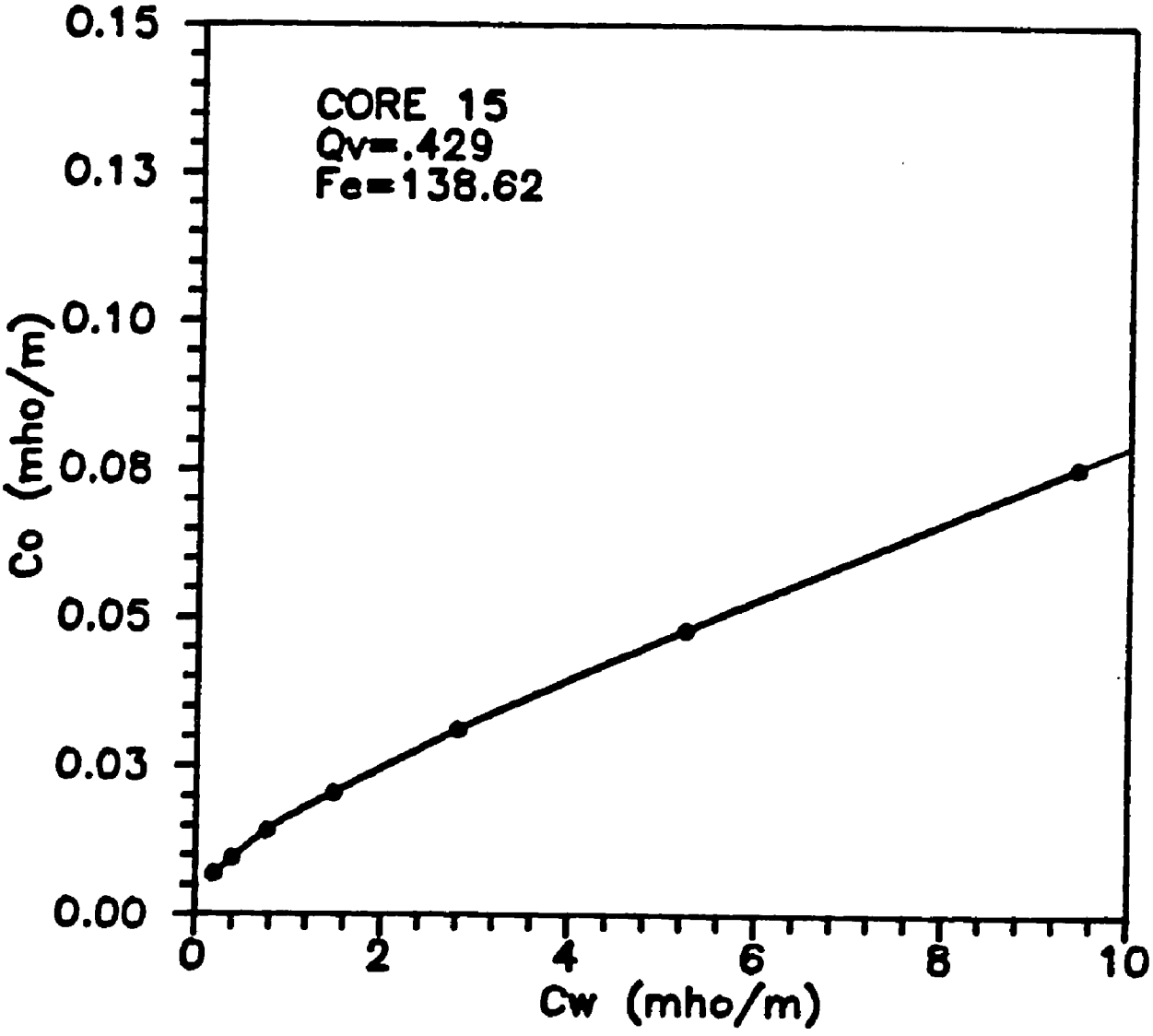
CORE 15
Qv=.429
Fe=138.62
Co (mho/m)
Cw (mho/m)
0.15
0.13
0.10
0.08
0.05
0.03
0.00
0
2
4
6
8
10

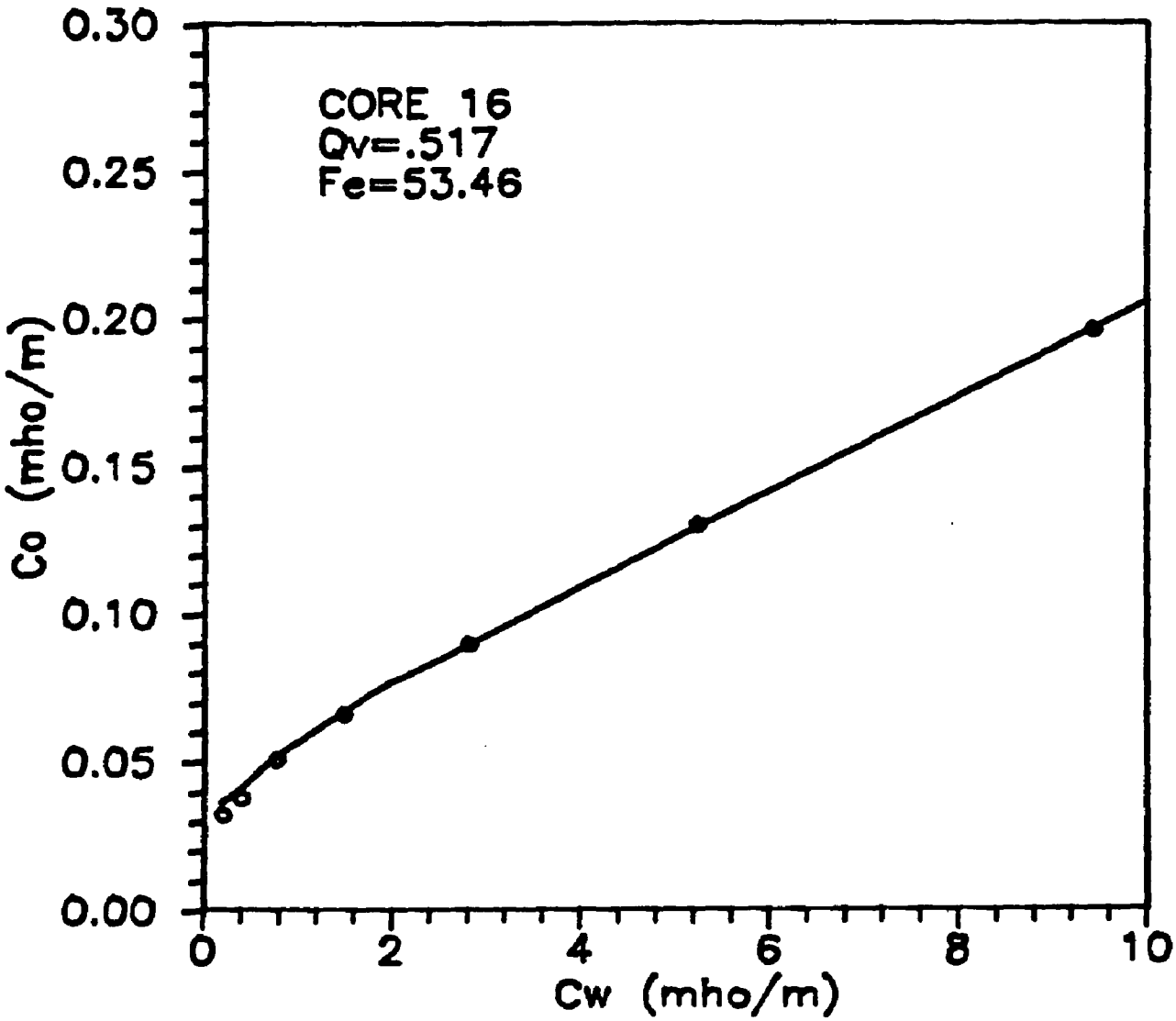
CORE 16
Qv=.517
Fe=53.46
Co (mho/m)
Cw (mho/m)
0.30
0.25
0.20
0.15
0.10
0.05
0.00
0
2
4
6
8
10

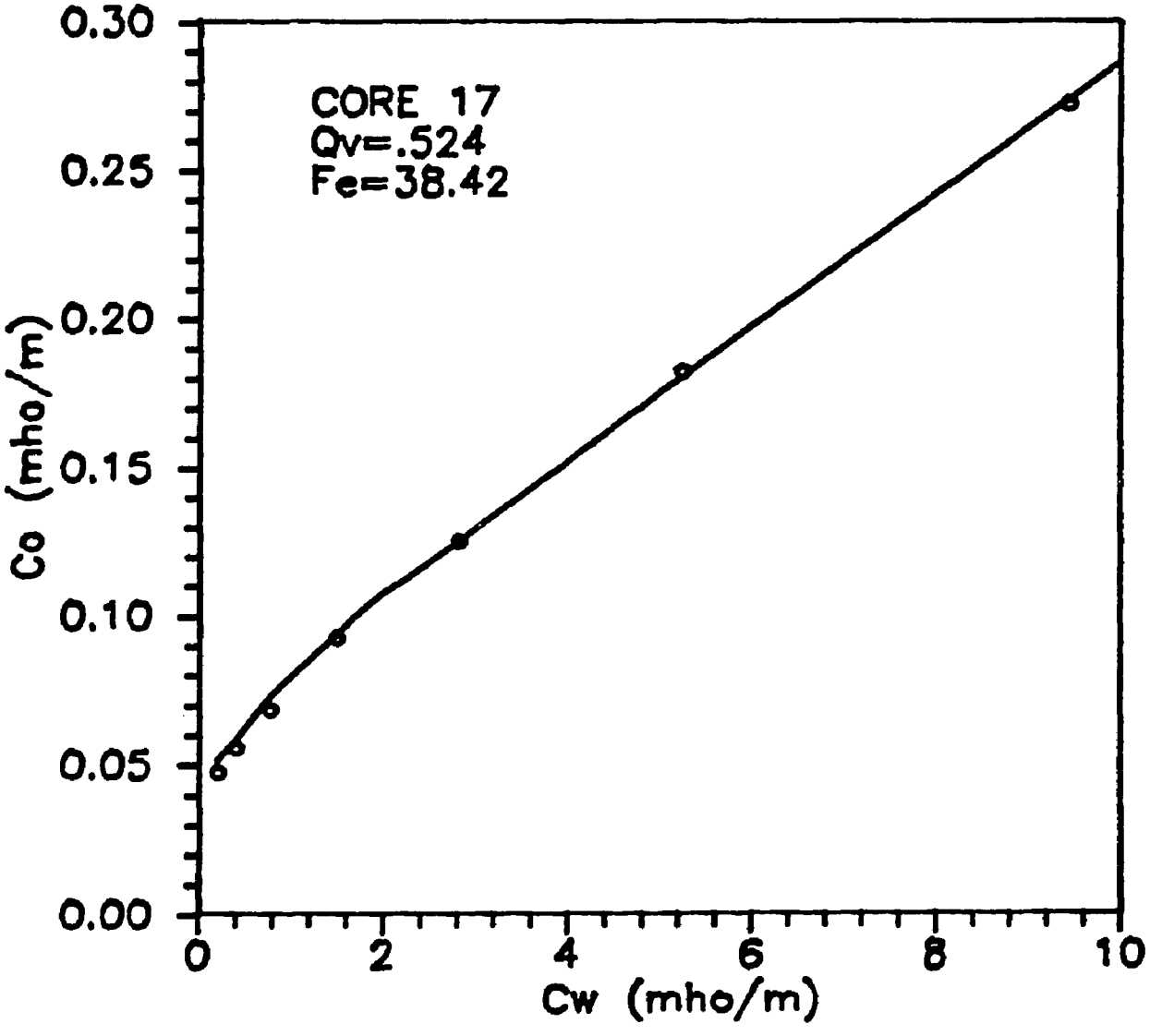
CORE 17
Qv=.524
Fe=38.42
Co (mho/m)
Cw (mho/m)
0.30
0.25
0.20
0.15
0.10
0.05
0.00
0
2
4
6
8
10

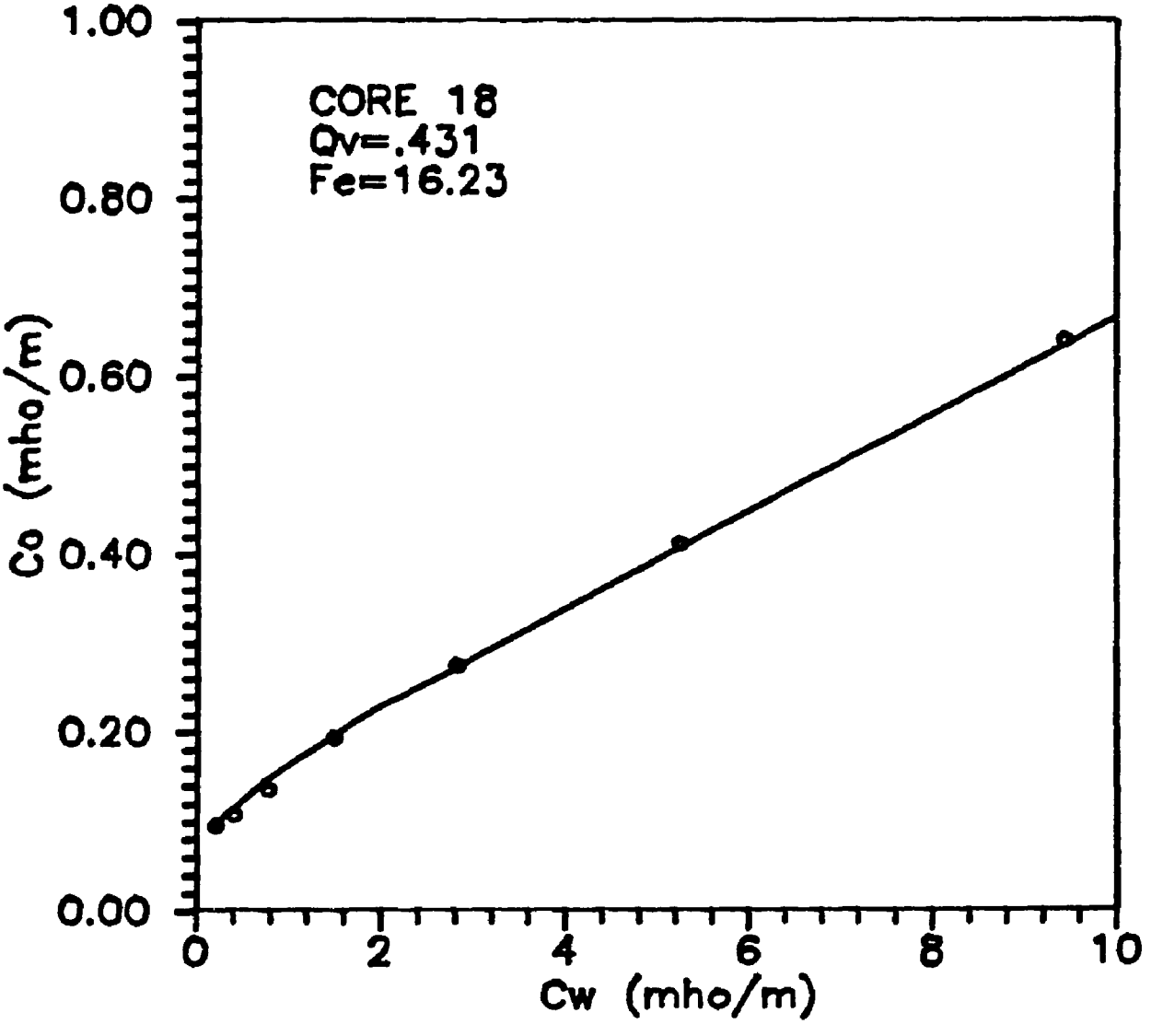
CORE 18
Qv=.431
Fe=16.23
1.00
0.80
0.60
0.40
0.20
0.00
Co (mho/m)
0
2
4
6
8
10
Cw (mho/m)

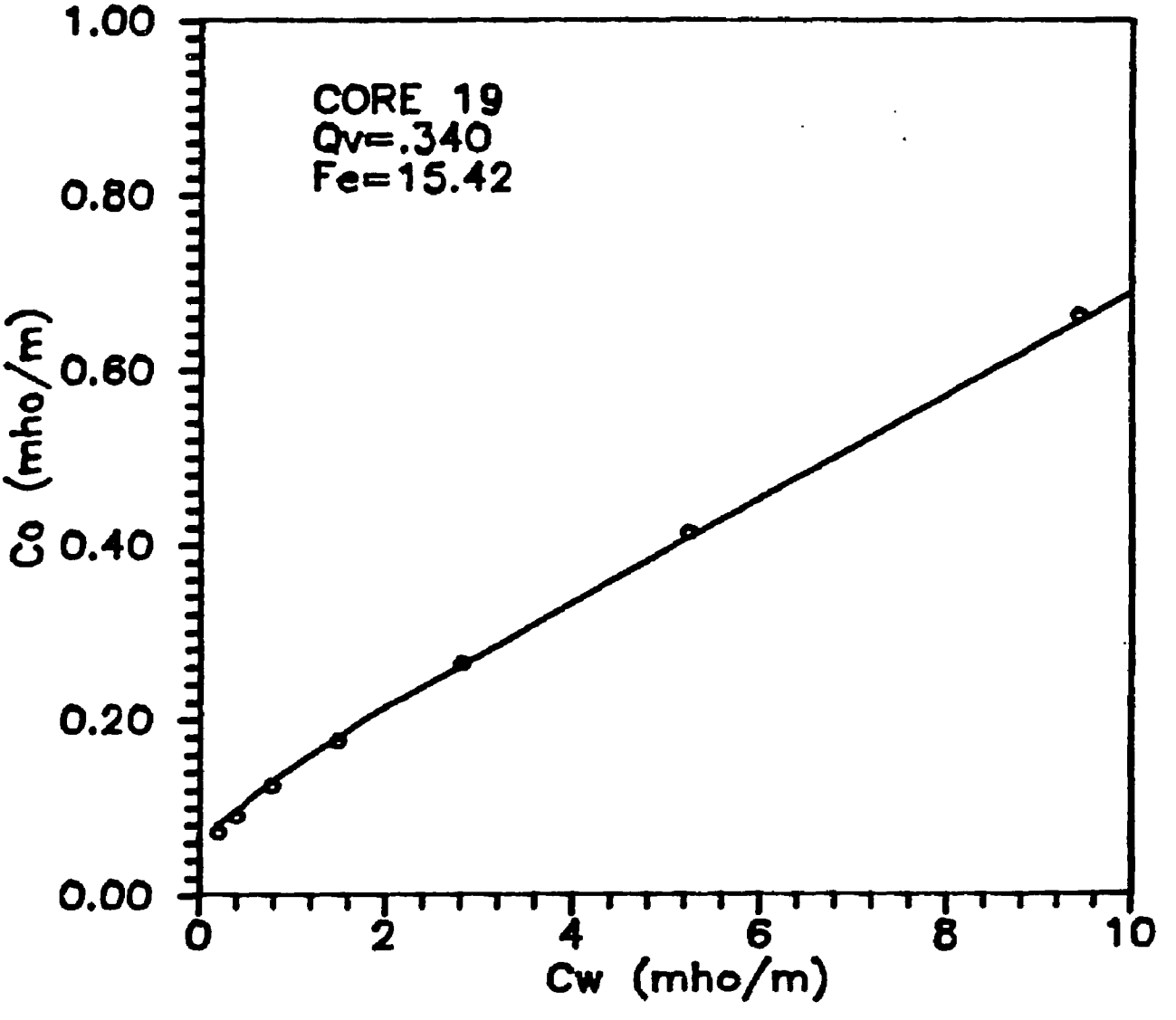
CORE 19
Qv=.340
Fe=15.42
Co (mho/m)
Cw (mho/m)
1.00
0.80
0.60
0.40
0.20
0.00
0
2
4
6
8
10

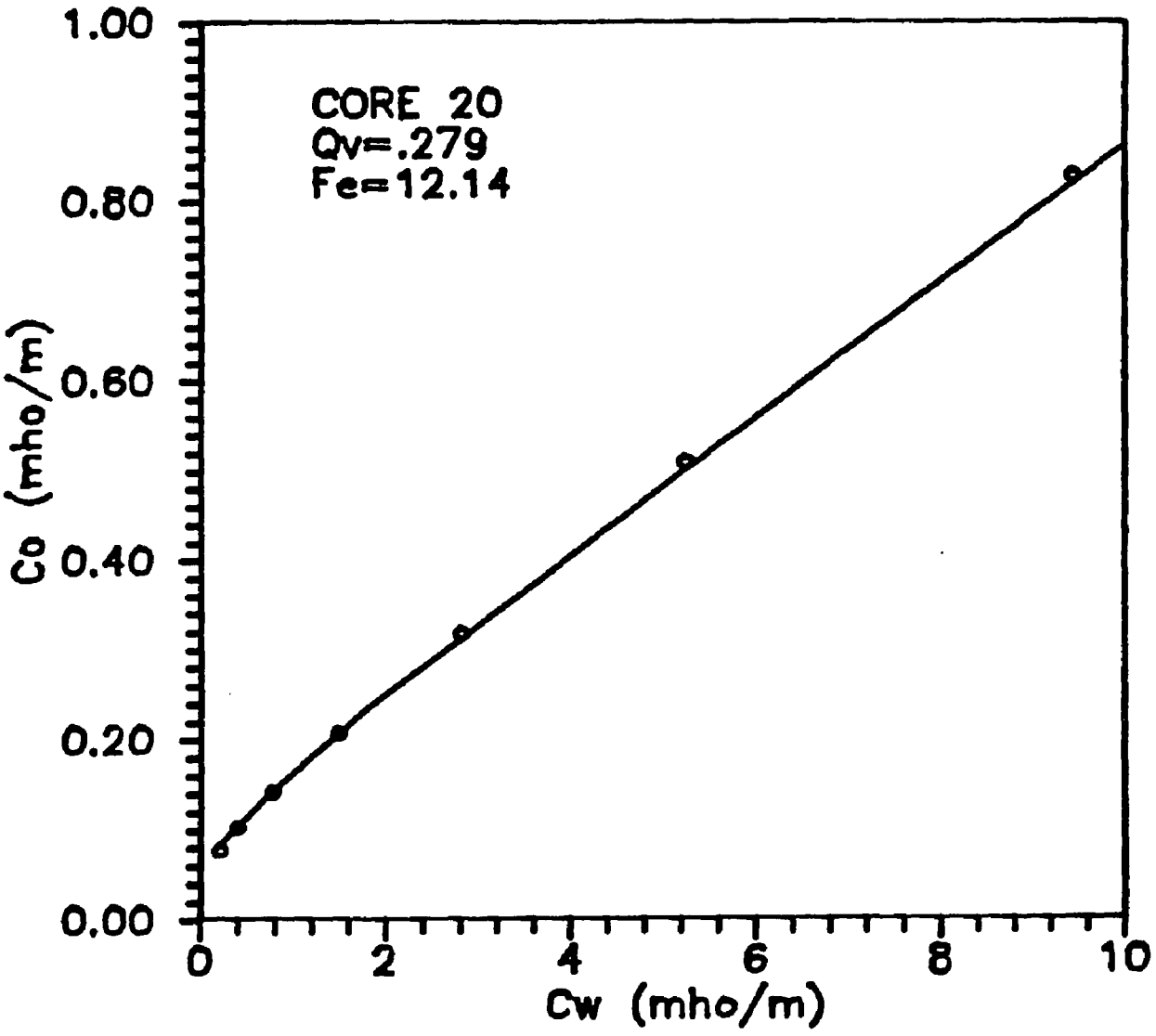
CORE 20
Qv=.279
Fe=12.14
1.00
0.80
0.60
0.40
0.20
0.00
Co (mho/m)
0
2
4
6
8
10
Cw (mho/m)

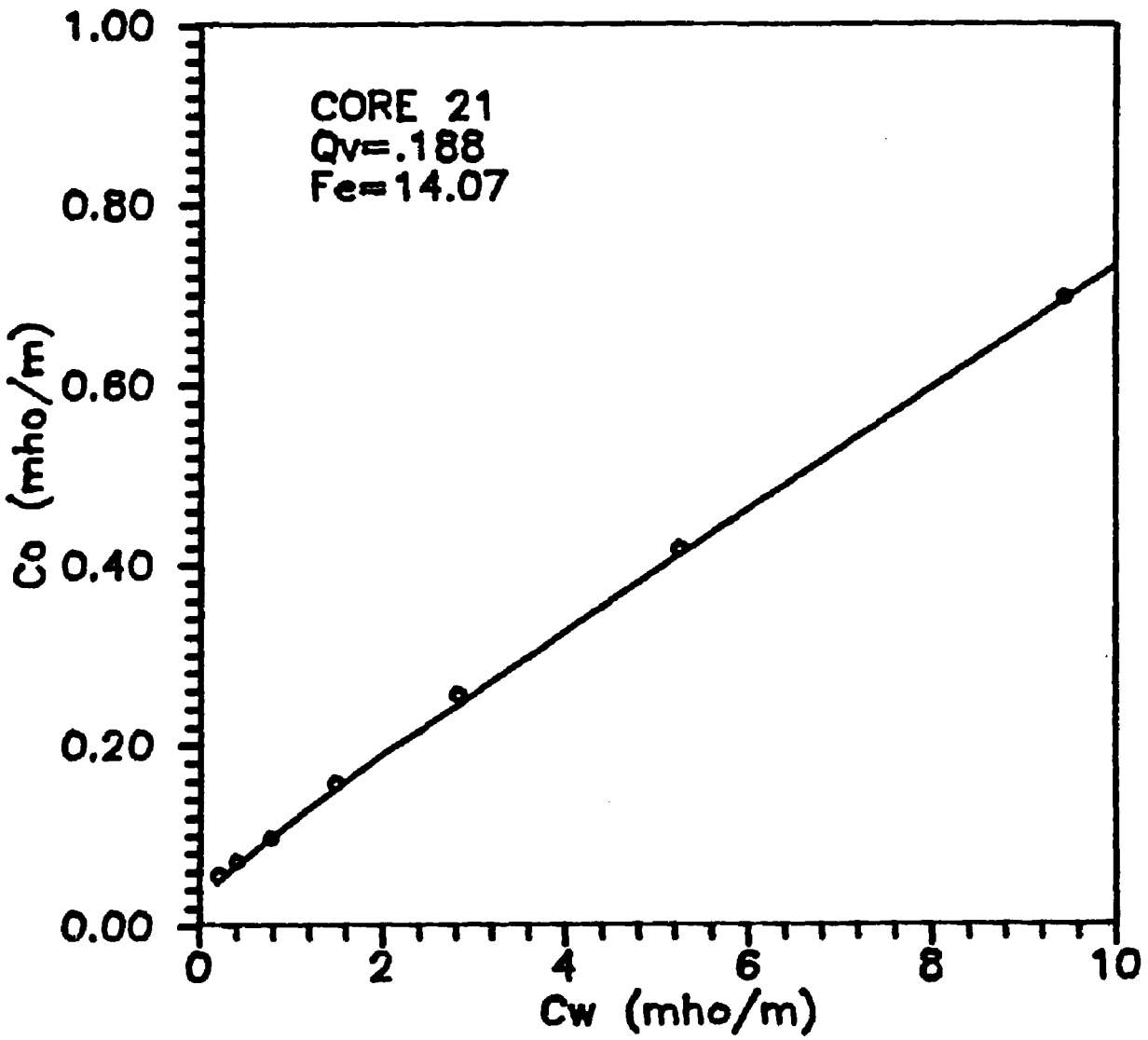
CORE 21
Qv=.188
Fe=14.07
1.00
0.80
0.60
0.40
0.20
0.00
Co (mho/m)
0
2
4
6
8
10
Cw (mho/m)

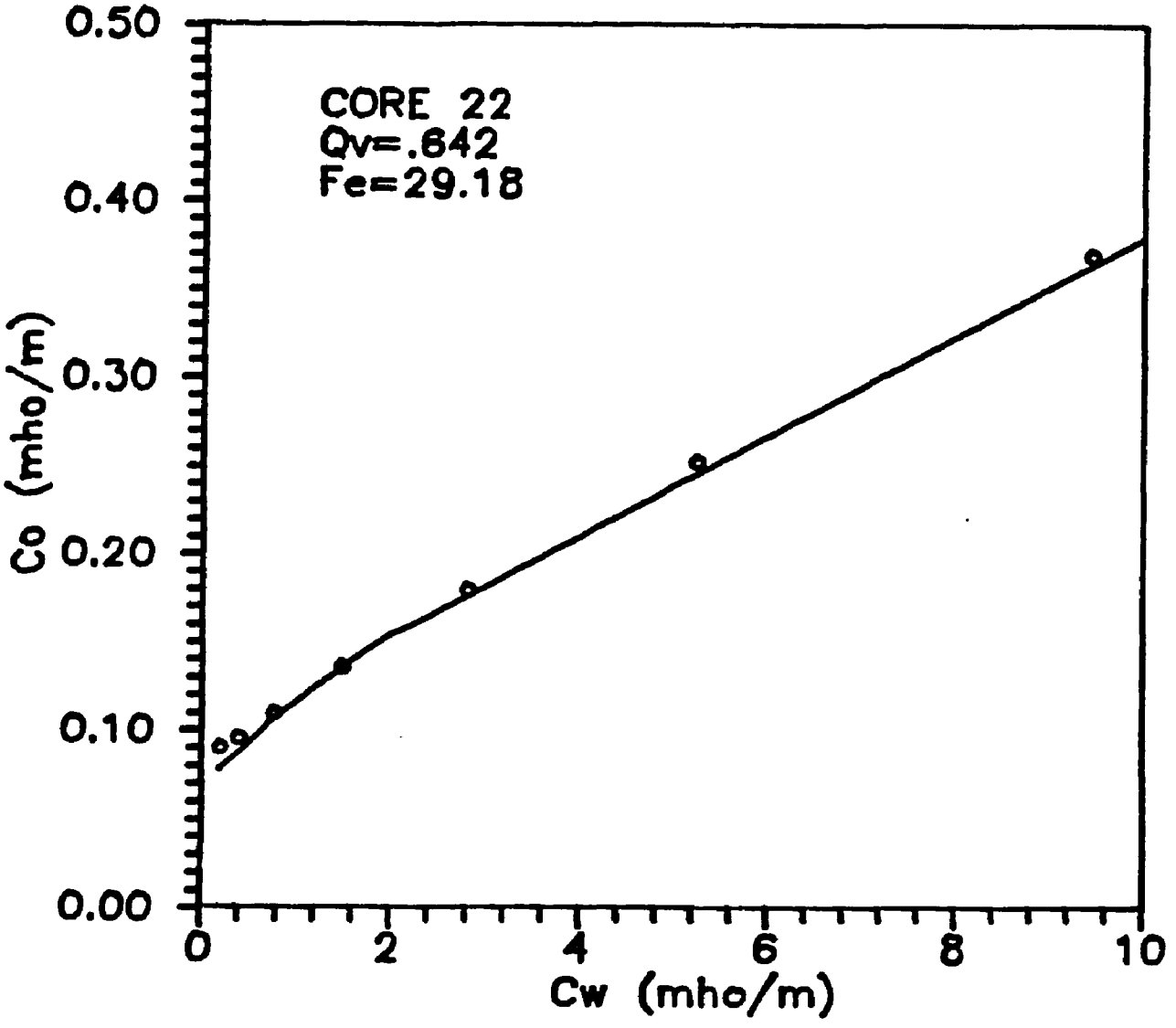
CORE 22
Qv=.642
Fe=29.18
0.50
0.40
0.30
0.20
0.10
0.00
Co (mho/m)
0
2
4
6
8
10
Cw (mho/m)

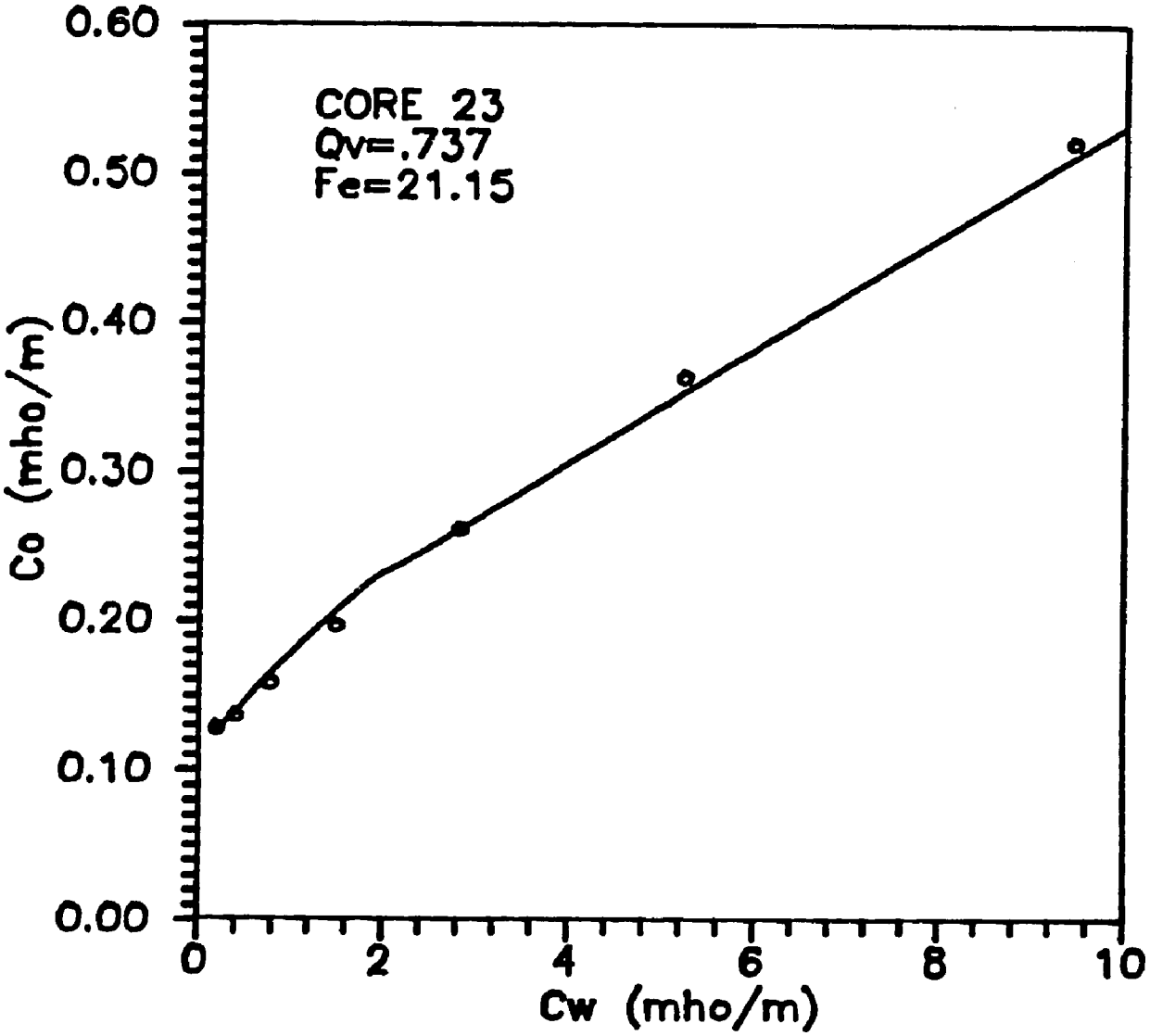
CORE 23
Qv=.737
Fe=21.15
Co (mho/m)
Cw (mho/m)
0.00
0.10
0.20
0.30
0.40
0.50
0.60
0
2
4
6
8
10

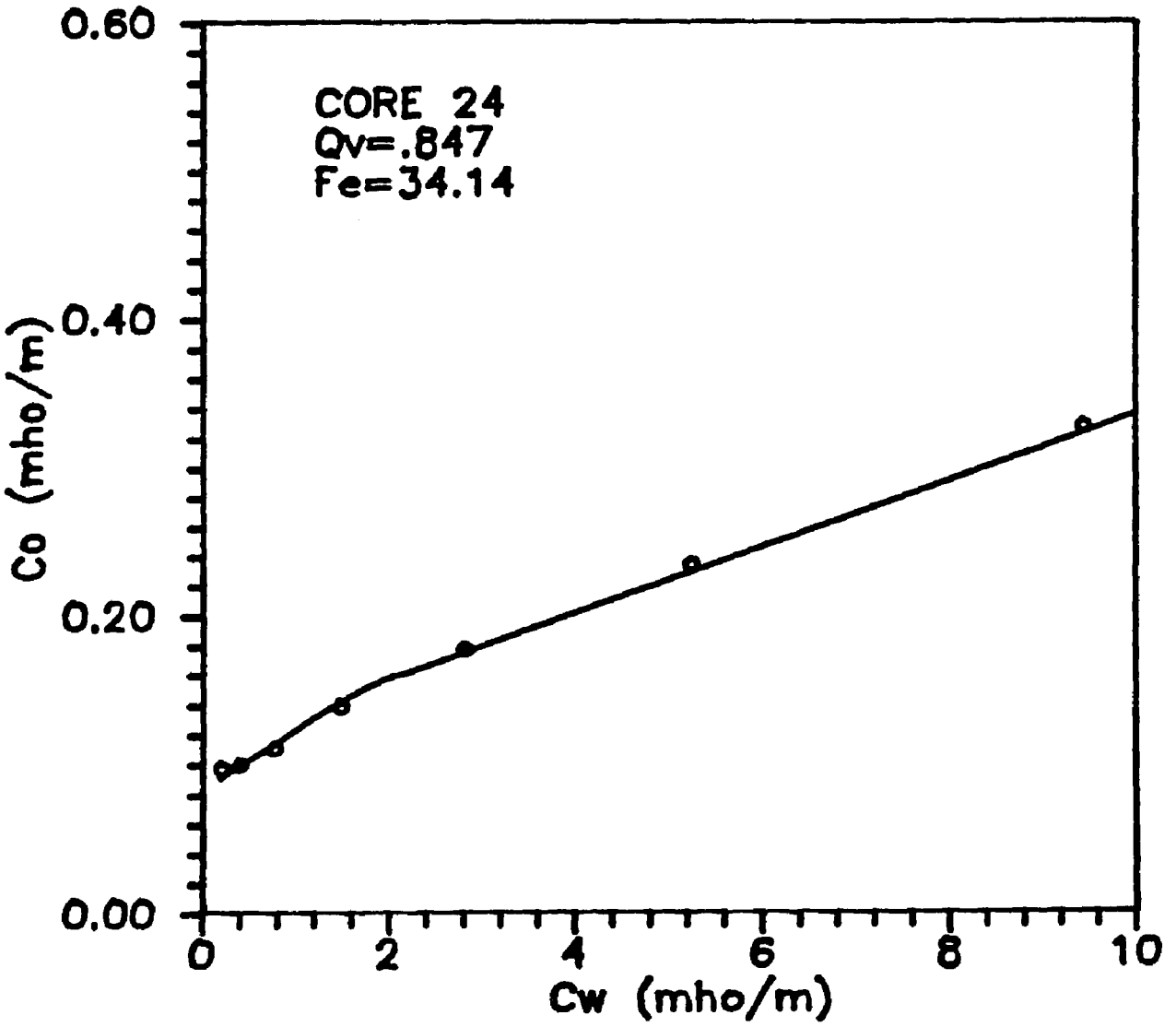
CORE 24
Qv=.847
Fe=34.14
0.60
0.40
0.20
0.00
Co (mho/m)
0
2
4
6
8
10
Cw (mho/m)

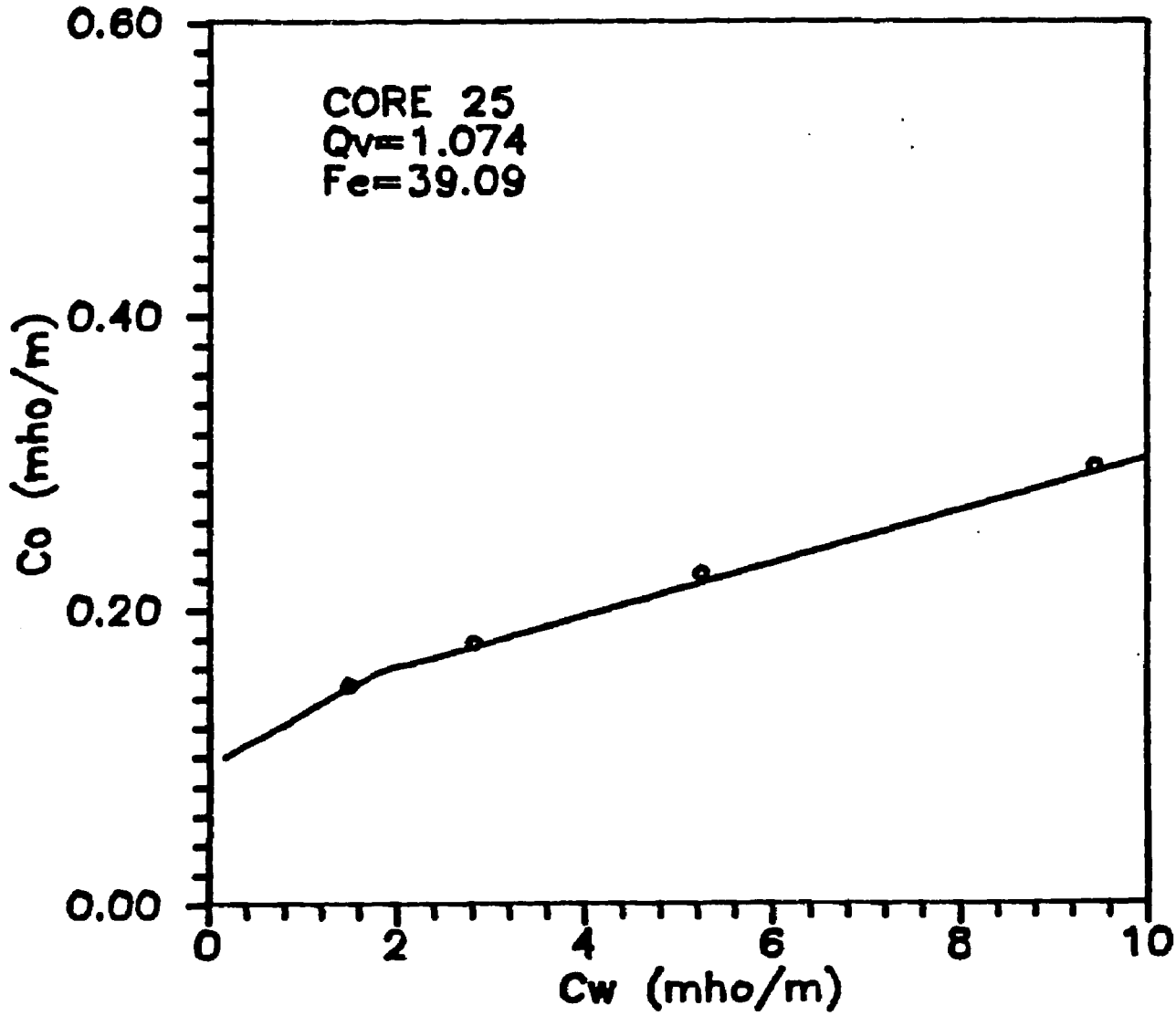
CORE 25
Qv=1.074
Fe=39.09
0.60
0.40
0.20
0.00
Co (mho/m)
0
2
4
6
8
10
Cw (mho/m)

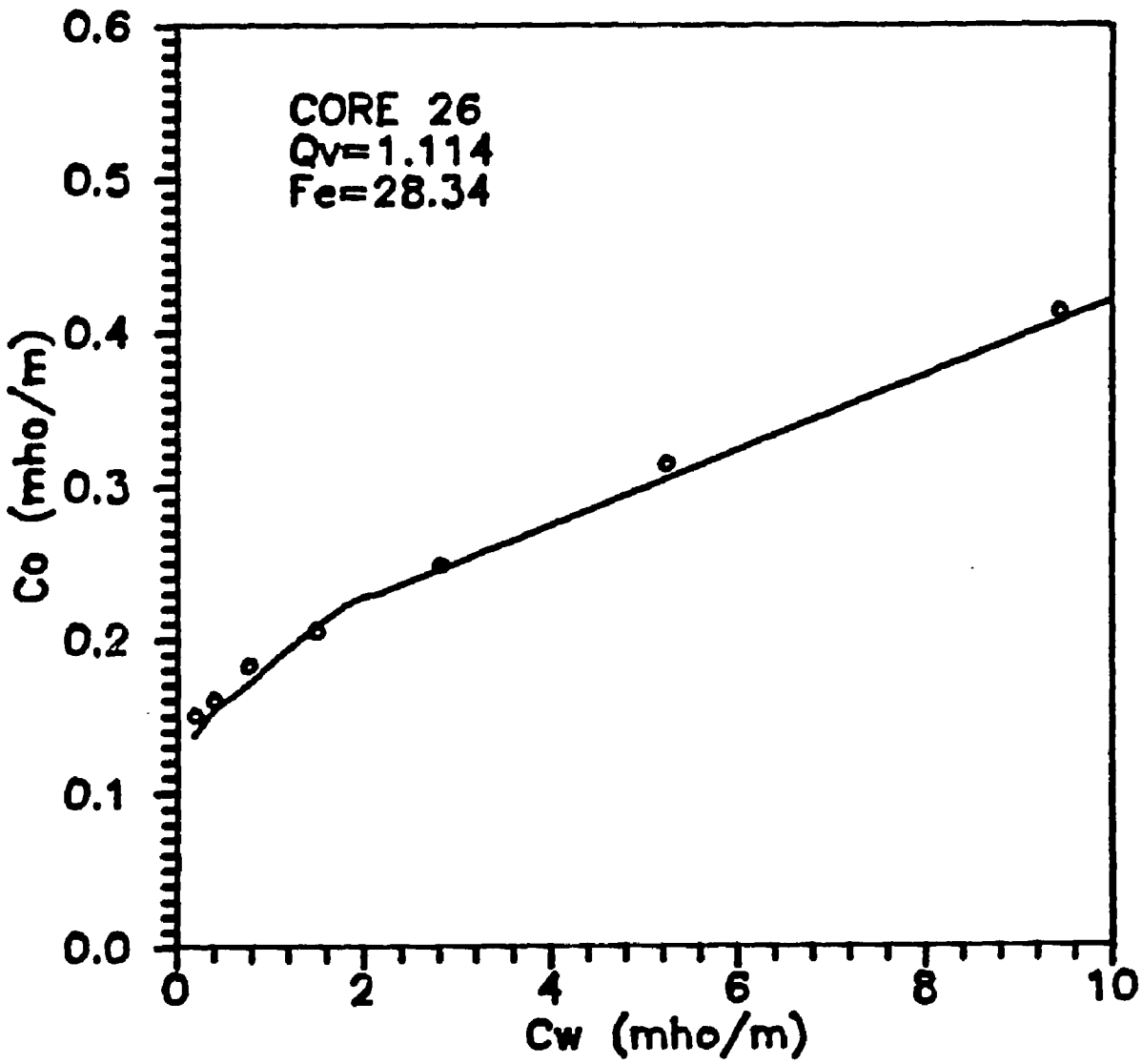
CORE 26
Qv=1.114
Fe=28.34
Co (mho/m)
Cw (mho/m)
0.0
0.1
0.2
0.3
0.4
0.5
0.6
0
2
4
6
8
10

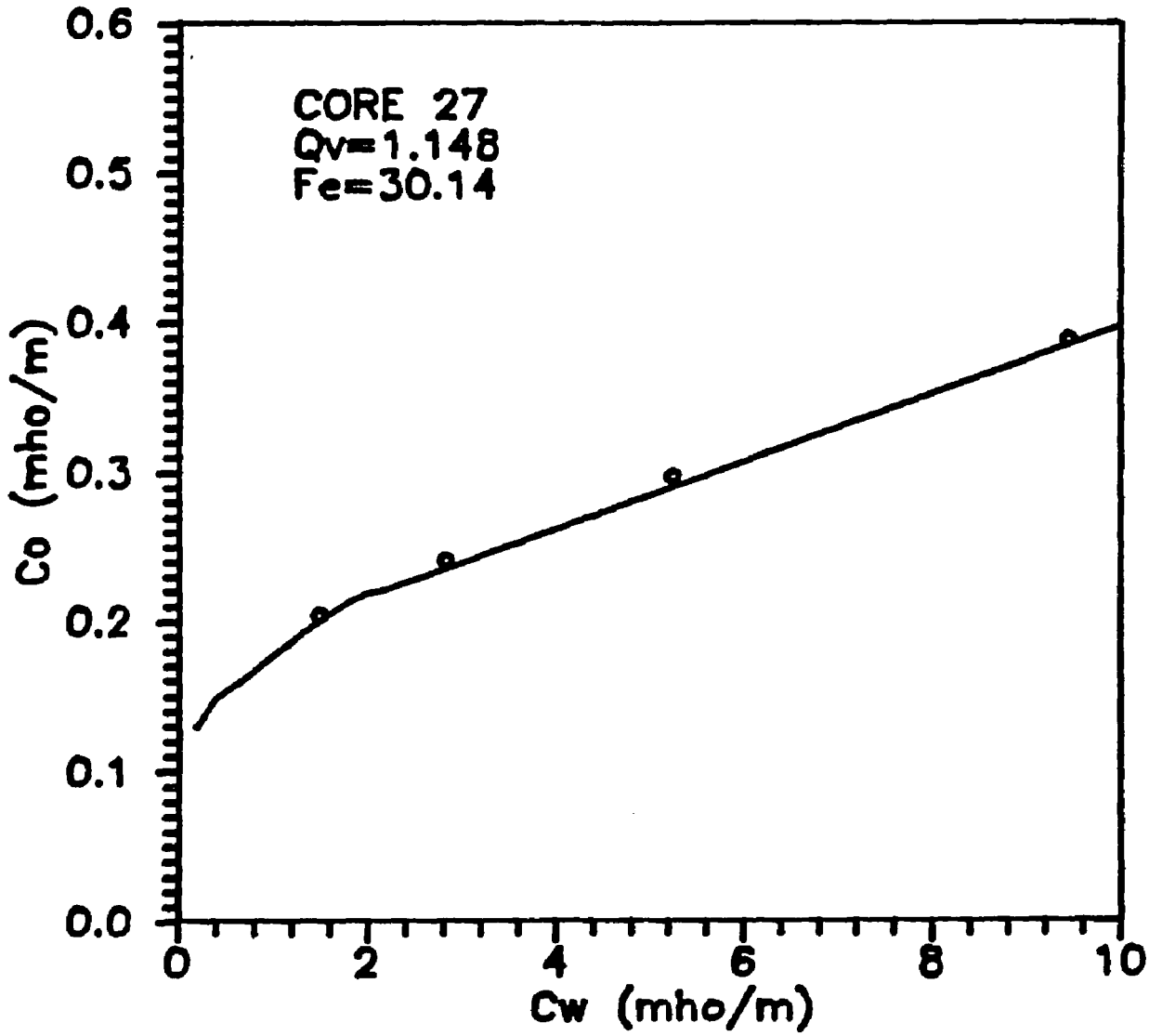
CORE 27
Qv=1.148
Fe=30.14
Co (mho/m)
Cw (mho/m)
0.0
0.1
0.2
0.3
0.4
0.5
0.6
0
2
4
6
8
10

APPENDIX C

Comparison of Experimental vs. Calculated Membrane Potentials

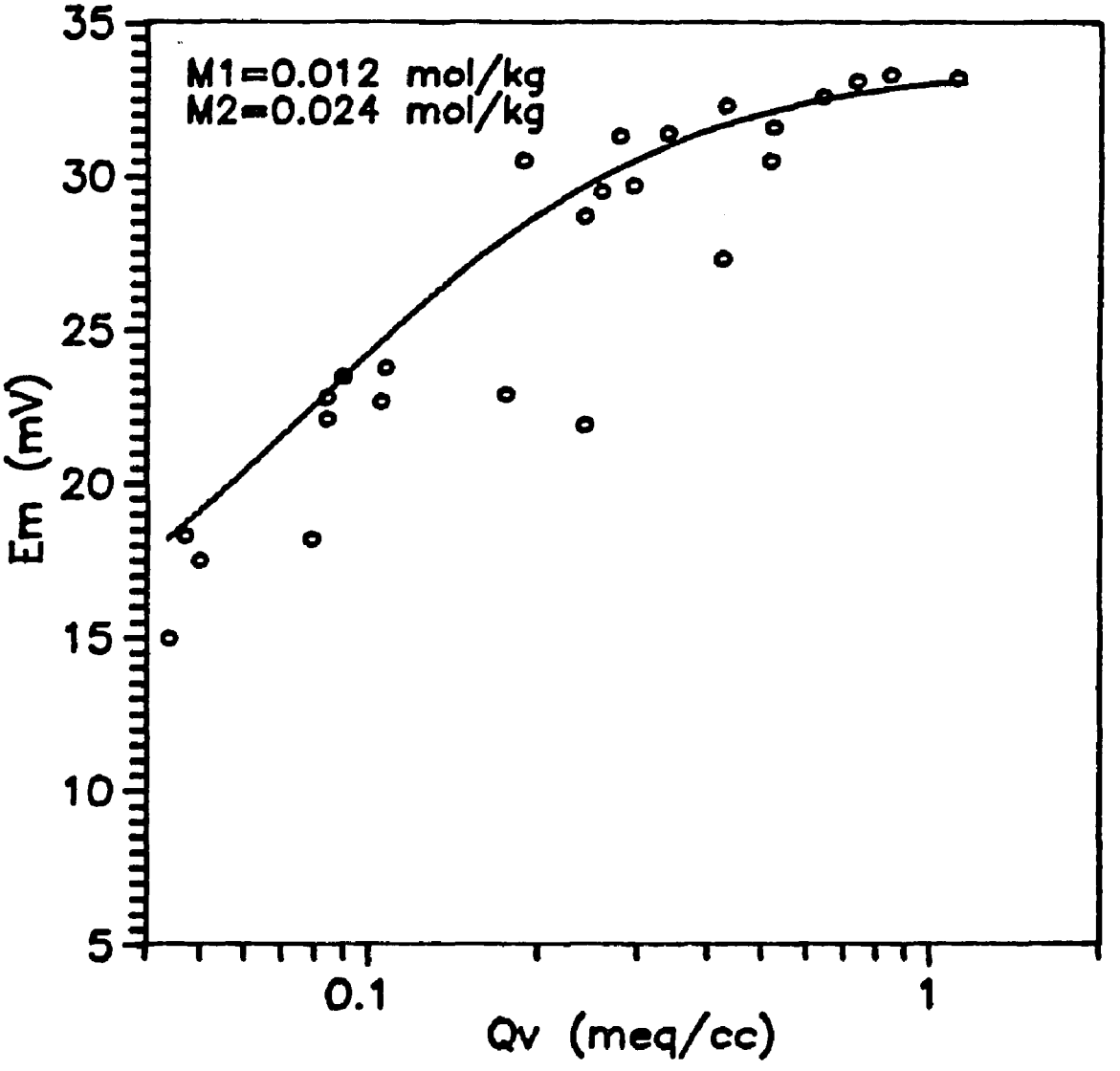
M1=0.012 mol/kg
M2=0.024 mol/kg
Em (mV)
35
30
25
20
15
10
5
0.1
1
Qv (meq/cc)

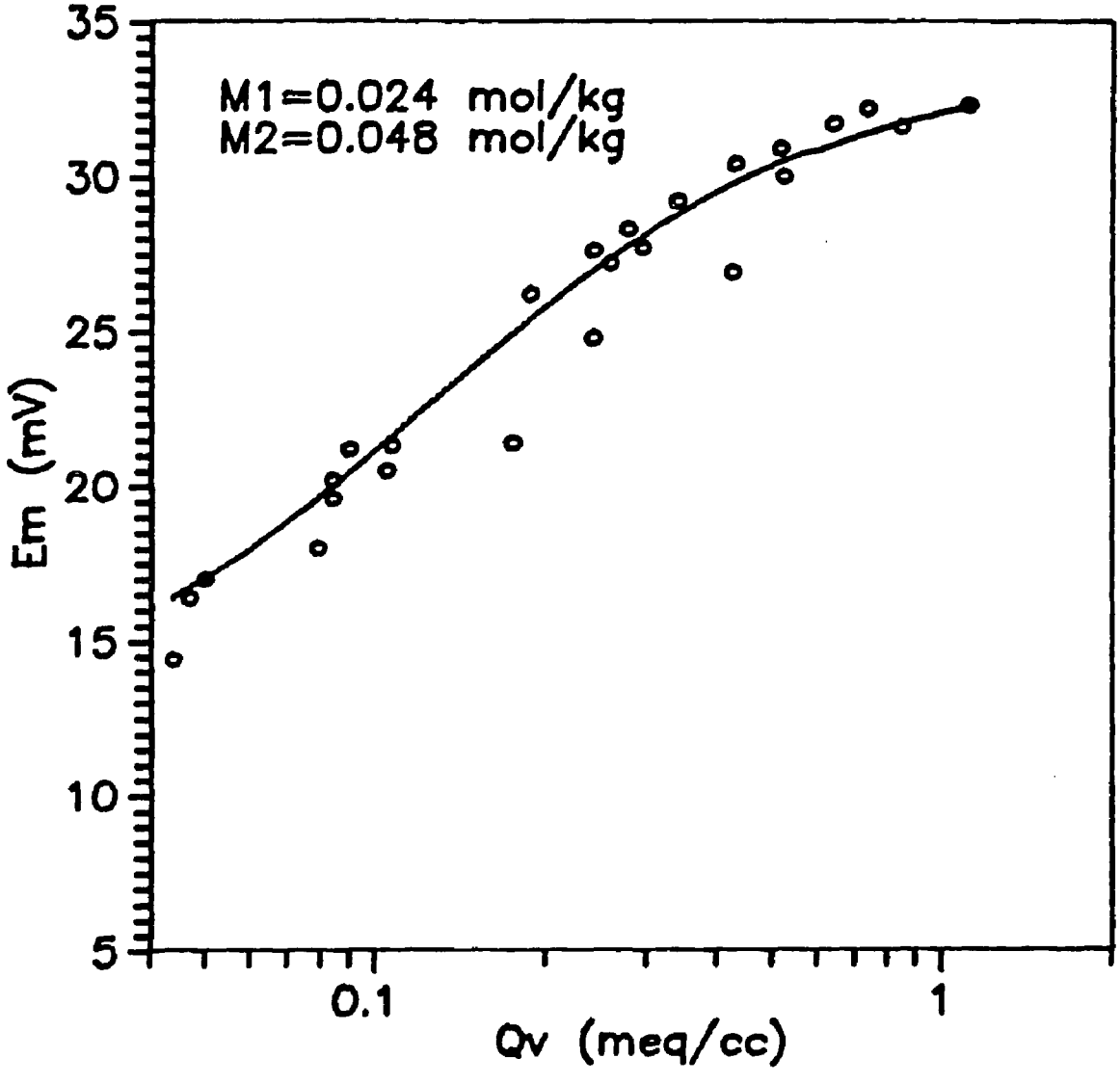
M1=0.024 mol/kg
M2=0.048 mol/kg
Em (mV)
35
30
25
20
15
10
5
0.1
1
Qv (meq/cc)

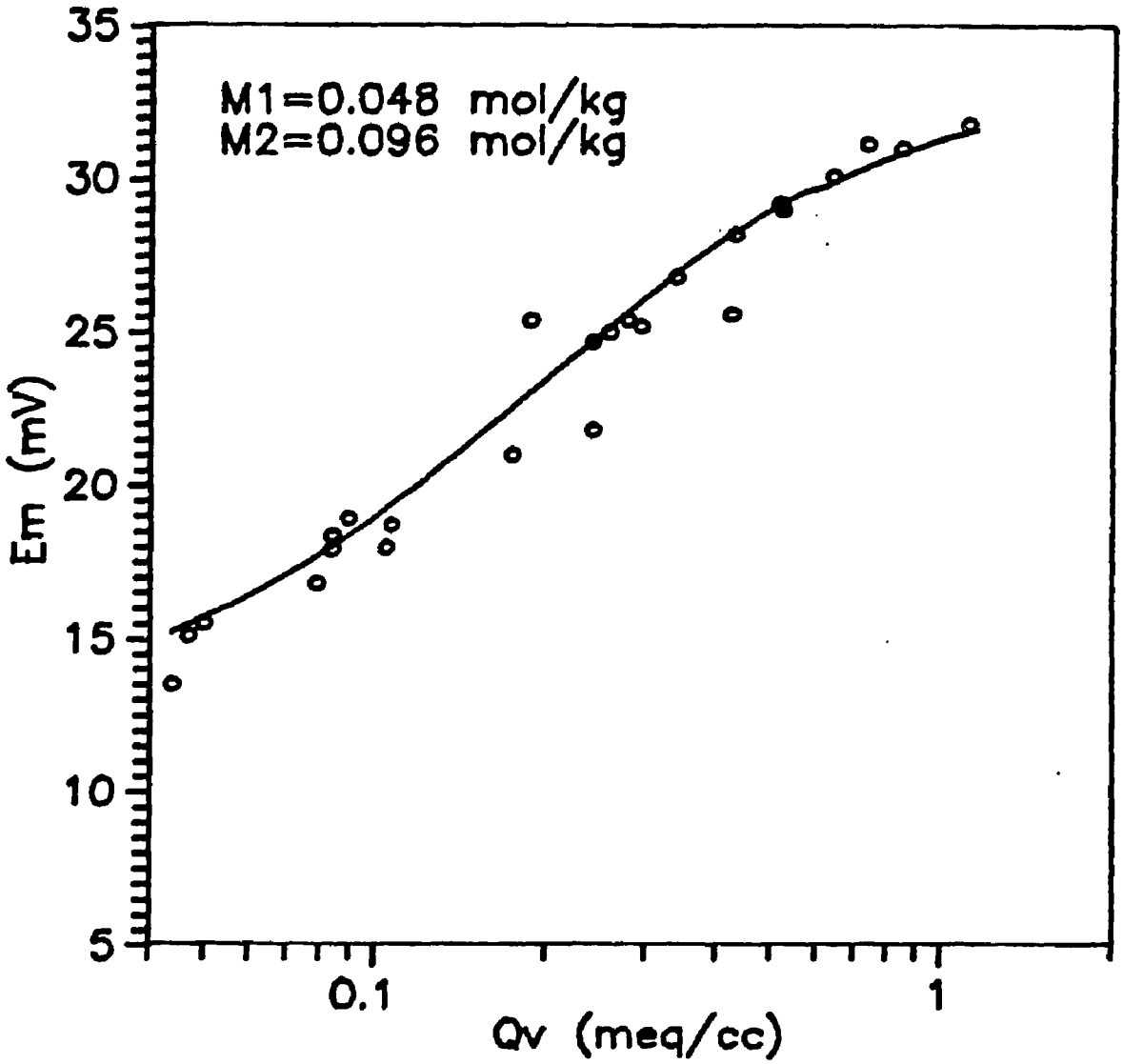
M1=0.048 mol/kg
M2=0.096 mol/kg
35
30
25
20
15
10
5
Em (mV)
0.1
1
Qv (meq/cc)

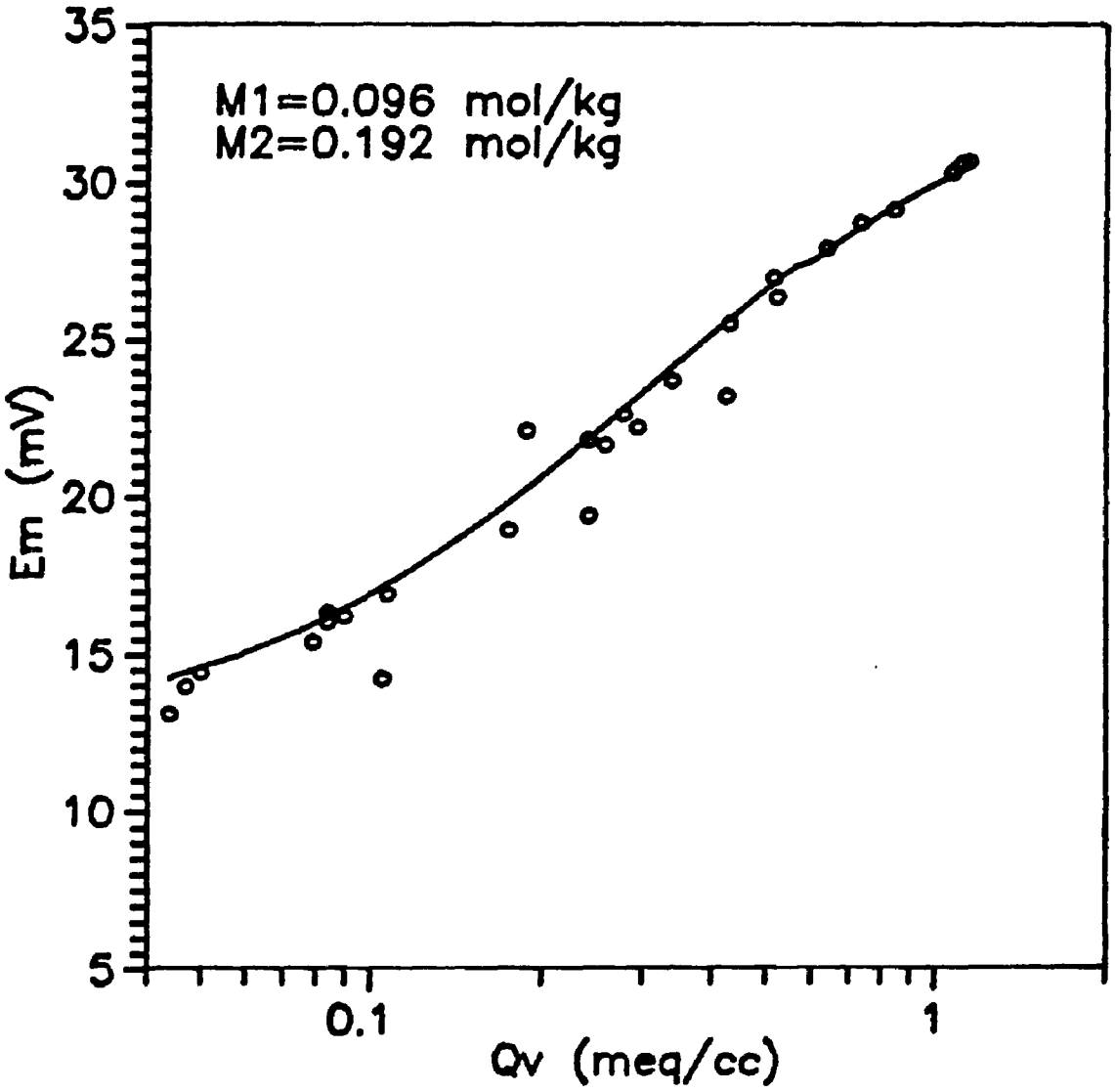
M1=0.096 mol/kg
M2=0.192 mol/kg
Em (mV)
Qv (meq/cc)
35
30
25
20
15
10
5
0.1
1

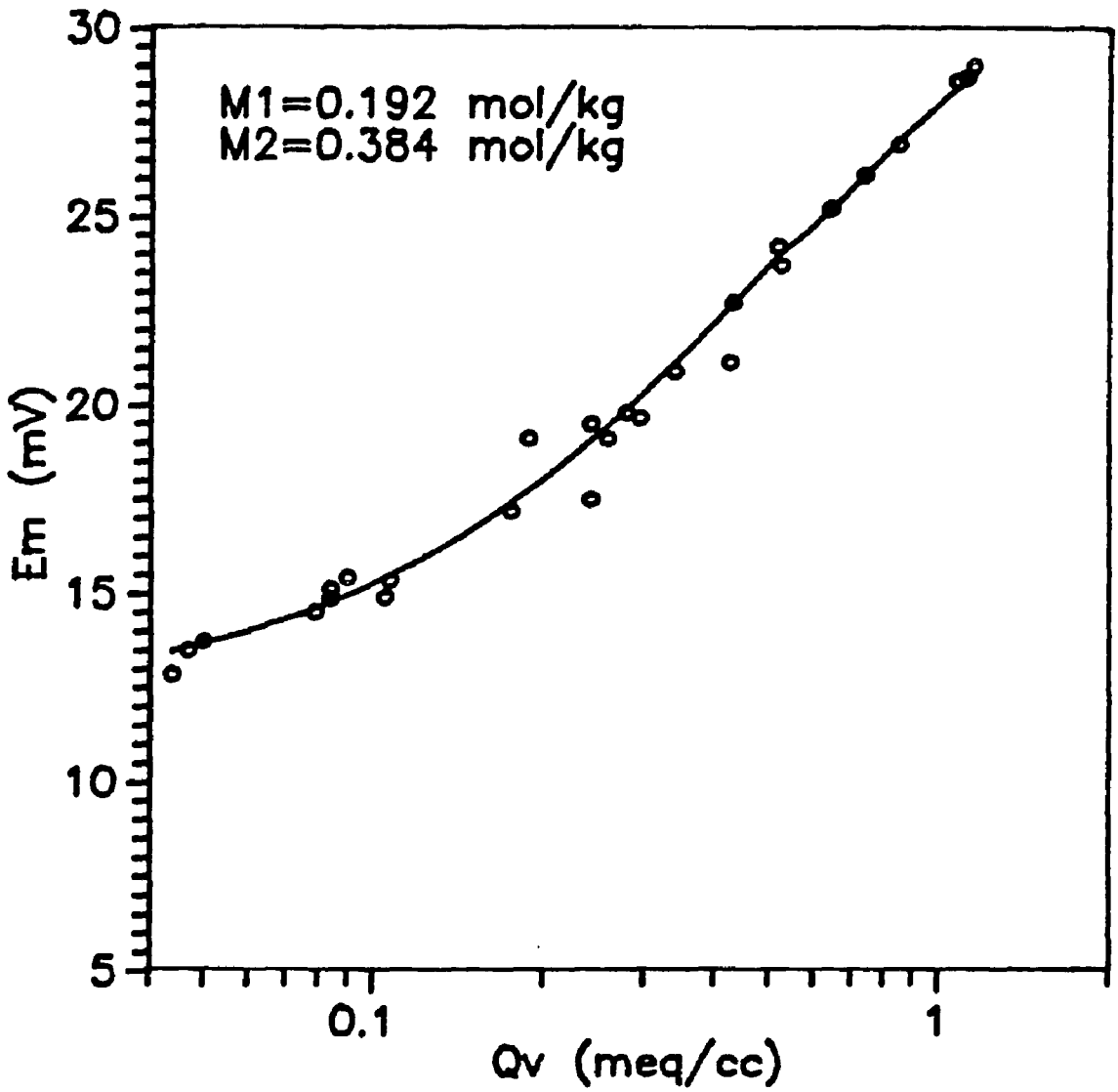
M1=0.192 mol/kg
M2=0.384 mol/kg
Em (mV)
30
25
20
15
10
5
0.1
1
Qv (meq/cc)

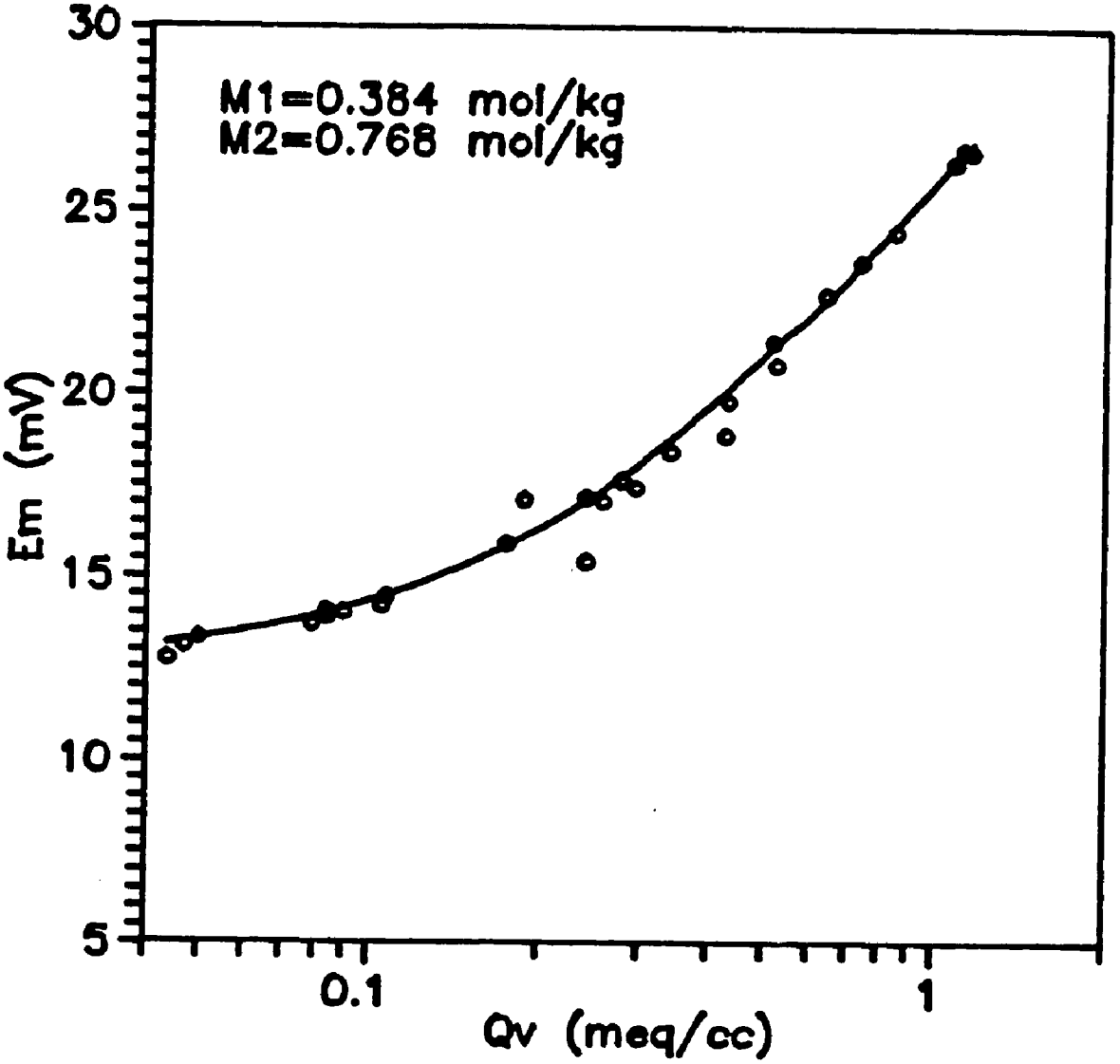
M1=0.384 mol/kg
M2=0.768 mol/kg
Em (mV)
30
25
20
15
10
5
0.1
1
Qv (meq/cc)

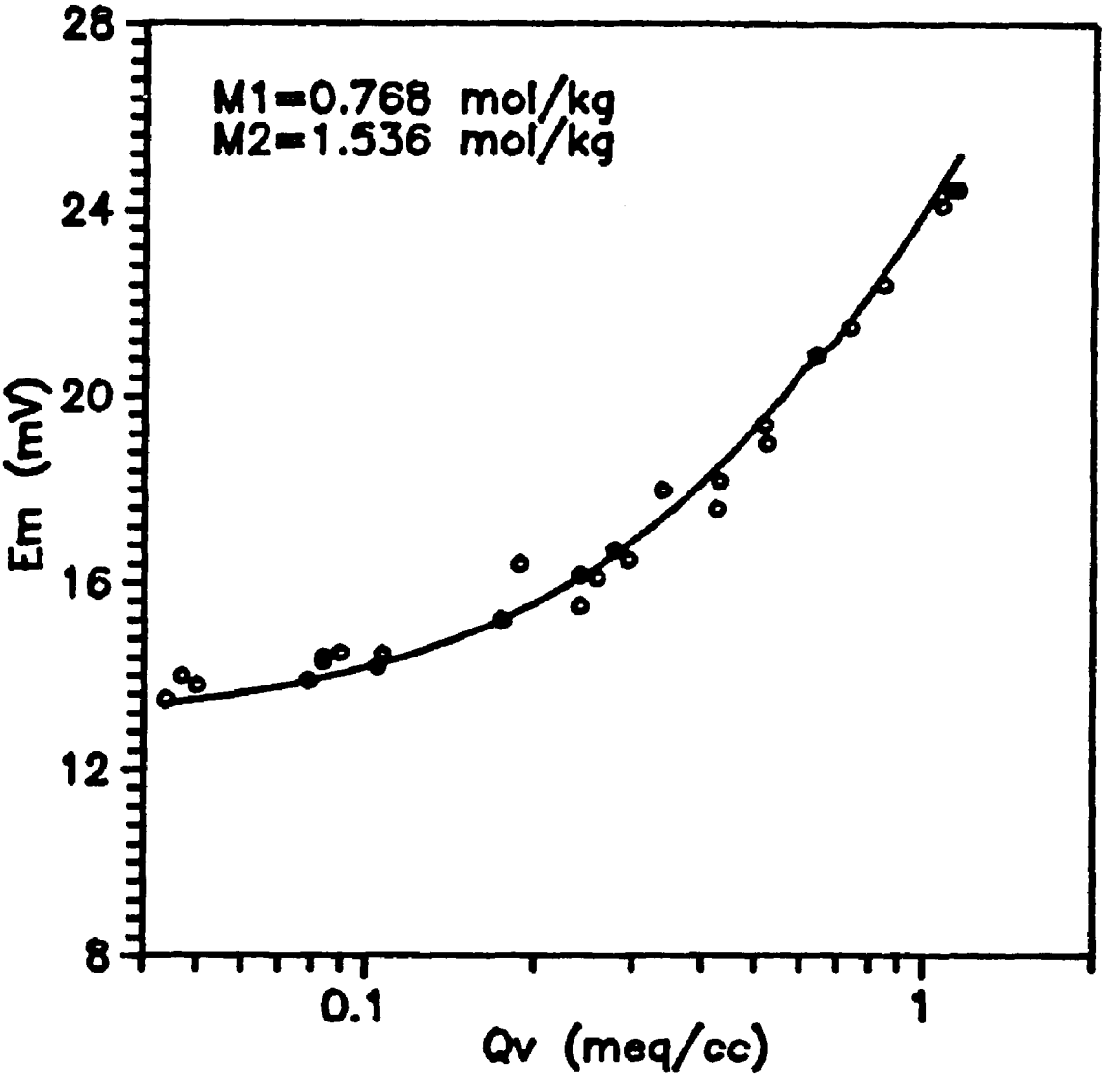
M1=0.768 mol/kg
M2=1.536 mol/kg
28
24
20
16
12
8
Em (mV)
0.1
1
Qv (meq/cc)

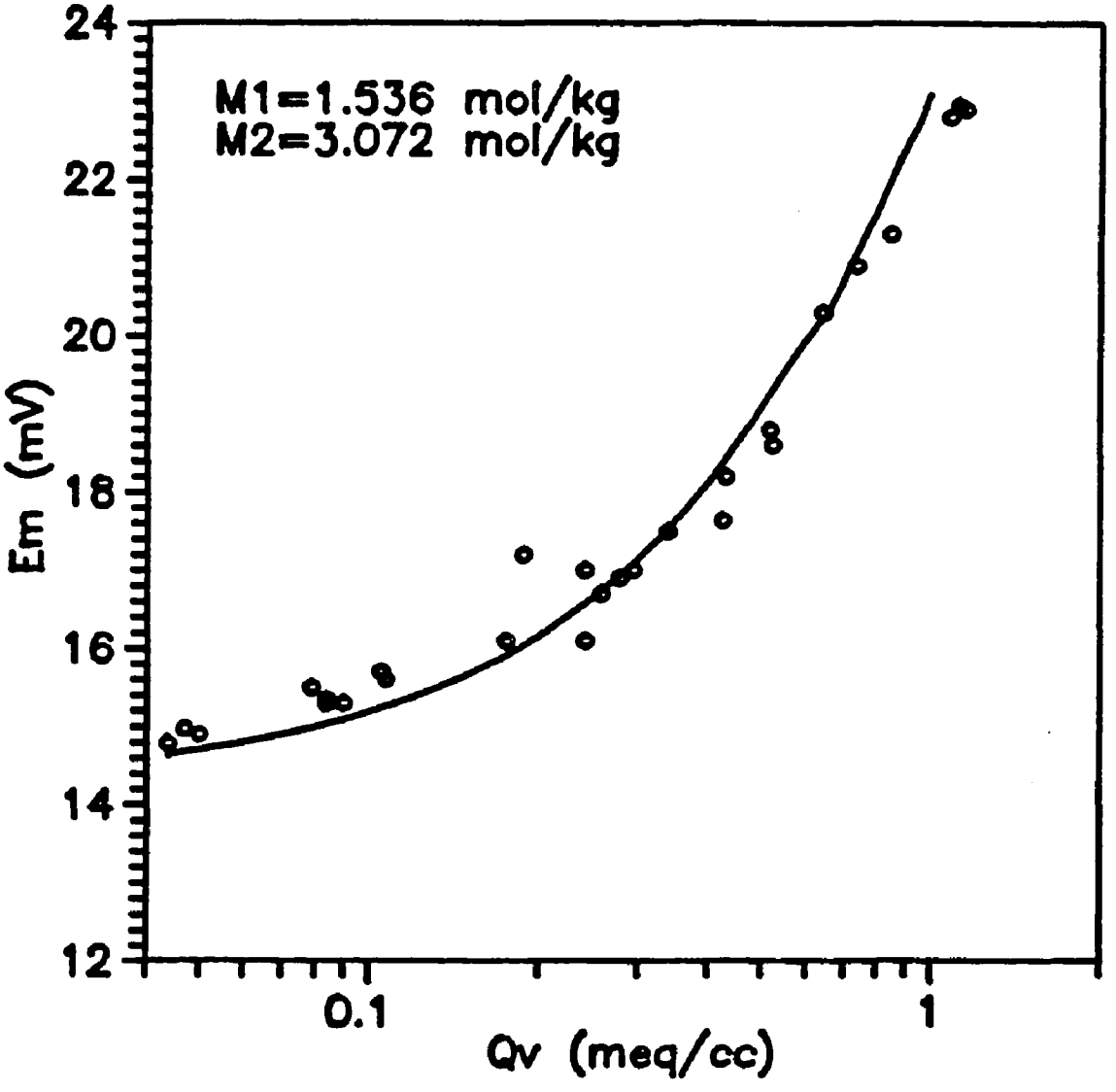
M1=1.536 mol/kg
M2=3.072 mol/kg
Em (mV)
Qv (meq/cc)
24
22
20
18
16
14
12
0.1
1

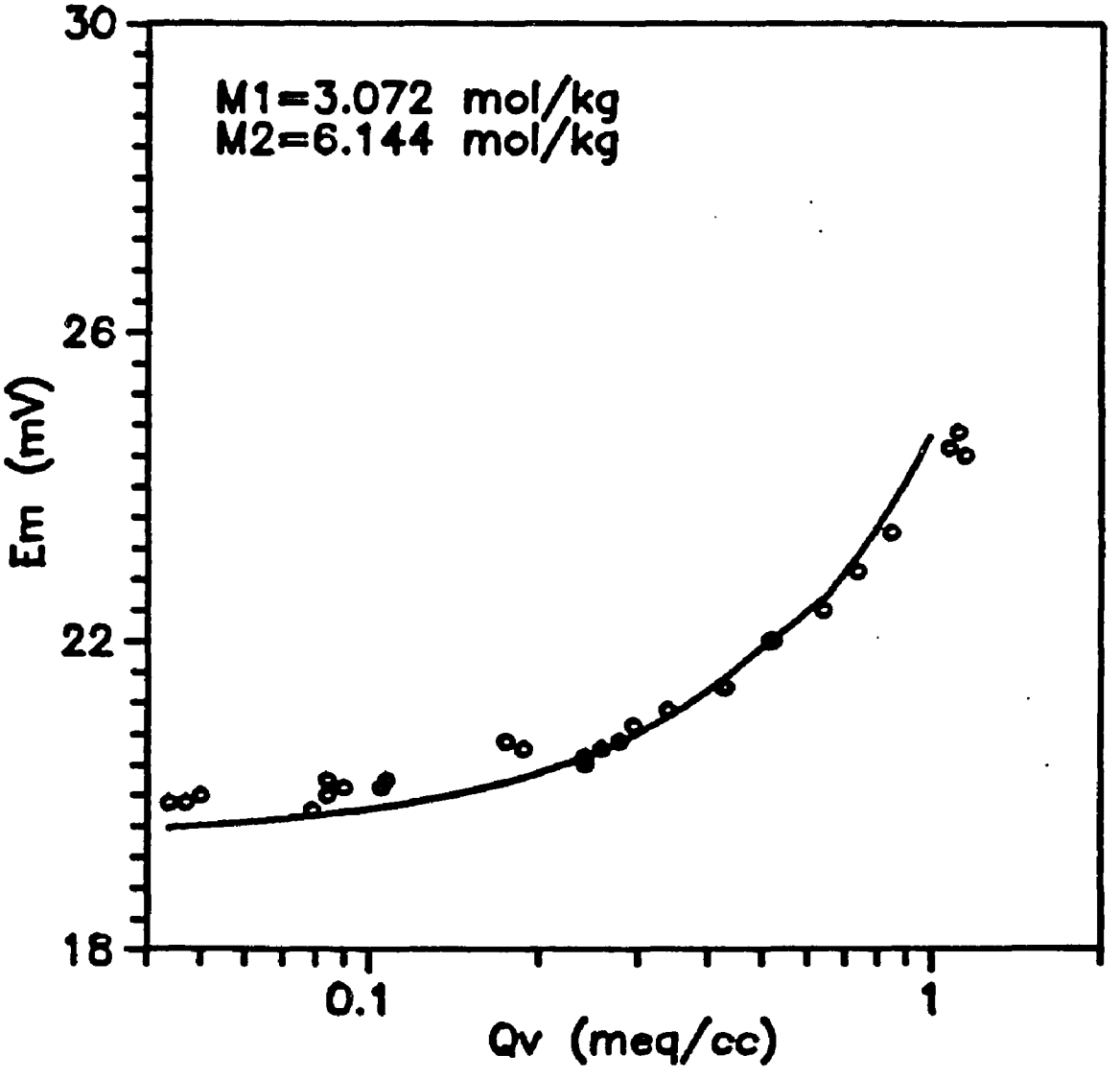
M1=3.072 mol/kg
M2=6.144 mol/kg
30
26
22
18
Em (mV)
0.1
1
Qv (meq/cc)

APPENDIX D

Experimental Data of Shaly Cores at Different Water Saturations

Table D.1

Data Used in the Test of the Saturation Equation

	Core 1		Core 2	
Cw	Sw	Ct	Sw	Ct
12.407	.473	.0691		
	.654	.1256		
	.868	.2099		
10.132	.463	.0588	.638	.3129
	.569	.0843	.711	.3847
	.750	.1371	.812	.4889
8.00	.463	.0490		
	.493	.0548		
	.665	.0931		
6.061	.471	.0410	.647	.2126
	.655	.0722	.713	.2556
			.840	.3396
3.058	.482	.0298	.590	.1148
	.591	.0423	.823	.1963
	.765	.0604		
1.015	.499	.0184	.600	.0606
	.669	.0259	.672	.0703
	.860	.0363	.768	.0844
			.895	.1036

(Core conductivities expressed in (mho/m)

Table D.1 (cont.)

Cw	Core 3 Sw	Core 3 Ct	Core 4 Sw	Core 4 Ct
12.407	.570	.1596	.464	.0816
	.730	.2449	.521	.1017
	.812	.2952	.595	.1254
	.867	.3315	.716	.1750
6.061	.601	.0991	.473	.0477
	.685	.1228	.510	.0534
	.747	.1406	.583	.0668
	.813	.1611	.695	.0872
3.058	.609	.0646	.480	.0293
	.706	.0787	.511	.0331
	.842	.1046	.570	.0387
			.665	.0481
1.015	.610	.0339	.464	.0158
	.695	.0392	.529	.0178
	.730	.0416	.594	.0204
	.861	.0516	.680	.0237

Table D.1 (cont.)

	Core 5		Core 6	
Cw	Sw	Ct	Sw	Ct
12.407	.437	.0777	.570	.1312
	.485	.0913	.628	.1585
	.557	.1131	.716	.2091
	.665	.1500		
	.856	.2244		
6.061	.449	.0449		
	.533	.0596		
	.659	.0818		
	.928	.1409		
3.058	.437	.0269	.540	.0394
	.485	.0312	.594	.0468
	.605	.0424	.678	.0590
	.719	.0600	.807	.0810
1.015	.431	.0139	.421	.0120
	.539	.0176	.535	.0185
	.671	.0221	.800	.0364
	.960	.0355		

Table D.1 (cont.)

Cw	Core 7 Sw	Core 7 Ct	Core 8 Sw	Core 8 Ct
12.407	.541	.2318	.435	.0733
	.589	.2746	.565	.1111
	.652	.3321	.712	.1582
	.725	.3923	.929	.2435
	.821	.5064		
6.061			.414	.0392
			.456	.0449
			.527	.0555
			.621	.0705
			.745	.0918
3.058	.528	.0781		
	.652	.1105		
	.794	.1496		
1.015	.510	.0374	.437	.0129
	.589	.0442	.541	.0161
	.693	.0550	.682	.0210
	.837	.0698	.929	.0314

Table D.1 (cont.)

	Core 9		Core 10	
Cw	Sw	Ct	Sw	Ct
3.058	.427	.0434	.434	.0944
	.558	.0717	.492	.1145
			.588	.1504
			.753	.2205
			.864	.2273
1.015	.455	.0216	.424	.0371
	.519	.0274	.478	.0435
	.594	.0345	.562	.0566
	.692	.0449	.662	.0718

Table D.2

Basic Petrophysical Data

Core	Porosity	Fe	Qv
1	.130	46.28	.328
2	.264	14.98	.240
3	.194	29.49	.260
4	.123	42.17	.199
5	.115	41.53	.188
6	.192	30.68	.196
7	.237	17.67	.177
8	.114	46.08	.187
9	.232	15.19	.098
10	.296	9.72	.121

APPENDIX E

Comparison of Calculated vs. Experimental Core Conductivities at Different Temperatures

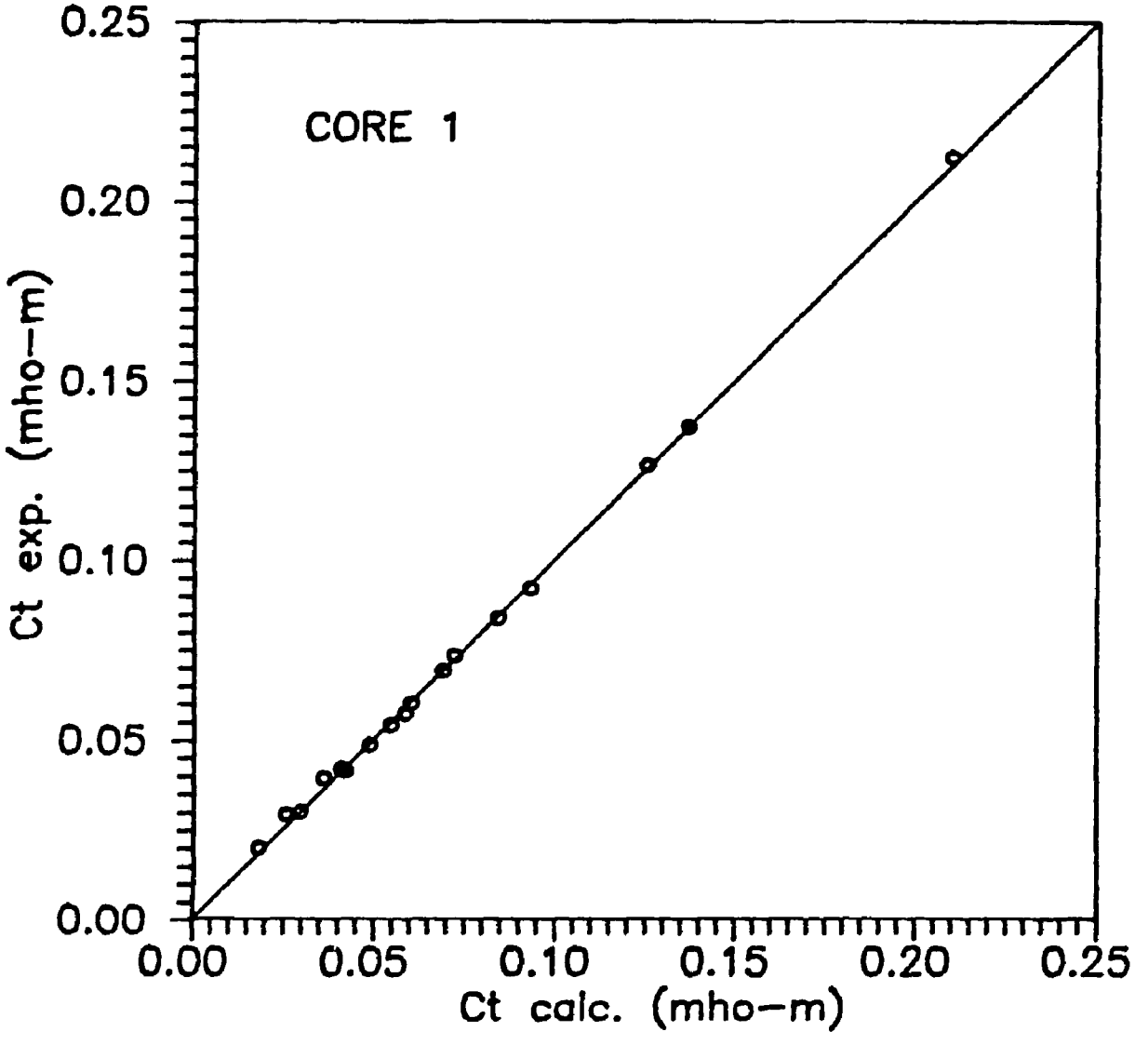
CORE 1
0.25
0.20
0.15
0.10
0.05
0.00
Ct exp. (mho-m)
0.00
0.05
0.10
0.15
0.20
0.25
Ct calc. (mho-m)

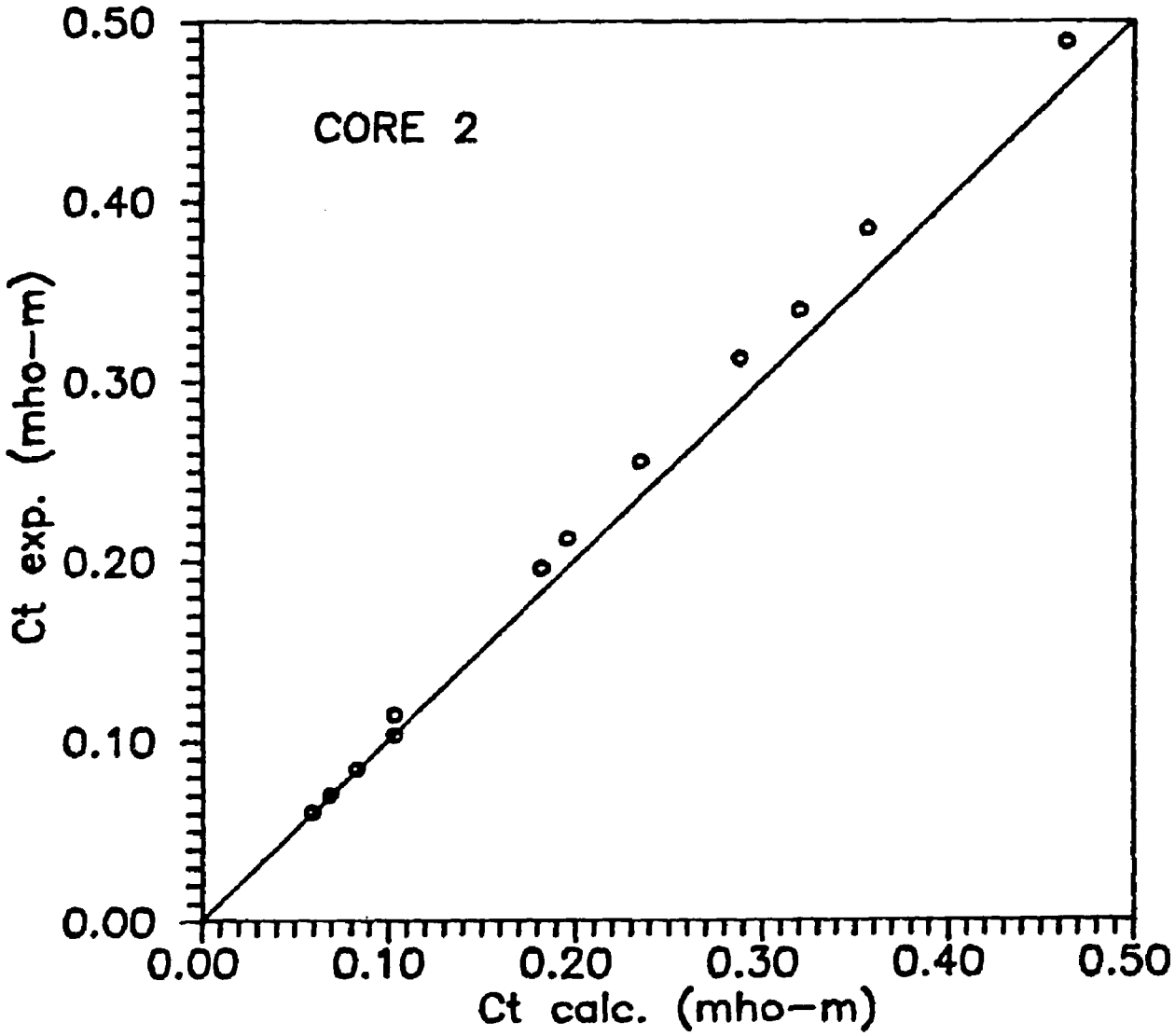
CORE 2
0.50
0.40
0.30
0.20
0.10
0.00
Ct exp. (mho-m)
0.00
0.10
0.20
0.30
0.40
0.50
Ct calc. (mho-m)

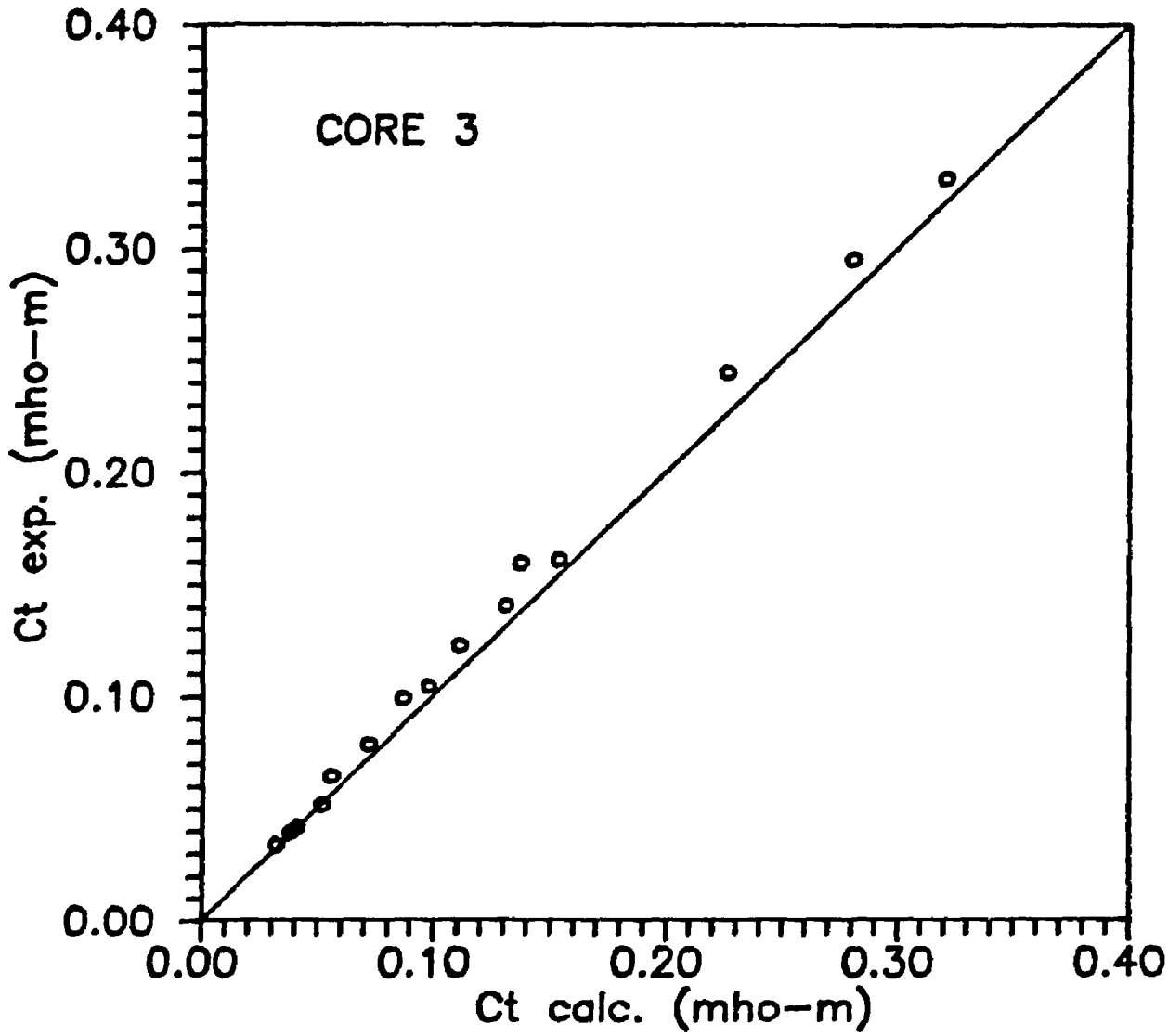
CORE 3
0.40
0.30
0.20
0.10
0.00
Ct exp. (mho-m)
0.00
0.10
0.20
0.30
0.40
Ct calc. (mho-m)

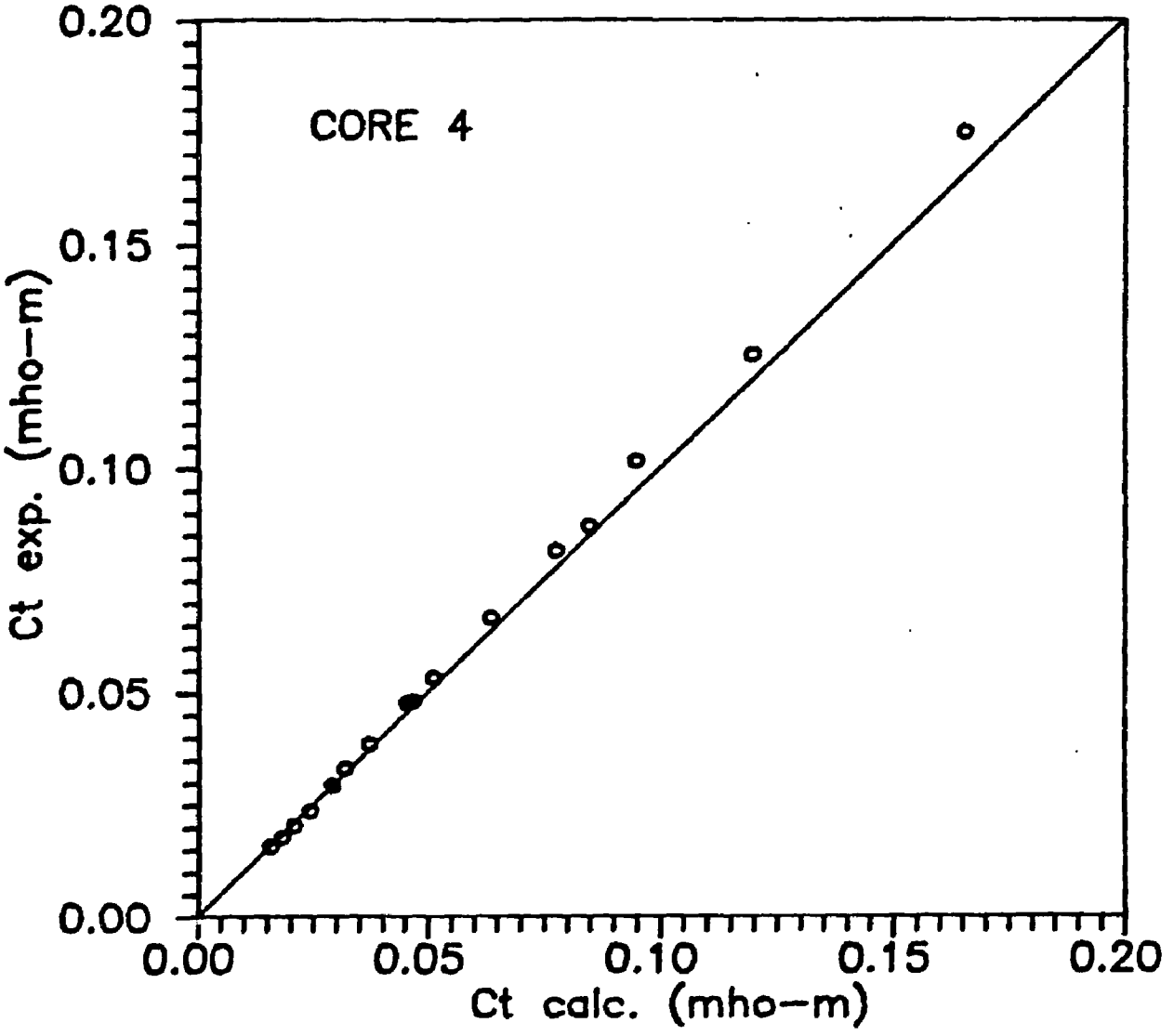
CORE 4
0.20
0.15
0.10
0.05
0.00
Ct exp. (mho-m)
0.00
0.05
0.10
0.15
0.20
Ct calc. (mho-m)

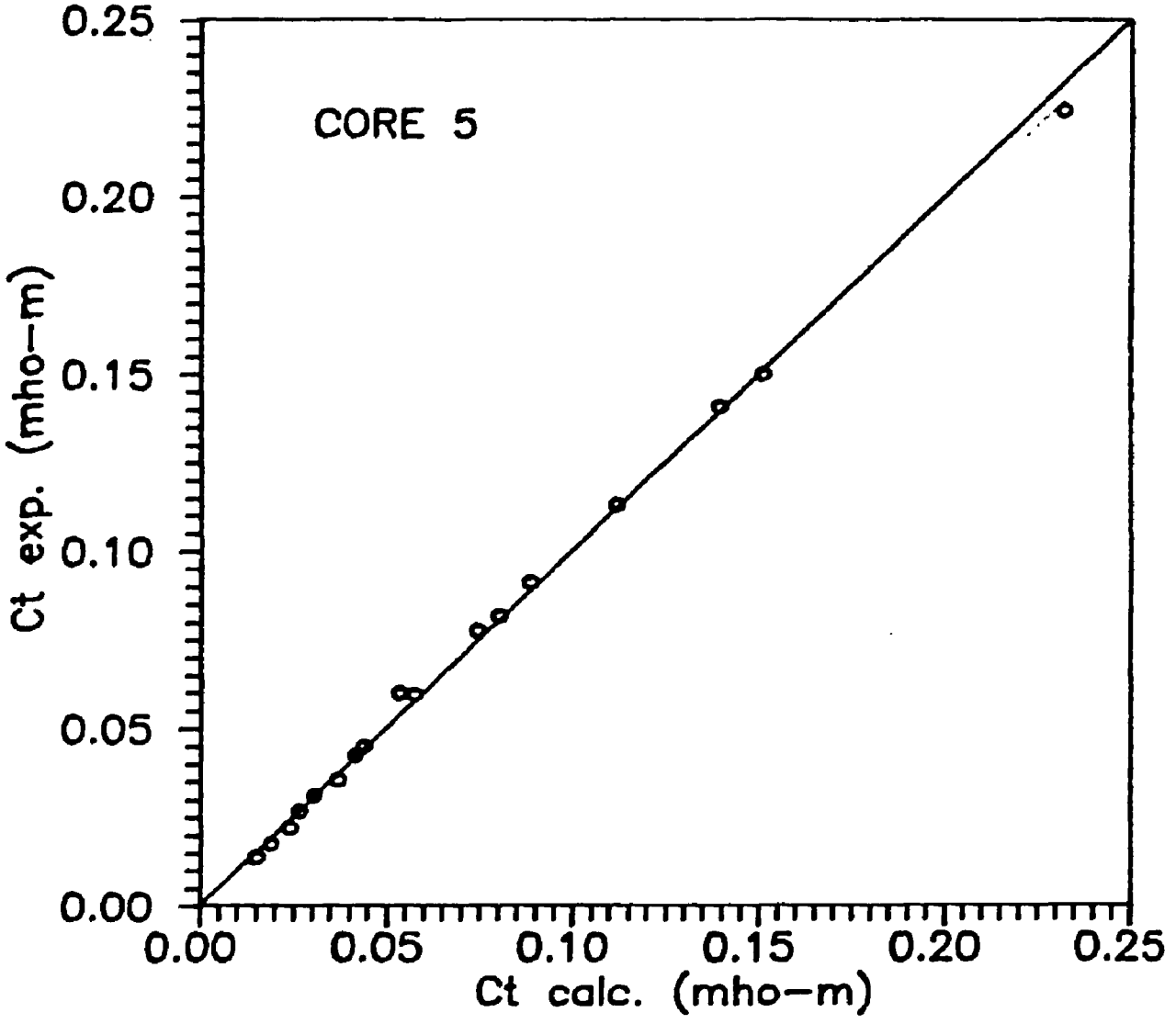
CORE 5
0.25
0.20
0.15
0.10
0.05
0.00
Ct exp. (mho-m)
0.00
0.05
0.10
0.15
0.20
0.25
Ct calc. (mho-m)

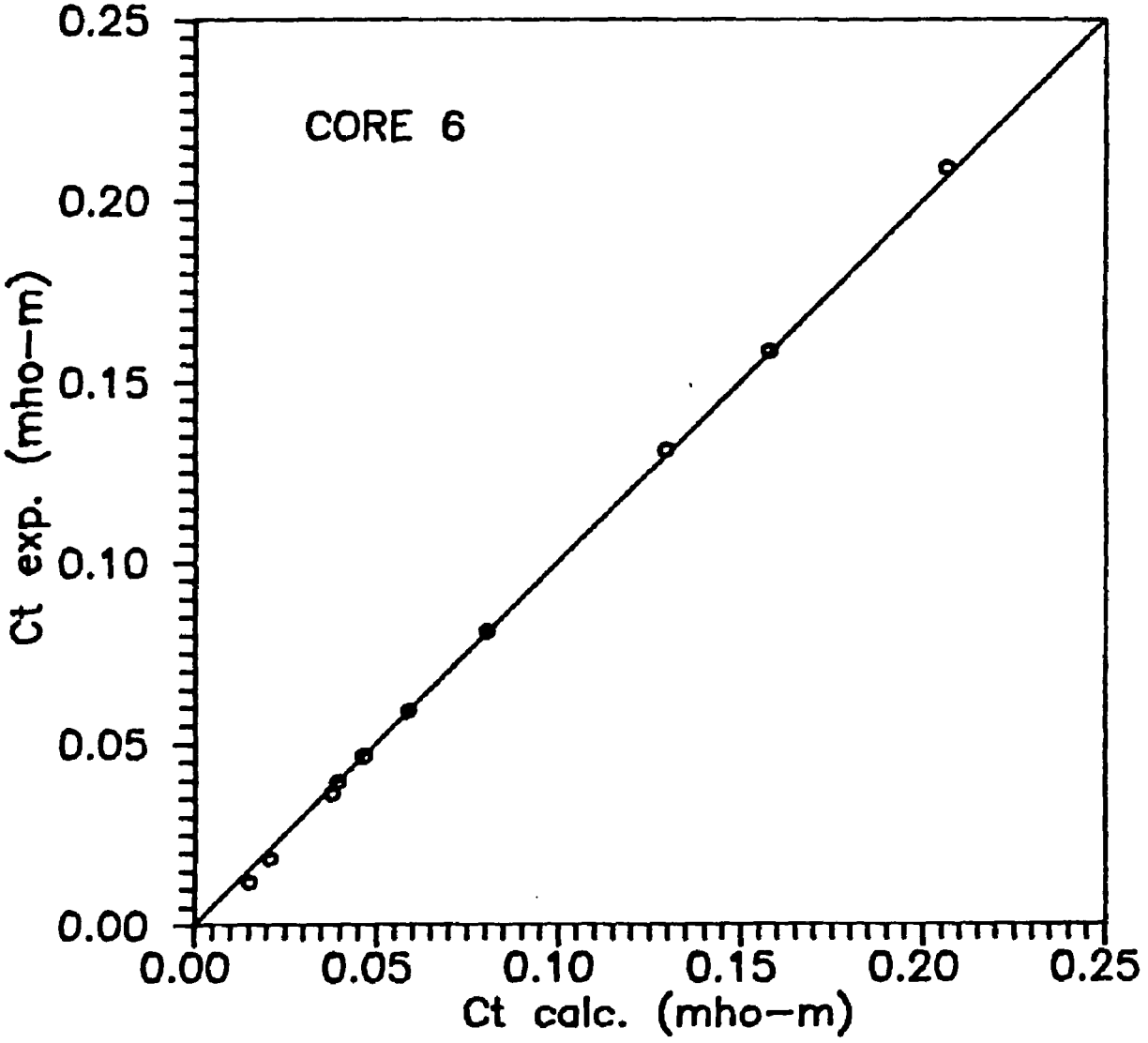
CORE 6
Ct exp. (mho-m)
Ct calc. (mho-m)
0.00
0.05
0.10
0.15
0.20
0.25

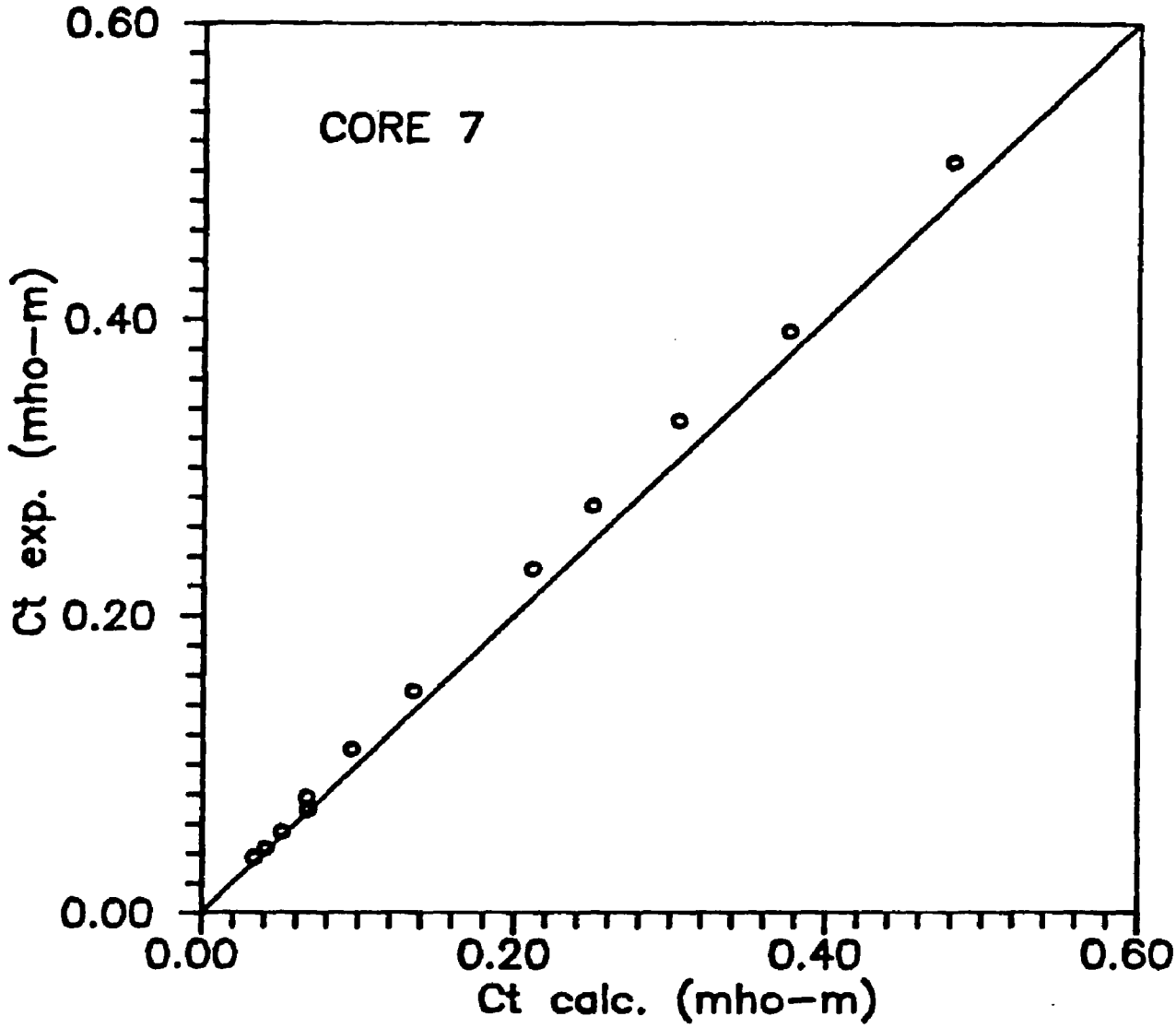
CORE 7
0.60
0.40
0.20
0.00
Ct exp. (mho-m)
0.00
0.20
0.40
0.60
Ct calc. (mho-m)

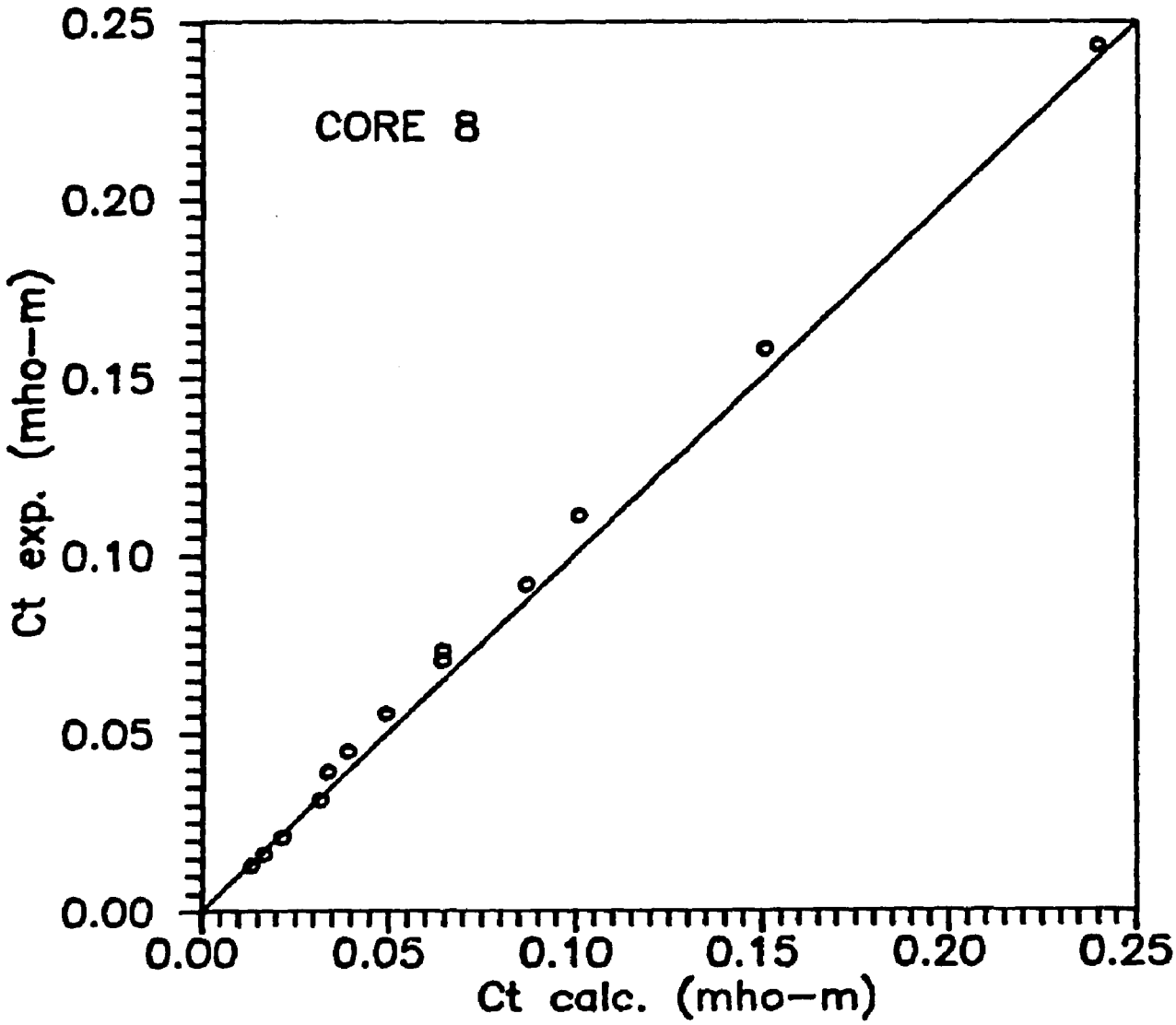
CORE 8
Ct exp. (mho-m)
Ct calc. (mho-m)
0.00
0.05
0.10
0.15
0.20
0.25

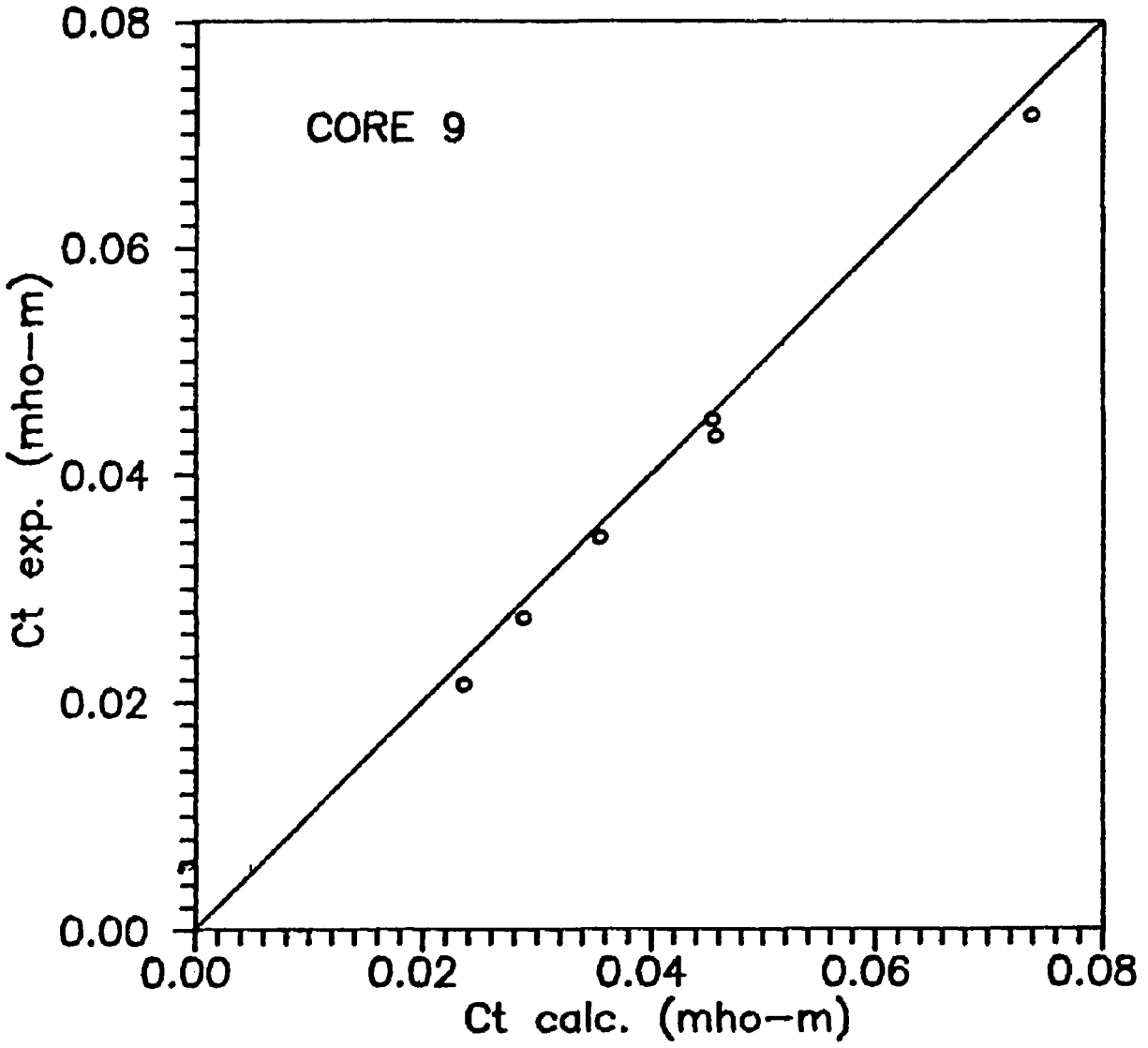
CORE 9
0.08
0.06
0.04
0.02
0.00
Ct exp. (mho-m)
0.00
0.02
0.04
0.06
0.08
Ct calc. (mho-m)

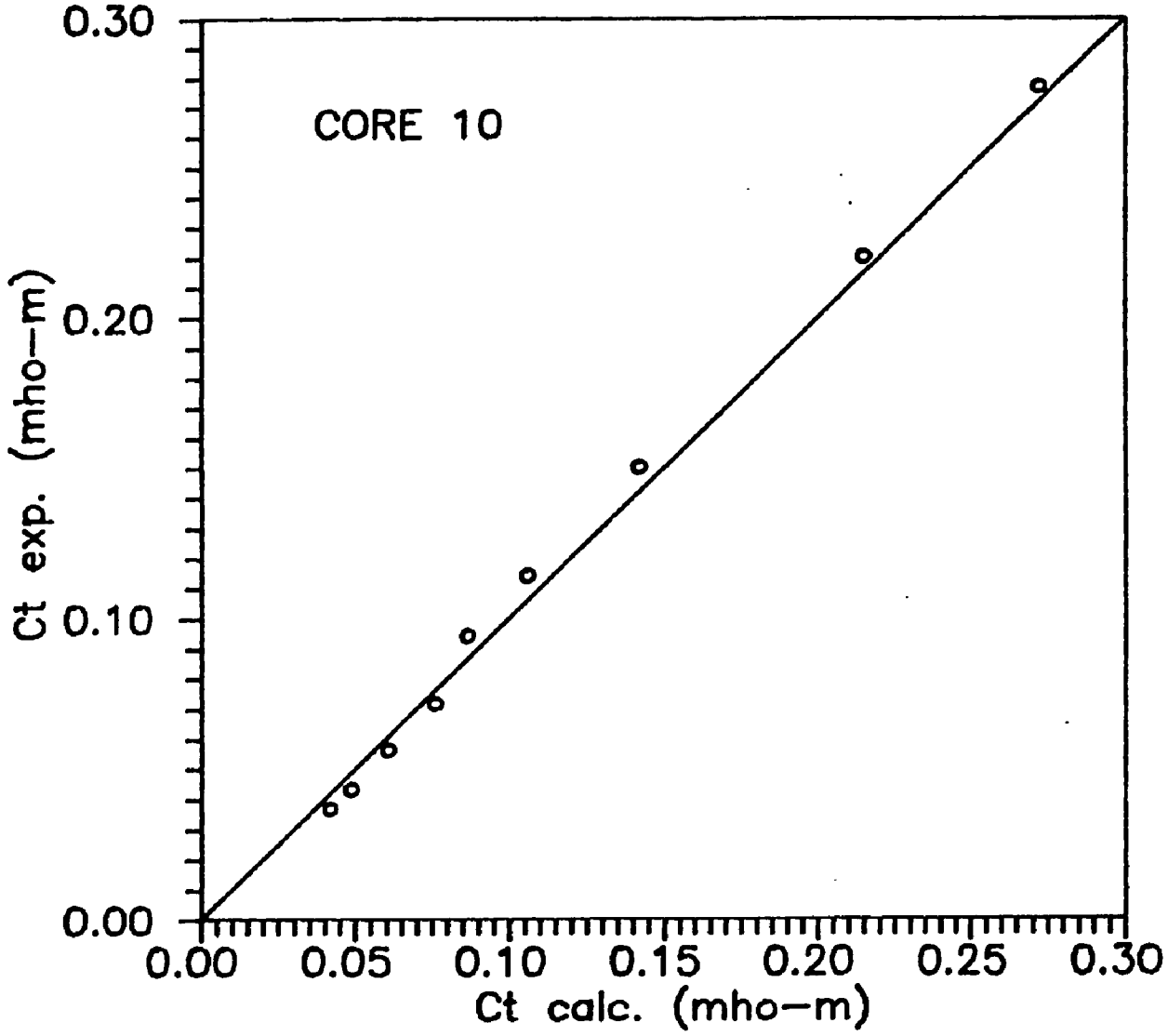
CORE 10
0.30
0.20
0.10
0.00
Ct exp. (mho-m)
0.00
0.05
0.10
0.15
0.20
0.25
0.30
Ct calc. (mho-m)

APPENDIX F

Core Conductivities at Different Temperatures

CORE CONDUCTIVITIES AT VARIOUS TEMPERATURES

CORE 1

	Core Conductivities, mho/m						
m_{NaCl}	22°C	50°C	80°C	110°C	140°C	170°C	200°C
0.090	0.101	0.163	0.235	0.309	0.376	0.448	0.522
0.260	0.350	0.574	0.809	1.040	1.240	1.430	1.590
0.858	0.899	1.410	1.970	2.500	3.020	3.430	3.780
1.760	1.510	2.360	3.400	4.350	5.230	5.950	6.480
4.740	2.740	4.340	6.200	7.960	9.520	10.84	11.77

CORE CONDUCTIVITIES AT VARIOUS TEMPERATURES

CORE 2

	Core Conductivities, mho/m						
m_{NaCl}	22°C	50°C	80°C	110°C	140°C	170°C	200°C
0.090	0.075	0.122	0.177	0.233	0.286	0.331	0.367
0.260	0.228	0.360	0.524	0.677	0.833	0.951	1.040
0.858	0.573	0.889	1.280	1.640	1.960	2.210	2.390
1.760	1.010	1.580	2.280	2.940	3.520	4.000	4.350
4.740	1.790	2.810	4.050	5.200	6.180	7.060	7.810

CORE CONDUCTIVITIES AT VARIOUS TEMPERATURES

CORE 3

	Core Conductivities, mho/m						
m_{NaCl}	22°C	50°C	80°C	110°C	140°C	170°C	200°C
0.090	0.049	0.079	0.116	0.155	0.191	0.226	0.259
0.260	0.132	0.214	0.314	0.413	0.504	0.576	0.639
0.858	0.317	0.497	0.702	0.902	1.090	1.260	1.380
1.760	0.530	0.860	1.220	1.560	1.860	2.140	2.320
4.740	0.956	1.550	2.240	2.840	3.360	3.800	4.180

CORE CONDUCTIVITIES AT VARIOUS TEMPERATURES

CORE 4

	Core Conductivities, mho/m						
m_{NaCl}	22°C	50°C	80°C	110°C	140°C	170°C	200°C
0.090	0.043	0.077	0.117	0.157	0.192	0.223	0.246
0.260	0.101	0.168	0.250	0.333	0.407	0.478	0.527
0.858	0.221	0.353	0.516	0.688	0.809	0.933	1.030
1.760	0.375	0.608	0.896	1.160	1.400	1.600	1.760
4.740	0.649	1.070	1.540	2.030	2.430	2.830	3.230

CORE CONDUCTIVITIES AT VARIOUS TEMPERATURES

CORE 5

	Core Conductivities, mho/m						
m_{NaCl}	22°C	50°C	80°C	110°C	140°C	170°C	200°C
0.090	0.077	0.132	0.198	0.264	0.327	0.380	0.408
0.260	0.169	0.281	0.426	0.559	0.690	0.793	0.879
0.858	0.362	0.572	0.840	1.090	1.340	1.540	1.700
1.760	0.562	0.922	1.349	1.770	2.130	2.430	2.730
4.740	0.973	1.570	2.306	3.030	3.650	4.160	4.620

CORE CONDUCTIVITIES AT VARIOUS TEMPERATURES

CORE 6

	Core Conductivities, mho/m						
m_{NaCl}	22°C	50°C	80°C	110°C	140°C	170°C	200°C
0.090	0.049	0.089	0.142	0.195	0.244	0.288	0.319
0.260	0.088	0.152	0.243	0.334	0.417	0.490	0.549
0.858	0.166	0.275	0.412	0.548	0.681	0.795	0.890
1.760	0.259	0.432	0.648	0.858	1.030	1.230	1.360
4.740	0.433	0.710	1.030	1.390	1.690	1.970	2.200

CORE CONDUCTIVITIES AT VARIOUS TEMPERATURES

CORE 7

	Core Conductivities, mho/m						
m_{NaCl}	22°C	50°C	80°C	110°C	140°C	170°C	200°C
0.090	0.116	0.190	0.318	0.435	0.546	0.642	0.720
0.260	0.184	0.322	0.502	0.694	0.859	1.010	1.120
0.858	0.295	5.100	7.700	1.030	1.270	1.490	1.660
1.760	0.430	0.711	1.120	1.480	1.800	2.080	2.340
4.740	0.720	1.200	1.790	2.350	2.870	3.310	3.650

CORE CONDUCTIVITIES AT VARIOUS TEMPERATURES

CORE 8

	Core Conductivities, mho/m						
m_{NaCl}	22°C	50°C	80°C	110°C	140°C	170°C	200°C
0.090	0.153	0.268	0.416	0.551	-----	-----	-----
0.260	0.277	0.484	0.719	0.980	1.230	1.410	1.540
0.858	0.480	0.816	1.210	1.610	1.960	2.270	2.510
1.760	0.706	1.200	1.770	2.370	2.920	3.330	3.650
4.740	1.160	1.920	2.850	3.670	4.560	5.200	5.800

CORE CONDUCTIVITIES AT VARIOUS TEMPERATURES

CORE 9

	Core Conductivities, mho/m						
m_{NaCl}	22°C	50°C	80°C	110°C	140°C	170°C	200°C
0.090	0.053	0.098	0.157	0.215	0.271	0.322	0.354
0.260	0.019	0.162	0.254	0.344	0.431	0.509	0.574
0.858	1.810	0.284	0.432	0.574	0.710	0.831	0.923
1.760	0.243	0.418	0.649	0.858	1.050	1.210	1.340
4.740	0.382	0.657	1.000	1.350	1.660	1.910	2.130

VITA

Milton Noel Lau was born in Guatemala City, Guatemala. He graduated from El Liceo Javier High School, Guatemala City in 1980. In 1980 he was an exchange student in Cleveland, Ohio, where we graduated from Euclid Senior High in 1981. In 1985 he received a Bachelor of Science in Petroleum Engineering, and in 1987 he was awarded a Master Degree in Petroleum Engineering. Both degrees were obtained from Louisiana State University. In August 1987, he joined the Petroleum Engineering Department at Louisiana State University to work towards a Ph. D.. He is a member of Tau Beta Pi, Pi Epsilon Tau, Phi Kappa Phi, the Society of Petroleum Engineers, and the Society of Professional Well Log Analysts.

DOCTORAL EXAMINATION AND DISSERTATION REPORT

Candidate: Milton Noel Lau

Major Field: Petroleum Engineering

Title of Dissertation: Development and Field Applications of Shaly Sand Petrophysical Models

Approved:

Major Professor and Chairman

Dean of the Graduate School

EXAMINING COMMITTEE:

William J. Moore

Robert Desbrandes

Adam T Bourgoyne Jr

William J Bernard

Lawrence J Young Jr

Date of Examination:

October 26, 1989